EVALUATION OF THE EFFECT OF LIPID METABOLISM ON THE HIPPO PATHWAY THROUGH A NOVEL EXTRACELLULAR MATRIX COMPLEX

Thesis submitted for the award of

DOCTOR OF PHILOSOPHY

By

Simge KARAGIL

School of Life Sciences, Pharmacy and Chemistry

Faculty of Science, Engineering and Computing

Kingston University London

55-59 Penrhyn Road

Kingston upon Thames

KT1 2EE

March 2023

DECLARATION OF WORK

I hereby confirm that this thesis entailed as 'Evaluation of the Effect of Lipid Metabolism on the Hippo Pathway through a Novel Extracellular Matrix Complex' is my own research conducted in School of Life Sciences, Pharmacy and Chemistry at Kingston University London between October 2019 and March 2023. The information derived from literature has been correctly indicated within the thesis and a list of references provided. None of this research has been previously submitted for another degree at this or any other institutions.

SIMGE KARAGIL

ACKNOWLEDGEMENTS

First of all, I would like to extend my sincere gratitude to my supervisor, Dr. Ahmed Elbediwy, for accepting me to participate in his research as well as for his direction and support by providing me with helpful comments, remarks, and engagement throughout the research's learning process. His recommendations helped me to direct the course of my study and led to a better version of my thesis. His assistance and guidance during this research project helped me to get good outcomes and shape my comprehension of this research project. I also want to express my gratitude to Dr. Michael Stolinski for his advice and recommendations during my research.

I would want to thank the Faculty of Science, Engineering, and Computing at Kingston University London for their financial assistance with this research endeavour.

Last but not least, I would want to give special thanks to my family, fiance, and friends for their patience and support during the period of completing this project. They supported and motivated me to complete this research since they always give credence to my success. They have always encouraged me at my darkest moments and shared my joy and sorrow. I was highly motivated during the write up of my thesis because of their love, trust, and constant presence at my side.

A HUGE THANKS TO YOU ALL ♡

ABSTRACT

The Hippo signalling pathway tightly governs tissue growth. Activation of the Hippo signalling pathway leads to phosphorylation and inactivation of transcriptional coactivators YAP and TAZ and their cytoplasmic retention, whereas inactivation of the Hippo signalling pathway leads to dephosphorylation and hyperactivation of YAP/TAZ and translocation into the nucleus to modulate a diverse range of cellular functions such as cell proliferation, migration differentiation and apoptosis. YAP/TAZ can act as a central hub relaying multiple signals and integrating diverse functions. The extracellular matrix (ECM) plays an important role in the regulation of the Hippo signalling pathway as do YAP/TAZ which can themselves be affected by cellular metabolism. Free fatty acids have been shown to regulate the transcriptional activity of YAP/TAZ. However, a link between the ECM, Hippo signalling pathway and lipids has not been previously descibed. This project shows a direct relationship between the Hippo signalling pathway, the ECM and exogenously supplied lipids. Furthermore, the project provides an understanding of how novel ECM components are involved in this regulation.

The Hippo signalling pathway effector YAP was shown to interact with ECM proteins; Talin, CD2AP, PDLIM7 and Ezrin by Co-immunoprecipitation leading to the characterisation of a novel protein complex coupling the Hippo signalling pathway, the ECM and lipids in a CaCo2 and Hep-G2 cell culture model system. Scratch assays were used to observe the effect of complex member proteins on cellular migration. Knockdown of YAP and Talin was shown to slow down the migration rate of CaCo-2 cells. Immunofluorescence (IF) imaging was used to describe the effect of the various complex member proteins on the stabilisation of YAP following siRNA knockdown of CD2AP/Talin/Ezrin to show that translocation of YAP

between nucleus and cytoplasm was affected.Depletion of talin resulted in inactivation of YAP by inducing its translocation from nucleus to cytoplasm in both CaCo-2 and Hep-G2 cells whereas depletion of CD2AP and Ezrin had no effect.

The availability of oleic acid (OA) and palmitic acid (PA), the most abundant fatty acids, on the Hippo signalling effector YAP and the novel components of the Hippo/ECM complex was described. The results obtained indicated that lipids leads to inhibition of YAP activity by significantly increasing the p-YAP levels. CaCo-2 cells treated with lipids showed a marked decrease in cellular migration. Oleic acid was shown to disrupt the interaction of YAP with CD2AP and the interaction of Talin with CD2AP. Addition of OA was shown to affect the localization of proteins of the identified complex by immunofluorescence microscopy. Upon OA treatment, nuclear YAP was decreased in both CaCo-2 and Hep-G2 cells.

The levels of lipid droplet formation following addition of OA in conjunction with the depletion of proteins within the complex was also evaluated in CaCo-2 and Hep-G2 cells. This provided a new insight into the relationship of lipid metabolism with the ECM and Hippo signalling pathway. Planarians have been used as a model organism in order to assess the effect of lipid metabolism in a physiological relevant system. The results gathered with OA *in-vivo* are consistent with the results obtained in the tested mammalian cell lines. Finally, the novel protein interactions and expression of specific genes with the Hippo signalling pathway upon addition of fatty acids was analysed by mass spectroscopy (MS) and RNA-Sequencing. Numerous YAP-interactors were obtained by MS analysis and most importantly, OA was shown to abolish the interaction of Ezrin and Radixin with YAP. The data obtained from RNA-Sequencing revealed that, expression of downstream target genes of YAP (MYC and ANKRD1) were downregulated whereas key upstream components of the

Hippo signalling pathway (FRMD6 and TAOK-1) were upregulated upon addition of oleic acid.

The data obtained therefore indicates that fatty acids in part interact/manipulate the Hippo signalling pathway to regulate its activation state through the newly described ECM complex.

TABLE OF CONTENTS

TABLE OF FIGURES

CHAPTER 1

CHAPTER 2

CHAPTER 3

CHAPTER 6

CHAPTER 7

ABBREVIATIONS

ACBT	Beta Actin
AKT	Protein Kinase B
AMOT	Angiomotin
AMOTL1	Angiomotin like 1
AMOTL2	Angiomotin like 2
AMPK	AMP-activated Protein Kinase
ANKRD1	Ankyrin Repeat Domain 1
BSA	Bovine Serum Albumin
CaCo-2	Colorectal Adenocarcinoma Cells
CapZ	Actin capping protein
CAPZA1	F-actin capping protein subunit alpha-1
CD2AP	CD2 associated protein
cDNA	Complementary Deoxyribonucleic Acid
cGAS	Cyclic GMP-AMP Synthase
c-Myc	Cellular Myc
CO_2	Carbon Dioxide
Co-IP	Co-immunoprecipitation
CRC	Colorectal Cancer
CST	Cell Signalling Technology
C-terminal	Carboxyl terminal
DAPI	4’,6-diamidino-2-phenylindole
DF	The degrees of freedom
dH_2O	Distilled Water
DMEM	Dulbecco’s Modified Eagle Serum

DNA	Deoxyribonucleic Acid
ECM	Extracellular Matrix
EDTA	*Ethylenediamine tetraacetic acid*
EGFR	Epidermal Growth Factor Receptor
EMT	Epithelial-Mesenchymal Transition
ERM	Ezrin, Radixin and Moesin
FA	Focal Adhesion
F-actin	Filamentous Actin
FAK	Focal Adhesion Kinase
FAS	Fatty Acid Synthase
FBS	Fetal Bovine Serum
FFAR1/4	Free Fatty Acid Receptor 1/4
FRMD6	FERM domain containing protein 6
FW	Forward
GAPDH	Glyceraldehyde-3-phosphate dehydrogenase
G-protein	Guanine nucleotide-binding protein
H_2O	Water
Hep-G2	Liver Hepatocellular Carcinoma Cells
HER2	Human Epidermal Growth Factor Receptor 2
HMGCR	30-hydroxylmethyl glutaryl coenzyme A reductase
Hpo	Hippo gene
IRF3	Interferon regulatory factor 3
JACOP	Junction-associated-coiled-coil protein
kDa	Kilodalton
LATS1/2	Large Tumor Suppressors 1 and 2

LD	Lipid Droplet
MALAT1	The metastasis-associated lung carcinoma transcript 1
Mats	Mob as tumor suppressor
mM	milliMolar
MOB1	Mps-one binder 1
MS	Mass Spectroscopy
MST1/2	Mammalian Sterile 20-like Protein Kinase 1 and 2
mTOR	The Mechanistic Target of Rapamycin
MW Marker	Molecular Weight Marker
NFAT	Nuclear Factor of Activated T-Cells
NHE1	Sodium-Hydrogen Antiporter 1
N-terminal	Amino-terminal
OA	Oleic Acid
OPTI-MEM	Reduced Serum Medium
P53	Tumor-suppressor transcription factor
PA	Palmitic Acid
PBS	Phosphate Buffered Saline
PBS-T	Phosphate Buffered Saline Tween
PCR	Polymerase Chain Reaction
PDK1	*Phosphoinositide-dependent kinase-1*
PDLIM	PDZ and LIM domain protein
Penstrep	Penicilin-Streptomycin
PFA	Paraformaldehyde
PI3K	Phosphoinositide 3-kinase
PIP2	Phosphatidylinositol 4,5-bisphosphate
PTPN14	Protein Tyrosine Phosphatase Non-Receptor Type 14

pYAP	Phospho – Yes-associated Protein
qPCR	Quantitave polymerase chain reaction
RNA	Ribonucleic Acid
RNAi	RNA Interference
RNAse	Ribonucleases
RNA-Seq	RNA-Sequencing
RT	Reverse Transcription
RT-qPCR	Reverse Transcription Polymerase Chain Reaction
RV	Reverse
S.Med	Schmidtea Mediterranea
S127	Serine 127
SAV1	Salvador
SCD1	Stearocyl-Coenzyme A-desaturase 1
Sd	Scalloped
SD	Standard Deviation
SDS-Page	Sodium Dodecyl Sulphate – Polyacrylamide Gel Electrophoresis
SH3	SRC homology 3 domain
SH3BP1	SH3 domain binding protein 1
siRNA	Small Interfering Ribonucleic Acid
SIRT1	SREBPs (sterol regulatory element binding protein) inhibitor
Src	Non-receptor tyrosine kinase
SREBP	Sterol Regulatory Element Binding Protein
STING	Stimulator of Interferon Genes
T567	Tyrosine 567
TAOK1	TAO kinase 1

TAZ	Transcriptional coactivator with PDZ-binding motif
TEAD	TEA domain transcription factor
TG	Triglyceride
TSCC	Tongue Squamous Cell Carcinoma
Tyr	Tyrosine
Wts	Warts
YAP	Yes-associated Protein
Yki	Yorkie
β1-integrin	Beta 1 Integrin
β-catenin	Beta-Catenin
µl	Microliter

CHAPTER 1. INTRODUCTION

1.0 INTRODUCTION

1.1 Regulation of Cellular Processes

The integrative control of biological processes such as cellular proliferation, differentiation and apoptosis are fundamental to sustain cell and tissue homeostasis in an organism (Watt, Harvey and Gregorevic, 2017). A principal question throughout biology is to try to decipher how organisms and their constituent parts recognise how much they need to grow and the triggers to stop upon reaching a certain size (Yimlamai, Fowl and Camargo, 2015; Zygulska, Krzemieniecki and Pierzchalski, 2017). For a developing tissue, cell proliferation is essential to boost organ size while proper differentiation is required to maintain the regular function of the newly developed organ (Yu and Guan, 2013). Loss of tightly controlled regulation controlling the growth of tissues and organisms can lead to development of numerous pathological disorders such as cancer (Yimlamai, Fowl and Camargo, 2015). Coordination of these processes is vital for the vast range of physiological and pathological conditions (Yu and Guan, 2013). Signalling pathways regulate these fundamental processes and thus it is important for researchers to investigate these pathways to better understand how organisms and their basic and fundamental processes can be regulated. One of these key regulatory pathways is the Hippo signalling pathway.

1.2 The Hippo Signalling Pathway

The Hippo signalling pathway has emerged as a significant biochemical signalling pathway which tightly governs tissue growth. The Hippo signalling pathway was first discovered by genetic screens in *Drosophila melanogaster* (fruit fly) as an evolutionarily conserved

regulator of cell differentiation and apoptosis (Kwon, Kim and Jho, 2021; Zygulska, Krzemieniecki and Pierzchalski, 2017).

The discovery of the first component of the hippo signalling pathway was in 1995 when the identification of tumor suppressor gene *Warts* (*Wts*) was found, as mutations in the *Wts* gene resulted in an abnormal rate of proliferation and cell shape changes during a genetic mosaic study in *Drosophila melanogaster* (Kwon, Kim and Jho, 2021; Zygulska, Krzemieniecki and Pierzchalski, 2017). The discovery of the upstream components of the Hippo signalling pathway was due to this finding of *Wts* gene and subsequent studies allowed the core of the pathway, comprising four members, to be revealed (Zygulska, Krzemieniecki and Pierzchalski, 2017). All of the four core proteins of the pathway; *Salvador* (*Sav*), *Hippo* (*Hpo*), *Warts* (*Wts*) and *Mob as tumor suppressor* (*Mats*) were identified through genetic screens in *Drosophila* (Staley and Irvine, 2012). The downstream components were the next to be discovered including the transcriptional activator *Yorkie* (*Yki*) and transcription factor *Scalloped* (*Sd*), establishing the main basis of the Hippo signalling pathway (Kwon, Kim and Jho, 2021). The pathway was thus named after mutations in the *Drosophila* serine/threonine kinase *hippo* gene (*hpo*) as loss of control of the functionality of this gene resulted in tissue wing overgrowth owing to excessive proliferation and decreased apoptosis (Shu *et al*., 2019; Yimlamai, Fowl and Camargo, 2015; Moya and Halder, 2016). The wings of the flies in question became grossly large and rounded thus resembling a Hippo which allowed the naming of the gene as *Hippo* (*hpo*) (Park and Guan, 2013). The *Hippo* gene was labelled as an organ size regulator in *Drosophila* (Bouchard *et al*., 2020). *Drosophila* mosaic genetic screens searching for additional genes revealed many other components of the Hippo signalling pathway, as gene mutations which resulted in gene loss of function led to strong overgrowth phenotypes (Park and Guan, 2013). Subsequent cellular, biochemical, and genetic studies over the years have

established that the core components of Hippo signalling pathway formed a key central kinase cascade which is highly conserved in mammals (Bea and Luo, 2018). What is intriguing is that the key components discovered in *Drosophila* are not only conserved in more advanced organisms such as mammals but also much simpler organisms such as flatworms (Fu, Plouffe and Guan, 2017; Hayashi, Yokoyama and Tamura, 2015).

1.2.1 Simple Organisms and the Hippo Signalling Pathway

In *Drosophila*, *Hippo (hpo), Salvador (sav), Warts (wts)* and *Mob as tumor suppressor (mats)* form the core kinase cassette of the Hippo signalling pathway. The *hpo-sav* complex phosphorylates and activates *Warts* and *Mats* which in turn phosphorylates and inactivates *Yki* (transcriptional co-activator) by sequestering it in the cytoplasm whereas, dephosphorylation of *Yki* promote transcriptional gene expressions by interacting with *Scallped (sd)* (DNA-binding transcription factor) in the nucleus as seen in Figure 1.0 (Hwang *et al*., 2015; Fu, Plouffe and Guan, 2017).

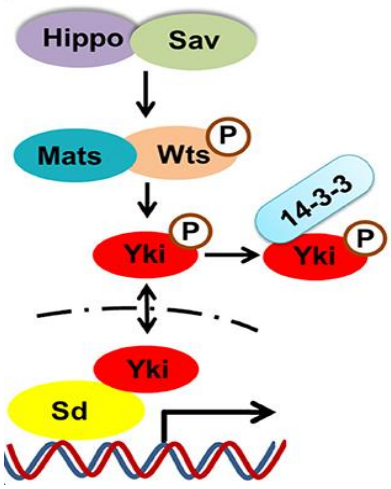

Figure 1.0 The schematic illustration of Hippo signalling pathway *in Drosophila melangoster.* The core components; *Hippo, Sav, Wts* and *Mats*. *Hippo-Sav* complex phosphorylate and activate *Wts*

and *Mats* which lead to phosphorylation of downstream *Yki* and its cytosolic retention by interacting with 14-3-3 protein. Whereas unphosphorylated *Yki* bind to transcription factor *Sd* in nucleus to regulate proliferation, differentiation, and survival (From; Cheng *et al*., 2020).

The Hippo signalling pathway as mentioned previously is conserved in various species from complex mammals to simple flatworms. The pathway is shown to be closely related and important in the regeneration process of Planarian flatworms (Hayashi, Yokoyama and Tamura, 2015). Planarians are flatworms belonging to members of the *Platyhelminthes* and are commonly found in freshwater brackish ponds (Makhutova *et al*., 2009; Yuwen *et al*., 2011). Planarians are an excellent model system for the study of key growth control and regeneration processes due to presence of a large pluripotent stem cell population spread throughout the planarian body (Cote, Simental and Reddien, 2019; Ge *et al*., 2022). Planarians, when cut in half can regenerate their body parts and maintain themselves; heads, tails, sides and became a complete worm within days owing to their regenerative ability (Reddien, 2018; Angerer *et al*., 2019).

The Hippo signalling pathway is not only important in the regeneration process of planarian it also plays an important role in tissue development and organ size control. Inhibition of the Hippo signalling pathway decreased rates of apoptosis and promoted cell dedifferentiation and cellular overgrowth by inducing cell-cycle arrest but without affecting body size and cell number (Pascual-Carreras *et al*., 2020; Ge *et al*., 2022; de Sousa *et al*., 2018). The same phenotype was observed when the core kinase elements of the Hippo signalling pathway; *salvador* and *warts* were inhibited (de Sousa *et al*., 2019). When the pathway, however was hyperactivated it resulted in an expansion of cell population improving the wound healing response and regeneration of the tissue (Pascual-Carreras *et*

al., 2020). Several further studies elucidated to the importance of the Hippo signalling cascade effector; *Yki* in multiple aspects of the pleiotropic process during regeneration including such key processes as stem cell proliferation, axial patterning and organ homeostasis (Lin and Pearson, 2017; Lin and Pearson, 2014). The planarian gene *Yorkie (yki)* was shown to be essential for the restriction of stem cell proliferation and maintanence of excretory system homeostasis of planarian. It was also shown that proper axial patterning required *Yorkie (yki).* Thus, *yki* seems to act as a key regulatory gene in planarians for the integration of cell regulation and spatial tissue patterning (Lin and Pearson, 2014). Since *yki* plays a major role in the regulation of growth control in simple organisms such as *Drosophila* and planarian, it is important to understand if this gene also plays a critical role in more complex organisms such as mammals and if it is conserved.

1.2.2 The Hippo Signalling Pathway in Cancer

After its initial discovery, the Hippo signalling pathway has been subjected to intensive study in mammals, and conservation of the mammalian pathway has been found (Meng, Moroishi and Guan, 2016; Ardestani and Maedler, 2016). The core aspects of the pathway comprising the core kinase cascade, transcription coactivators and DNA-binding partners were found to be conserved in mammals with its role as a highly conserved regulator of mammalian organ size control being reported (Meng, Moroishi and Guan, 2016; Watt, Harvey and Gregorevic, 2017). The core components of the mammalian Hippo signalling pathway include a kinase cascade composed of two types of serine/threonine kinases; mammalian sterile 20-like protein kinases 1 and 2 (MST1/2) and large tumor suppressors 1 and 2 (LATS 1/2) as core kinases which are orthologs of the Drosophila *Hpo* and *Wts* respectively (DeRan *et al*., 2014; Bae and Luo, 2018; Kwon, Kim and Jho, 2021). The

downstream effectors of mammals; Yes-associated protein (YAP) and transcriptional coactivator with PDZ-binding motif (TAZ); are the orthologs of *Drosophila Yki* and several associated regulatory proteins like Salvador (SAV1), Mps-one binder 1 (MOB1) function together to transmit both extracellular and intracellular signals to core cassette and transcriptional complexes (such as TEA domain transcription factors; TEAD; an ortholog of sd) respectively for controlling cell fate (Ardestani, Lupse and Maedler, 2018; Ardestani and Madler, 2016). Any disorder in the mammalian Hippo signalling pathway leading to a loss of the pathways tightly controlling the growth regulation can initiate development and progression of cancer as represented in Figure 1.1 (Yimlamai, Fowl and Camargo, 2015).

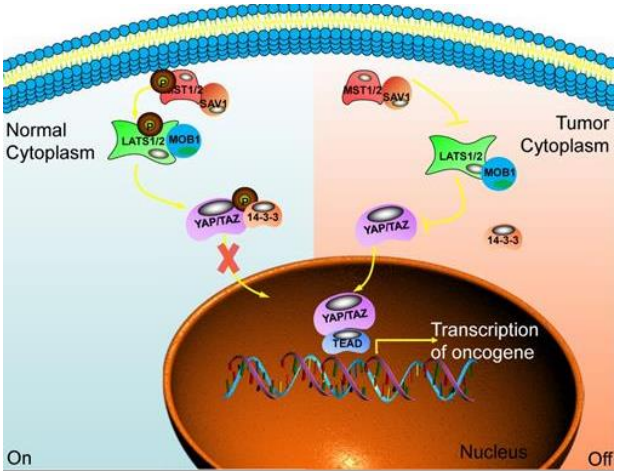

Figure 1.1 Hippo signalling pathway in cancer. Hippo signalling pathway is active in normal cells and YAP/TAZ is sequestered in cytoplasm. In cancer cells, the hippo signalling pathway is deregulated where YAP/TAZ translocate into the nucleus promoting the transcription of various oncogenes elevating the formation of tumours (From; Wang *et al*., 2021).

Cancer is a serious, complex genetic disease abundant across the world with the ultimate outcome of death if untreated due to uncontrollable cell proliferation and cancer cell metastasis (Han, 2019; Lamar *et al*., 2012; Snigdha *et al*., 2019). Cancer cells invade surrounding tissue, enter into the blood circulation, survive and proliferate to distant

organs and result in metastatic tumours. The signalling cascades involved in cancer initiation and survival are well-designed to promote metastatic progression by regulating the expression of target genes that are progenitors of prometastatic processes (Lamar *et al*., 2012). Activation of oncogenic genes are crucial to initiate the uncontrolled proliferation of cancerous cells (Snigha *et al*., 2019). The finding of a highly proliferative overgrowth phenotype in *Drosophila melangoster* is due to a loss of function in the *Hpo* gene and is suggestive that the gene acts as a tumour suppressor by controlling organ growth and thus the Hippo signalling pathway is anti-cancerous (Cunningham and Hansen, 2022; Johnson and Halder, 2014). Many studies have exhibited that dysregulation of the Hippo signalling pathway is associated with a vast range of human cancers by inducing hyperproliferation, invasion and metastasis (Calses *et al*., 2019). Aberrantly elevated levels and nuclear localised transcriptional coactivator Yes-associated protein (YAP) has been encountered in the vast majority of solid tumours with its role to promote expression of genes required for proliferation, thus clearly demonstrating that YAP acts as an oncogene in cancer (Xiao and Dong, 2021; Johnson and Halter, 2014; Lamar *et al*., 2012; Hsu *et al*., 2020). Any disorder in Hippo signalling can cause hyperactivation of YAP/TAZ and thus initiate tumour cell migration by causing ectopic cell proliferation (Wang *et al*., 2021; Harvey, Zhang and Thomas, 2013). The Hippo signalling pathway is also found to be deregulated by sensing the changes in cell microenvironment (Wang *et al*., 2021; Harvey, Zhang and Thomas, 2013). Alterations in the tumour microenvironment such as microarchitecture of tumour, stiffness of the cell, pressure of interstitial fluid and solid stresses could promote inactivation of the Hippo signalling pathway leading to cancer progression and resistance to all manner of cancer treatments (Cai, Wang and Meng, 2021).

1.3 Hippo Signalling Pathway Activation

The Hippo signalling pathway comprises of two principal modules; the serine/threonine kinase cascade controlled by diverse range of upstream signals and the transcriptional module activating the downstream target genes (Cunningham and Hansen, 2022). Once the Hippo signalling pathway is activated; in the "ON" state, the upstream MST1/2 kinases form a complex with the regulatory protein SAV1, which in turn phosphorylates and activate the LATS1/2 kinases at their hydrophobic motif. Subsequently, an auto-inhibitory motif in the LATS1/2 kinases form a complex with MOB1 leading to phosphorylation of the LATS activation loop thence increasing their kinase activity (DeRan *et al.,* 2014; Ardestani and Madler, 2016; Ardestani and Maedler, 2017; Yu and Guan, 2013). Activated LATS1/2 directly phosphorylate and inactivate YAP; the transcriptional coactivator and TAZ; the YAP paralog transcriptional coactivator on various serine residues (Zhao, Li, Lei and Guan, 2010). Interaction of LATS1/2 with YAP/TAZ are mediated via PPxY motifs on LATS1/2 and WW domains on YAP/TAZ (Yu and Guan, 2013). Phosphorylation of the transcriptional coactivators YAP/TAZ promotes YAP/TAZ nuclear exclusion, cytoplasmic retention and its ubiquitin-dependent degradation thereby inhibiting their transcriptional regulatory activity resulting in inhibition of target gene transcription (Ardestani and Maedler, 2017; Ardestani, Lupse and Maedler, 2018; Ardetani and Maedler, 2016; Maugeri-Sacca and Maria, 2018). The most communal phosphorylation site in YAP is at serine residue 127 as phosphorylation at S127 site is essential to sequester YAP in cytoplasm by binding to a mediator of cytoplasmic retention protein 14-3-3 (Cunningham and Hansen, 2022; Kwon, Kim and Jho, 2021; Han, 2019).

Conversely, when the Hippo signalling pathway is in its "OFF" state, the kinase cascade leads to dephosphorylation and hyperactivation of YAP/TAZ and their translocation into

the nucleus to exert their roles in gene expressions involved in proliferation, migration, and anti-apopotosis (Yu and Guan, 2013; Zeng and Dong; 2021). Translocation of YAP between the cytoplasm and nucleus occurs rapidly as nuclear translocation of YAP is required for the initiation of Hippo target gene expression (Kwon, Kim and Jho, 2021). Accumulation of YAP/TAZ in the nucleus induces target gene expression by binding to the TEA domain transcriptional factor family (TEAD) (a homolog of sd) and allows modulation of a diverse range of cellular functions such as proliferation, migration, differentiation and apoptosis as represented in Figure 1.2 (Ardestani and Maedler, 2017; DeRan *et al.,* 2014; Ardestani and Maedler, 2016). YAP and TAZ do not have intrinsic DNA-binding domains but instead regulate gene expression through interacting with transcription factors TEAD1-4 to mediate the main transcriptional output of the mammalian Hippo signalling pathway (Meng, Moroishi and Guan, 2016; Yu and Guan, 2013; Han, 2019). The primary regulatory target of Hippo signalling is the YAP transcriptional coactivator (Yimlamai, Fowl and Camargo, 2015). Overexpression of YAP or inactivation of Hippo signalling pathway may lead to massive tissue overgrowth thus tumour progression. However, excessive “ON” state thus hyperactivation of MST or LATS kinases, assists cell death which is generally associated with neurodegenerative and cardiovascular diseases and with metabolic abnormalities such as diabetes (Shu *et al.,* 2019; Ardestani, Lupse and Maedler, 2018).

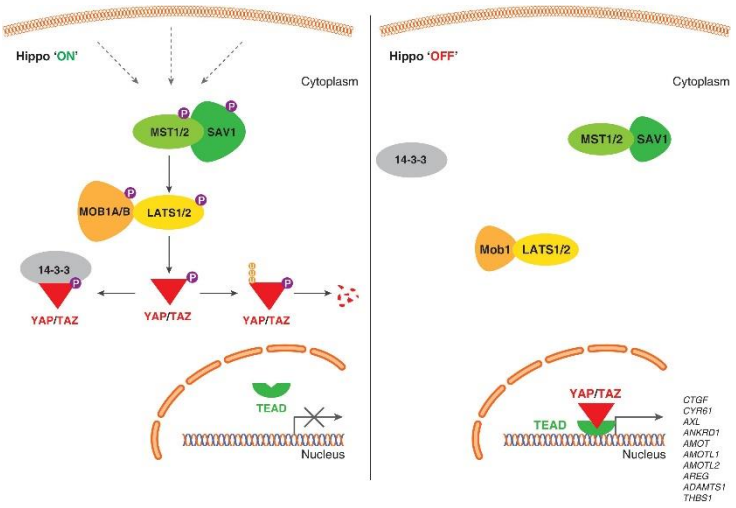

Figure 1.2 Schematic illustration of mammalian Hippo signaling pathway. 'ON' state of Hippo signaling pathway (left), leads to phosphorylation of transcriptional co-activators YAP/TAZ. Phosphorylated YAP/TAZ proteins recruit 14-3-3 proteins to stimulate cytoplasmic retention or proteolytic degradation. 'OFF' state of Hippo signaling pathway (right), the kinase cascade dephosphorylates YAP/TAZ proteins and localize to nucleus leading to complex formation with TEAD transcription factors to regulate transcriptional activity of diverse cellular functions (From; Boopathy and Hong, 2019).

The Hippo signalling pathway does not possess a specific cell surface receptor or ligands thus its activation can be regulated by diverse input signals (Werneburg, Gores and Smoot, 2020). Multiple upstream signals activate the core kinase cascade to coordinate the localization of oncogenic transcriptional coactivators; YAP and TAZ (Bae and Luo, 2018). Recent studies cemented that the Hippo signalling pathway can be activated by myriad of intrinsic and extrinsic signals. Upstream factors controlling the Hippo signalling pathway ranges from cell-to-cell contact and mechanical signals to G-protein coupled receptor ligands and metabolic pathways, and various other inputs are being discovered on a regular basis (Bae and Lou, 2018; Maugeri-Sacca and Maria, 2018). It is also been shown that the

Hippo signalling pathway effector YAP can also be activated independently of the hippo signalling pathway by cellular mechanotransduction (Gumbiner and Kim, 2014).

1.4 Hippo Signalling and Mechanotransduction

Living cells are constantly subjected to mechanical cues and signals and able to convert these mechanical forces in the environment into biochemical and behavioural responses through the extracellular matrix and can adapt to the extracellular environmental changes though a process called mechanotransduction (Maxwell and Roskelley, 2015; Seong, Wang and Wang, 2013; Shamsan and Odde, 2019; Sun, Guo and Fässler, 2016). The process of mechanotransduction includes the sensing of mechanical stimuli, transmission of the stimuli into biochemical signals to promote a signalling cascade and lastly regulating the expression of target genes to drive functional physiological roles (Virdi and Pethe, 2021; Cai, Wang and Meng, 2021; Seo and Kim, 2018). Mechanotransduction relies on mechanically induced alterations in the conformation of proteins or inhibition of signalling protein endocytosis leading to such processes as cytoskeleton rearrangements, cell division modulation and differentiation. Translation of the mechanical forces and deformations into biochemical signals ultimately influence gene expression, cell shape changes and cell fate decisions (Mohri, Del Rio Hernandez and Krams, 2017). YAP/TAZ, are central components of mechanotransduction by way of acting as mechanotransducers or tension sensors to transmit mechanical forces for the regulation of biological outcomes (Cai, Wang and Meng, 2021; Seo and Kim, 2018). Mechanotransduction is vital for cellular processes such as cell adhesion, motility, proliferation, migration, differentiation and survival (Aw Yong *et al*., 2017; Maxwell and Roskelley, 2015). Thus the mechanotransduction process involves both the external environment and internal signalling. The extracellular matrix (ECM) has a

crucial role among all the mechanical forces in the determination of cellular functionality (Virdi and Pethe, 2021). Various mechanical cues regulating YAP are represented in Figure 1.3.

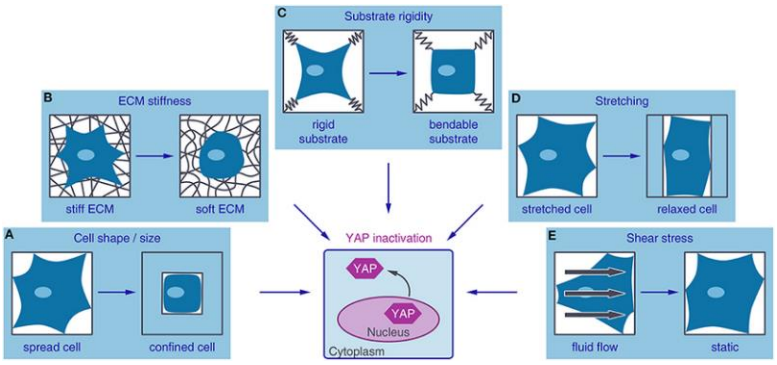

Figure 1.3 Various mechanical cues regulate the activity of YAP. In stiff ECM (B), stretched-spread cell (A&D), rigid substrate (C) and fluid shear stress where the intracellular tension is high, YAP is active and localized to the nucleus. At low contractile forces, soft ECM, small area, bendable substrate, static media and relaxed cell, YAP retains in cytoplasm in its inactive form (From; Fisher *et al*., 2016).

1.4.1 Focal Adhesions

Cells are physically bound to the extracellular matrix (ECM) microenvironment through the transmembrane receptor integrins and focal adhesions (FAs). Focal adhesions are subcellular structures at the main sites of ECM attachment acting as a scaffold for the activation of downstream signalling pathways involving mechanical tension (Hoskin *et al*., 2015; Shen *et al*., 2018). Focal adhesions are large and dynamic multiprotein complexes comprise of various protein layers with the integral components integrins, vinculin, talin and focal adhesion kinase (Figure 1.4). Thus, FAs relay mechanical responses at the plasma membrane from integrin complexes by providing a linkage amongst the intracellular cytoskeleton and the ECM. These protein complexes behave as mechanosensors and

integrators to regulate a diverse sequence of signalling molecules, including Hippo signalling (Rausch and Hansen, 2020).

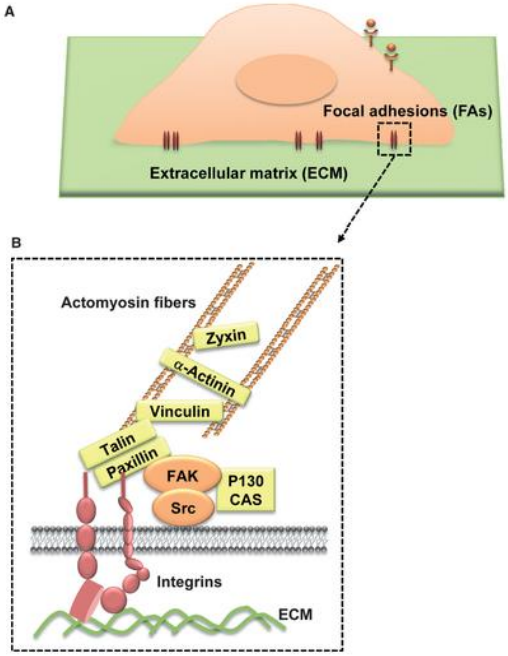

Figure 1.4 Focal adhesions. (A) FAs linking the cell to extracellular matrix (ECM). (B) Structure of focal adhesion. Interaction of FAs with ECM recruits signalling proteins (orange) and structural proteins (yellow) via transmembrane integrin receptor (red), connecting actomyosin fibres (From; Seong, Wang and Wang, 2013).

Focal adhesions are the main site of interaction for both interior and exterior mechanotransduction thus exterior mechanical signals are sensed at FAs and translated by integrin-related signalling pathways into biochemical information to maintain cellular function (Seong, Wang and Wang, 2013; Maxwell and Roskelley, 2015). Focal adhesions are important for cellular mechanosensing as they behave as a linker among ECM-integrin interaction and cytoskeleton (Zhao, Lykov and Tzeng, 2022).

1.4.2 Integrin and Talin Signalling

Signals sensed through the Hippo signalling pathway mediate the ECM signal transduction through a prominent involvement of integrins (Yang *et al*., 2021). Activation of integrins are important for cell adhesion, migration and ECM assembly processes. Integrins are heterodimeric transmembrane proteins comprised of eighteen alpha and eight β subunits connecting the ECM and the intracellular environment (Lin, Chun and Kang, 2016; Tadokoro *et al*., 2003; Li *et al*., 2017). Integrin activation is usually mediated via the integrin subunit cytoplasmic tail and regulated by different biochemical signalling pathways. Integrin-mediated mechanical signals can regulate the migration, invasion and metastasis of tumor cells (Tadokoro *et al*., 2003; Li *et al*., 2017). Physical connection amongst the ECM, integrins and the cellular cytoskeleton is critical in various signalling cascade for the cellular migration, adhesion and ECM remodelling (Zhang *et al*., 2008). Extensive biological studies elucidated that talin which is a large focal adhesion protein is essential for regulating various integrin-mediated cell adhesion dependent processes like growth, differentiation and migration (Liang *et al*., 2018). Talin is a critical protein in integrin-mediated adhesion complexes as it acts as a linker between integrins and the actin cytoskeleton (Rahikainen *et al*., 2019; Zhang *et al*., 2008). Talin is the first protein mediating the formation of cell-matrix adhesions as the head domain of talin modulates integrin-ECM affinity and its rod domain directly interacts with integrins (Rahikainen *et al*., 2017; Zhang *et al*., 2008).

Talin is a large 270 kDa actin-binding cytoskeletal protein and was first discovered in 1983 as a focal adhesion and ruffling membrane component (Gough and Goult, 2018). Talin has emerged as a key cytosolic protein in integrin activation mediating adhesion of integrins to the ECM (Klapholz and Brown, 2017; Chinthalapudi, Rangarajan and Izard, 2018). Talin

proteins reside at focal adhesions providing a connection to intracellular networks and the ECM by simultaneously coupling with the actin cytoskeleton and membrane integrins through its interaction with β integrin tail domains and F-actin fibers (Tadokoro *et al*., 2003; Haining, Lieberthal and del Río Hernández, 2016; Seong, Wang and Wang, 2013; Rahikainen *et al*., 2019). Talins as focal adhesion scaffold proteins are crucial determinants of adhesion complex integrity and therefore required for sustained cell growth and generation of traction force (Rahikainen *et al*., 2019). Talin's are comprised of long N-terminal globular head domain, flexible C-terminal rod domain and these are interconnected by a calpain-sensitive linker as shown in Figure 1.5 (Chinthalapudi, Rangarajan and Izard, 2018; Gough and Goult, 2018). The head domain contains a 4.1 FERM domain with 4 subdomains (F0-F3) providing a site for binding to the cytoplasmic β-integrin subunit to form cell-matrix adhesions, whereas the talin rod domain consisting of 13 helical bundles contains diverse binding sites for the vinculin ECM protein to provide a linkage to an actin cytoskeleton by extension to ECM (Haining, Lieberthal and del Río Hernández, 2016; Seong, Wang and Wang, 2013; Kelley *et al*., 2020; Rahikainen *et al*., 2017; Chinthalapudi, Rangarajan and Izard, 2018). Mechanical forces sensed by talins are known to be involved in crucial cellular processes (Rahikainen *et al*., 2019).

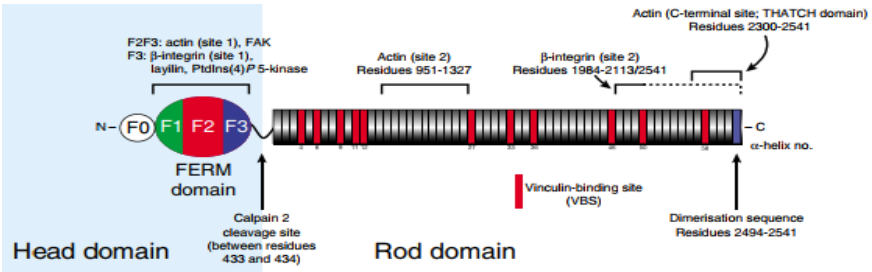

Figure 1.5 Organization of talin domains. The globular talin head region with a FERM domain connected via linker to the talin rod domains with several binding sites to actin, vinculin (From; Critchley and Gingras, 2008).

The regulated binding of talin to integrin β tails represents the essential final step for the integrin activation pathways (Qi *et al*., 2016; Calderwood, 2004). Transmission of mechanical stretching forces through α-helical rod subdomains leads to an unfolding of the talin rod domain disclosing critical binding sites to allow the recruitment of vinculin for stabilizing the linkage between integrin and actin cytoskeleton. Interaction between talin and vinculin provides structural support to the linkage between the actin cytoskeleton and the ECM leading to reorganization of the cellular cytoskeleton (Figure 1.6) (Haining, Lieberthal and del Río Hernández, 2016; Broders-Bondon *et al*., 2018; Rahikainen *et al*., 2019). Both talin and vinculin are located at cell-matrix adhesion sites and are ideal candidates for mechanotransduction as binding of vinculin to focal adhesion complexes are enhanced upon the application of force (Broders-Bondon *et al*., 2018). This mechanism is mechanosensitive as it strengthens adhesion upon force exertion to mediate the recruitment of a diverse range of signalling proteins (Goult, Yan and Schwartz, 2018; Rahikainen *et al*., 2019). Integrin activation by talins is called inside-out activation as integrins are converted into a high-affinity conformation for their ECM ligand by talins, as talins are key proteins for organising integrin affinity and their attachment to the cell membrane is a requisite for integrin activation, FA formation and stability (Klapholz and Brown, 2017; Chinthalapudi, Rangarajan and Izard, 2018). Integrins, thus play an important role in mediating signals from the extracellular matrix (ECM) and various connections have been assigned between integrins and activity of YAP (Misra and Irvine, 2018). Immunoprecipitation and mass spectroscopy analysis identified novel interactors of YAP linked to the ECM, these include the Enigma family proteins which are members of integrin adhesome with conserved PDZ and LIM domains. Talin2 was also found to bind YAP directly in mass spectroscopy analysis from the same study; thus, talin-family members could be a

novel and important interactor of the Hippo signalling pathway in the context of the ECM (Elbediwy *et al*., 2018).

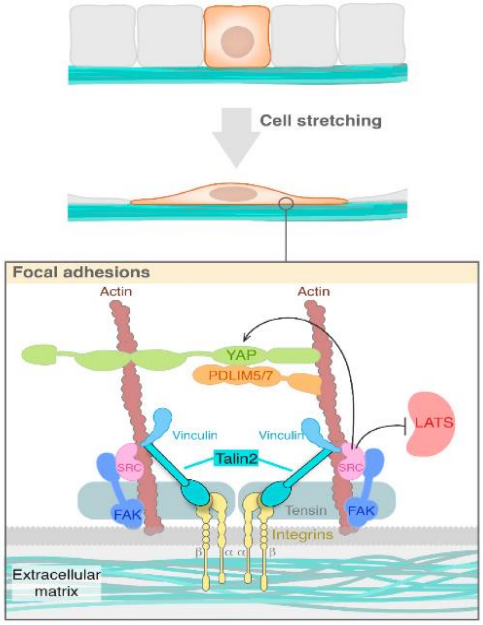

Figure 1.6 Regulation of YAP through the ECM; activity and stability of YAP involves a range of proteins including talin, vinculin and PDLIM family proteins. External forces sensed by integrins are transmitted to talin family members allowing YAP and accessory proteins to act as a mechanosensors (From; Cobbault *et al*., 2020).

In vertebrates, there are 2 talin isoforms encoded by separate genes, *talin1* and *talin2* with conserved intron-exon boundaries sharing 74% sequence identity (Gough and Goult, 2018; Kelly *et al*., 2020). Although talin1 and talin2 have distinct functions, both are localized at focal adhesions when cells are in fully spread and elongated conditions (Zhang *et al*., 2008; Kelley *et al*., 2020). The precise role of talin2 is not clear, however; Talin 1 was found to contribute to the regulation of focal adhesion dynamics, cell migration and invasion. Talin1 is expressed almost in every tissues; liver, kidney, stomach, lungs, muscles whereas expression of talin2 is found to be mainly in heart, brain, testis and muscles (Liang *et al*.,

2018; Zhao, Lykov and Tzeng, 2022). Talin2 is usually localized at larger, more stable focal adhesions and fibrillary adhesions and found to function distinctly in the regulation of cell invasion with a higher affinity for specific integrin receptors when compared to talin1. Talin2 was found to regulate focal adhesion assembly and kinase signalling in the absence of talin1 (Qi *et al*., 2016; Kelley *et al*., 2020). Previously published data showed that the head domain (TH2) of talin2 occupies stronger binding to the β-integrin tails than the talin1 head domain (TH1) with a higher affinity which is inevitable to generate traction force and cell invasion. Strong binding of talin2 with β-integrin tails generates traction force which in turn localizes with invadopodia and drives invadopodium-mediated matrix degradation; a principle machinery of cancer cell invasion. Talin2 can aggregate into large assemblies and stabilize invadopodia as it controls larger and more stable focal adhesion formation. (Qi *et al*., 2016). It has been reported that talin2 is essential for cell migration, invasion, tumorigenesis and metastasis, although exogenous expressed levels of talin2 could suppress tumorigenesis. The role for talin in cancer is highly regulated by mechanical cues. Dysregulation of talin activators can lead to aberrant integrin activation and mechanotransduction changes in cell invasion, migration and survival. YAP translocates into nucleus upon force-dependent unfolding of talin for the expression of genes critical in cancer progression. Thus, communication of cells with their microenvironment via integrin-mediated focal adhesion complexes which connect the cytoskeleton to ECM is crucial to control cell progression (Seong, Wang and Wang, 2013; Tadokoro *et al*., 2003, Elosegui-Artola *et al*., 2017).

1.5 Src Activation and the Hippo Signalling Pathway

Conformational changes in talin upon sensing force exertion induces activation of YAP, by encouraging focal adhesion signalling. The regulation of YAP is linked with numerous focal adhesion signalling molecules such as focal adhesion kinase (FAK), the PDZ and LIM domain containing proteins; PDLIM5/PDLIM7 and Src-family tyrosine kinases. Engagement of integrin with an ECM substrate initiates the FAK and Src tyrosine kinase activation (Davis and Tapon, 2019; Dasgupta and McCollum, 2019). Focal adhesion signalling via FAK and Src kinases modulate the Hippo signalling pathway and activity of YAP/TAZ. Both FAK and Src have been exhibited to increase the activation and nuclear localization of YAP. FAK phosphorylates YAP on Tyr357 and MOB1 on Tyr26 directly to activate YAP whereas Src promote YAP activity (Dasgupta and McCollum, 2019). Src can directly phosphorylate YAP at multiple positions; Tyr-341, Tyr-357 and Tyr-394 to promote YAP activation and transcription of anti-apoptotic genes (Cunnigham and Hansen, 2022; Dasgupta and McCollum, 2019). Abnormal activity of Src has been shown to induce tumorigenesis in a YAP-dependent manner and elevated levels of Src in breast cancer tissue correlated with an accumulation of active YAP (Lamar *et al*., 2019; Si *et al*., 2017). FAK and Src signalling are thus seen as negative regulators of the Hippo signalling pathway (Kim and Gumbiner, 2015).

1.6 Cell-Cell Contact

A key critical extracellular stimuli which can regulate the Hippo signalling pathway is contact-dependent signalling. The physical contact of cells triggers cell-cycle arrest by the cytoplasmic retention of YAP/TAZ through the activation of Hippo core kinases. Cell-cell contact, and cell density are determinants of the subcellular YAP localization (Cai, Wang and Meng, 2021). YAP/TAZ is well-known for its function in sensing mechanical stimuli like

matrix stiffness, cell density and stretch (Mohri, Del Rio Hernandez and Krams, 2017). A fundamental characteristic of normal cells is to arrest proliferation upon reaching a confluency which is known as cell contact inhibition. In contrast, cancer cells can escape cell contact inhibition and invade host tissue leading to metastasis.

Cell-cell contact at high cell density, activates the Hippo signalling pathway by perceiving neighbouring cells through junctional structures leading to suppression of YAP activity. This is mediated by an increase in adherent and tight junctions formation and protein localisation contributing to activation of LATS kinases which in turn results in sequestration of YAP/TAZ in the cytoplasm or proliferation arrest (Ko and Guan, 2018; Meng, Moroishi and Guan, 2016; Park and Guan, 2013). Thus, at high cell density when the cells are in confluent condition, YAP is strongly phosphorylated by LATS1/2 and localised in the cytoplasm (Zheng and Pan, 2019; Dobrokhotov *et al*., 2018).

Cell connections are major regions where cell proteins interact therefore, cell junction associated proteins are located on the cellular membrane consisting of tight junctions and adherin junctions (Cai, Wang and Meng, 2021; Wang *et al*., 2021). Angiomotin (AMOT); is a cell-cell junctional related protein found to regulate the signal transduction of the Hippo signalling pathway with its tumor-supressing potential (Zhao *et al*., 2011; Zhao *et al*., 2012; Wang *et al*., 2021; Yang and Wang, 2017). The Angiomotin family proteins (AMOT, AMOTL1 and AMOTL2) have been specified as a negative regulators of YAP as they result in the suppression of its activity (Kim *et al*., 2016; Moleirinho *et al*., 2017). The inactivation of YAP via AMOT is driven by two independent molecular mechanisms. Angiomotin can directly associate with YAP and sequester YAP in the cytoplasm/along cell junctions independently

of phosphorylation (Yang and Wang, 2017; Moleirinho *et al*., 2017; Seo and Kim, 2017). Angiomotin can also suppress the activity of YAP by acting as a scaffold protein and promote its phosphorylation via LATS kinases at the previously mentioned target phosphorylation sites (Seo and Kim, 2017; Moleirinho *et al*., 2017). Angiomotin-family proteins are recently discovered components of the Hippo signalling pathway as shown in Figure 1.7 (Seo and Kim, 2017; Zhao *et al*., 2011).

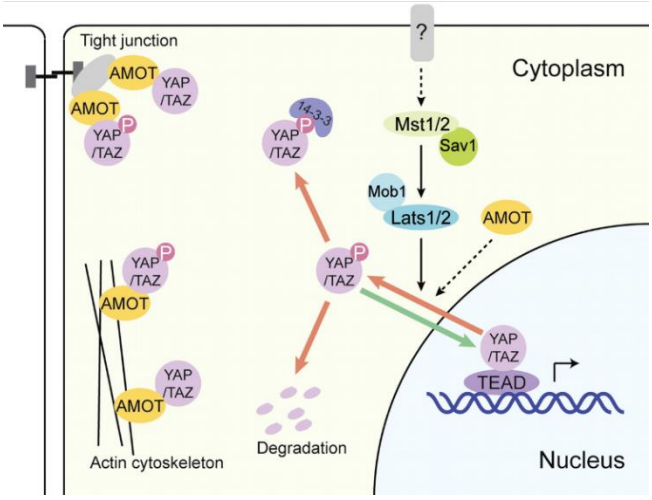

Figure 1.7 Angiomotin (AMOT) in the regulation of YAP/TAZ. AMOT can inhibit and sequester YAP/TAZ in cytoplasm by directly interacting with Yap/TAZ or by phosphorylating YAP/TAZ via LATS1/2 kinases. (From; Zhao *et al*., 2011)

When cell-cell contact is lost with one another, YAP can translocate to the nucleus due to this loss of polarity. Subcellular localization of YAP is determined by the mechanical tension consequently from the spread of cell contact over their basal substrate and substrate stiffness as a reflection of cell density (Elbediwy *et al*., 2018). At low cell density when cells are found in sparse condition, the level of YAP dependent hippo phosphorylation is low and YAP is nuclear localized (Zheng and Pan, 2019; Dobrokhotov *et al*., 2018).

Recent reviews have illustrated how YAP regulation by the Hippo signalling pathway may have a crucial role in mediating cell contact inhibition. LATS tumour suppressors phosphorylate and inhibit YAP resulting in its cytoplasmic localization. Overexpression of YAP antagonizes density-dependent YAP regulation and contact inhibition. In human cancer cells, YAP expression levels and nuclear localization was shown to be strongly elevated. Constitutive YAP activation may lead to escape of contact inhibition thus providing an advantage for YAP-overexpressing cancer cell to grow and invade the surrounding tissues. In Hippo signalling pathway deficient cancer cells, loss of cell contact inhibition can be restored by the blockage of endogenous YAP function. This evidence supports the role of YAP in contact inhibition (Zhao *et al*., 2007). Changes in cytoskeletal integrity and cell shape affect YAP via LATS/Hippo kinases or independently of Hippo signalling pathway. The integrin-focal adhesion complex is the central mechanosensor to detect ECM changes (Chakraborty *et al*., 2017).

1.7 ECM Stiffness

YAP and TAZ have also been found to be regulated directly by the extracellular matrix (ECM) (Moroishi, Hansen and Guan, 2015). The mechanical signals within the ECM are fundamental in cellular input to maintain proliferation and differentiation. Cells sense chemical composition and physical properties of the ECM through integrin adhesions (Zhao, Lykov and Tzeng, 2022). The ECM defines the cell behaviour by controlling the organization of the internal cytoskeleton and cellular trafficking (Chakraborty and Hong, 2018; Cai, Wang and Meng, 2021). Behaviour of the cell is influenced by the mechanical elasticity or stiffness of the ECM. Aberrant cell behaviour can result from the mechanosensitivity driven by the alterations in ECM stiffness. This stiffness gives a

mechanical signal to control the cellular fate and to choose between proliferation and apoptosis (Dupont, 2016). Mechanical forces emerging from the surrounding matrix also regulate YAP/TAZ activity (Ko and Guan, 2018). Extracellular matrix stiffness coordinates the subcellular localization of YAP and TAZ through modifications of cell geometry and cytoskeletal tension (Meng, Moroishi and Guan, 2016). When a cell senses stiffness from the ECM, spreading and migration is changed accordingly with the amount of ECM stiffness resulting in regulation of YAP/TAZ activity. A stiffened ECM and stretched cell shape leads to activation of YAP and TAZ promoting transcription of target genes, whereas their activity is inhibited when cells encounter a soft ECM environment and adapt to a round cell shape (Zanconato *et al*., 2016; Islam *et al*., 2021). Cells on stiff surfaces thus indicate activated YAP/TAZ with a high level of YAP/TAZ localized in the nucleus and subsequent activity of transcription factors, whilst cells on soft surface show YAP/TAZ inhibition through LATS activation and return to cytoplasm thus triggering cellular apoptosis (Yu and Guan, 2013; Koo and Guan, 2018). A stiffer ECM results in higher cell proliferation rate and displays invasive phenotypes by increasing the expression and activity of adhesion receptors. (Dupont, 2016). Solid tumours show high level of ECM stiffness and crosslinking, encouraging an invasive phenotype in cancer cells with a correlation of elevated YAP/TAZ activity and thus their nuclear localization. Increase in ECM stiffness can also disrupt the epithelial polarity resulting in migration and metastasis (Maxwell and Roskelley, 2015; Dobrokhotov *et al*., 2018). In addition, a stiff matrix, and attachment of cells to the ECM induces the β1-integrin-FAK-Src-PI3K-PDK1 pathway to facilitate nuclear translocation of YAP and transcriptional activation by inhibiting LATS1/2 activity. YAP/TAZ accumulation in the nucleus of cancer cells triggers the transcriptional activity of YAP/TAZ target genes for proliferation, invasion and metastasis (Dobrokhotov *et al*., 2018; Meng, Moroisho and Guan, 2016). Talin linking the integrins to F-actin acts as a molecular tension sensor and

detects forces produced over a certain stiffness threshold; above 5 kPa (Davis and Tapon, 2019; Lomakin, Nader and Piel, 2017). This stiffness initiates unfolding of talin by conformational changes, the unfolded talin binds and activates Vinculin which in turn increases focal adhesions and promote YAP/TAZ nuclear translocation (Virdi and Pethe, 2021; Seo and Kim, 2017).

Thus, YAP/TAZ bear a great importance in driving tumorigenesis as its dysregulation and sustained activation drives irrepressible growth (Zhang *et al*., 2019). The rearrangement of the cytoskeleton upon various mechanical cues is highly related with the alterations of YAP/TAZ activity (Yu and Guan, 2013).

1.8 Extracellular Matrix (ECM) Proteins

1.8.1 CD2-Associated Protein (CD2AP)

Mechanical and cytoskeletal checkpoints affect cellular proliferation by regulating YAP and TAZ. Physical and architectural characteristics like cell shape, stretching and stiffness of ECM drive out alterations in cytoskeletal structure and tension leading to mechanical stresses. F-actin capping protein, CapZ was previously identified to restrict activation of YAP/TAZ in cells with low mechanical stress by acting as a gatekeeper at tissue-level checkpoint (Aragona *et al*., 2013). CD2-associated protein (CD2AP) was also found to interact with CapZ in a study conducted by Elbediwy *et al*. (2012).

CD2-associated protein (CD2AP) was first discovered in mouse T cells acting as a CD2 cell adhesion protein-interacting partner (Lehtonen, Zhao and Lehtonen, 2002; Adair *et al*.,

2014). CD2-associated protein (CD2AP) is a cytoplasmic multidomain scaffolding protein and is expressed commonly in epithelial cells, immune cells and neurons (Schiffer *et al*., 2004; Lehtonen, Zhao and Lehtonen, 2002; Zhao *et al*., 2013). The CD2AP protein is comprised of three N-terminus Src homology 3 (SH3) domains, a proline-rich domain and a coiled-coiled domain at the C-terminus (Schiffer *et al*., 2004). Each region of the protein is assigned for different functions. The conserved SH3 domains are essential for interacting with variety of signalling molecules, cytoskeleton regulators and apoptosis modulators containing a target recognition sequences. The binding sites for SH3 domains are provided by the proline-rich region of the CD2AP protein where protein-protein interactions are modulated by the C-terminus coiled-coiled domain. CD2-associated protein is an essential protein for the assembly of the actin cytoskeleton at cell-cell junctions by controlling the adhesion, motility and morphology of the cell (Lehtonen, Zhao and Lehtonen, 2002; Wang and Brieher, 2019). Thus, CD2AP and its role in connecting the actin cytoskeleton to proteins at the plasma membrane functions as a regulator of actin assembly (Lehtonen, Zhao and Lehtonen, 2002).

CD2-associated protein regulates actin dynamics by binding to CapZ. CD2-associated protein brings CapZ to the barbed ends of F-actin resulting in modifications in polymerized actin which in turn leads to membrane deformation and tight junction modifications (Cummins *et al*., 2018; Elbediwy *et al*., 2012). This junction formation and regulation of actin-membrane assembly involves a RhoTPase regulating GAP known as SH3BP1 and its resulting complex proteins. The SH3BP1 complex is comprised of CD2AP, CapZ and JACOP (a key constituent of adherens junctions) (Elbediwy *et al*., 2012).

CapZ was shown to restrict YAP/TAZ activity of cells experiencing low mechanical stress and interaction of CD2AP with CapZ is a requirement for junction formation and actin assembly (Aragona *et al*., 2013; Elbediwy *et al*., 2012). There is no clear evidence of an interaction of CD2AP and YAP, however, they might interact at some point when cells encounter mechanical stress.

1.8.2 Ezrin

Many of the membrane-cytoskeletal interactions are organized by an evolutionary conserved group of proteins called the ERM proteins which is comprised of Ezrin-Radixin-Moesin (Ponuwei, 2016; Marsick *et al*., 2012). The ERM family proteins act as a cross-linker between the actin cytoskeleton and plasma membrane, providing a path for signal transduction in response to extracellular cues (Arpin *et al*., 2011; Song *et al*., 2020). ERM proteins are implicated in cell polarity, adhesion and migration (Song *et al*., 2020). ERM proteins are generally located at cell surface structures like filopodia, microvilli, ruffling membranes and adhesion sites where the plasma membrane integrate with the actin cytoskeleton (Kawaguchi and Asano, 2022; Ponuwei, 2016). ERMs comprise an N-terminal FERM domain, α helices domain and C-terminal domain with an F-actin binding site (Arpin *et al*., 2011; Kawaguchi and Asano, 2022). ERM proteins have fundamental role as scaffolding for adaptor and signalling molecules assisting transduction of signals amongst intracellular and extracellular parts of the cell. They have a pivotal role in the regulation of cellular processes like membrane dynamics, cytoskeletal-membrane interaction and cell signalling (Ponuwei, 2016; Marsick *et al*., 2012). Ezrin, a key member of the ERM family proteins is a cytoskeletal linker due to its capability of interaction with both actin filaments and the plasma membrane (Quan *et al*., 2018; Quan *et al*., 2019; Hugo *et al*., 1998).

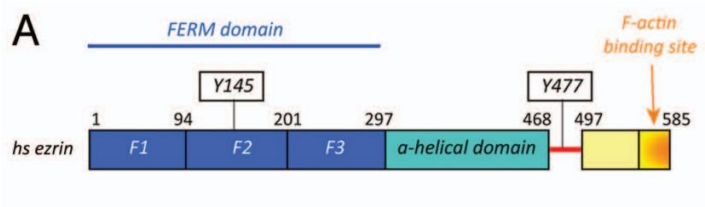

Figure 1.8. Structure of the human ezrin. Ezrin comprising of N-terminal FERM domain and C-terminal domain of F-actin binding site linked with α-helical rich domain (From; Arpin *et al*., 2011).

The N-terminal domain (FERM) of ezrin is densely present at the plasma membrane allowing its interaction with membrane components, while the C-terminal region is associated with the actin cytoskeleton for F-actin binding (Arpin *et al*., 2011; Quan *et al*., 2018). The structure of human ezrin is represented in Figure 1.8. The interaction of membrane and the cytoskeleton is crucial for basic cellular processes, thus ezrin have been assigned to have a role in a diverse range of cellular functions including the morphology and integrity of the cells (Quan *et al*., 2018). Ezrin has been implicated as an important regulator of cancer progression and metastasis as highly expressed ezrin was found in multiple invasive malignancies (Hoskin *et al*., 2015). Conformational changes of the protein leads to its activation. Phosphorylation of ezrin at its Thr657 site at the C-terminal region restricts its interaction with membrane domains and stabilises its interaction with the actin cytoskeleton, thus inhibiting the signalling molecules from implementing diverse downstream effects (Antelmi *et al*., 2013; Xue *et al*., 2020). A clear correlation was found between phosphorylated ezrin and expression of YAP. Ezrin and YAP have a considerable role in the initiation and progression of cancers and are found to be overexpressed in multiple malignancies. In a previous study, depletion of ezrin in skin fibroblast was found to reduce the size of the fibroblast and decrease proliferation by interfering with YAP nuclear translocation and results in inhibition of YAP target gene expression (Quan *et al*.,

2018). Ezrin also promotes proliferation and invasion of cancer cells via activation of epithelial to mesenchymal transition (EMT). Ezrin is normally located at apical structures however, when cells obtain a metastatic phenotype and lose their apical-basal polarity, ezrin translocate to the cytoplasm and plasma membrane leading to an initiation of EMT related proteins and thus cancer cell invasion (Ponuwei, 2016). Conformation changes in ezrin result in activation of ezrin as the N-terminal FERM domain of ezrin binds to the membrane lipid phosphatidylinositol 4,5-biphosphate (PIP2) and this results in T567 phosphorylation at the proteins C-terminus. It has been demonstrated that phospho (T567)-ezrin is overexpressed in more aggressive metastatic cancer types and is enriched in invadopodia resulting in protein-protein signalling complexes with NHE1, β1-integrin and EGFR. Phospho (T567)-ezrin is also associated with lipid rafts in invadopodia as its binding to PIP2 promotes the activation of lipid raft signalsome leading to a regulation of invadopodia proteolytic activity and invasion (Antelmi *et al*., 2013).

1.9 The Hippo Signalling Pathway and Lipids

YAP and TAZ have been implicated in the context of cellular metabolism as their activity can also be regulated by metabolic cues such as lipids, glucose and other metabolic signals (Koo and Guan, 2018). Lipids are the prominent building blocks of cell membranes and bear critical importance in the maintenance of cells by regulating enzymatic functions and supplying energy (Lee, Cho and Jho, 2022). The presence of lipids is a crucial element of cell proliferation as they are used as the precursors of cell membrane fragments. The regulation of lipid metabolism like uptake, synthesis and hydrolysis of lipids is crucial to sustain cellular homeostasis and its dysregulation largely results in progression of cancer due to metabolic alterations promoting the proliferation, migration, invasion and metastasis (Bian et al.,

2020). The major lipids which are essential for the biogenesis of cell membranes and also acting as a signalling molecules are fatty acids, phospholipids and cholesterol. High levels of cell proliferation execute an extreme demand for lipid and cholesterol production which can be accomplished by an increase in cellular lipid and cholesterol regulation levels or *de novo* synthesis (Koo and Guan, 2018). An increased synthesis and uptake of lipids drive progression of cancer and alterations in lipid metabolism promote the activation of oncogenic signalling pathways resulting in cancer cell proliferation (Fu et al., 2020). Thus, lipids play an important role in the maintenance of metastatic cancer phenotype and lipid metabolism can provide metabolic biomarkers for the diagnosis of cancer (Fu et al., 2020), hence a fundamental link between metabolomics and cancer initiation.

1.9.1 Lipid/Cholesterol Regulation

Two lipogenic transcription factors known as sterol regulatory element binding proteins 1c and 2 (SREBP-1c and SREBP-2) control the regulation of lipid and cholesterol levels by modulating the expression of genes required for lipid synthesis, transport and de novo lipogenesis (Lee, Cho and Jho, 2022; Liu, Liu and Song, 2021). SREBP-1c is mainly involved in the regulation of lipogenic processes in fatty acid and triglyceride biosynthesis whereas SREBP2 activates genes for synthesizing cholesterol (Aylon *et al*., 2016; Shu *et al*., 2019). Recent studies have discovered that SREBPs and the Hippo-YAP signalling pathway is closely connected to lipid metabolism through as yet unknown mechanism. SREBPs were found to coordinate the metabolism of both triglyceride and cholesterol by acting as downstream effectors of a Hippo-YAP signalling axis in hepatocytes (Shu *et al.,* 2019). YAP, is a novel co-activator of both SREBP-1 and SREBP-2 which directly interacts with the target gene promoters of SREBPs; FAS (fatty acid synthase) and HMGCR (30-hydroxylmethyl glutaryl

coenzyme A reductase) to induce expression of enzymes involved in lipogenesis and cholesterol synthesis (Kashihara and Sadoshima, 2019; Shu *et al*., 2019; Di Benedetto *et al*., 2021). Inhibition of YAP-SREBPs complexes downregulate cell lipid and cholesterol levels. Thus the 'OFF' state of Hippo signalling results in dephosphorylation and translocation of YAP into the hepatocyte nucleus and function as SREBP-1 and SREBP-2 co-activators leading to lipogenesis and cholesterol synthesis (Shu *et al*., 2019). A study conducted by Aylon *et al.* (2016) stated that upstream regulators of YAP can restrain SREBPs in a Hippo-YAP independent manner. LATS2 was shown to restrict SREBPs activity; a key regulator of lipid and cholesterol metabolism via a non-canonical Hippo signalling manner (Aylon *et al*., 2016; Shu *et al*., 2019). LATS2 incorporates with p53 (a tumour-suppressor transcription factor) weakening by disrupting the endoplasmic reticulum located on SREBPs precursors causing inhibition of both transcriptional activities of SREBPs and expression of lipogenic enzymes (Ardestani, Lupse and Maedler, 2018). The deletion of LATS2 in mice hepatocytes induced elevated levels of cholesterol synthesis and de novo lipogenesis due to increased SREPBs target gene expression and resulted in metabolic disorders (Nguyen-Lefebvre *et al*., 2021). This novel interaction between LATS2 and lipid/cholesterol metabolism is mediated through the inhibitory interaction of a tumour suppressor, LATS2 and SREBPs clarifying LATS2 as a gatekeeper of SREBPs activity whose deregulation disturb lipid/cholesterol homeostasis and leads to excessive cholesterol accumulation (Aylon *et al*., 2016; Shu *et al*., 2019). MST1 is also a negative regulator of SREPBs, as it was found to inhibit SREBPs through activation of LATS or stabilization of SREBPs inhibitor; SIRT1 (Ardestani, Lupse and Maedler, 2018; Nguyen-Lefebvre *et al*., 2021). Thus, like LATS2, MST1 was also found to result in increased lipid accumulation upon deletion. Both Hippo core components (LATS2 and MS1T1) act as a SREBPs activity controllers for lipid and cholesterol homeostasis as illustrated in Figure 1.9. (Ardestani, Lupse and Maedler, 2018).

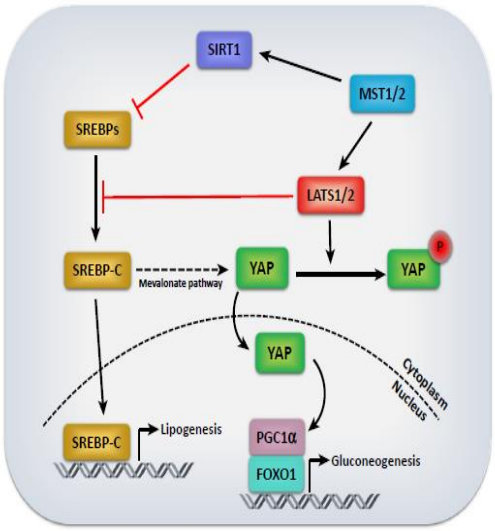

Figure 1.9 Regulation of lipid metabolism by Hippo signalling pathway. The core Hippo kinases MST and LATS suppresses lipogenesis by inhibiting master regulators of lipogenesis; SREBPs. MST1 also inhibits SREBPs through activation of LATS or stabilization of SREBPs inhibitor; SIRT1 (From; Ardestani, Lupse and Maedler, 2018).

1.9.2 De novo Synthesis

Fatty acid de novo synthesis is the major metabolic hallmark for oncogenic transformation in cancer cells in order to maintain membrane synthesis and produce signalling molecules (Yamaguchi and Taouk, 2020). Stearocyl-Coenzyme A-desaturase 1 (SCD1) is an enzyme involved in mono-unsaturated fatty acid synthesis and has been thought to play a crucial role in malignant tumour formation by favouring an accelerated proliferation rate (Koo and Guan, 2018; Zhang *et al*., 2018; Ibar and Irvine, 2020). Recent studies revealed that SCD1 assisted transcriptional activity of YAP/TAZ by translocating YAP/TAZ to the nucleus, and vice a versa when SCD1 is inhibited in lung adenocarcinoma cells. This finding suggests a favourable role for SCD1 and unsaturated fatty acids in the activation of YAP/TAZ. Although the precise mechanism of action is not clear yet, SCD1 may regulate YAP/TAZ activity by depending on the activity of the canonical Wnt/β-catenin pathway but independently of

the Hippo signalling pathway (Figure 1.10). Previously published reports have confirmed that YAP and TAZ are integral components of the β-catenin destruction complex. Upon Wnt activation, YAP/TAZ dissociates from the complex to translocate to the nucleus and function as a regulator of transcriptional activity (Zhang *et al*., 2018; Koo and Guan, 2018). Increase in the synthesis of unsaturated fatty acids induces activation of Wnt ligands which in turn promotes SCD1 to mediate the dissociation of β-catenin and YAP/TAZ from the destruction complex encouraging target gene transcription (Zhang *et al*., 2018). Besides the SCD1 enzyme in fatty acid metabolism, transcriptional activity of YAP/TAZ can also be regulated by free fatty acids themselves (Zhang *et al*., 2018).

A recent study conducted by Yuan *et al.* (2017) proposed the most common saturated fatty acid, palmitic acid (PA) could inhibit endothelial cell proliferation, migration and tube formation through dysregulation of the Hippo-YAP pathway. Palmitic acid induces increased expression of the Hippo signalling pathway kinase MST1 and YAP phosphorylation resulting in subsequent inhibition of nuclear YAP and its function. Palmitic acid induces mitochondrial damage to activate IRF3 through the activation of cytosolic DNA sensors cGAS and STING (Yuan *et al*., 2017). Activated IRF3 binds to the MST1 promotor to induce transcription of MST1 which in turn leads to YAP phosphorylation to mediate inhibition of endothelial cell proliferation and migration (Figure 1.10) (Yuan *et al*., 2017; Koo and Guan, 2018). Observation of palmitic acid's effect on the Hippo-YAP pathway suggest that lipid metabolism might regulate the activity of YAP/TAZ (Yuan *et al*., 2017; Koo and Guan, 2018).

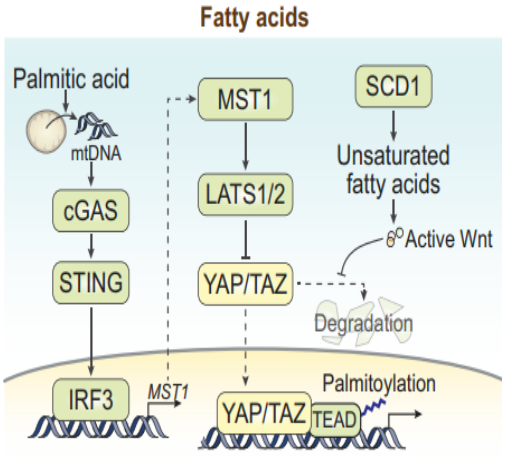

Figure 1.10 Regulation of YAP/TAZ by palmitic acid (PA) and unsaturated fatty acids. Palmitic acid activates cGAS-STING pathway and increases MST1 transcription leading to YAP/TAZ inhibition. Unsaturated fatty acids synthesized by SCD1 stabilize YAP/TAZ through Wnt signalling (From; Koo and Guan, 2018).

Oleic acid (OA) is a commonly occurring, monounsaturated fatty acid found in olive oil and is classified as a non-essential fatty acid which has been defined to regulate immune function and health (Sales-Campos *et al*., 2013; Giulitti *et al*., 2021). Oleic acid was found to induce a protective effect on breast cancer, and an anti-inflammatory effect on auto-immune diseases (Sales-Campos *et al*., 2013). Moreover, hepatocellular carcinoma cells administered with oleic acid show a reduction of cellular migration and invasion considerably (Giulitti *et al*., 2021). However, the mechanism underlying its functionality has not yet been identified.

The most abundant dietary fatty acids; saturated palmitic acid (PA) and monounsaturated oleic acid (OA) are esterified into triglycerides (TG) and afterwards transferred to adipocytes and the liver for their distribution to organs. Against the accumulation of triglycerides upon fatty acid overload, lipid droplets act as a TG deposits to prevent lipotoxicity (Eynaudi *et al*., 2021). Lipid droplets have emerged as highly dynamic organelles consisting of a neutral lipid core of triglycerides and cholesterol esters enclosed by a

monolayer of phospholipids, cholesterol and specific coat proteins (Khaldoun *et al*., 2014; Accioly *et al*., 2008; Lee and Ridgway, 2018). Several proteomics studies have revealed that lipids droplets are embedded with various proteins and presence of specific proteins on the LD surface result in diverse functionality such as membrane trafficking and intracellular signalling (Demignot, Beilstein and Morel, 2014). Proteins on the LD surface facilitate their movement along the cytoskeleton to allow their interaction with alternative cellular organelles and signalling molecules. A proteomics study by Ding *et al*., identified that both Talin1 and Talin2 were associated with lipid droplets isolated from mouse adipocytes (Ding *et al*., 2012).

Even though the role of Hippo signalling pathway in organ growth regulation is well-characterized field, the metabolites and metabolic pathways which regulate the Hippo signalling pathway are relatively unknown. Dysregulation of these pathways may allow translocation YAP to the nucleus, leading to its activation thus transcription of pro proliferative and anti-apoptotic genes which can lead to disruption of metabolic pathways which are fundamental in diseases such as cancer, obesity and diabetes. There is increasing evidence that manipulation of cellular glucose and lipid metabolism could affect YAP/TAZ activation.

1.10 Aims

The aims of my project is to establish an association between the Hippo signalling pathway and lipids. This will be done through a newly characterised extracellular matrix protein complex. The primary aim is to characterize a novel protein complex coupling the Hippo signalling pathway and the ECM and to assess if this complex is regulated by the manipulation of lipids. The secondary aim is to use Planarian as an *in-vivo* model organism

to study the effect of lipid metabolism on the Hippo signalling pathway. And last aim is to use mass spectroscopy (MS) and RNA-Sequencing analysis to determine the novel protein interactions within the complex and expression of specific genes associated with Hippo signalling pathway during lipid metabolism.

1.11 Objectives

- To charecterize a novel extracellular matrix complex.

- To determine the effects of exogenous lipids on protein interactions within the complex and the expression of specific genes associated with the Hippo signalling pathway.

- To determine the role of the novel complex in lipid droplet formation as a way of establishing a relationship between the Hippo signalling pathway and lipids.

- To use Planarians as an *in-vivo* model organism to verify the effects of lipid on the Hippo signalling pathway in a whole organism.

1.12 Hypothesis

Lipid metabolism plays an important role in the functionality of Hippo signalling pathway through the novel extracellular matrix complex. I believe that a novel protein complex couple the Hippo signalling pathway, the ECM and lipids and in the course of my project I aim to identify this. The addition of extracellular lipids (oleic acid and palmitic acid) I hypothesise will attenuate the interaction of any discovered ECM proteins with YAP; the transcriptional co-activator of the Hippo signalling pathway causing dyregulation of cellular function. Finally, I will show that an *in-vivo* model organism; planarian will verify the effects of lipid manipulation on the Hippo signalling pathway physiologically. In addition, the

binding partners of YAP within the complex and speicif genes associated with the Hippo signalling pathway will change by the manipulation of exogenous lipids, strengthening the role of lipid metabolism on the Hippo signalling pathway through the novel ECM proteins within the complex.

CHAPTER 2 – MATERIALS AND METHODS

2.0 MATERIALS AND METHODS

2.1 EXPERIMENTAL PROCEDURES

All cell culture procedures contained within this thesis were implemented under a sterile laminar flow hood and handled with aseptic techniques throughout. Cell culture media was stored at 4^{o}C and warmed prior using at 37^{o}C.

2.1.1 Cell Culture Maintenance of Liver Hepatocellular Carcinoma (Hep-G2) Cells and Colorectal Adenocarcinoma (CaCo-2) Cells

Hep-G2 and CaCo-2 cells were kept in Nunc 6-well plates (Thermoscientific) and maintained with DMEM (Dulbecco's Modified Eagle Medium including D-Glucose, L-Glutamine and Pyruvate) supplemented with 10% Fetal Bovine Serum (FBS) and 1% Penstrep. Cells were grown at 5% Carbon Dioxide (CO_2) at 37^{o}C using a Thermofisher HERACELL 150i CO_2 incubator. When cells reached 70% confluency, cells were passaged briefly, the media aspirated and washed with 1 ml DPBS (without calcium chloride and magnesium chloride). 500 µl of 0.05% Trypsin/EDTA was added upon DPBS removal and the cells were incubated for 5 minutes in 5% CO_2 at 37^{o}C for Hep-G2 or 15 minutes for CaCo-2 to allow detachment of the cells. Cells were seeded in a fresh 6-well plate with fresh DMEM (with antibiotics Penicilin-Streptomycin). Trypsinized cells were gently aspirated with a pipette to ensure all cells were detached and homogenized before seeding. This was performed as a 1:3 split for Hep-G2 cells and 1:6 split for CaCo-2 cells for stock. The seeded cells were returned to the incubator of 5% CO_2 at 37^{o}C. The cells were seeded in 6, 12, 24 or 48 well plates depending on the experiments to be performed.

2.1.2 siRNA Transfection

2.1.2.1 Preparation of Hep-G2 and CaCo-2 Cells for siRNA Transfection

Hep-G2 and CaCo-2 cells were split at 33% confluency and 50% confluency from a confluent well for siRNA transfection respectively (or 150-200k cells per well was seeded). Cells, pre-transfection are required to be seeded in antibiotic free media due to cytotoxicity of the reagent. Pre-prepared 6-well plates, were trypsinized as previously stated. Two 10 ml falcon tubes with 5 ml of DMEM media were prepared for two different cell lines. After the incubation period, trypsinised Hep-G2 and CaCo-2 cells in each well (total 3 wells for CaCo-2 and 2 wells for Hep-G2) were added into the falcon tube containing the 5 DMEM. Both falcon tubes containing the Hep-G2 and CaCo-2 cells were centrifuged for 3 minutes at 1000 rpm and 20 ^{o}C to obtain a cell pellet using the Thermo-Scientific Sorvall Legend RT+ Centrifuge. Supernatants were discarded and pellet at the bottom of the tube for each cell line was re-suspended in 6 ml of DMEM without antibiotics. Cells then seeded to a 6-well plate with each well containing a 1 ml of cells with antibiotic free DMEM (around 150-200k cells). Two 6-well plates (one plate for Hep-G2 cells and other plate for CaCo-2 cells) were incubated for 2 hours before cells are ready for transfection with designated siRNA. Depending on the designed experiment, the cells were seeded in 12, 24 or 48 well plates for siRNA transfection.

2.1.2.2 siRNA Transfection

After 2 hours of incubation, each well of the 6-well plate of Hep-G2 and CaCo-2 cells prepared before (in 2.1.2.1) was labelled as control and rest of the wells for the proteins of interest. 12 eppendorf tubes were prepared, 2 for control and 10 for the proteins of interest (these are designated as tube A) and 12 for Lipofectamine mix (these are

designated tube B). 125 µl of OPTI-MEM media was added into each tube. For the tubes labelled as control and the protein of interest siRNA (tube A); 5 µl of siRNA was added accordingly. For tube B centrifuge tubes, 5 µl of the transfection reagent RNAimax lipofectamine was added. Each tube was vortexed and incubated for 5 minutes at room temperature. After incubation, the tubes containing the transfection reagent were transferred to the corresponding tubes containing the siRNA. Tubes were vortexed after the transfer and incubated for 10 minutes at room temperature. According to the labels on wells, cells were transfected directly with 250 µl of Lipofectamine/siRNA complexes and incubated for 72 hours in an incubator of 5% CO_2 at 37^oC. After 24 hours of transfection the DMEM without antibiotics was replaced with antibiotic containing DMEM to prevent contamination. The volume of each reagent used for the siRNA transfection was adjusted for the experiments designed in 12, 24 or 48 well plates accordingly, and the cells were prepared for either immunoblotting or immunofluorescence respectively.

2.1.3 Oleic and Palmitic Acid Treatments

CaCo-2 and Hep-G2 cells were split into a 12-well plate for the oleic acid and palmitic acid treatments. While cells were trypsinizing a 12-well plate was prepared by the addition of 500 µl of complete DMEM media into each well. After trypsinisation, trypsinised cells were added into a 12 well plates and left in an incubator at 5% CO_2 at 37^oC for 24 hours. 1 well was used as a control and 3 wells were used to treat cells with oleic acid in various concentrations. The final volume in each well was required to be 500 µl. After the centrifuge tubes were prepared accordingly with the designated oleic acid concentrations; the old media was aspirated out of the 12 well plate and components in the tubes were added into the wells according to labels whereas for control labelled well only 500 µl of

DMEM (+) media was added with BSA. After 4 hours of treatment, cells were lysed and stored in -20 ^{o}C ready for immunoblotting. The same procedure was repeated for palmitic acid treatments in concentrations of 0.5 mM, 1 mM and 2 mM. Finally, in order to perform dual treatments, CaCo-2 cells were treated with combination of both oleic and palmitic acid as stated concentrations of 2 mM and 0.5 mM respectively. Each experiment was repeated 3 times, N=3.

2.1.4 Lipid Staining in CaCo-2 and Hep-G2 Cells

CaCo-2 and Hep-G2 cells were seeded into 10 wells of 24-well plate using 25k and 50k split respectively with 250 µl of DMEM media (no antibiotics) and transfected with control, YAP, CD2AP, Talin and Ezrin siRNAs according to the siRNA transfection protocol in 2.1.2. After 72 hours of transfection, the 5 wells of the 10 wells were treated with 1 mM oleic acid for both cell lines and incubated for 24 hours in 5% CO_2 at 37^{o}C. After 24 hours of incubation with oleic acid, 1 µl of LipidSpot^{TM} 488 Lipid Droplet Stain (Biotium, Cat:70065-T) and 0.25 µl of DAPI were added into all 10 wells for both cell lines and incubated for 30 minutes then pictures were taken by using the Floid microscope. The cells were then lysed and stored in -20^{o}C for SDS-Page analysis. Each experiment was repeated 3 times, N=3.

2.1.5 Scratch Assay

CaCo-2 cells were split into 6 well and 12 well plates at high confluence for scratch assay analysis (1 and 0.5x10^{6} respectively). Cells in 6 well plates were scratched using the edge of a p200 pipette tip and treated with 2 mM oleic and 0.5 mM palmitic acid. Pictures were taken at time 0 and after 24h using a microscope connected specialist imaging tablet to observe the rate of cellular migration. CaCo-2 cells split into 12-well plates were transfected

with designated siRNAs using Lipofectamine RNAimax as described in 2.1.2.2 and after 48 hours cells were scratched and time 0 pictures were taken. After 24 hours, again pictures were taken to observe the effect of knockdown of specific proteins on cellular migration. Cells were then lysed using a lysis buffer and stored in -20^{o}C for SDS-Page analysis. Each experiment was repeated 3 times, N=3.

2.1.6 Cell Lysis

Lysis buffer was prepared by addition of NuPage 2X sample buffer and 10X sample reducing agent. To lyse cells, media in each well of the plates was aspirated out and washed 3 times with PBS carefully. The amount of the lysis buffer to be added for cell lysis procedure was pre-determined by assigning the confluency of cells in each well. After the addition of lysis buffer cells were homogenized with 25 gauge needle and cell extracts were scraped using cell scraper and collected into a 1.5 ml centrifuge tubes. Samples were denatured by heating at 95 ^{o}C for 10 minutes on a heating block. The samples were then placed into a freezer at -20 ^{o}C and stored until the SDS-PAGE process.

2.1.7 SDS-PAGE

To conduct SDS-PAGE; primarily, preparation of separating and stacking gels were done according to the instructions given in the materials section. 10% polyacrylamide gel was prepared using Bio-Rad gel cassettes between the 1.5 mm thick glasses by consecutive addition of the separating and stacking gels. Afterwards, gel cassettes were placed inside the electrophoresis tank and loaded with 1X running buffer. 10 µl of MW marker (Thermoscientific) and 20 µl of previously prepared samples were uploaded onto the gel. Electrophoresis tank was attached to the power pack and run for 1 hour at 180V.

2.1.8 Western Blot

The Bio-Rad Trans-blot system was used to transfer gels onto a 0.45 um nitrocellulose membrane (Sigma Aldrich). Transfer of proteins onto the membrane requires the sandwich of sponge-filter paper-membrane-gel-filter paper-sponge (starting from the red side) in 1X transfer buffer. The Biorad transfer tank was then attached to power unit and run for 90 minutes at 100V in 1X transfer buffer. After completion, the membranes were gathered, rinsed with water, and then treated with amido black for 20 seconds and again rinsed with water to observe protein levels. Destain solution was added and placed on a shaker for 10 minutes. This step was repeated 1 more time. The membranes were then washed with PBS for 5 minutes to remove the destain solution and allow the membrane to be neutralized. Membranes were then incubated in 5% milk / PBS-T for 15 minutes on a shaker to minimalize the non-specific binding of the primary antibody. Afterwards, the membranes were then incubated in primary antibody solution overnight at 4 ^{o}C on a Stuart Seea-saw rocker. The membranes were washed 3 times with PBS-T for 10 minutes before incubating with the secondary antibody (LI-COR infrared antibodies). The correspondent secondary antibody was applied in 10 ml of PBS-T and incubated for 90 minutes at room temperature on Stuart Seea-saw rocker without light (black box or foil wrapped). After incubation, the membranes were washed 3 times with PBS-T and 2 times with PBS for 10 minutes to remove the tween and then imaged by using LI-COR Biosciences Western Blot Scanner. Total protein levels were quantified using the LI-COR Biosciences Western Blot Scanner to obtain normalization graphs.

2.1.9 Immunoprecipitation with Antibody-Magnetic Bead Conjugate

Thirty µl of protein A/G mix magnetic beads (MCE®) were washed 3 times with 500 µl of wash buffer. Beads were incubated with selected antibodies (at designated concentrations) for 2 hours at room temperature by gently mixing the mixture on a rotator. After incubation, antibody-magnetic bead complex was captured with a magnetic bead separator (MagRack6) and unbound antibody was discarded. Antibody-bead mixture was washed twice with 500 µl of wash buffer. After CaCo-2 cells seeded in 15 cm plates reached the desired confluency of 90%, cells were placed on ice and washed twice with ice-cold PBS. Cells were lysed by the addition of 1200 µl of lysis buffer (0.5% Triton X-100 in PBS) containing 100 µl of phosphatase and 100 µl of protease inhibitors. Cells were scraped and then lysed using a syringe and needle by homogenizing 6 times into a 1.5 ml of centrifuge tube. Cell lysates tubes were then incubated on ice with the addition of 30 µl of beads for 30 minutes to inhibit unspecific binding and tubes were occasionally inverted every 5 minutes. After incubation of cell lysates with magnetic beads, the beads were removed. 1000 µl of cell lysate were added into the antibody-bead mixture and the lysate-bead/antibody conjugate mixture was gently re-suspended. 20 µl of cell lysate was added into tube labelled as input without any magnetic beads. The lysate-bead/antibody complex was incubated for 90 minutes at 4°C with mixing on Stuart Seea-saw rocker. Beads were collected with a magnetic separator and the unbound sample was removed. Beads were washed 3 times with 500 µl of lysis buffer and then 3 times with 500 µl of wash buffer. 80 µl of sample buffer was added to the tube containing the beads and 100 µl of sample buffer was added to the input tubes containing only the cell lysate and samples were heated at 96-100°C for 10 minutes on a heat-block. The samples were then stored at -20^{o}C until the down-stream process for SDS-PAGE analysis. Each experiment was repeated 4 times, N=4.

2.1.10 Mass Spectroscopy

The samples for the mass spectroscopy analysis were prepared by co-immunoprecipiation as stated in 2.1.9. CaCo-2 cells were seeded in two 15 cm plates and when cells reached the desired confluency of 90%, one of the plate was treated with 2 mM oleic acid and lysed after 4 hours of incubation. Cell samples of 3 independent experiments were pooled together. Two tubes of YAP Ab-bead-lysate complexes were prepared for MS analysis as one tube was treated with oleic acid and the other tube was untreated. For mass spectroscopy, the samples were subjected to SDS-Page analysis. Samples were loaded and first run at 100V for 2-5 minutes, stopped and more sample was loaded into the gel until the whole sample was loaded. The gel was run at 180V for 1h. After completion, the gel was gathered, rinsed with dH_2O, and then treated with Commasie blue stain (0.75g Comassie brilliant blue R-250(VWR) + 60 ml methanol + 20 ml glacial acetic acid filled upto 200 ml with dH_2O) on a shaker for 30 minutes. After 30 minutes, the stain was removed and the gel was rinsed with dH_2O two times for 5 minutes on a shaker. Destain solution was added and the gel was placed on a shaker for 30 minutes. After 30 minutes, destain was removed and fresh destain was added and the gel was left on a shaker overnight. The protein of interests on the gel were cut and the samples were sent off for mass spectroscopy analysis.

2.1.11 RNA Sequencing

CaCo-2 cells were split into 6-well plate. After reaching a desired confluency of 70%, 3-wells of the 6-well plate were treated with 2 mM of oleic acid and incubated for 4 hours at 37^{o}C. After incubation, cells were centrifuged down using the Thermoscientific Sorvall Legend

RT+ Centrifuge and cell samples of 3 independent experiments were pooled together and sent to GENEWIZ for RNA sequencing analysis on dry ice.

2.1.12 Immunofluorescence Microscopy

Coverslips (Thermoscientific) were double sterilized by ethanol sterilizing and autoclaving. Primarily, the coverslips were added into 100% ethanol and incubated for 30 minutes. After incubation, 10 circular filter papers were added into a glass petri dish then coverslips removed with tweezers from ethanol were added onto the filter paper and a new layer started until all the coverslips were added into the glass petri dish. The top was finished with 10 circular filter papers and the lid was taped with autoclave tape and the coverslips were autoclaved. Sterile coverslips were placed into each well of 48-well plate using a curved, high precision tweezers. CaCo-2 and Hep-G2 cells were seeded onto the coverslips in 1:10, 1:15, 1:30 or 1:60 depending on the experiment and incubated in 5% Carbon Dioxide (CO_2) at 37^{o}C until the desired confluency is reached. Once the cells are in desired confluency, the cells were fixed using a 4% Paraformaldehyde solution (Thermoscientific) in a fume cupboard for 20 minutes. After fixation, cells were blocked with a blocking buffer comprising of Glycine+BSA+PBS for 30 minutes if proceeding to primary antibody incubation or stored in blocking buffer at 4^{o}C. The chosen primary antibodies were diluted in Ab dilution buffer comprising of blocking buffer and 0.2 % Triton. Primary antibodies (1/200) were added 100 µl per well onto fixed cells and incubated overnight at 4^{o}C. The cells were washed 3 times with PBS and the 100 µl of complementary fluorescent secondary antibodies (1/300) and DAPI (1/2000) diluted in Ab dilution buffer were added and cell plate was incubated for 2 hours in dark conditions at room temperature. The cells were then washed 3 times with PBS and each well was filled up to top with PBS for allowing

the removal of coverslips for the mounting process. The coverslips were mounted using a Prolong gold antifade mountant (Invitrogen). A drop of mounting medium was placed on a microscope slide (Fisher), the coverslip was removed carefully from 48-well plate using a tweezers, dabbed on a tissue for residual water and then the coverslip was placed onto the drop of Prolong gold antifade mountant with the cells upside down. The coverslip was pressed slightly with a tweezers for ensuring the well distribution of the mounting medium. The slides were then placed in a slide folder and incubated at 4^{o}C for 2 hours before use or for long term storage. The IF slides were prepared at different conditions according to protocols like oleic acid treatments, siRNA knockdowns, etc. The IF images were taken using the Evos fl Fluorescence Miscroscope at 20X magnification. Each experiment was repeated 4 times, N=4.

2.1.13 Planarian Experiments

2.1.13.1 *Dugesia Lugubris* and *Schmidtea Mediterranea* Microinjection

The petri dish containing ice was covered with a layer of blue roll to slow down the movement of worms for easier injection. A worm was placed onto the paper using a plastic pipette and placed under a motic AE31 dissecting microscope. The worm was screened for any abnormalities such as extra eyes before the injection and picture taken. The experimental fatty acids were administered with a micro-syringe with 1 ml needle and 1 µl of oleic acid or palmitic acid was injected into the tail region of the worm. After injection, a picture was taken and the worm was gently taken using forceps and placed into a tank with Planarian water containing ocean salts (1g/L) and bioactive tapsafe. Physical changes were observed over time after 1 and 2 weeks and pictures taken. The same steps were repeated for each treatment (sham, oleic acid and palmitic acid). Two species of Planarian;

Dugesia Lugubris and *Schmidtea Mediterranea* were used for the treatments. The *Schmidtea Mediterranea* worms injected with oleic and palmitic acid were compared to controls to analyse the expression of *Hippo* and *Yorkie* genes by qPCR reaction. Oleic acid treated *S.Mediterranea* worms were used to evaluate wound resolution comparative to sham worms. The *Dugesia Lugubris* worms were used to compare whole worms against regenerating trunk fragments and oleic acid treatment with analysis of the expression of *Hippo* and *Yorkie* genes by qPCR reaction. *Dugesia Lugubris* was cut into 3 pieces of head, trunk and tail using a sterile disposable scalpel. A cut was made at the base of the head and at the top of the tail of the worm and head and tail regions of the worm were placed into a tank to recover. A trunk region of the worm was injected with the oleic acid as indicated and physical changes were observed over time. Figure 2.0 indicates a schematic diagram for the microinjection of the whole (B) worms and trunk section (C) of the worms.

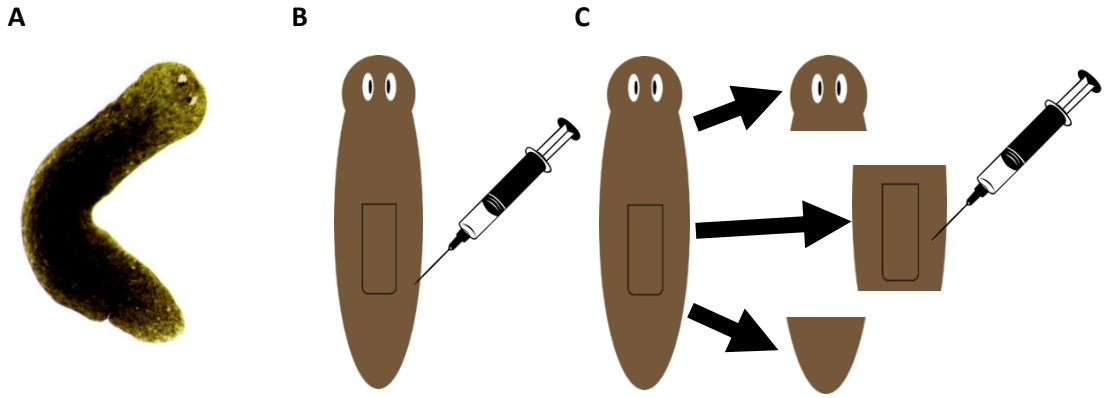

Figure 2.0 A schematic diagram illustrates the microinjection of whole Planaria and trunk part of the Planaria.

(A)An image showing the actual Planaria species; Dugesia Lugubris. (B) Schematic diagram illustrating the microinjection into the tail region of the whole Planaria. (C) Schematic diagram illustrating the microinjection of the trunk section of a Planaria.

2.1.13.2 RNA Extraction

The homogenizer was cleaned using 70% ethanol (IMS). The worm was added into a homogenizer containing 500 µl of RNAzol. The homogenised worm was transferred into an Eppendorf tube and 500 µl of 100% isopropanol was added into the tube containing the RNAzol and worm. The tube was allowed to stand for 10 minutes at room temperature then centrifuged at 12,000 x g for 10 minutes. The supernatant was discarded and the white RNA pellet was collected at the bottom of the tube. The white RNA pellet was washed with 400 µl of 75% ethanol and centrifuged at 8,000 x g for 2 minutes at room temperature. The wash step was repeated 1 more time. The supernatant was discarded and pellet was dissolved in 200 µl of RNAse free H_2O by vortexing at room temperature for 2-5 minutes. The concentration of extracted RNA was measured using NanoVue Plus™. This process was repeated for each worm injected with different treatments. The samples were then stored at -20°C for the next process of cDNA synthesis.

2.1.13.3 cDNA Synthesis

The reaction was prepared on ice into a 20 µl sterile PCR tube. In a tube 4 µl of iScript RT supermix, 1 µl of RNA sample and 15 µl of nuclease-free water were added. The complete reaction mix was incubated in a thermal cycler (ProFlex PCR System) according to the protocol; 5 minutes at 25°C for priming, 20 minutes at 46°C for reverse transcription and 1 minute at 95°C for RT inactivation. Once the cycle completed, the the DNA concentration was measured using NanoVue Plus™. This process was repeated for each RNA sample. The samples were then stored in -20°C for the qPCR reaction.

2.1.13.4 Quantitative-PCR Reaction

The cDNA samples were diluted according to their concentrations to obtain 10 ng for each cDNA sample. 5 µl of sybr green readymix, 0.25 µl of FW primer, 0.25 µl of RV primer, 1 µl of cDNA and 3.5 µl of nuclease-free H_2O were added into tubes for each Hippo, Yorkie and housekeeper gene beta actin (ACBT). Primers are as follows;

Hippo; FW: CGAGCACTGTTTATGATTCCTTC and RV: CTCGGCTTGCAAGTCTGAGTC

Yorkie; FW: GTTTGGATGAATTATTCGAAGTGG and RV: CACAATACAAAAGAAACCACATGG

ACBT; FW: ACACCGTACCAATCTATG and RV: GTGAAACTGTAACCTCGT

Once the wells of PCR plate are made up with the primers, cDNA and readymix, the plate was sealed with a clear tape and centrifuged down for few seconds to ensure all the components are inside the wells and then the plate was placed into the Eco PCRmax machine and run for 1 hour until all the cycles (40 cycles) are completed. The cycle protocol is as follows;

The cycle protocol; UDG Incubation; 2 minutes at $50^{O}C$

Polymerase Activation; 5 minutes at $95^{O}C$

PCR Cycling; 15 seconds at $94^{O}C$

1 minute at $60^{O}C$

Melt Curve; 15 seconds at $95^{O}C$

15 seconds at $55^{O}C$

15 seconds at $95^{O}C$

2.1.13.5. Statistical Analysis

The statistical data obtained was generated using a Graphpad Prism 8. The significance of the data collected from the qPCR reactions was determined using two-way ANOVA test. A BONFERRONI's post hoc multiple comparisons test was conducted to examine the significance between treatments and controls and $p<0.05$ was considered significant for comparisons of oleic/palmitic acid treated Planarian versus control. The significance for wound resolution of oleic acid treated *Schmidtea Mediterranea* was calculated by Mann Whitney U test, significant at $**p<0.05$.

2.1.14 Statistical Analysis

The data was demonstrated as mean ± standard deviation (SD). Statistical importance was defined by T-Test (n.s = not significant ($p>0.05$), * $p\leq 0.05$, ** $p\leq 0.01$, and *** $p\leq 0.001$). Samples were normalized relative to control samples. The representative N-values were indicated in figure legends.

CHAPTER 3. CHARACTERISATION OF A NOVEL PROTEIN COMPLEX LINKING THE EXTRACELLULAR MATRIX/HIPPO PATHWAY

CHAPTER 3. CHARACTERISATION OF A NOVEL PROTEIN COMPLEX LINKING THE EXTRACELLULAR MATRIX/HIPPO PATHWAY

The extracellular matrix plays an important role in the regulation of the Hippo signalling pathway (Moroishi, Hansen and Guan, 2015), however the link between the ECM, Hippo signalling pathway and lipid metabolism is not well characterised.

This chapter, therefore focuses on the characterisation of a novel protein complex which couples the Hippo signalling pathway, the ECM and is influenced by lipids (Chapter 4). Hep-G2 and CaCo-2 cells were used in this research because of their physiological suitability and importance to lipid metabolism, the extracellular matrix and Hippo signalling pathway. Primarily, the interaction between the Hippo signalling pathway effector YAP and the ECM protein Talin2 was validated using a Co-immunoprecipitation assay to confirm previous research by mass spectroscopy showing this potential interaction (Elbediwy *et al*., 2018). A candidate approach was used in the identification of components which may bind to this YAP/Talin2 complex, with three other components of the complex, the ECM/actin linked proteins CD2AP and PDLIM7 and finally the polarity protein Ezrin identified. These proteins were chosen due to their link to key signalling pathways which intersect the Hippo signalling pathway indirectly as well as looking at evidence from previous assays and publications (Zhao *et al*., 2013; Xue *et al*., 2020). We wanted to determine if siRNA mediated knockdowns of any of these specific proteins of the complex would influence other key members of complex and stabilisation of YAP. Transfection efficiency of cells via siRNA-mediated knockdowns was evaluated by immunoblot analysis.

The cellular morphology and the rate of proliferation/migration upon knockdown of specific ECM proteins in CaCo-2 cells was also performed using scratch assays. Finally, immunofluorescence imaging was used to decipher the effect of complex members on

stabilisation on YAP. The translocation of YAP between nucleus and cytoplasm in the context of siRNA of CD2AP/Talin/Ezrin was assessed by using immunofluorescence stains.

3.1 Analysis of protein-protein interactions by Co-immunoprecipitation

Firstly an experiment was undertaken to validate protein-protein interactions using co-immunoprecipitation (Co-IP). CaCo-2 cells were incubated with selected antibodies against proteins of interest conjugated to beads. The inputs and Co-IP fractions were subjected to immunoprecipitation and interacting proteins were analysed by immunoblotting. Each experiment was repeated 3 times, N=3. The interaction between the Talin and YAP was validated in Figure 3.0 as YAP immunoprecipitates were found to contain talin, thus showing a clear protein-protein interaction. In mass spectroscopy data (see chapter 6), ezrin was found to be one of the binding partners of YAP which was also confirmed by co-immunoprecipiation assay in Figure 3.0 as a binding partner of YAP. Talin was not only found to interact with YAP but, was also found to interact with the extracellular matrix proteins, PDLIM7 and CD2AP as shown in Figure 3.1 and 3.2 respectively. Further co-immunoprecipiation assays were performed and the CD2AP protein was co-immunoprecipitated with both PDLIM7 and YAP (Figure 3.1 and 3.2). This confirms that all the proteins interacted with one other leading to the characterisation of a novel complex linking the Hippo signalling pathway and the extracellular matrix (ECM).

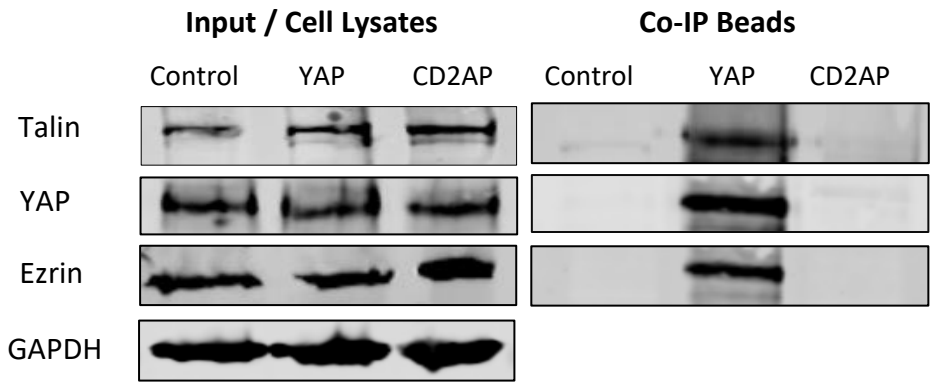

Figure 3.0. Co-Immunoprecipitation showing the interaction of Talin and Ezrin with YAP. CaCo-2 cells were incubated with antibodies against proteins of interest conjugated to beads. Both inputs and Co-IP fractions were subjected to immunoprecipitation and proteins present were analysed by immunoblotting. Talin and Ezrin immunoprecipitates were found to contain YAP showing protein-protein interactions. Representative blots from one experiment are displayed amongst 4 independent repeats.

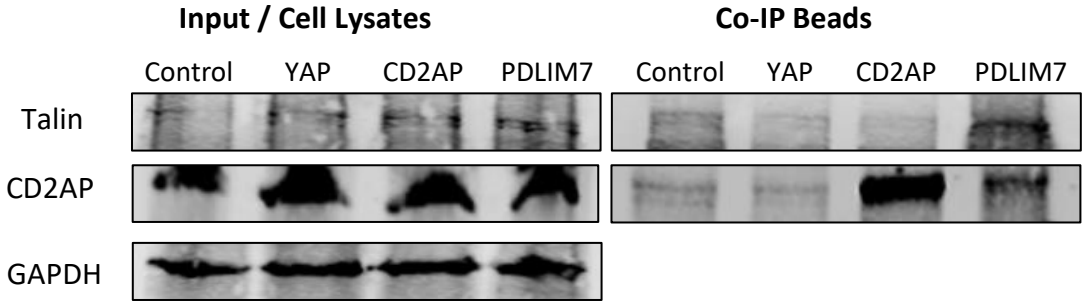

Figure 3.1. Co-Immunoprecipitation showing the interaction of Talin and CD2AP with PDLIM7. CaCo-2 cells were incubated with antibodies against proteins of interest conjugated to beads. Both inputs and Co-IP fractions were subjected to immunoprecipitation and proteins present were analysed by immunoblotting. Talin and CD2AP immunoprecipitates were found to contain PDLIM7 showing co-immunoprecipitations. Representative blots from one experiment are displayed amongst 4 independent repeats.

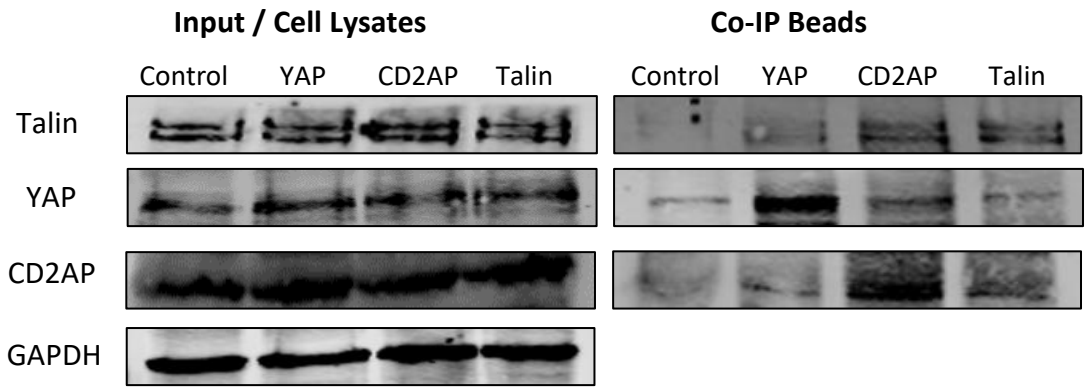

Figure 3.2. Co-Immunoprecipitation showing the interactions of Talin, YAP and CD2AP. CaCo-2 cells were incubated with antibodies against the proteins of interest pre-conjugated to beads. Both inputs and Co-IP fractions were subjected to immunoprecipitation and proteins present were analysed by immunoblotting. Talin and YAP immunoprecipitates were found to contain CD2AP, and CD2AP immunoprecipitates were found to contain both YAP and Talin showing the co-immunoprecipitations. Representative blots from one experiment are displayed amongst 4 independent repeats.

3.2 Transfection efficiency of Hep-G2 cells via YAP siRNA

Hep-G2 cells were transfected with YAP specific siRNA to knockdown the Hippo signalling pathway effector, YAP. A quantification graph in Figure 3.3(B) was generated from immunoblot analysis upon siRNA transfection. The experimental data exhibited that transfection of Hep-G2 cells with YAP siRNA was effective in the downregulation of YAP as YAP level was dramatically reduced in siRNA transfected cells. This also allowed us to assess the specificity of the YAP antibody for further studies. Decreased expression of total YAP was also observable in the comparison of control siRNA versus YAP siRNA with a reduced signal in the western-blot image as shown in Figure 3.3(A).

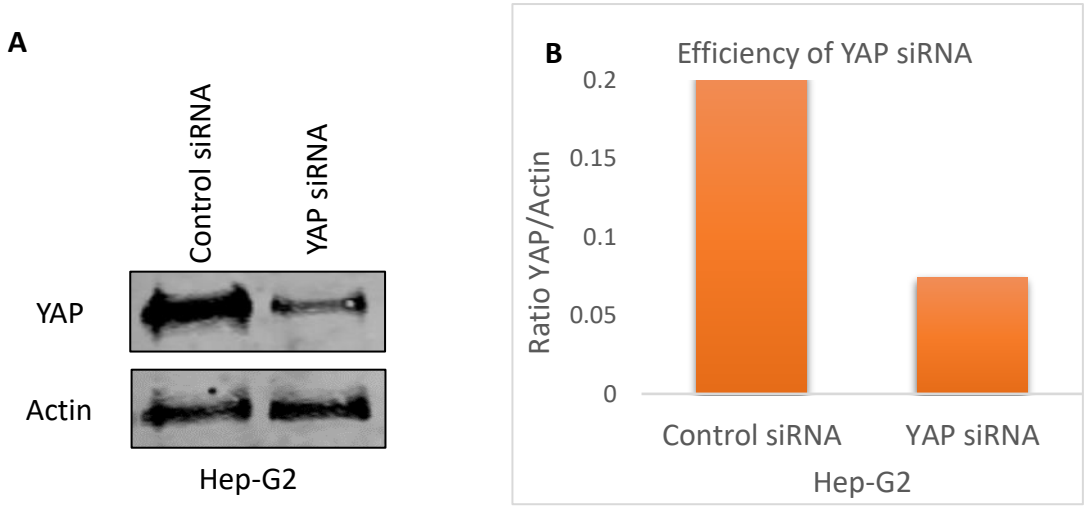

Figure 3.3. Optimization of siRNA YAP knockdown in Hep-G2 cell line. (A) Western blot image of YAP in control siRNA and YAP siRNA treated cells. (B) Quantification graph YAP levels in control and YAP siRNA treated cells.

3.3 Transfection efficiency of CaCo-2 cells via siRNA-mediated knockdown of YAP, CD2AP, Talin and Ezrin

CaCo-2 cells were transfected with siRNAs for specific proteins of interest and the efficiency of knockdowns was assessed by immunoblotting. The expression of YAP, Ezrin, Talin and CD2AP was silenced and the efficiency of their depletion represented in Figures 3.4, 3.5, 3.6 and 3.7 respectively. A quantification graph for siRNA-mediated knockdown of YAP, Ezrin, Talin and CD2AP was generated from immunoblot analysis upon siRNA transfection. The experimental data obtained suggest that transfection of CaCo-2 cells with siRNAs for the corresponding proteins was effective in the downregulation of each proteins expression levels thus giving us confidence that when we use the corresponding siRNA that the effects we see will be due to the depletion of the protein/s in question rather than off target effects. This was also seen quite clearly in immunoblot images in 3.4-3.7 (A).

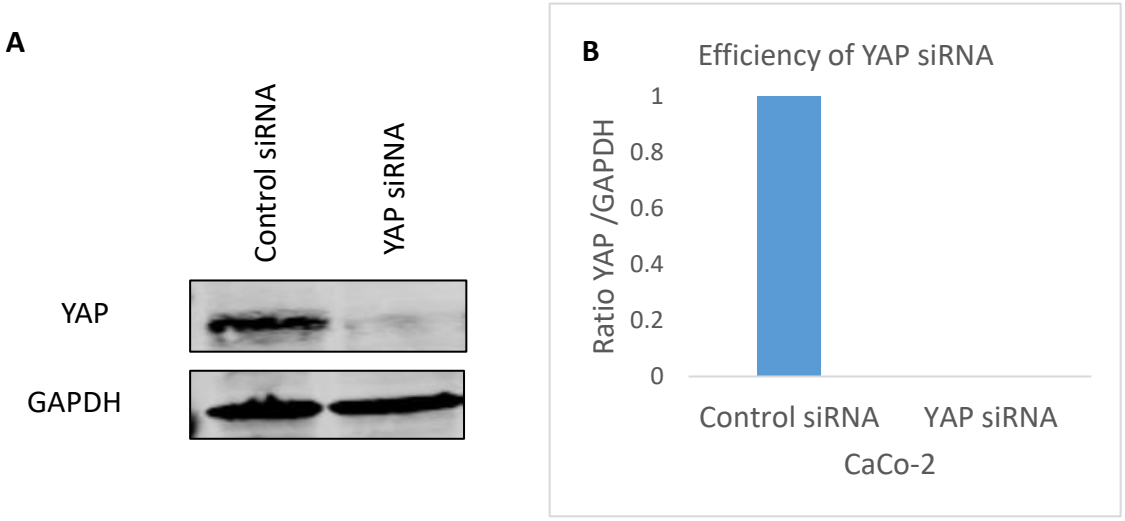

Figure 3.4. Expression level of YAP depletion in CaCo-2 cells was assessed by blotting for YAP. (A)Western blot image of YAP siRNA and control siRNA. Optimization of YAP knockdown assessed by immunoblotting. GAPDH was used as a loading control. (B) Quantification graph of YAP levels in control and YAP siRNA treated cells.

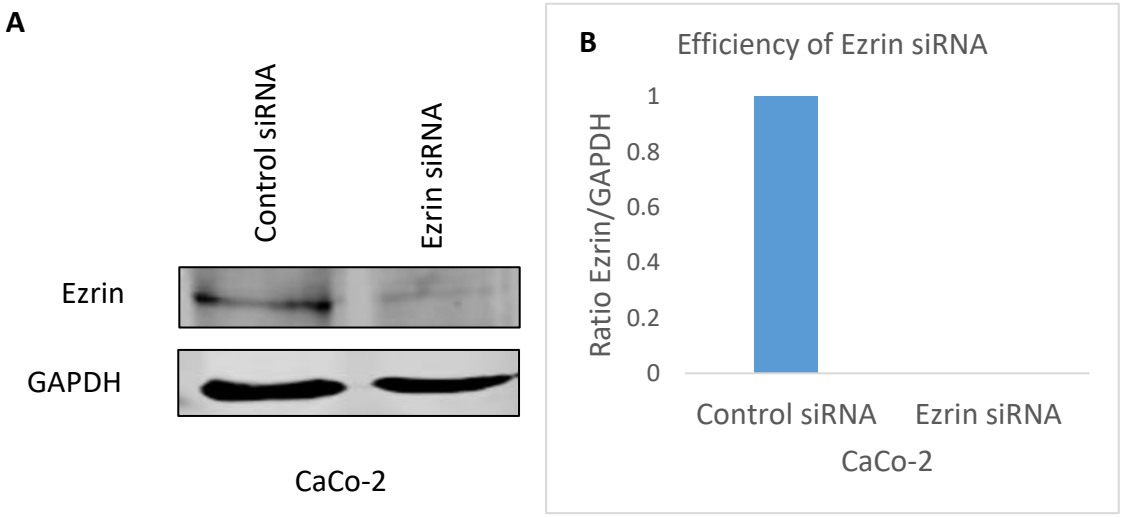

Figure 3.5. Expression level of Ezrin depletion in CaCo-2 cells was assessed by blotting for Ezrin.

(A)Western blot image of Ezrin siRNA and control siRNA. Optimization of Ezrin knockdown assessed by immunoblotting. GAPDH was used as a loading control. (B) Quantification graph of Ezrin levels in control and Ezrin siRNA treated cells.

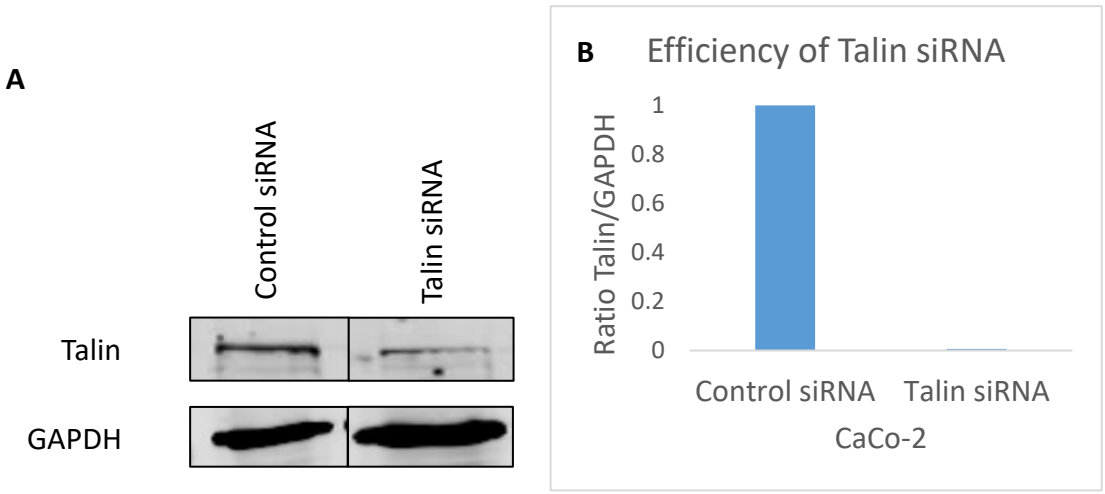

Figure 3.6. Expression level of Talin depletion in CaCo-2 cells was assessed by blotting for Talin. (A)Western blot image of Talin siRNA and control siRNA. Optimization of Talin knockdown assessed by immunoblotting. GAPDH was used as a loading control. (B) Quantification graph of Talin levels in control and Talin siRNA treated cells.

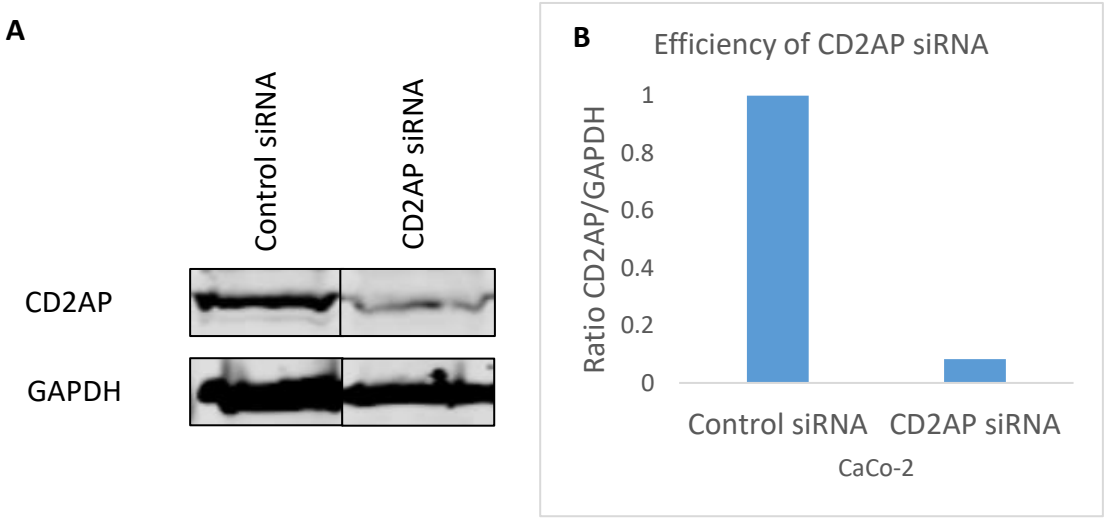

Figure 3.7. Expression level of CD2AP depletion in CaCo-2 cells was assessed by blotting for CD2AP. (A)Western blot image of CD2AP siRNA and control siRNA. Optimization of CD2AP knockdown assessed by immunoblotting. GAPDH was used as a loading control. (B) Quantification graph of CD2AP levels in control and CD2AP siRNA treated cells.

3.4 Rate of cellular migration upon siRNA knockdown of specific proteins

The expression of specific proteins was diminished by siRNA-mediated knockdown (Figures 3.4-3.7) and scratch assays were subsequently used to observe the effect on the rate of cellular migration and if it had a significant effect. The CaCo-2 cells were cultured and transfected with either control, YAP, Talin, CD2AP or Ezrin siRNAs. After transfection, cells were left for 48 hours before being subjected to a scratch with time 0 images being taken. The rate of cellular migration was analysed after 24 hours, indicated in Figures 3.8 and 3.9. Each experiment was repeated 3 times, N=3. Rates of cellular migration were significantly affected with knockdowns of YAP and Talin. Figure 3.8 (A) represents the cells at time 0 and Figure 3.8 (B) after 24 hours. Thus, knockdown of YAP and Talin slowed down the migration rate of cells when compared to control cells; scratch areas remained open after the silencing of YAP and Talin while in control cells the wound completely closed. This is in contradiction to, CD2AP and Ezrin siRNA transfections as cells migrated at the same rate with as controls (Figure 3.9). The rate of migration can be seen from the quantification graphs in Figures 3.8(C) and 3.9(C).

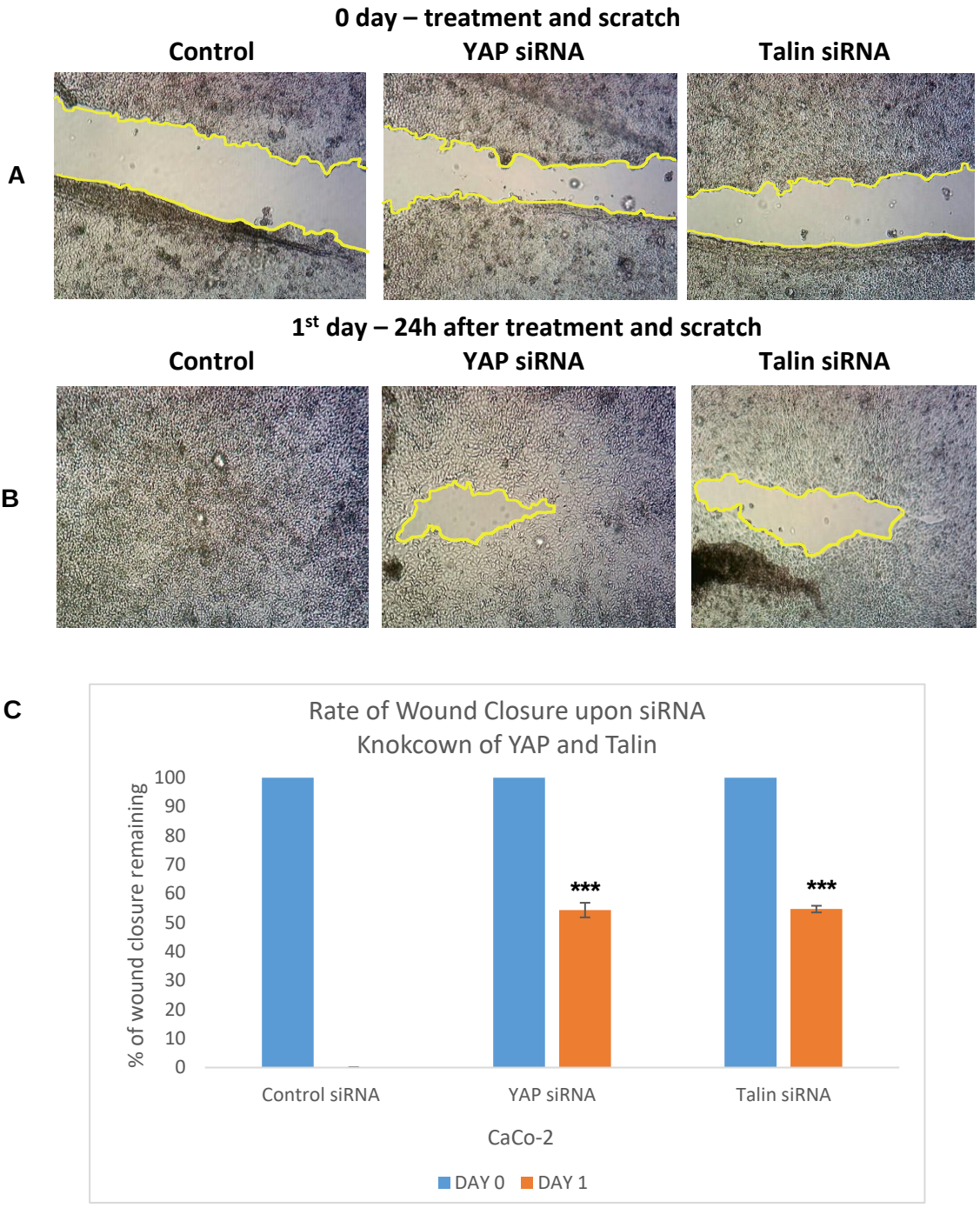

Figure 3.8. Scratch assay analysis with siRNA-mediated knockdowns in CaCo-2 cell line.

Representative brightfield images of scratch assay samples of control cells (A) and cells transfected with YAP and Talin siRNA (B) showing cellular migration at indicated time points at 20X magnification (Time 0 & 24h after). (C) Quantitative graph showing the rate of wound closure upon siRNA depletion of YAP and Talin compared to control siRNA. Graph was obtained from the pooled data of 3 independent experiments and represented as mean ± standard deviation (SD), N=3. Statistical importance of control versus YAP and Talin siRNAs was determined by T-Test with a significant p values of ***$p \leq 0.0001$.

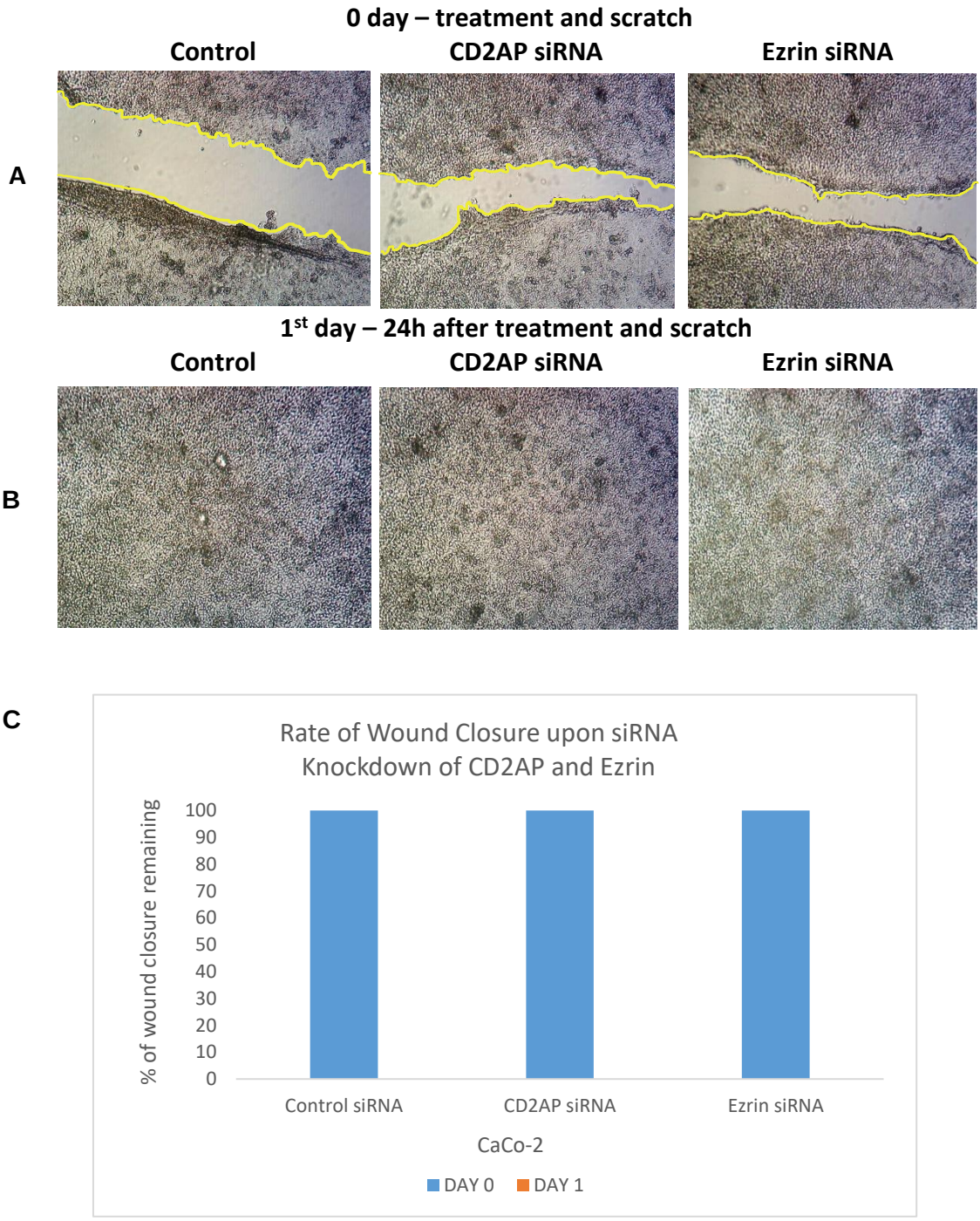

Figure 3.9. Scratch assay analysis with siRNA-mediated knockdowns in CaCo-2 cell line. Representative brightfield images of scratch assay samples of control cells (A) and cells transfected with CD2AP and Ezrin siRNA (B) showing cellular migration at indicated time points at 20X magnification (Time 0 & 24h after). (C) Quantitative graph showing the rate of wound closure upon siRNA depletion of CD2AP and Ezrin compared to control siRNA. Graph was obtained from the pooled data of 3 independent experiments, N=3.

3.5 Effect of Talin1 and Talin2 silencing on YAP phosphorylation

3.5.1 Hep-G2 Cells

To examine the role of talin1 and talin2 on YAP activity, endogenous talin1 and talin2 were silenced by siRNA transfection in Hep-G2 cells. The knockdown of Talin1 resulted in decreased level of YAP phosphorylation as shown in Figure 3.10. However, quantification graphs generated from immunoblot analysis upon Talin2 transfection clearly indicates that knockdown of Talin2 resulted in an increase in the phosphorylation level of YAP. Inhibition of YAP by Talin2 knockdown is shown by a significant increase in the phosphorylation levels of YAP in S127 site with an evident increase of signal in immunoblot analysis shown in Figure 3.11.

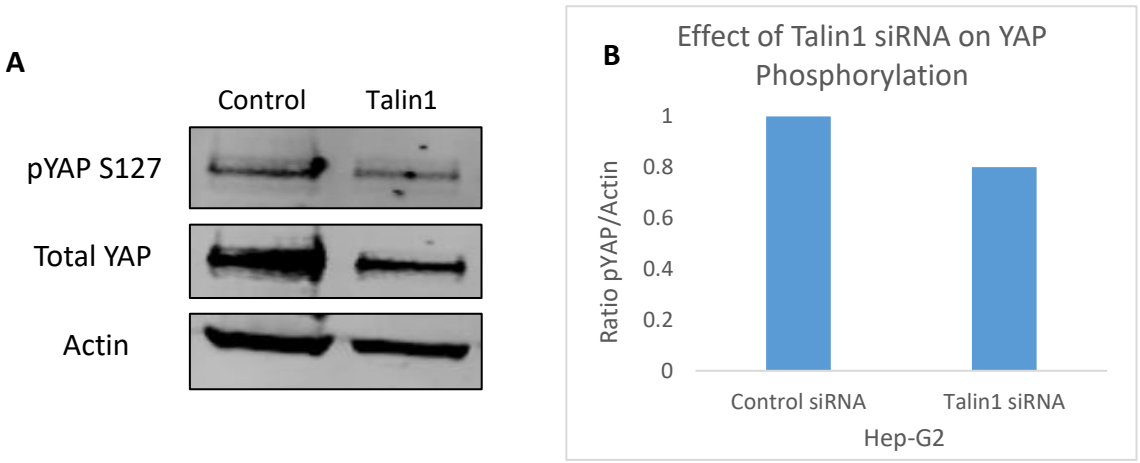

Figure 3.10. Effect of Talin1 siRNA-mediated knockdown on YAP phosphorylation in Hep-G2 cells.(A)Western blot image of pYAP s127 site in control siRNA and Talin1 siRNA treated cells. (B) Quantification graph of YAP phosphorylation levels with Actin. (C) Quantification graph of YAP phosphorylation levels with total YAP.

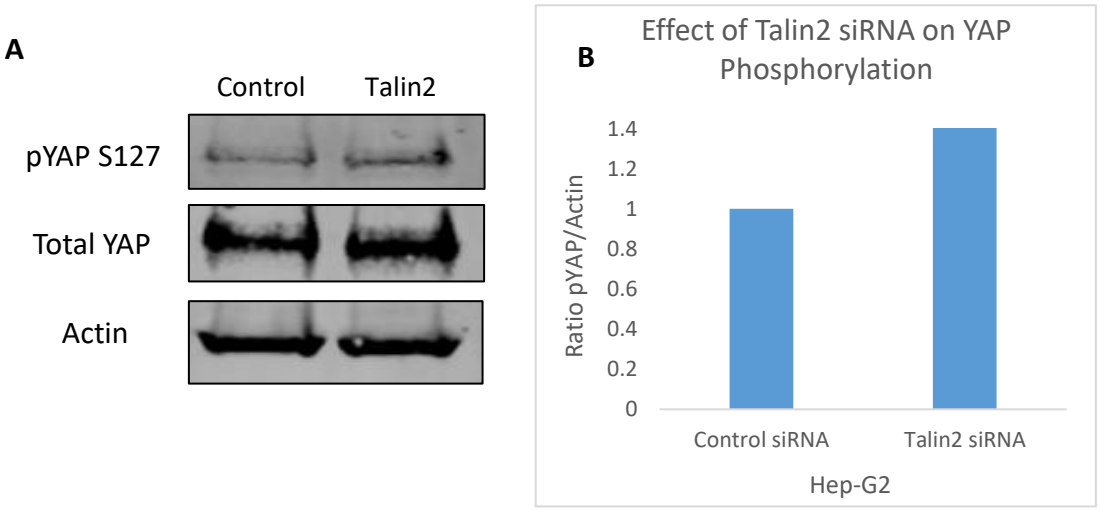

Figure 3.11. Effect of Talin2 siRNA-mediated knockdown on YAP phosphorylation in Hep-G2 cells.(A)Western blot image of pYAP s127 site in control siRNA and Talin2 siRNA treated cells. (B) Quantification graph of YAP phosphorylation levels with Actin. (C) Quantification graph of YAP phosphorylation levels with total YAP.

3.5.2 CaCo-2 Cells

The effect of Talin1 and Talin2 on the activity of YAP in CaCo-2 cells was analysed by silencing the expression of endogenous Talin1 and Talin2 using siRNA-mediated knockdown. CaCo-2 cells were transfected with Talin1 siRNA, Talin2 siRNA and combination of Talin1 and Talin2 siRNA respectively. Figure 3.12(A) represents an evident decrease of signal in the immunoblot image of pYAP S127 site in siRNA-treated cells compared to control. Quantification graphs generated from the immunoblot analysis upon knockdown of Talin1, Talin2 and Talin1+2 (Figure 3.12(B)), provide a clear indication of a significant decrease in YAP phosphorylation levels in the S127 site. The talin knockdown result reinforces the notation that YAP and talin not only interact, but potentially can affect pYAP

levels due to some unknown pathway interaction that needs to be investigated in future studies.

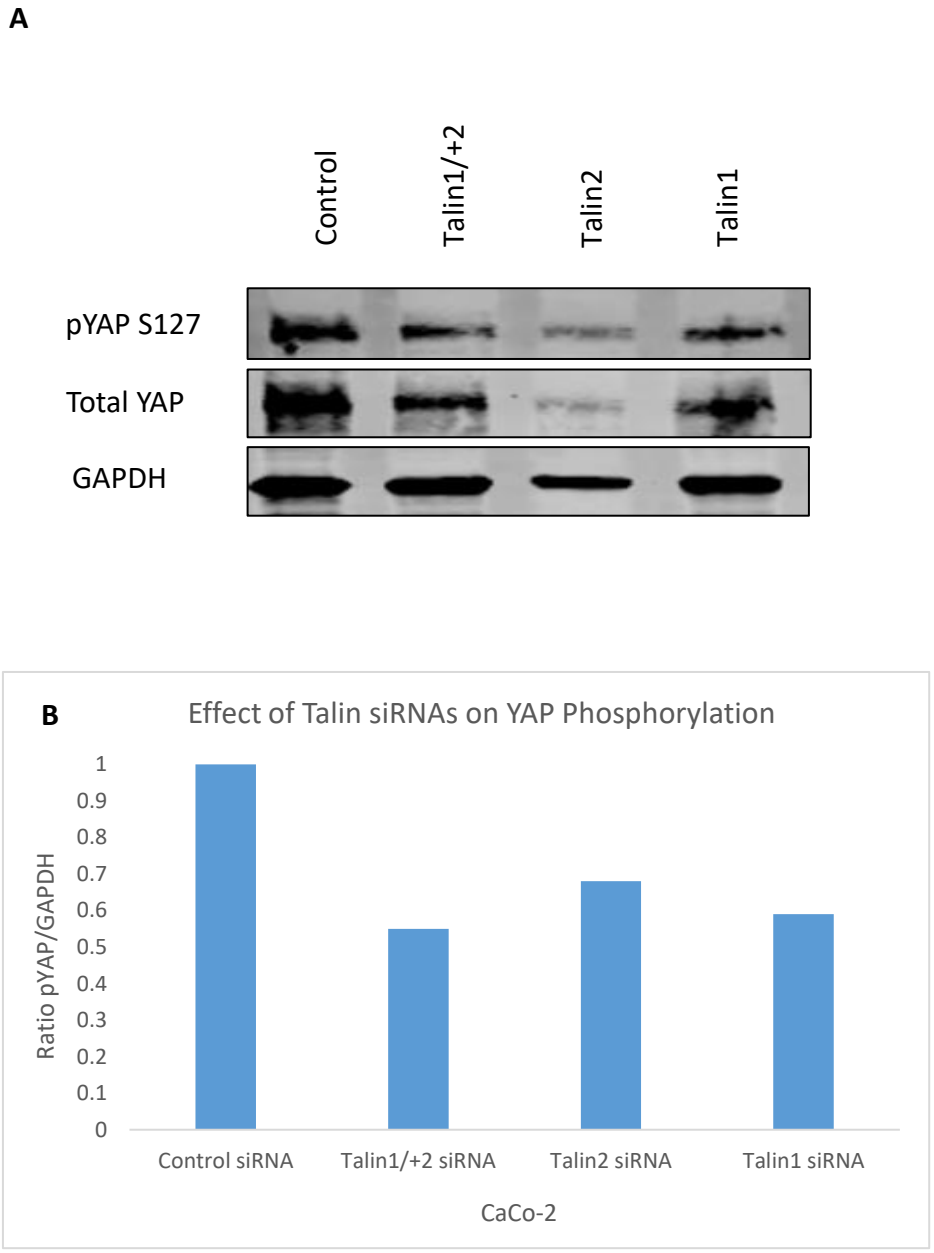

Figure 3.12. Effect of Talin1 and Talin2 siRNA-mediated knockdowns on YAP phosphorylation in CaCo-2 cells.(A)Western blot image of pYAP s127 site in control, Talin1, Talin2 and combined Talin1/+2 siRNA treated cells. (B) Quantification graph of YAP phosphorylation levels with GAPDH.

3.6 Translocation of YAP upon siRNA-mediated knockdown of CD2AP, Talin and Ezrin

3.6.1 CaCo-2 Cells

Primarily, the CaCo-2 cells were transfected with control siRNA and cellular localization of YAP, CD2AP, Talin and Ezrin was determined by immunofluorescence staining in confluent and sparse CaCo-2 cells before silencing the members of the complex. Cells were fixed after 72 hours of transfection using 4% PFA. Coverslips were stained for proteins (A)YAP, (B)CD2AP, (C)Talin, (D) Ezrin. DAPI (blue) used for staining the cell nuclei and CY3(red) was used to stain proteins. Images were taken with Evos fl Fluorescence microscope at 20X magnification. Each experiment was repeated 3 times, N=3. YAP was observed in a clear cytoplasmic state in confluent cells, while YAP translocated to the nucleus in sparse condition, represented in Figure 3.13(A) and 3.14(A) respectively as cell density is one of the prominent regulator of YAP translocation (Zhao *et al*., 2007; Cai, Wang and Meng, 2021). CD2AP, Talin and Ezrin are cytoplasmic proteins and can be clearly seen around the nucleus of the cells in both confluent and sparse conditions of control siRNA treated CaCo-2 cells in Figure 3.13 and 3.14.

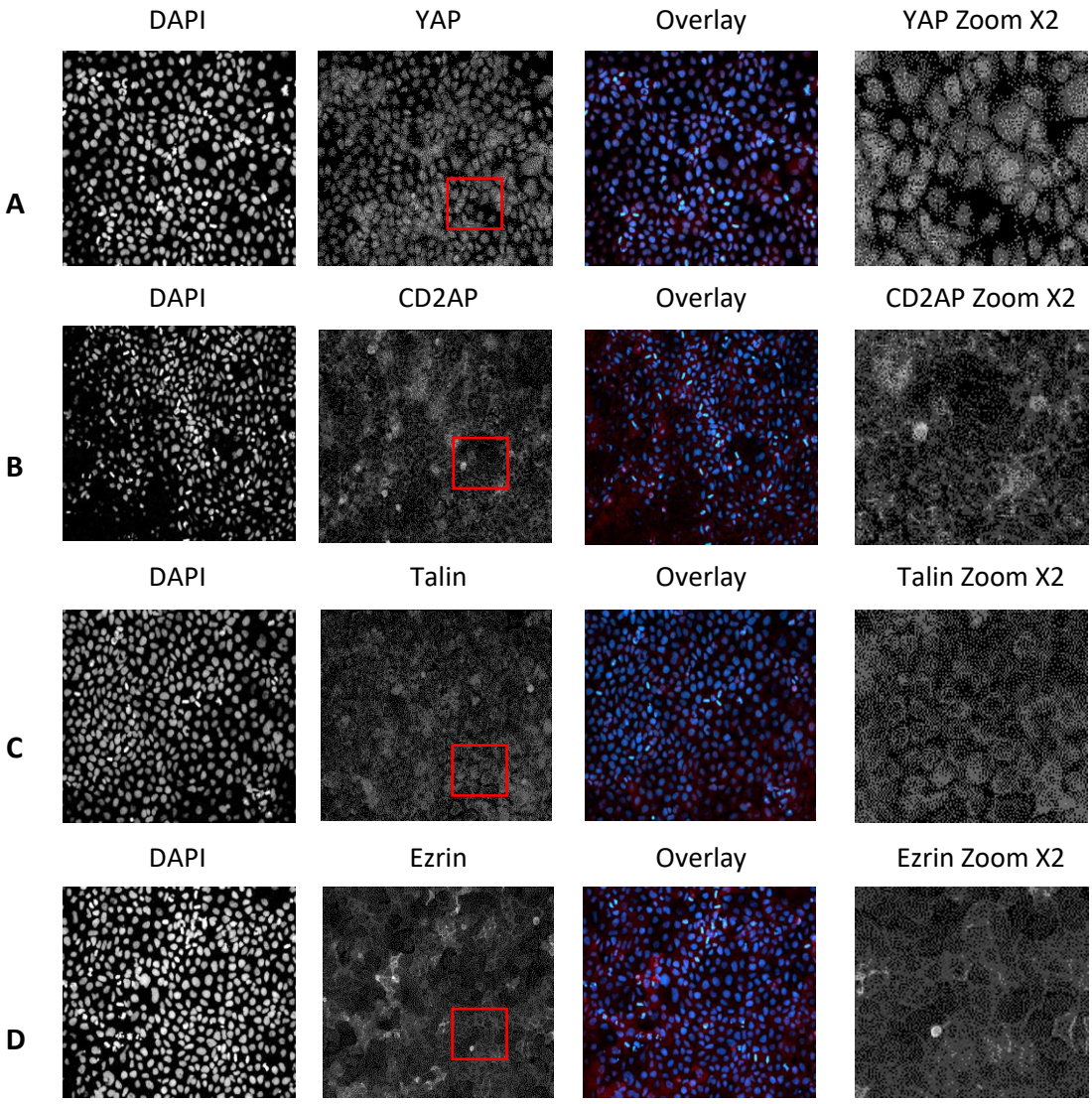

Figure 3.13. Cellular localization of YAP, CD2AP, Talin and Ezrin determined by immunofluorescence staining in confluent CaCo-2 cells treated with Control siRNA. CaCo-2 cells were transfected with control siRNAs. Cells were fixed after 72hours using 4% PFA. Coverslips were stained for proteins indicated. DAPI (blue) used for staining the cell nuclei and CY3 (red) used for all proteins; (A)YAP, (B)CD2AP, (C)Talin, and (D) Ezrin. Images were taken with Evos fl Fluorescence microscope at 20X magnification. For each protein, an inset of the image is provided in the last panel at a 2X zoom to show the localisation of proteins more clearly. Representative IF images from one experiment are displayed amongst 4 independent repeats.

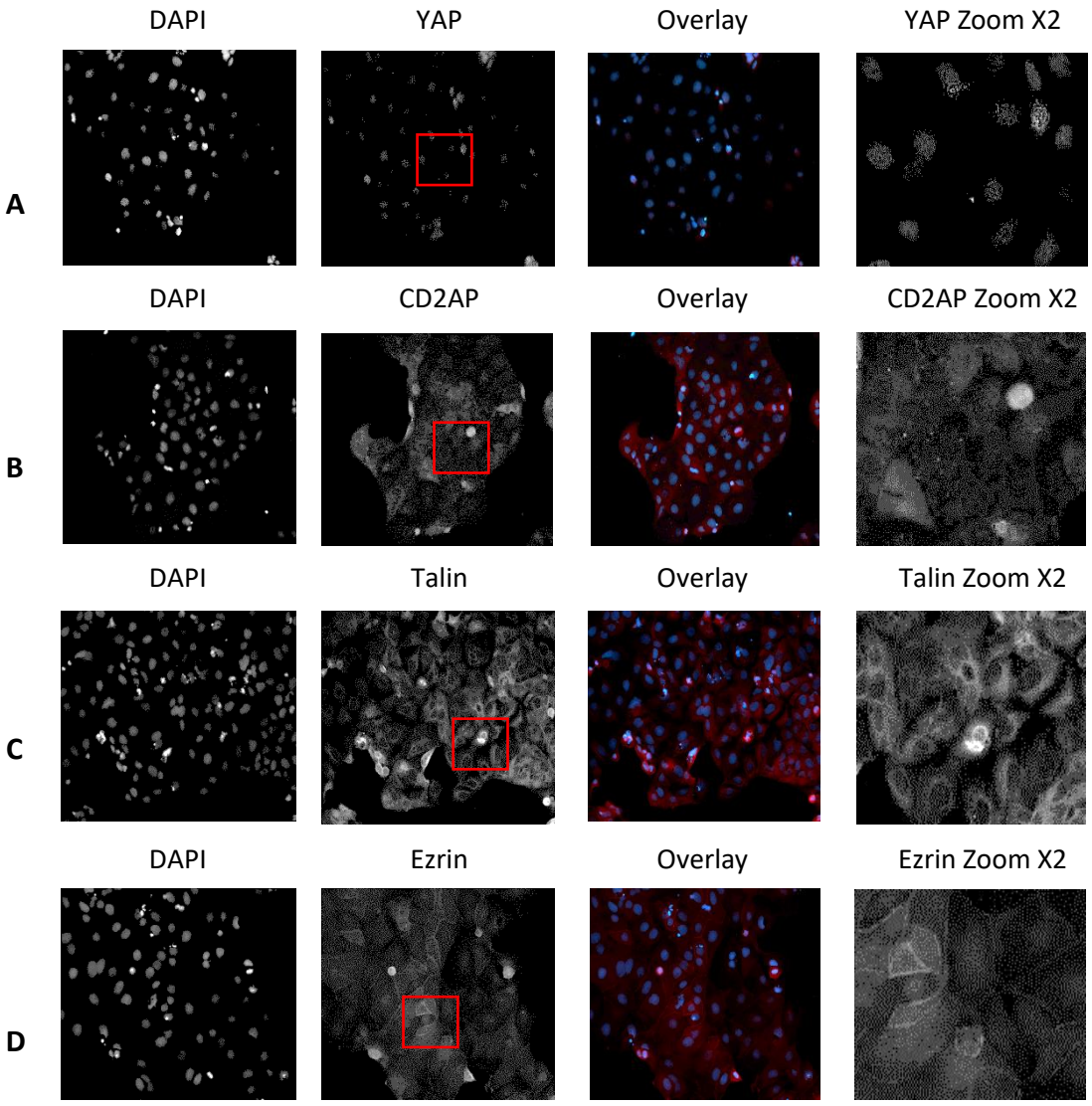

Figure 3.14. Cellular localization of YAP, CD2AP, Talin and Ezrin determined by immunofluorescence staining in sparse CaCo-2 cells treated with Control siRNA. CaCo-2 cells were transfected with control siRNAs. Cells were fixed after 72hours using 4% PFA. Coverslips were stained for proteins indicated. DAPI (blue) used for staining the cell nuclei and CY3 (red) used for all proteins; (A)YAP, (B)CD2AP, (C)Talin, and (D) Ezrin. Images were taken with Evos fl Fluorescence microscope at 20X magnification. For each protein, an inset of the image is provided in the last panel at a 2X zoom to show the localisation of proteins more clearly. Representative IF images from one experiment are displayed amongst 4 independent repeats.

Expression of the YAP was silenced to observe the effect of its depletion on subsequent members of the complex; CD2AP, Talin and Ezrin in confluent CaCo-2 cells in Figure 3.15. The siRNA was clearly effective in silencing YAP as YAP was depleted in YAP siRNA transfected cells compared to control siRNA in terms of loss of antibody signal. The knockdown of YAP affected all the members of complex as less protein was observed upon depletion of YAP in comparison to control cells in Figure 3.13. However, silencing of YAP had an enormous impact on CD2AP as its expression was significantly decreased with YAP knockdown in comparison to control in Figure 3.13(B). In the sparse condition, no effect was observed on the level of CD2AP, Talin and Ezrin (Figure 3.16) upon depletion of YAP when compared to sparse control cells (Figure 3.14).

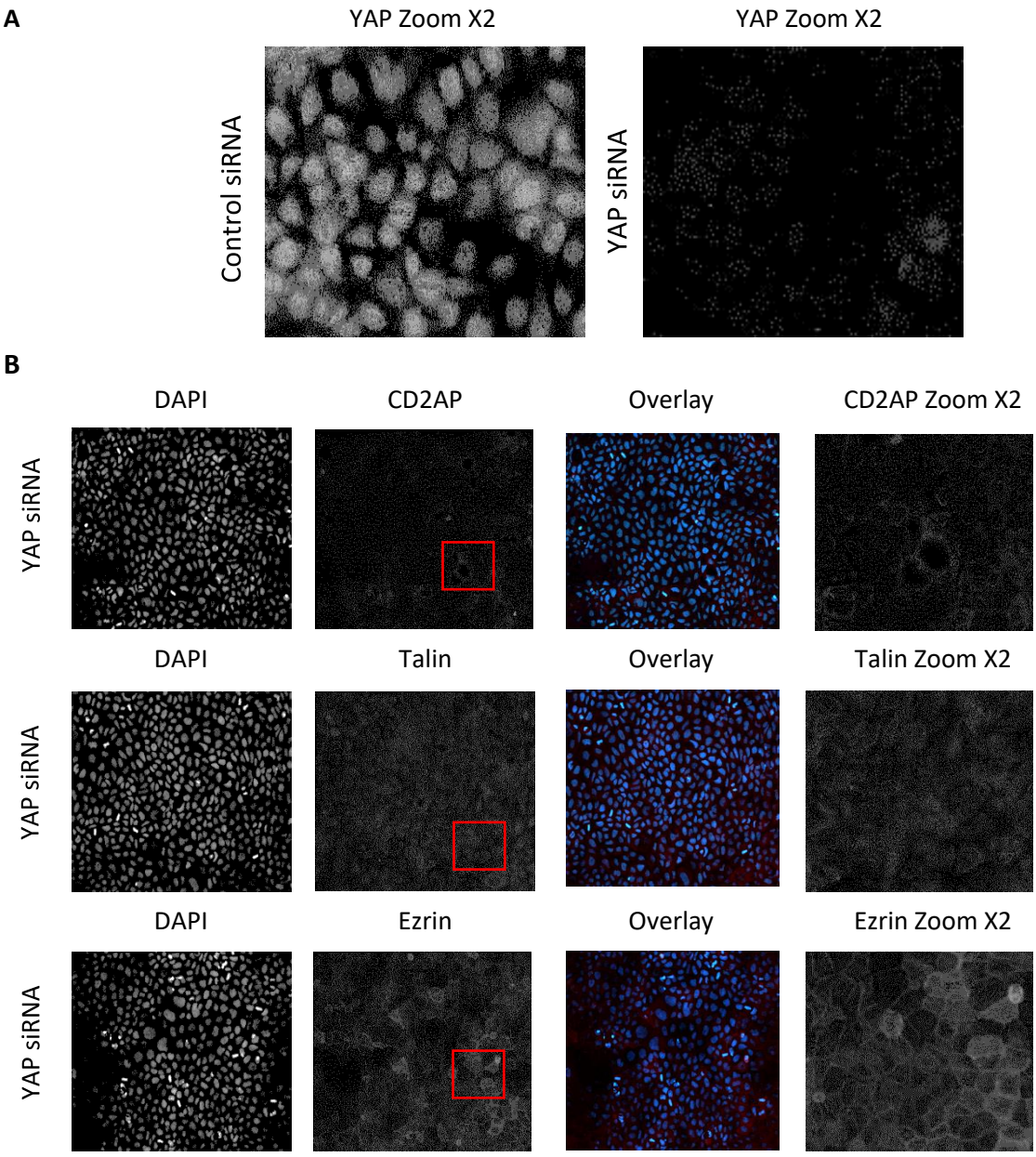

Figure 3.15. The depletion of YAP and cellular localization of CD2AP, Talin and Ezrin upon siRNA mediated knockdown of YAP determined by immunofluorescence staining in confluent CaCo-2 cells. CaCo-2 cells were transfected with YAP siRNA. Cells were fixed after 72hours using 4% PFA. Coverslips were stained for proteins indicated. DAPI (blue) used for staining the cell nuclei and CY3 (red) used for all proteins; YAP, CD2AP, Talin, and Ezrin. Images were taken with Evos fl Fluorescence microscope at 20X magnification. For each protein, an inset of the image is provided in the last panel at a 2X zoom to show the localisation of proteins more clearly upon knockdown of YAP. Representative IF images from one experiment are displayed amongst 4 independent repeats.

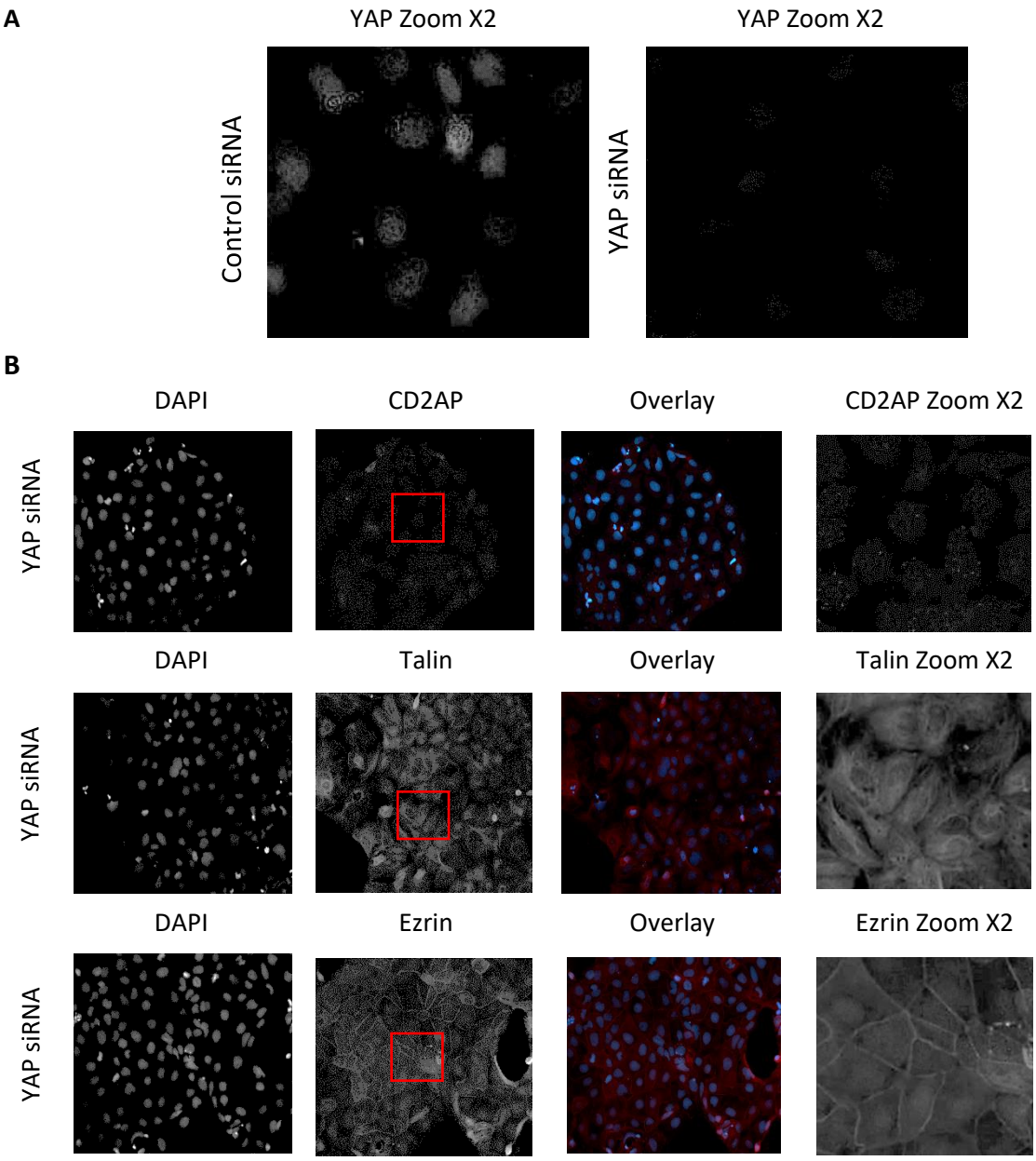

Figure 3.16. The depletion of YAP and cellular localization of CD2AP, Talin and Ezrin upon siRNA mediated knockdown of YAP determined by immunofluorescence staining in sparse CaCo-2 cells. CaCo-2 cells were transfected with YAP siRNA. Cells were fixed after 72hours using 4% PFA. Coverslips were stained for proteins indicated. DAPI (blue) used for staining the cell nuclei and CY3 (red) used for all proteins; YAP, CD2AP,Talin, and Ezrin. Images were taken with Evos fl Fluorescence microscope at 20X magnification. For each protein, an inset of the image is provided in the last panel at a 2X zoom to show the localisation of proteins more clearly upon knockdown of YAP. Representative IF images from one experiment are displayed amongst 4 independent repeats.

CD2-associated protein (CD2AP) expression was silenced by CD2AP siRNA to assess the translocation of YAP. Knockdown of CD2AP was effective when compared to control in confluent and sparse CaCo-2 cells as indicated in Figure 3.17 and 3.18 respectively. The translocation and expression of YAP was not changed upon silencing of CD2AP in both confluent and sparse CaCo-2 cells in comparison to control as seen in Figure 3.17 and 3.18 respectively showing that depletion of CD2AP is not efficient to shuttle YAP between the nucleus and cytoplasm.

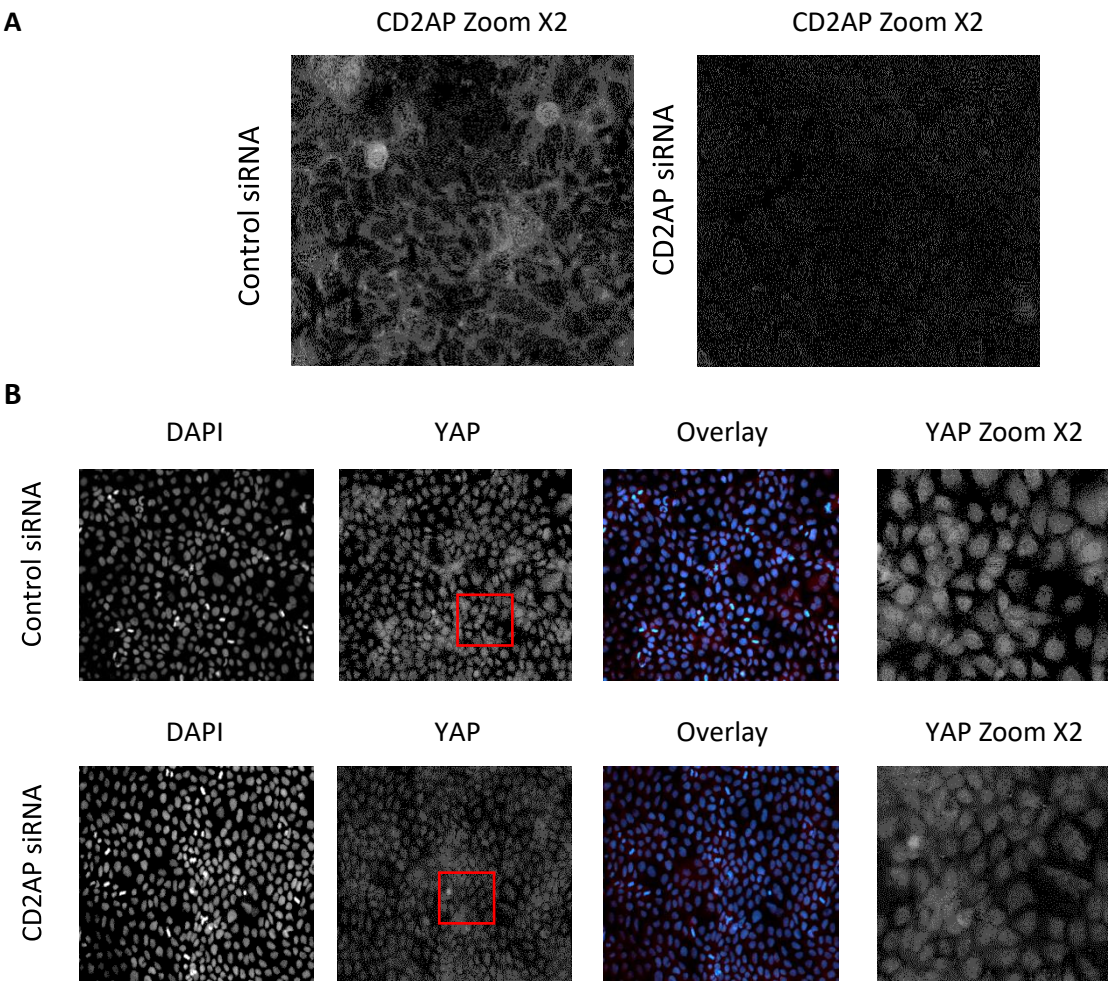

Figure 3.17. The depletion of CD2AP and cellular localization of YAP upon siRNA mediated knockdown of CD2AP determined by immunofluorescence staining in confluent CaCo-2 cells. CaCo-2 cells were transfected with CD2AP siRNA. Cells were fixed after 72hours using 4% PFA. Coverslips were stained for proteins indicated. DAPI (blue) used for staining the cell nuclei and CY3 (red) used to stain CD2AP and YAP. Images were taken with Evos fl Fluorescence microscope at 20X magnification. For each protein an inset of the image is provided in the last panel at a 2X zoom to show the localisation of proteins more clearly. Representative IF images from one experiment are displayed amongst 4 independent repeats.

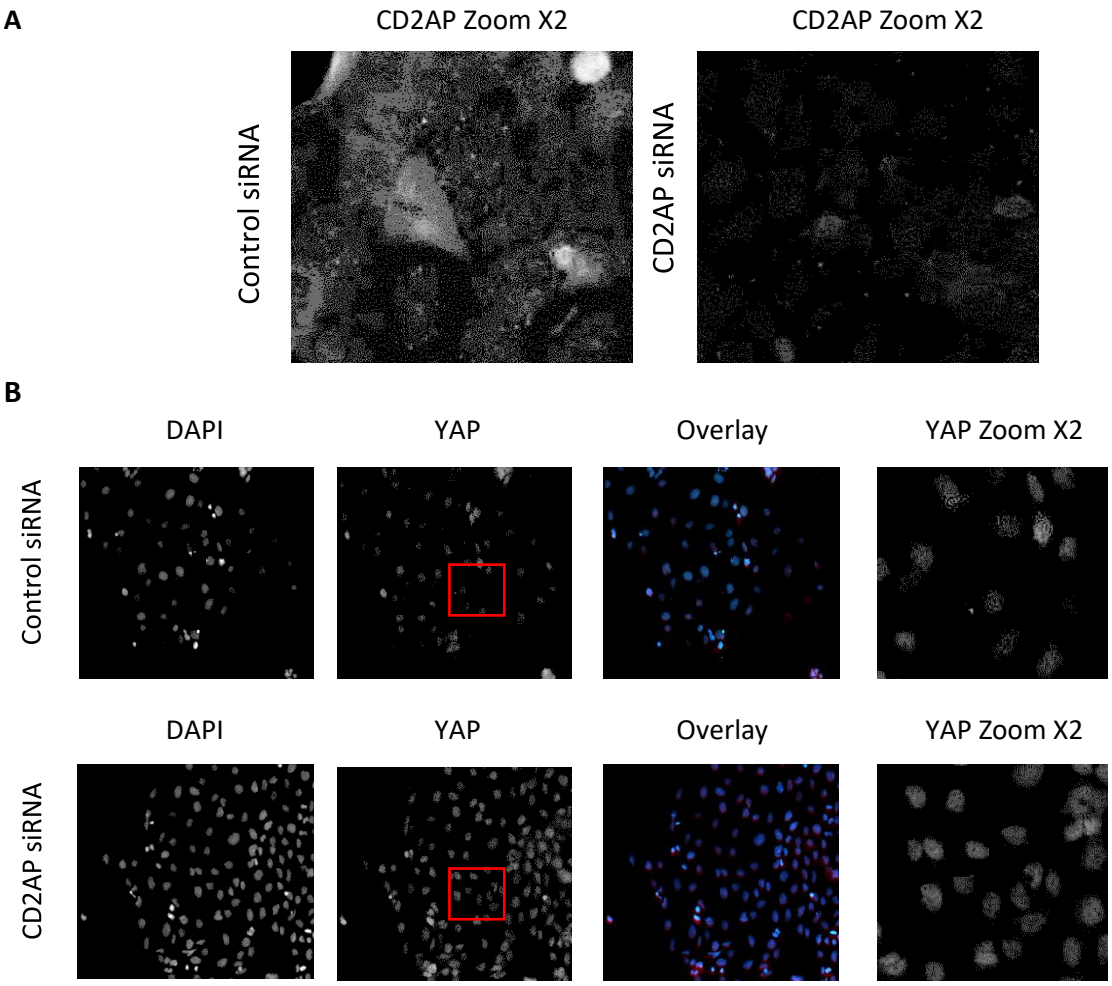

Figure 3.18. The depletion of CD2AP and cellular localization of YAP upon siRNA mediated knockdown of CD2AP determined by immunofluorescence staining in sparse CaCo-2 cells. CaCo-2 cells were transfected with CD2AP siRNA. Cells were fixed after 72hours using 4% PFA. Coverslips were stained for proteins indicated. DAPI (blue) used for staining the cell nuclei and CY3 (red) used to stain CD2AP and YAP. Images were taken with Evos fl Fluorescence microscope at 20X magnification. For each protein, an inset of the image is provided in the last panel at a 2X zoom to show the localisation of proteins more clearly. Representative IF images from one experiment are displayed amongst 4 independent repeats.

Expression of talin was depleted via siRNA-mediated knockdown to determine the translocation of YAP in confluent and sparse CaCo-2 cells. The efficiency of knockdown in comparison to control siRNA was indicated in Figure 3.19 and 3.20 and shows the effective depletion of Talin. YAP was translocated from nucleus to cytoplasm upon depletion of talin in both confluent and sparse conditions. Thus, YAP was inactivated upon knockdown of Talin. The transition of YAP from a nuclear state into a more cytoplasmic state was clearly evident under both confluent and sparse conditions in Figure 3.19 and 3.20 consecutively. The immunofluorescence images indicated that presence of talin is important for the activation of YAP as talin is known to promote nuclear localisation and activation of YAP by triggering FAK and Src activation (Dasgupta and McCollum, 2019).

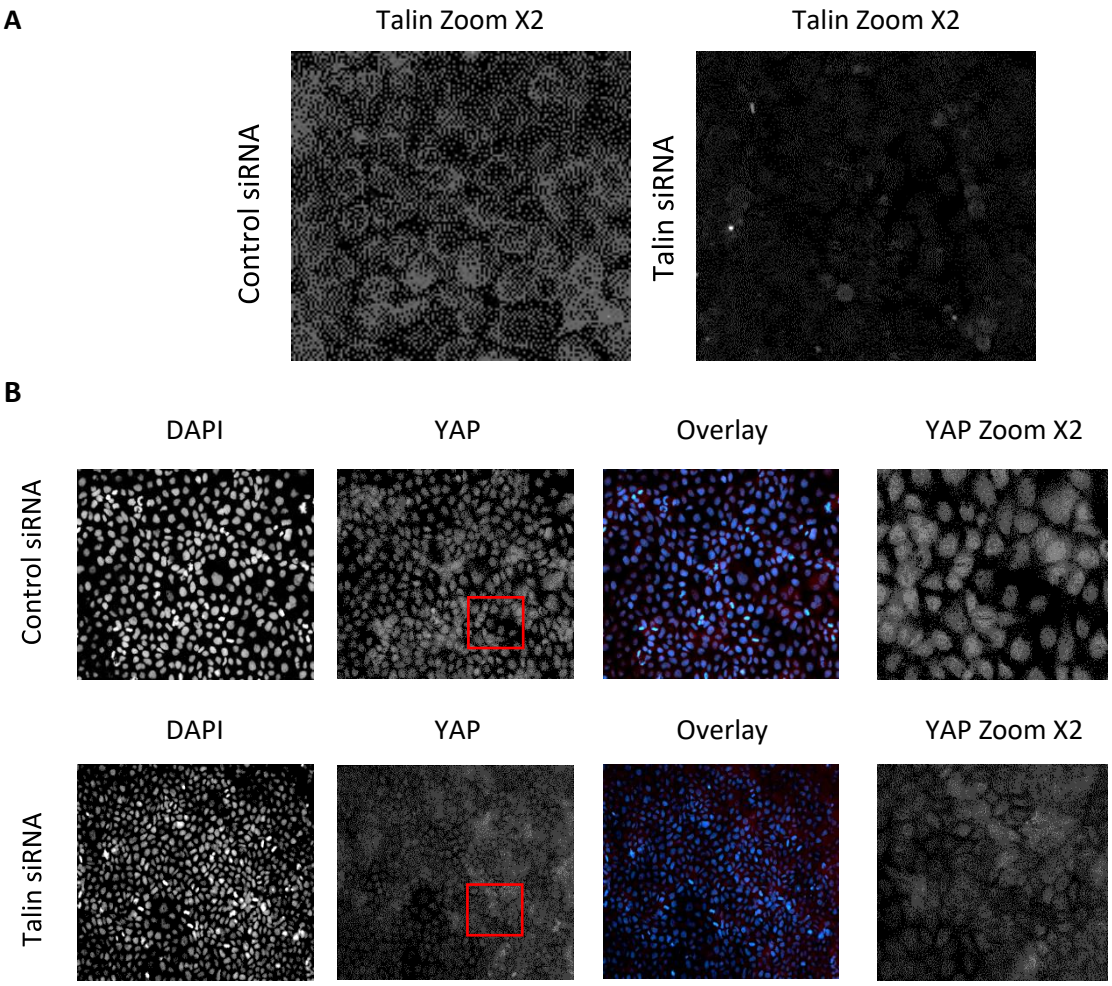

Figure 3.19. The depletion of Talin and cellular localization of YAP upon siRNA mediated knockdown of Talin determined by immunofluorescence staining in confluent CaCo-2 cells. CaCo-2 cells were transfected with Talin siRNA. Cells were fixed after 72hours using 4% PFA. Coverslips were stained for proteins indicated. DAPI (blue) used for staining the cell nuclei and CY3 (red) used to stain Talin and YAP. Images were taken with Evos fl Fluorescence microscope at 20X magnification. For each protein, an inset of the image is provided in the last panel at a 2X zoom to show the localisation of proteins more clearly. Representative IF images from one experiment are displayed amongst 4 independent repeats.

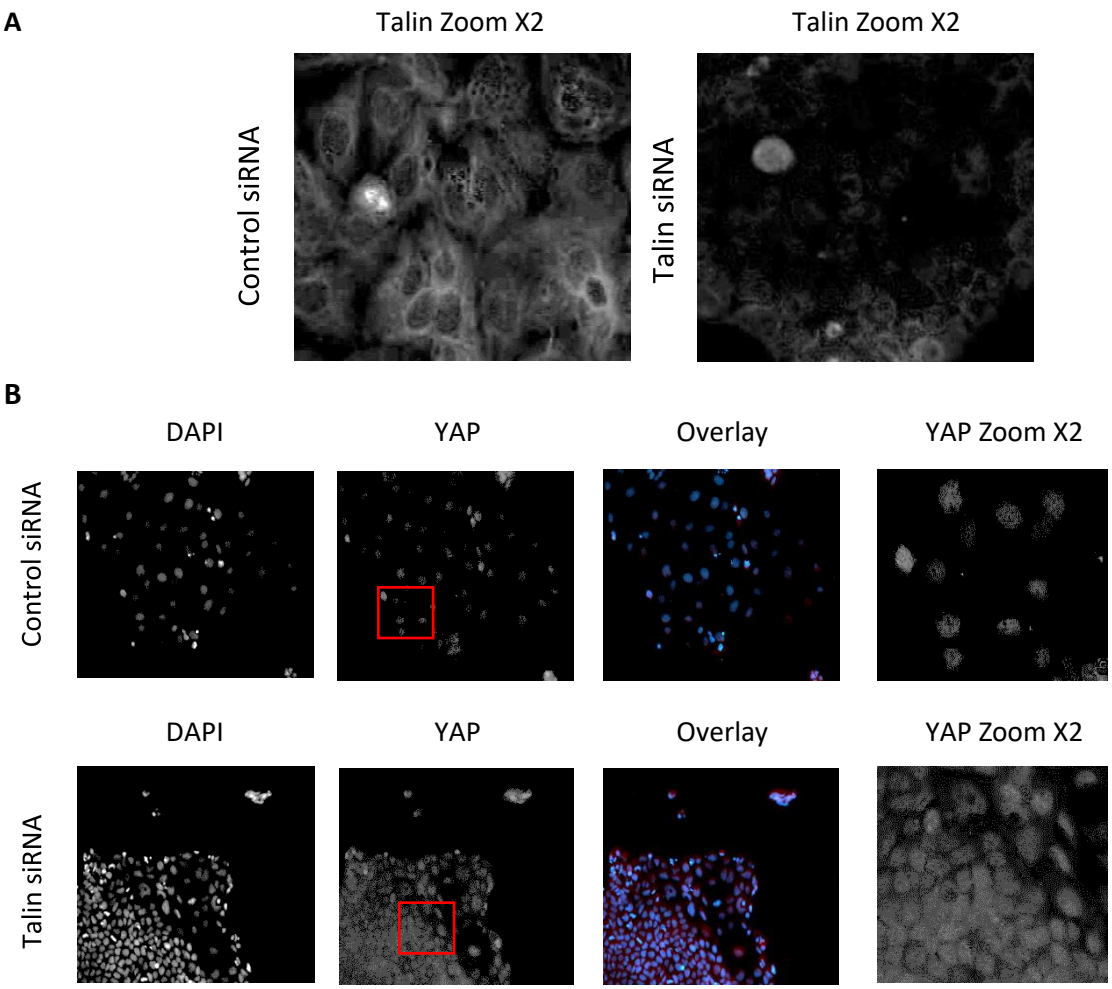

Figure 3.20. The depletion of Talin and cellular localization of YAP upon siRNA mediated knockdown of Talin determined by immunofluorescence staining in sparse CaCo-2 cells. CaCo-2 cells were transfected with Talin siRNA. Cells were fixed after 72hours using 4% PFA. Coverslips were stained for proteins indicated. DAPI (blue) used for staining the cell nuclei and CY3 (red) used to stain Talin and YAP. Images were taken with Evos fl Fluorescence microscope at 20X magnification. An inset of focused image is provided in the last panel to show Talin and the location of YAP more clearly upon depletion of Talin. Representative IF images from one experiment are displayed amongst 4 independent repeats.

Ezrin was depleted and translocation of YAP was determined via immunofluorescence staining in confluent and sparse CaCo-2 cells. The expression of ezrin was effectively suppressed which can be clearly seen in Figures 3.21 and 3.22. Ezrin knockdown does not seem to affect YAP translocation however, YAP in ezrin depleted cells was more

cytoplasmic compared to control under both confluent and sparse conditions compared to control siRNA (Figure 3.21 and 3.22), this could be due to the fact that ezrin is involved in the nuclear translocation of YAP.

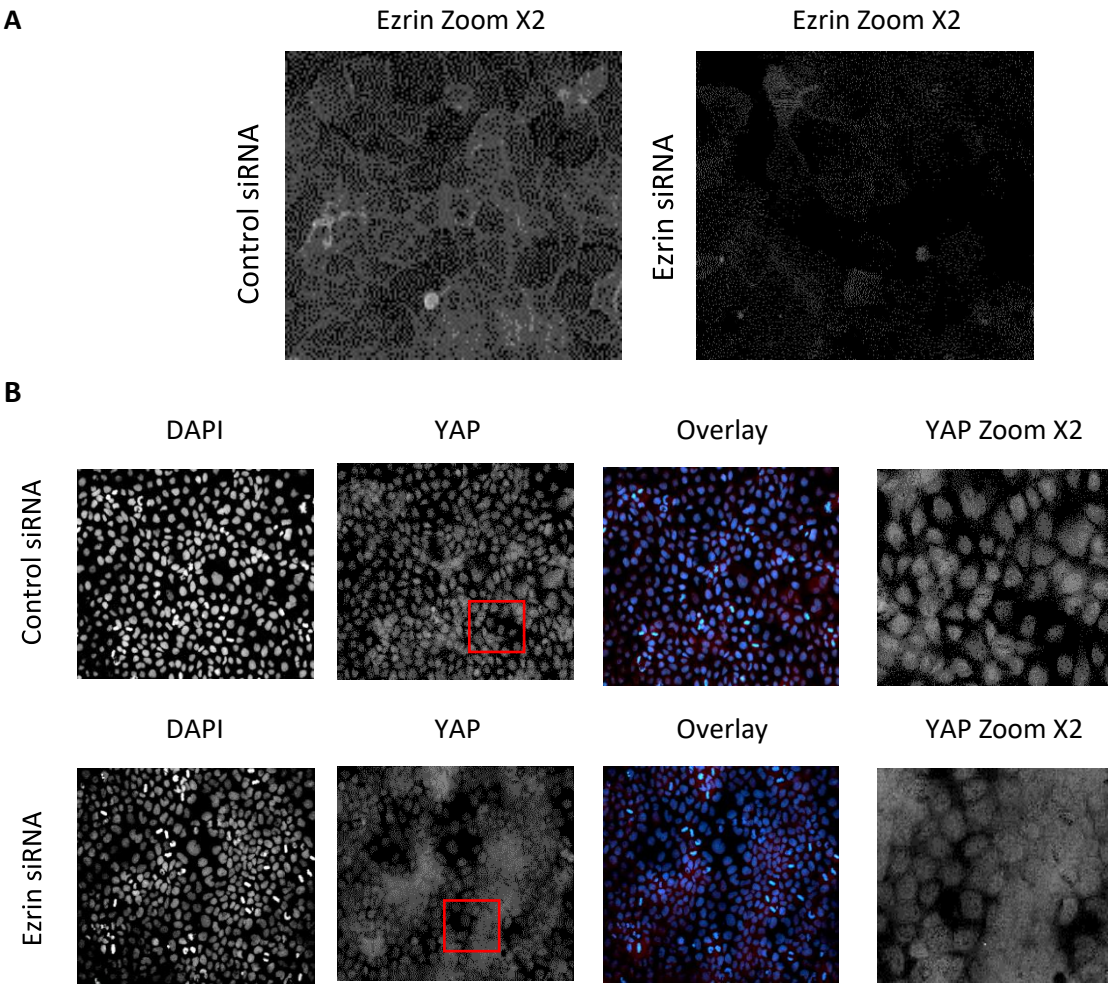

Figure 3.21. The depletion of Ezrin and cellular localization of YAP upon siRNA mediated knockdown of Ezrin determined by immunofluorescence staining in confluent CaCo-2 cells. CaCo-2 cells were transfected with Ezrin siRNA. Cells were fixed after 72hours using 4% PFA. Coverslips were stained for proteins indicated. DAPI (blue) used for staining the cell nuclei and CY3 (red) used to stain Ezrin and YAP. Images were taken with Evos fl Fluorescence microscope at 20X magnification. For each protein, an inset of the image is provided in the last panel at a 2X zoom to show the localisation of proteins more clearly. Representative IF images from one experiment are displayed amongst 4 independent repeats.

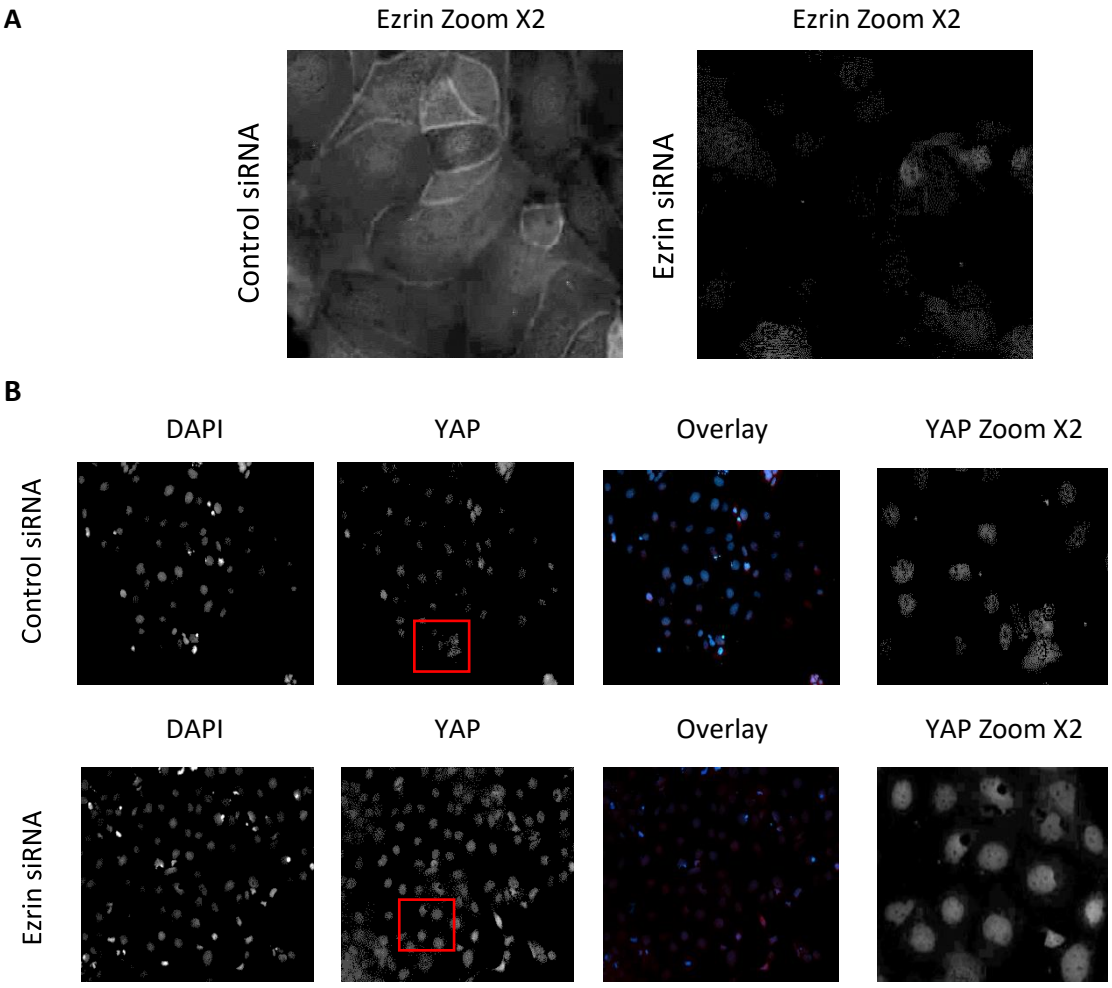

Figure 3.22. The depletion of Ezrin and cellular localization of YAP upon siRNA mediated knockdown of Ezrin determined by immunofluorescence staining in sparse CaCo-2 cells. CaCo-2 cells were transfected with Ezrin siRNA. Cells were fixed after 72hours using 4% PFA. Coverslips were stained for proteins indicated. DAPI (blue) used for staining the cell nuclei and CY3 (red) used to stain Ezrin and YAP. Images were taken with Evos fl Fluorescence microscope at 20X magnification. For each protein, an inset of the image is provided in the last panel at a 2X zoom to show the localisation of proteins more clearly. Representative IF images from one experiment are displayed amongst 4 independent repeats.

3.6.2 Hep-G2 Cells

Hep-G2 cells were transfected with control siRNA and cellular localization of YAP, CD2AP, Talin and Ezrin was determined by immunofluorescence staining in confluent and sparse Hep-G2 cells before silencing the members of the complex. Cells were fixed after 72 hours of transfection using 4% PFA. Coverslips were stained for proteins (A)YAP, (B)CD2AP, (C)Talin and (D) Ezrin. DAPI (blue) used for staining the cell nuclei and CY3(red) was used to stain proteins. Images were taken with Evos fl Fluorescence microscope at 20X magnification. YAP was in cytoplasmic state in confluent cells where it was much more nuclear in sparse condition indicated in Figure 3.23(A) and 3.24(A) respectively as cellular density is the primary regulator of YAP nuclear/cytoplasmic shuttling (Zhao *et al*., 2007; Cai, Wang and Meng, 2021). Cytoplasmic proteins CD2AP, Talin and Ezrin can be clearly observed in both confluent and sparse conditions of control siRNA treated Hep-G2 cells in Figures 3.23 and 3.24.

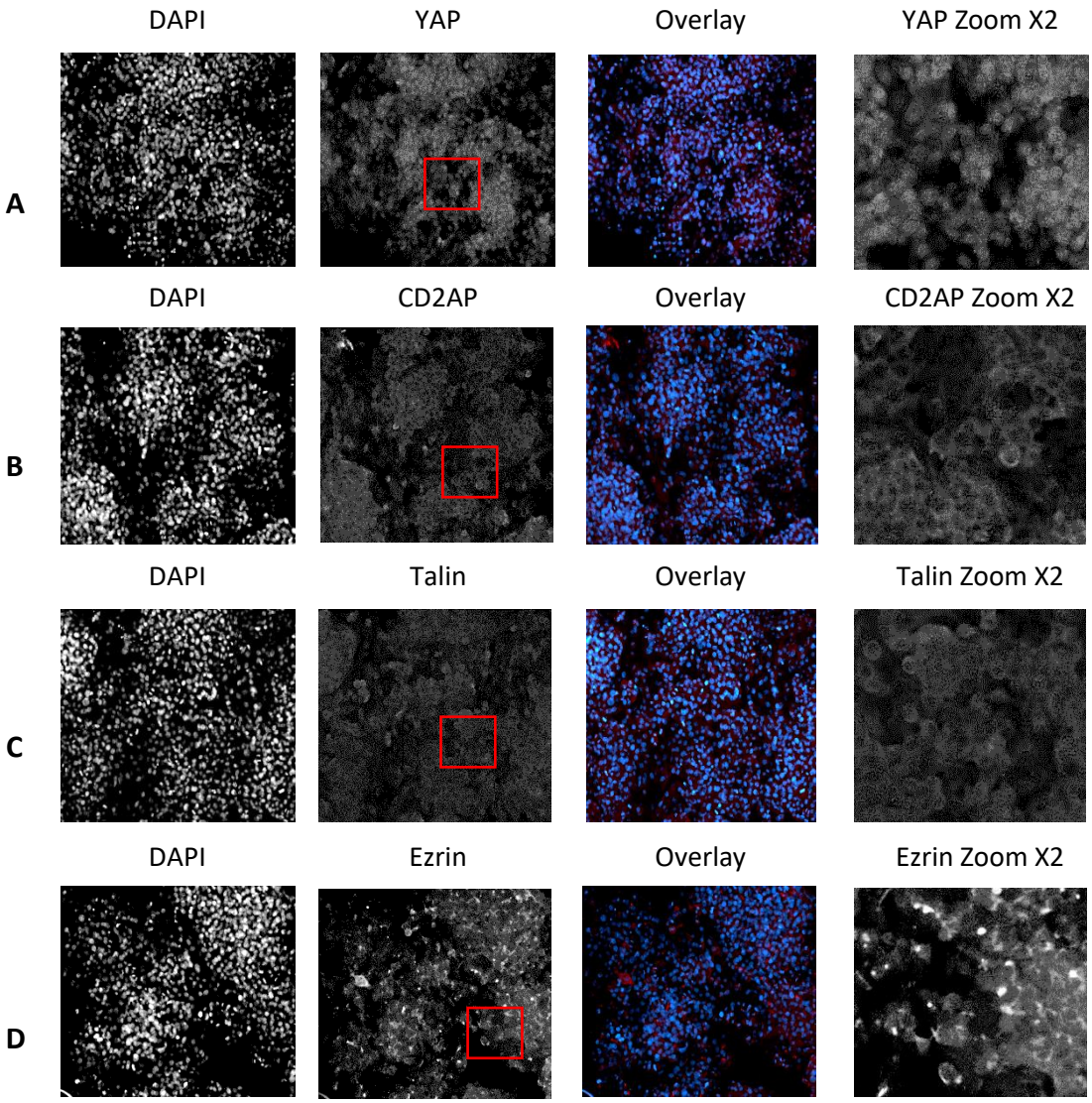

Figure 3.23. Cellular localization of YAP, CD2AP, Talin and Ezrin determined by immunofluorescence staining in confluent Hep-G2 cells treated with Control siRNA. Hep-G2 cells were transfected with control siRNAs. Cells were fixed after 72hours using 4% PFA. Coverslips were stained for proteins indicated. DAPI (blue) used for staining the cell nuclei and CY3 (red) used for all proteins; (A)YAP, (B)CD2AP, (C)Talin, and (D)Ezrin. Images were taken with Evos fl Fluorescence microscope at 20X magnification. For each protein, an inset of focused image is provided in the last panel to show the location of proteins more clearly. Representative IF images from one experiment are displayed amongst 4 independent repeats.

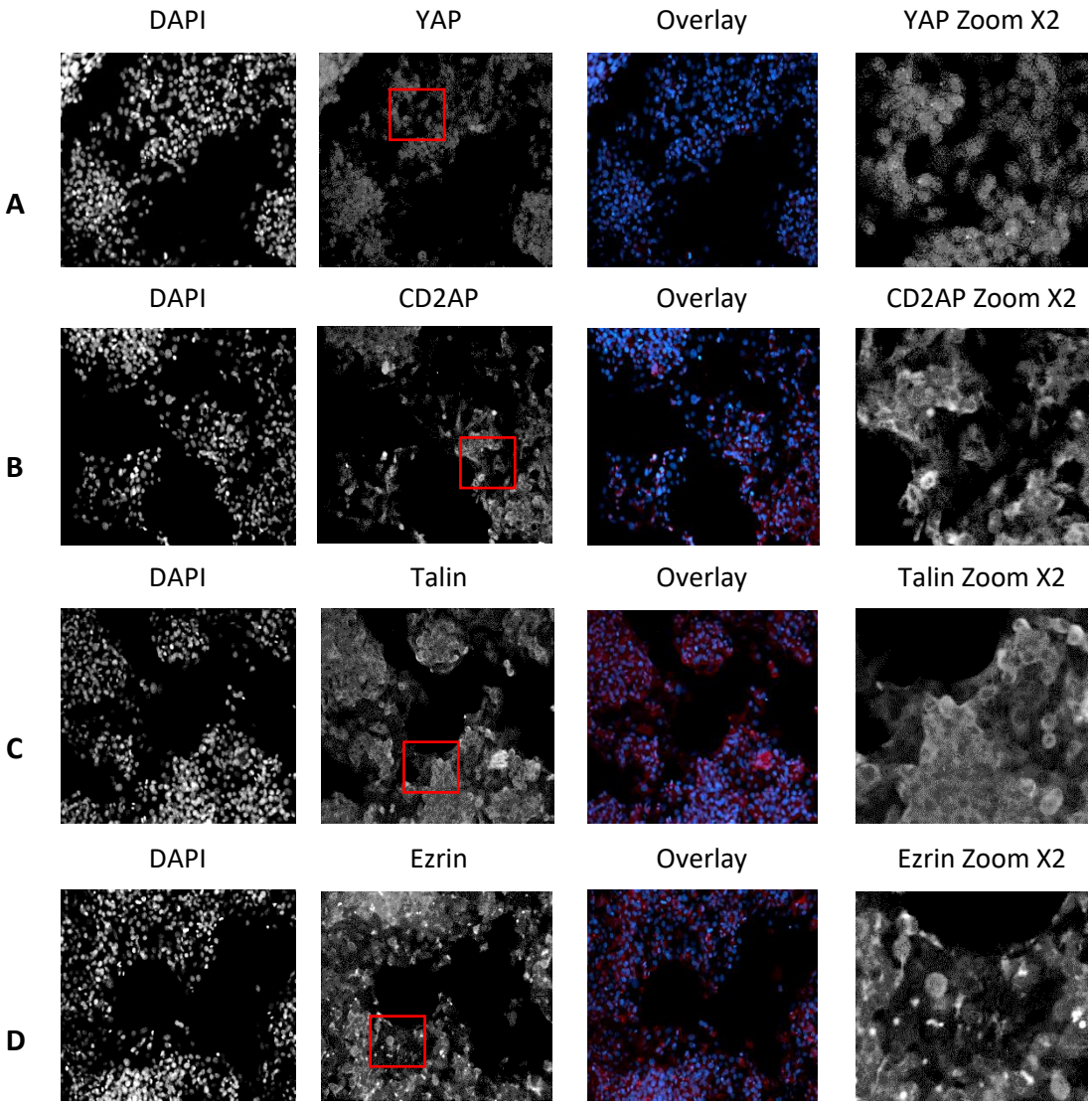

Figure 3.24. Cellular localization of YAP, CD2AP, Talin and Ezrin determined by immunofluorescence staining in sparse Hep-G2 cells. Untreated Hep-G2 cells were stained with complex proteins. Cells were fixed after 72hours using 4% PFA. Coverslips were stained for proteins indicated. DAPI (blue) used for staining the cell nuclei and CY3 (red) used for all proteins; (A)YAP, (B)CD2AP, (C)Talin, and (D)Ezrin. Images were taken with Evos fl Fluorescence microscope at 20X magnification. For each protein, an inset of the image is provided in the last panel at a 2X zoom to show the localisation of proteins more clearly. Representative IF images from one experiment are displayed amongst 4 independent repeats.

Expression of the YAP was silenced to observe the effect on the members of the complex; CD2AP, Talin and Ezrin in confluent and sparse Hep-G2 cells in Figures 3.25 and 3.26. The siRNA was effective in silencing YAP, as YAP antibody signal was clearly diminished in YAP siRNA transfected confluent and sparse cells compared to control siRNA. The members of the complex; CD2AP, Talin and Ezrin do not seem to be affected by the depletion of YAP under both confluent and sparse conditions as represented in Figures 3.25 and 3.26. The morphology of the cell could be the reason for not observing any effect in the components of the complex upon depletion of YAP.

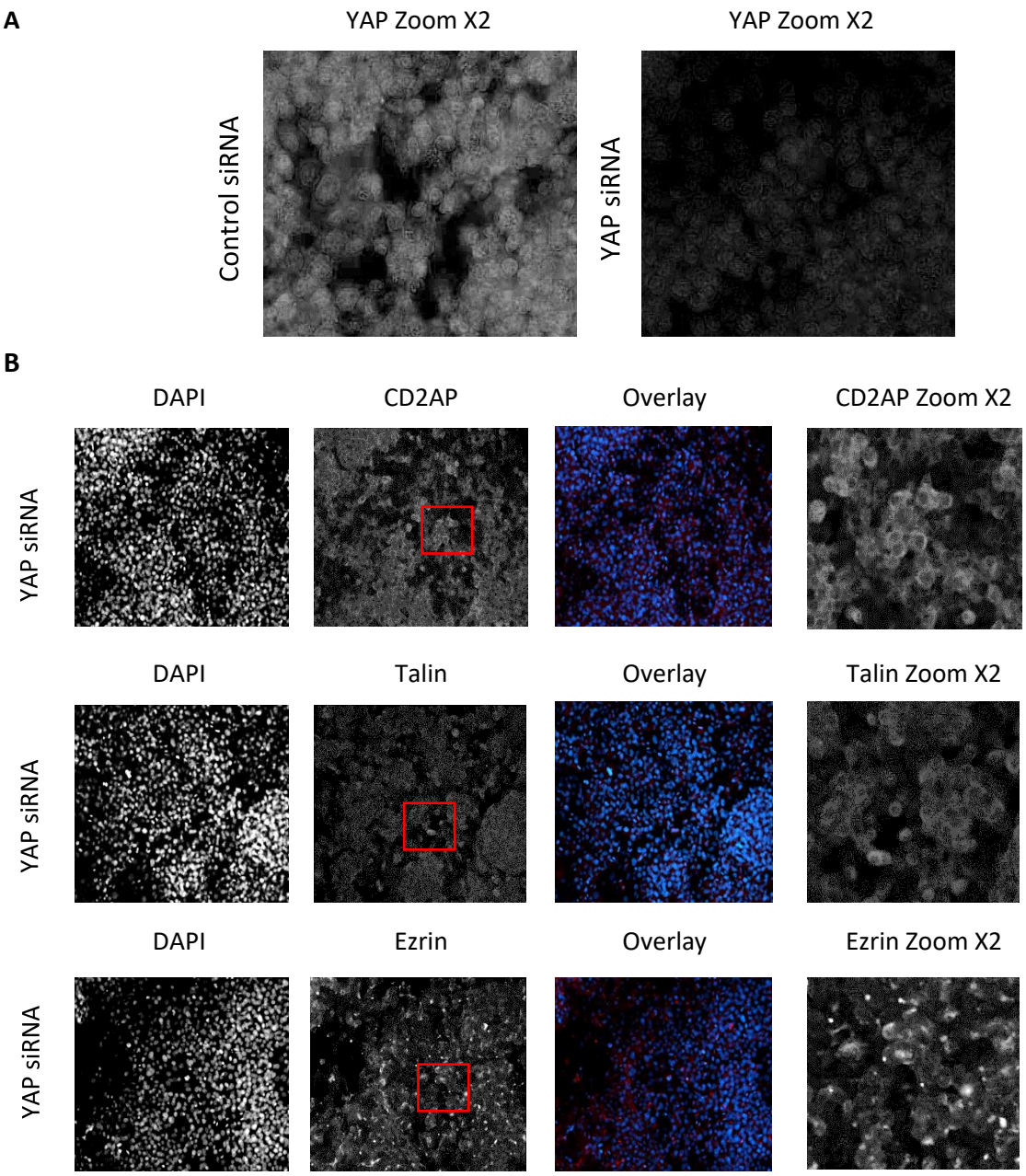

Figure 3.25. The depletion of YAP and cellular localization of CD2AP, Talin and Ezrin upon siRNA mediated knockdown of YAP determined by immunofluorescence staining in confluent Hep-G2 cells. Hep-G2 cells were transfected with YAP siRNA. Cells were fixed after 72hours using 4% PFA. Coverslips were stained for proteins indicated. DAPI (blue) used for staining the cell nuclei and CY3 (red) used for all proteins; YAP, CD2AP,Talin, and Ezrin. Images were taken with Evos fl Fluorescence microscope at 20X magnification. For each protein, an inset of the image is provided in the last panel at a 2X zoom to show the localisation of proteins more clearly. Representative IF images from one experiment are displayed amongst 4 independent repeats.

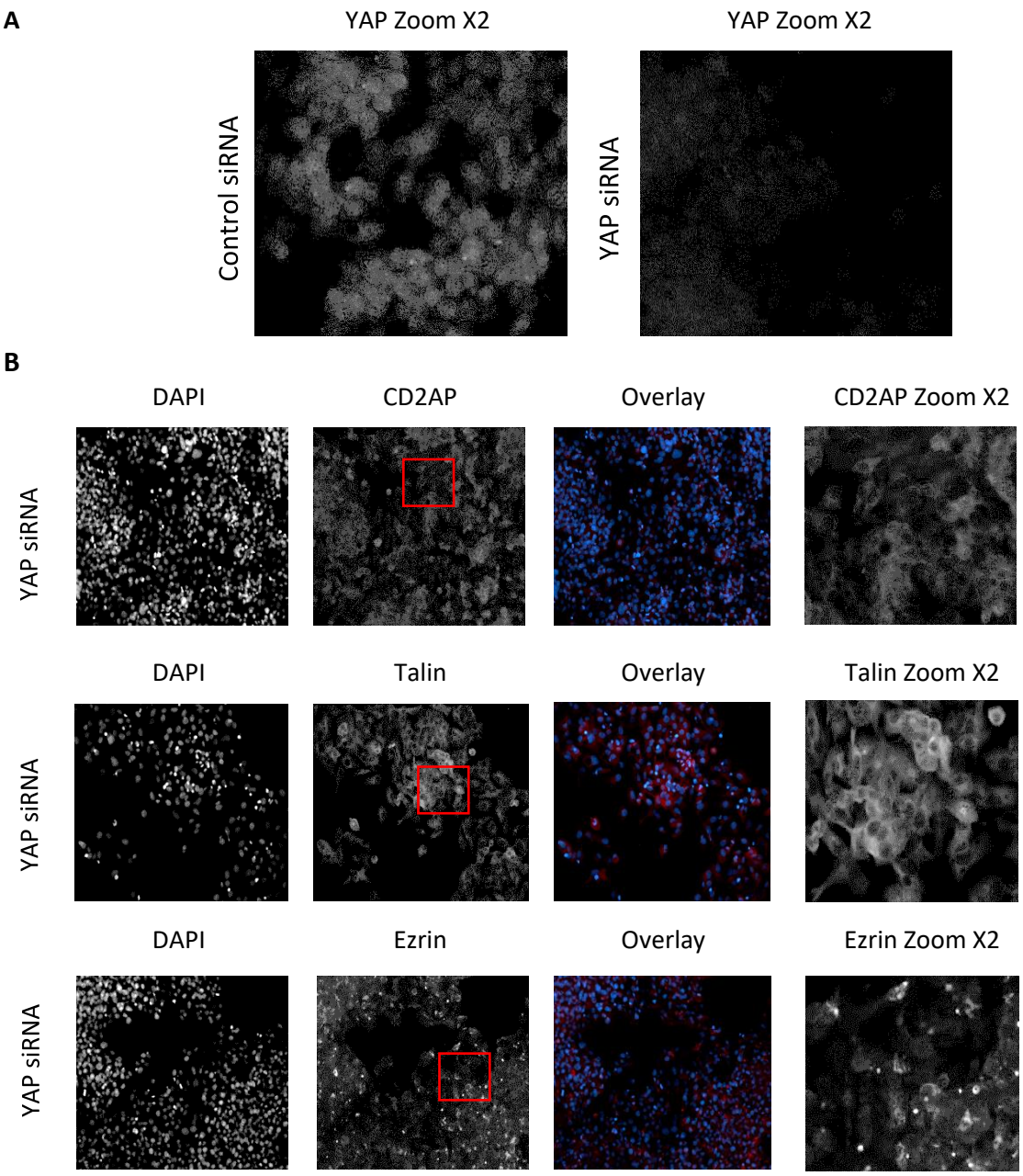

Figure 3.26. The depletion of YAP and cellular localization of CD2AP, Talin and Ezrin upon siRNA mediated knockdown of YAP determined by immunofluorescence staining in sparse Hep-G2 cells.

Hep-G2 cells were transfected with YAP siRNA. Cells were fixed after 72hours using 4% PFA. Coverslips were stained for proteins indicated. DAPI (blue) used for staining the cell nuclei and CY3 (red) used for all proteins; YAP, CD2AP, Talin, and Ezrin. Images were taken with Evos fl Fluorescence microscope at 20X magnification. For each protein, an inset of the image is provided in the last panel at a 2X zoom to show the location of proteins more clearly. Representative IF images from one experiment are displayed amongst 4 independent repeats.

CD2-associated protein (CD2AP) expression was silenced by CD2AP siRNA to assess the translocation of YAP. Knockdown of CD2AP was effective when compared to control in confluent and sparse Hep-G2 cells as indicated in Figure 3.27 and 3.28 respectively. The translocation of YAP was not changed upon silencing of CD2AP but the expression of YAP was less in confluent cells upon depletion of CD2AP in comparison to control as represented in Figure 3.27 where in sparse cells YAP was nuclear and not affected (Figure 3.28).

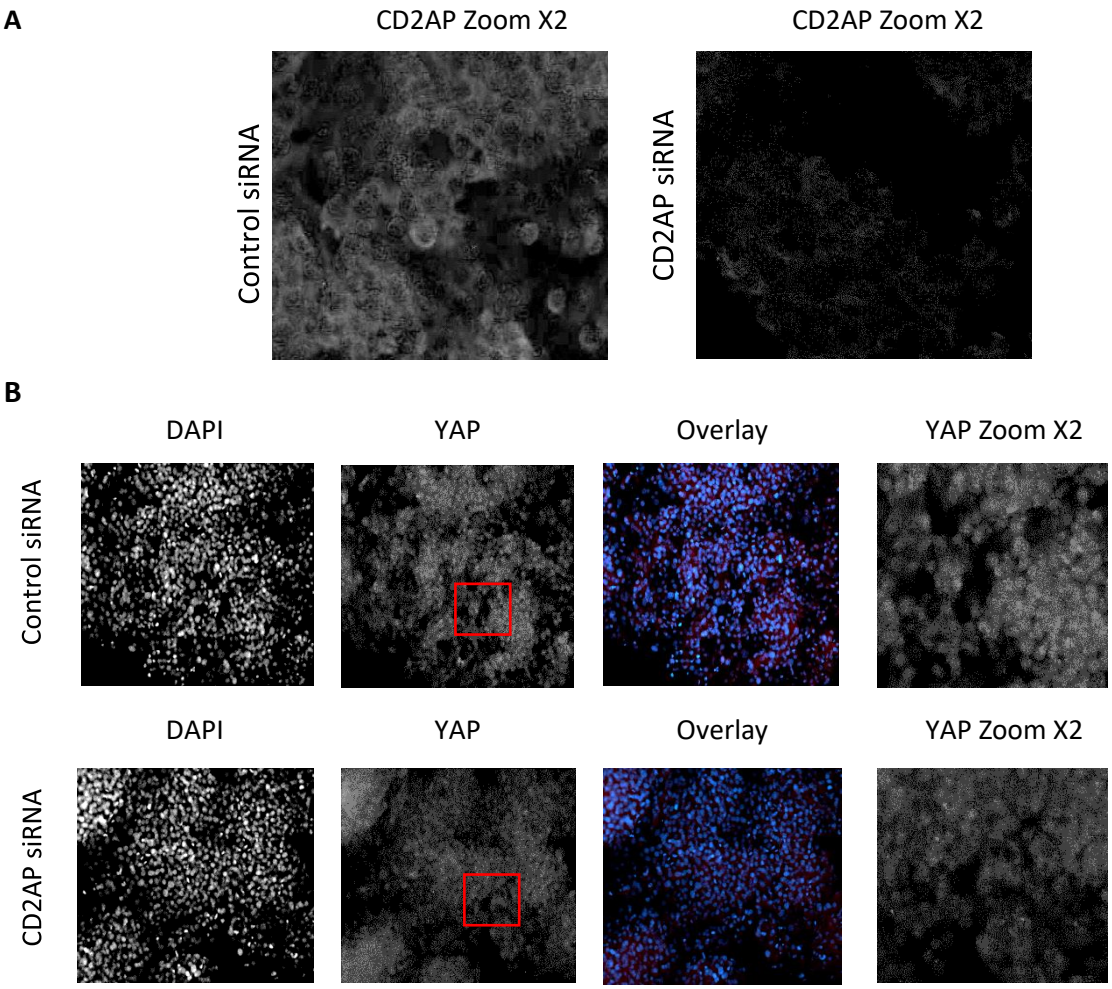

Figure 3.27. The depletion of CD2AP and cellular localization of YAP upon siRNA mediated knockdown of CD2AP determined by immunofluorescence staining in confluent Hep-G2 cells. Hep-G2 cells were transfected with CD2AP siRNA. Cells were fixed after 72hours using 4% PFA. Coverslips were stained for proteins indicated. DAPI (blue) used for staining the cell nuclei and CY3 (red) used to stain CD2AP and YAP. Images were taken with Evos fl Fluorescence microscope at 20X magnification. For each protein, an inset of the image is provided in the last panel at a 2X zoom to show the location of proteins more clearly. Representative IF images from one experiment are displayed amongst 4 independent repeats.

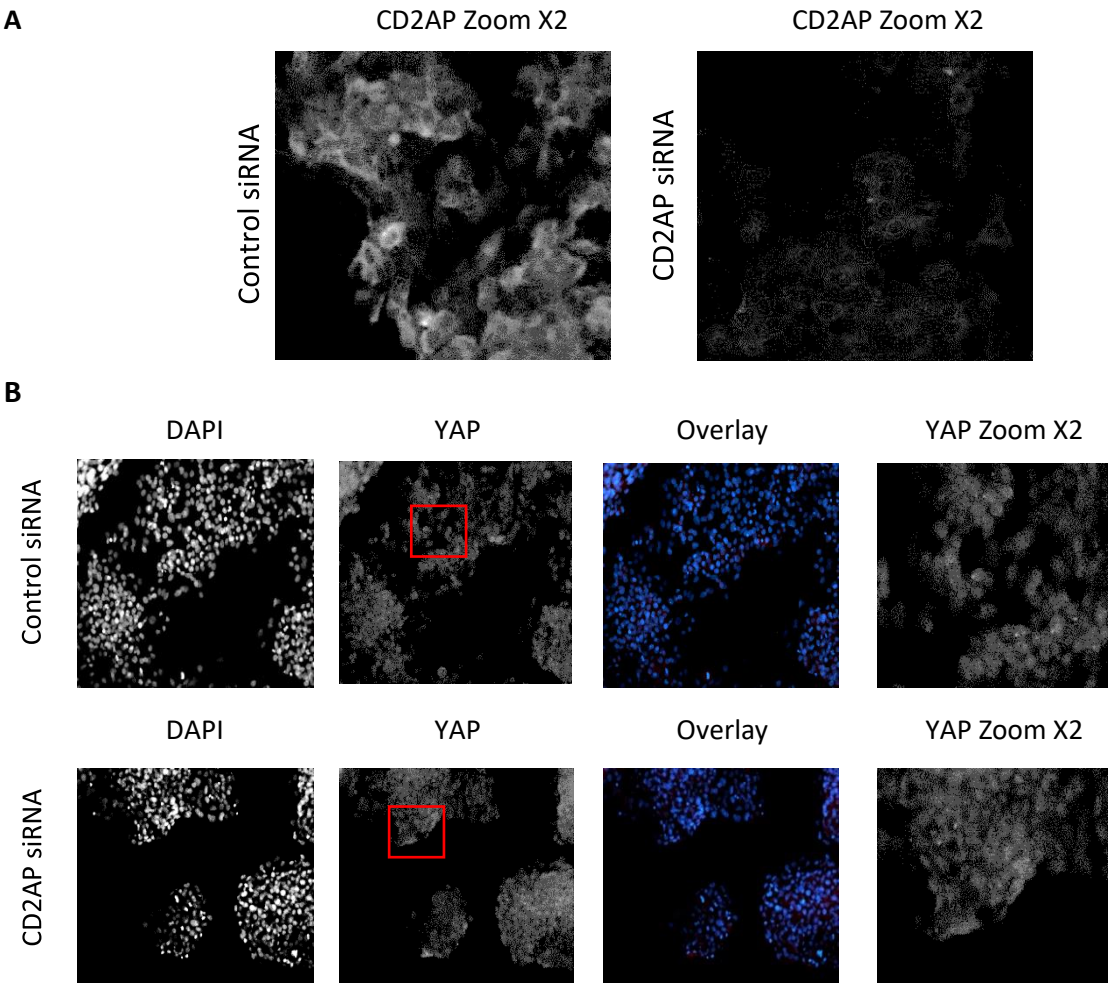

Figure 3.28. The depletion of CD2AP and cellular localization of YAP upon siRNA mediated knockdown of CD2AP determined by immunofluorescence staining in sparse Hep-G2 cells. Hep-G2 cells were transfected with CD2AP siRNA. Cells were fixed after 72hours using 4% PFA. Coverslips were stained for proteins indicated. DAPI (blue) used for staining the cell nuclei and CY3 (red) used to stain CD2AP and YAP. Images were taken with Evos fl Fluorescence microscope at 20X magnification. For each protein, an inset of the image is provided in the last panel at a 2X zoom to show the location of proteins more clearly. Representative IF images from one experiment are displayed amongst 4 independent repeats.

Expression of talin was depleted via siRNA-mediated knockdown to determine the translocation of YAP in confluent and sparse Hep-G2 cells. The efficiency of knockdown in comparison to control siRNA indicated in Figure 3.29 and 3.30 showing the depletion of Talin. Upon knockdown of Talin, YAP was observed to be more cytoplasmic at both

confluent and sparse conditions (Figure 3.29 and 3.30) as Talin is involved in the activation of YAP thus its nuclear translocation (Dasgupta and McCollum, 2019).

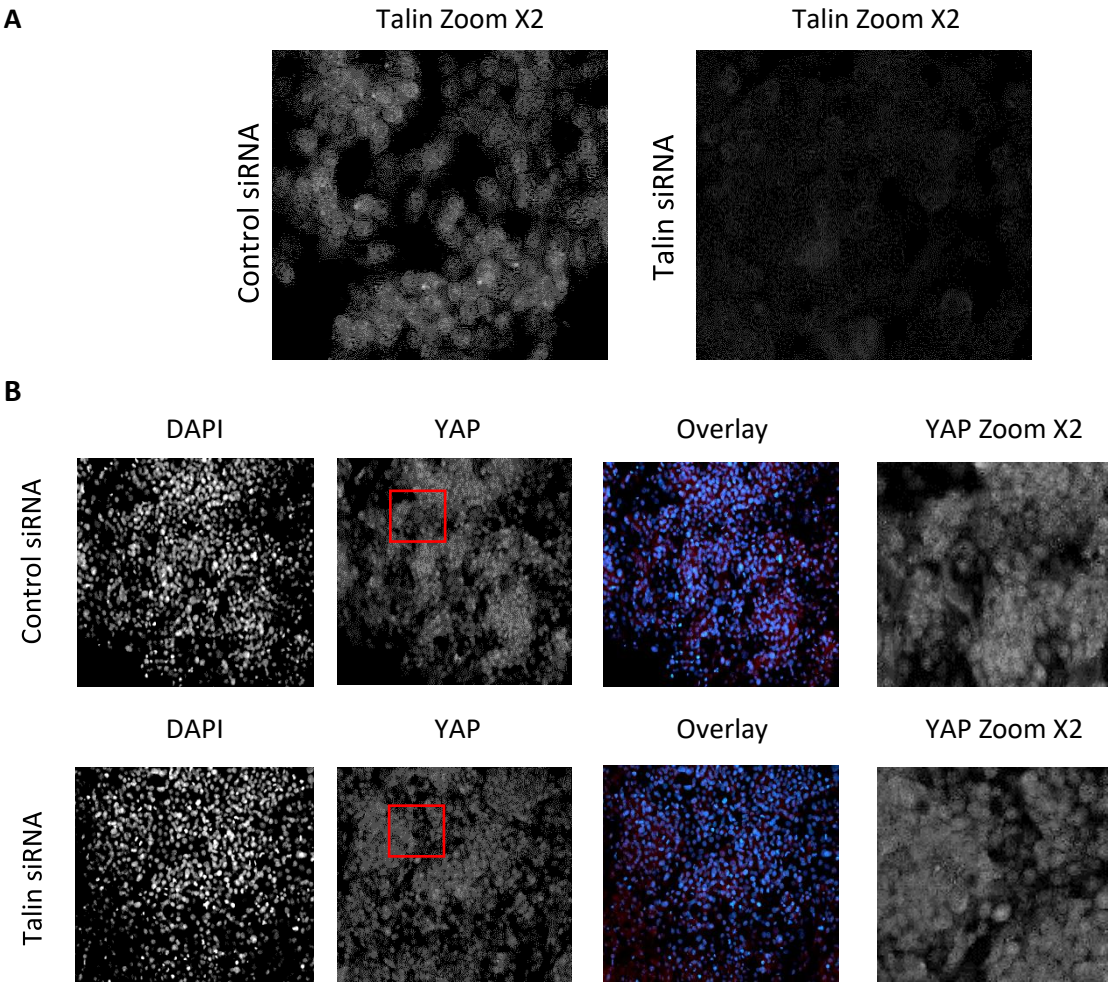

Figure 3.29. The depletion of Talin and cellular localization of YAP upon siRNA mediated knockdown of Talin determined by immunofluorescence staining in confluent Hep-G2 cells. Hep-G2 cells were transfected with Talin siRNA. Cells were fixed after 72hours using 4% PFA. Coverslips were stained for proteins indicated. DAPI (blue) used for staining the cell nuclei and CY3 (red) used to stain Talin and YAP. Images were taken with Evos fl Fluorescence microscope at 20X magnification. For each protein, an inset of the image is provided in the last panel at a 2X zoom to show the location of proteins more clearly. Representative IF images from one experiment are displayed amongst 4 independent repeats.

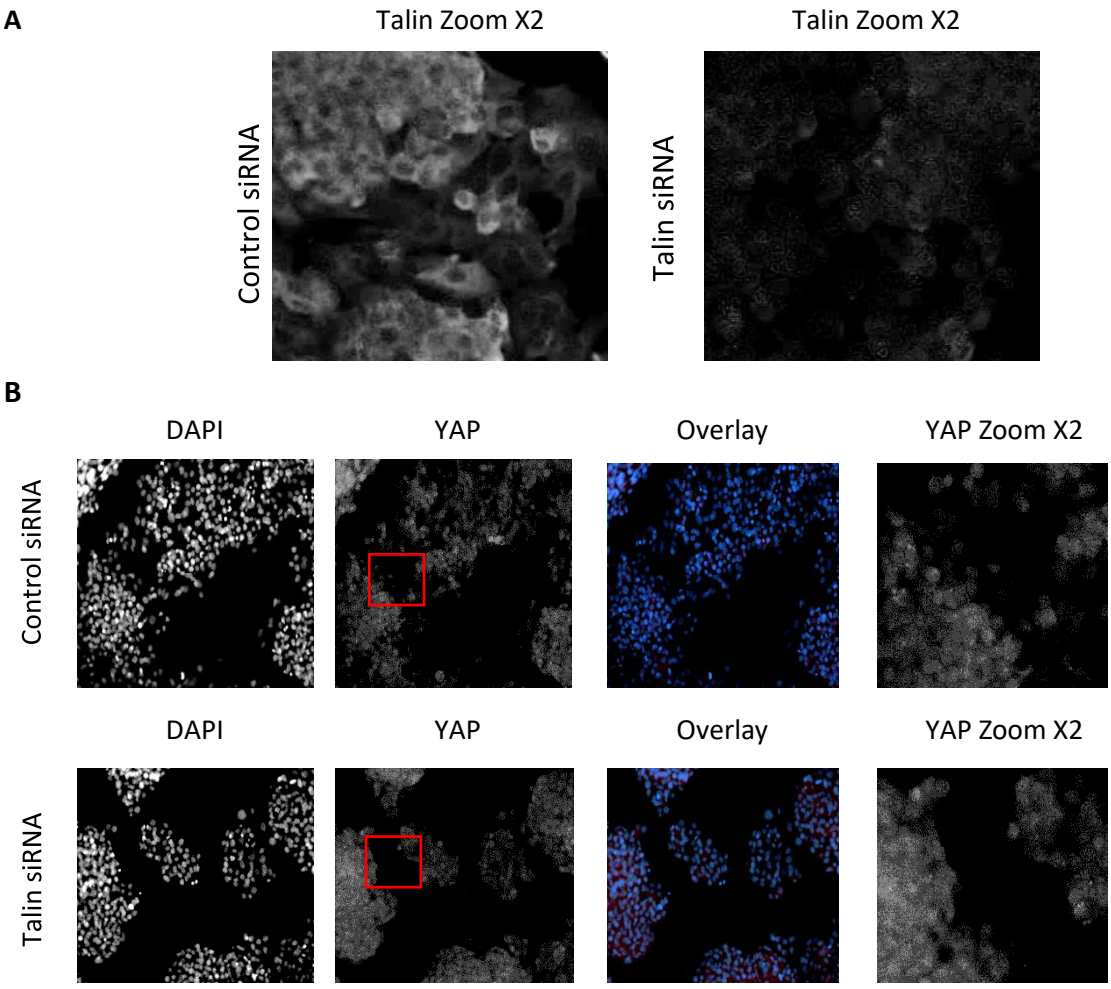

Figure 3.30. The depletion of Talin and cellular localization of YAP upon siRNA mediated knockdown of Talin determined by immunofluorescence staining in sparse Hep-G2 cells. Hep-G2 cells were transfected with Talin siRNA. Cells were fixed after 72hours using 4% PFA. Coverslips were stained for proteins indicated. DAPI (blue) used for staining the cell nuclei and CY3 (red) used to stain Talin and YAP. Images were taken with Evos fl Fluorescence microscope at 20X magnification. For each protein, an inset of the image is provided in the last panel at a 2X zoom to show the location of proteins more clearly. Representative IF images from one experiment are displayed amongst 4 independent repeats.

The Ezrin was depleted and translocation of YAP was determined via immunofluorescence staining in confluent and sparse Hep-G2 cells. The expression of ezrin was effectively suppressed which can be clearly seen in Figure 3.31 and 3.32. Ezrin knockdown did not affect YAP translocation under both confluent and sparse conditions compared to control

siRNA (Figure 3.31 and 3.32). The regulation of YAP by ezrin might be different in Hep-G2 cells.

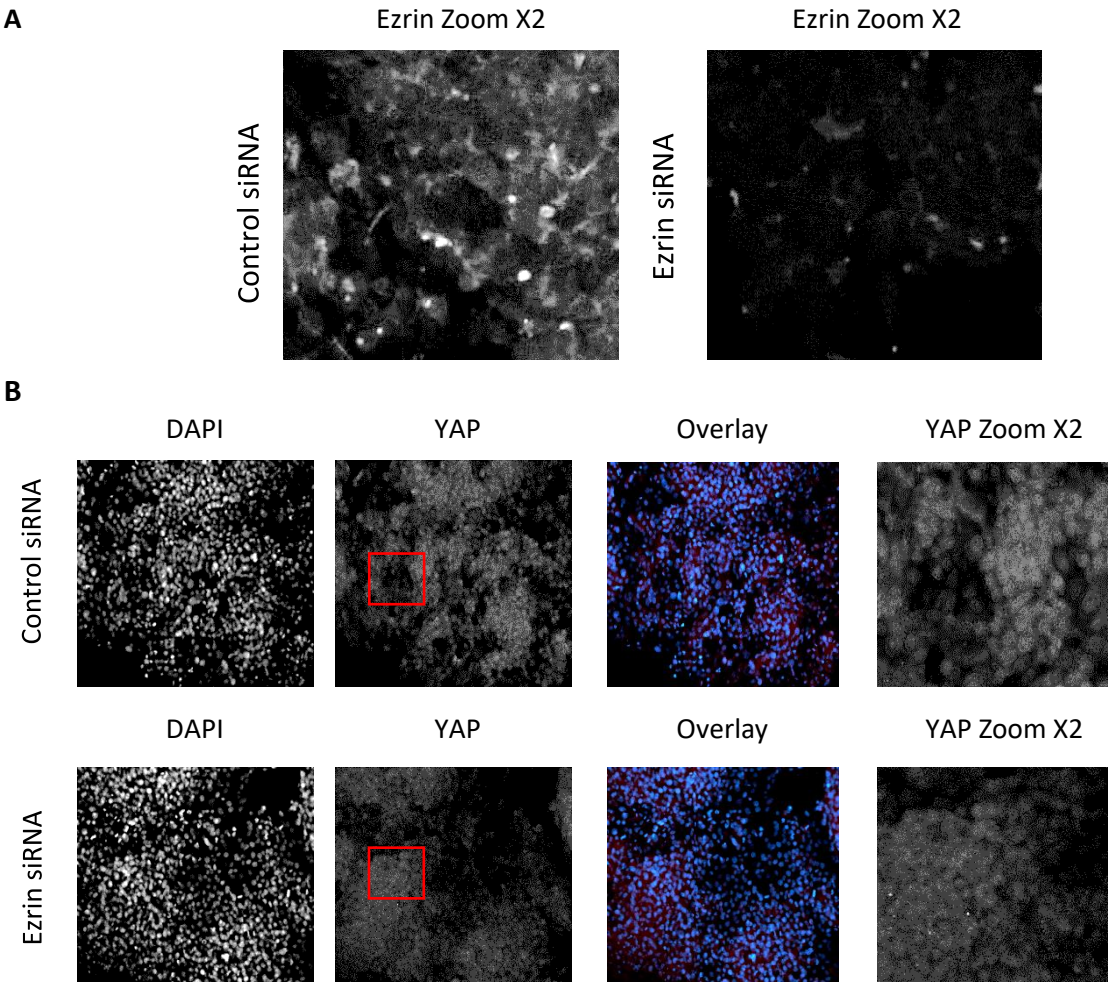

Figure 3.31. The depletion of Ezrin and cellular localization of YAP upon siRNA mediated knockdown of Ezrin determined by immunofluorescence staining in confluent Hep-G2 cells. Hep-G2 cells were transfected with Ezrin siRNA. Cells were fixed after 72hours using 4% PFA. Coverslips were stained for proteins indicated. DAPI (blue) used for staining the cell nuclei and CY3 (red) used to stain Ezrin and YAP. Images were taken with Evos fl Fluorescence microscope at 20X magnification. For each protein, an inset of the image is provided in the last panel at a 2X zoom to show the location of proteins more clearly. Representative IF images from one experiment are displayed amongst 4 independent repeats.

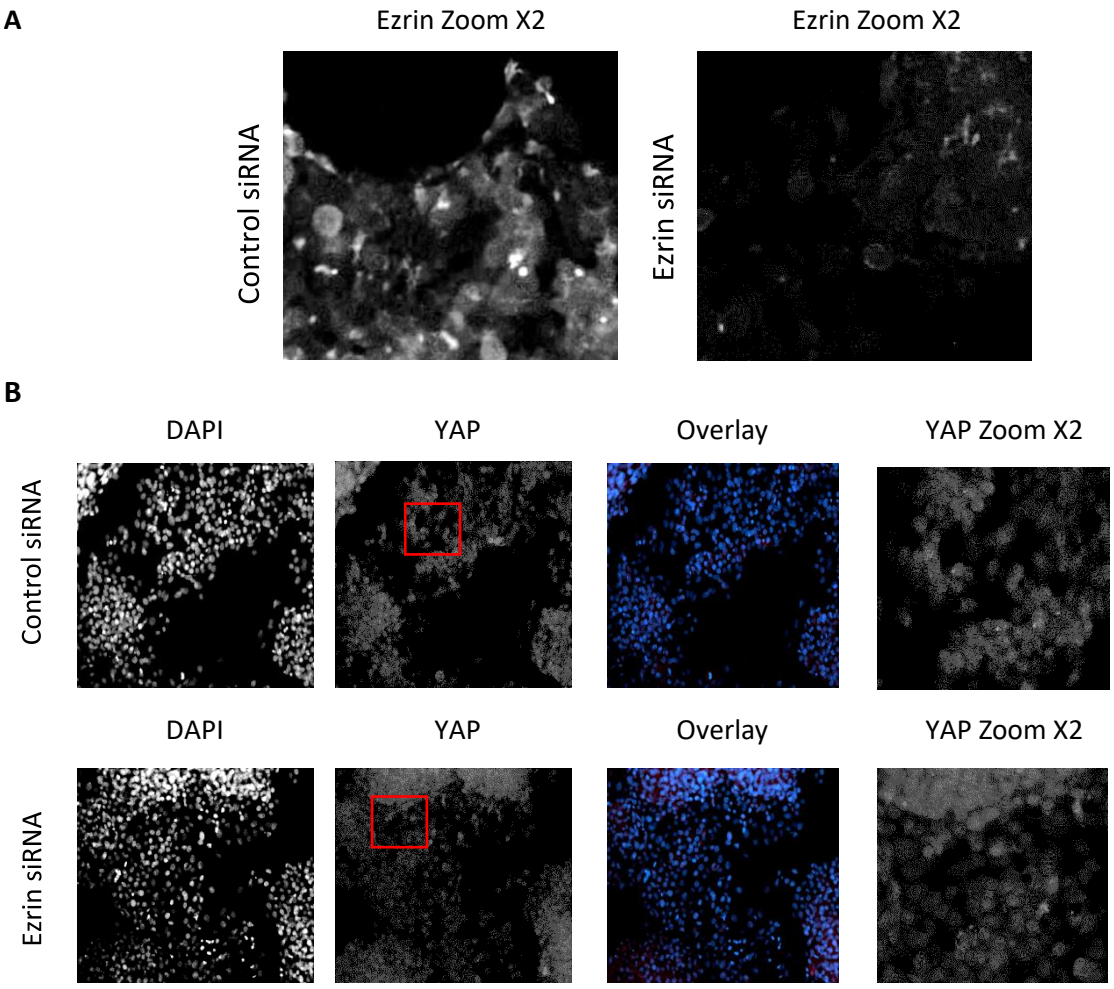

Figure 3.32. The depletion of Ezrin and cellular localization of YAP upon siRNA mediated knockdown of Ezrin determined by immunofluorescence staining in sparse Hep-G2 cells. Hep-G2 cells were transfected with Ezrin siRNA. Cells were fixed after 72hours using 4% PFA. Coverslips were stained for proteins indicated. DAPI (blue) used for staining the cell nuclei and CY3 (red) used to stain Ezrin and YAP. Images were taken with Evos fl Fluorescence microscope at 20X magnification. For each protein, an inset of the image is provided in the last panel at a 2X zoom to show the location of proteins more clearly. Representative IF images from one experiment are displayed amongst 4 independent repeats.

CHAPTER 4. EFFECT OF LIPID METABOLISM ON THE HIPPO SIGNALLING PATHWAY

CHAPTER 4. EFFECT OF LIPID METABOLISM ON THE HIPPO SIGNALLING PATHWAY

Lipid metabolism is a fundamental aspect of an organism, involved in synthesis of cell membranes, essential for cellular function by supplying energy (Santos and Schulze, 2012; Lee, Cho and Jho, 2022). Lipids play an important role in signal transduction and are crucial elements of cell proliferation as they are involved in synthesis of cell membranes as precursors (Koo and Guan, 2018; Abrass, 2004). Cells tightly regulate the synthesis and degradation of lipids to maintain an energy homeostasis and to control their functions in signalling as alterations in lipid metabolism can have an impact on cellular proliferation, differentiation and growth (Santos and Schulze, 2012; Abrass, 2004). The activity of Hippo signalling pathway effectors, YAP/TAZ have been implicated to be regulated by signals from lipids and glucose in context of cellular metabolism but how metabolic processes regulate the pathway is relatively obscure (Koo and Guan, 2018). Dysregulation of the Hippo signalling pathway can lead to disruption of metabolic pathways fundamental in diseases such as cancer, obesity and diabetes (Nguyen-Lefebvre *et al*., 2021).

This chapter will focus on the effect of lipid metabolism on the Hippo signalling pathway as there is increasing evidence to show that manipulation of lipid metabolism could affect YAP/TAZ activation (Koo and Guan, 2018; Yamaguchi and Taouk, 2020). Chapter 3 introduced a novel ECM/Hippo complex. The next aspect is to assess if this is regulated by lipid manipulation. In this chapter, assessment of cellular morphology and the effect of migration upon addition of lipids was determined in CaCo-2 cells. CaCo-2 cells were treated with lipids and cellular migration was analysed over time with scratch assay closure. A notable effect was observed on cellular migration upon lipid treatment. Cells were treated with various concentrations of two types of lipids: oleic acid or palmitic acid to observe their relationship with YAP and the activation state of the protein by assessing YAP

phosphorylation levels and thus the effect on Hippo signalling pathway activity. The pYAP (S127) antibody directly measures the serine residue which the upstream kinase of the Hippo signalling pathway LATS phosphorylates YAP to inactivate the protein. Thus, western-blot analysis was performed to assess the activity of YAP by quantifying its phosphorylation levels upon lipid treatment. Immunofluorescence microscopy was then used to evaluate levels of lipid droplet composition by addition of oleic acid in conjunction with siRNA mediated knockdown of proteins within the novel complex as characterised in chapter 3 both in CaCo-2 and Hep-G2 cell lines. In addition, localisation of proteins of the complex was observed upon treatment of cells with oleic acid by immunofluorescence. In summary, this chapter summarises the effect of lipid metabolism on the Hippo signalling pathway effector YAP and components of the ECM/Hippo signalling pathway.

4.1 Lipid treatment and cellular migration

CaCo-2 cells were treated with either 2 mM oleic acid or 0.5 mM palmitic acid and the rate of cellular migration evaluated in comparison to control cells with assessment at time 0 and 24 and 48 hours post scratch. The experiment was repeated 3 times, N=3. Scratch assays were used for assessment of cellular migration. Colorectal cancer cells treated with lipids showed a marked decrease in cell migration compared to control. The images in the first row of Figure 4.0 show scratched images at time 0 after immediate lipid treatment. The second and third rows of images indicate the scratched images after 24 and 48 hours of lipid treatments respectively. After 48 hours, the scratched well in control cells completely closed, whereas the scratched wells in both oleic and palmitic acid treated cells were still open which suggests a clear deceleration in cellular migration after treating the cells with lipids possibly due to the lipids causing an inactivation on YAP (Figure 4.0 (D)).

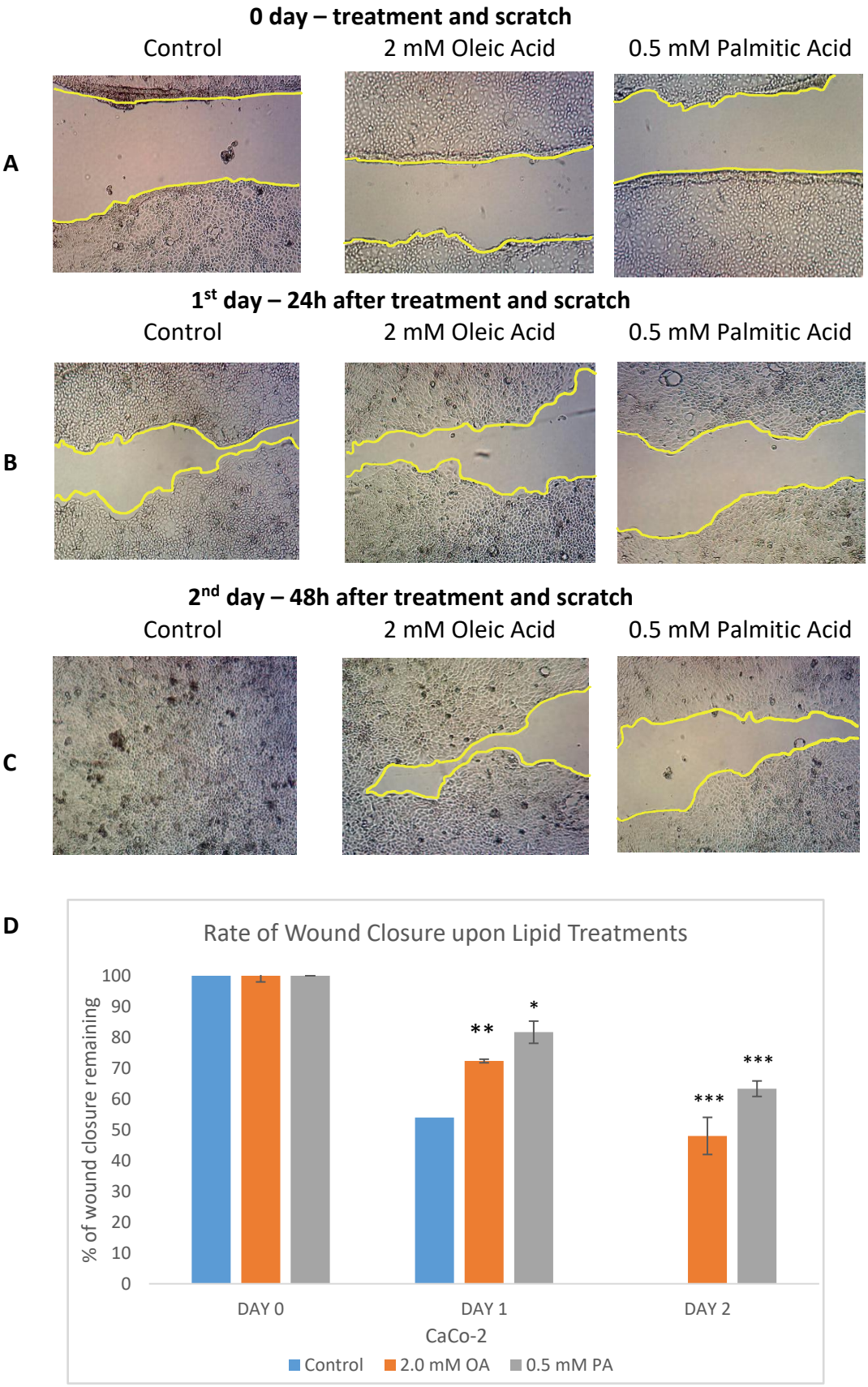

Figure 4.0 Scratch assay analysis with Oleic and Palmitic Acid treatments in CaCo-2 cell line. Representative brightfield images of scratch assay wells comparing control cells and cells treated with either 2 mM Oleic Acid or 0.5 mM Palmitic acid showing cellular migration at indicated time points (Time 0 (A) , 24h (B) and 48h (C)). Representative images of N=3 experiments. (D)

Quantitative graph showing the rate of wound closure upon OA and PA treatments compared to control siRNA. Graph was obtained from the pooled data of 3 independent experiments and represented as mean ± standard deviation (SD), N=3. Statistical importance of control versus OA and PA was determined by T-Test with a significant p values of *$p \leq 0.05$, ** $p \leq 0.01$ and ***$p \leq 0.0001$.

4.2 Effect of various oleic acid concentrations on YAP phosphorylation in CaCo-2 cells

CaCo-2 cells were then treated with various concentrations of the lipid oleic acid to observe if there was an effect of oleic acid directly on YAP phosphorylation levels to explain the observation seen with the decrease in cellular migration (Figure 4.0) and whether this was an effect on YAP directly. In order to evaluate the activity of YAP, western-blot analysis was carried out and phosphorylation levels of YAP at its serine 127 site was assessed. CaCo-2 cells were initially treated with oleic acid at varying concentrations of 1 mM, 0.5 mM and 0.1 mM for 4 hours. Each OA treatment was repeated 4 times, N=4. Oleic acid treatment at the different concentrations was not distinguishable to the control from the immunoblot image in Figure 4.1(A). However, quantification of the immunoblot by use of a graph in Figure 4.1(B) shows that the treatment of cells with the highest concentration of oleic acid (1 mM), increased the pYAP levels compared to control cells which corresponds with deactivation of YAP however, the increase was not statistically significant. Phosphorylation levels of YAP with 0.5 mM and 0.1 mM oleic acid stimulation also seemed to cause a slight decrease in the level of pYAP compared to control but again the decrease is not statistically significant. As seen in the quantification graph, Figure 4.1(B), a higher concentration of oleic acid treatment of CaCo-2 cells resulted in a further increase in phosphorylation level of YAP but this was not the significant.

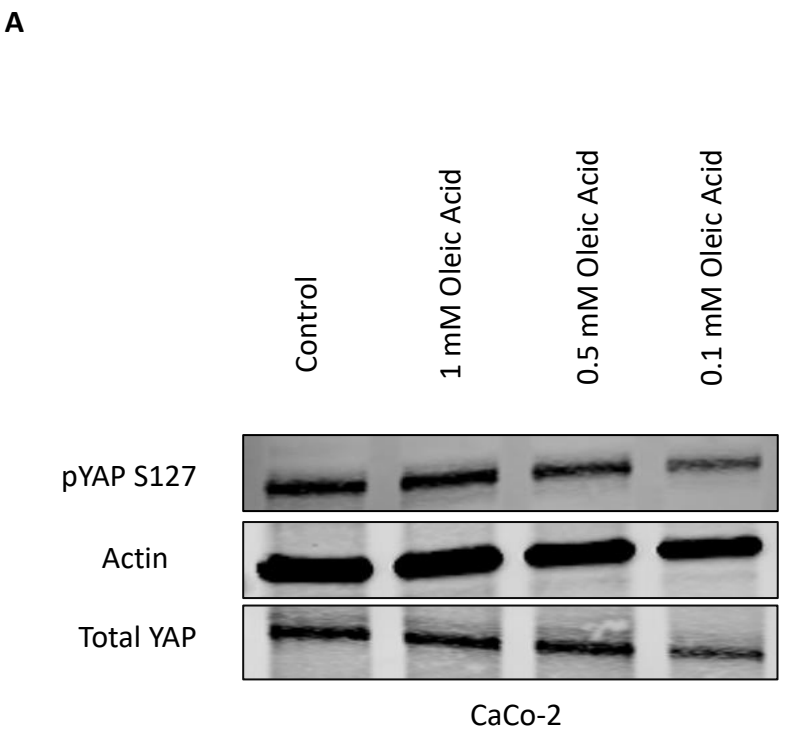

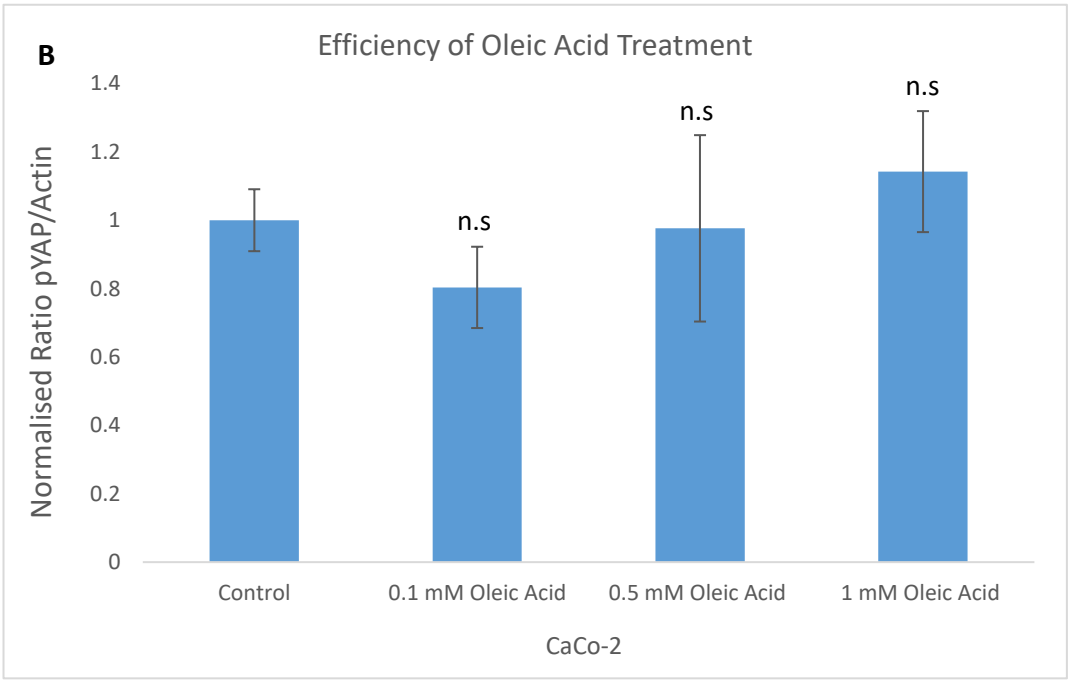

Figure 4.1 Effect of oleic acid treatments in different concentrations (1 mM, 0.5 mM and 0.1 mM respectively) on YAP (S127 site) phosphorylation in CaCo-2 cell line by western-blot analysis.(A) Western blot image of the effect of oleic acid treatments with different concentrations on phosphorylation levels of YAP in Caco-2 cells. Representative blots from one experiment (n=4) are displayed amongst four repeats per experiment (B) Quantification graph of phosphorylation levels of YAP upon treatment of oleic acid with various concentrations compared to control cells. Graph

was obtained from the pooled data of 4 independent experiments and represented as mean ± standard deviation (SD), N=4. Statistical importance of control versus different concentrations of oleic acid was determined by T-Test relating to YAP (S127) phosphorylation levels with p values above 0.05 which are statistically not-significant; $p>0.05$.

As low concentrations had no significant effect on YAP phosphorylation, higher concentrations of oleic acid were tested but still had no effect on YAP phosphorylation and thus activation. CaCo-2 cells were treated with concentrations of 1 mM, 1.5 mM, 2 mM and 2.5 mM oleic acid in Figures 4.2 and 4.3. The CaCo-2 cells stimulated with 2 mM oleic acid resulted in an increase in YAP phsophorylation. The increase was subtle in western-blot images represented in Figure 4.2(A) and Figure 4.3(A) but an evident inactivation of YAP with an increase in its phosphorylation level was indicated in the quantification graphs, Figure 4.2(B) and Figure 4.3(B). The 1 mM OA did not have any obvious effect on pYAP levels as previously observed thus acted as a good internal control, whereas 1.5 mM and 2.5 mM oleic acid concentrations increased the YAP phosphorylation levels but not as significantly as 2 mM oleic acid. This could be due to oversaturation of cells with oleic acid where 2 mM appears to be the optimum point at which an effect can be observed.

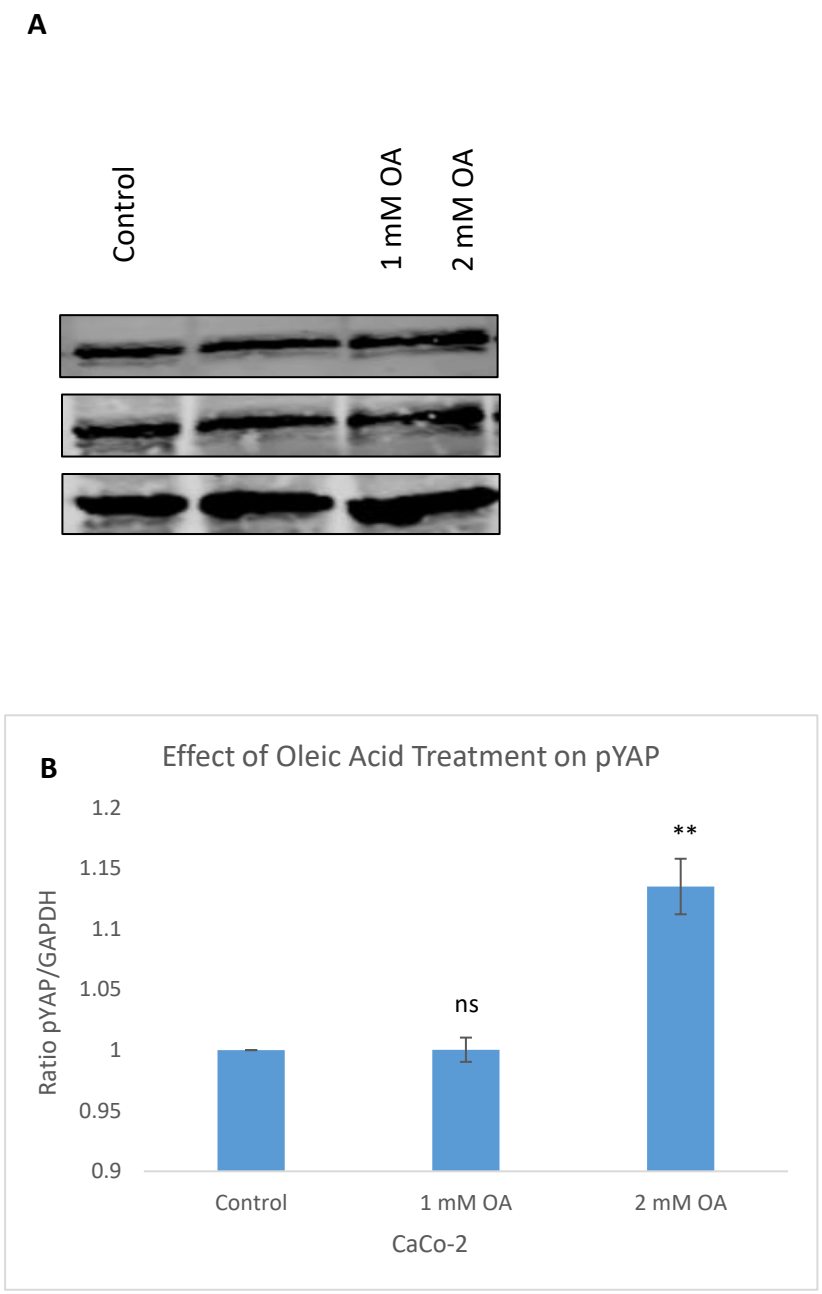

Figure 4.2 Effect of higher concentrations of oleic acid on YAP phosphorylation in CaCo-2 cell line. (A) Western blot image of the effect of oleic acid treatments with 1 mM and 2 mM concentrations on phosphorylation levels of YAP in Caco-2 cells. (B) Quantification graph of phosphorylation levels of YAP versus GAPDH upon treatment of oleic acid with various concentrations compared to control cells. (C) Quantification graph of pYAP versus total YAP upon treatment of oleic acid with various concentrations compared to control cells. Graph was represented as mean ± standard deviation (SD), N=1. Statistical importance of control versus different concentrations of oleic acid was determined by T-Test relating to YAP (S127) phosphorylation levels with p values of $p>0.05$ (n.s, statistically not-significant) and $^{**}p\leq0.01$ (statistically significant).

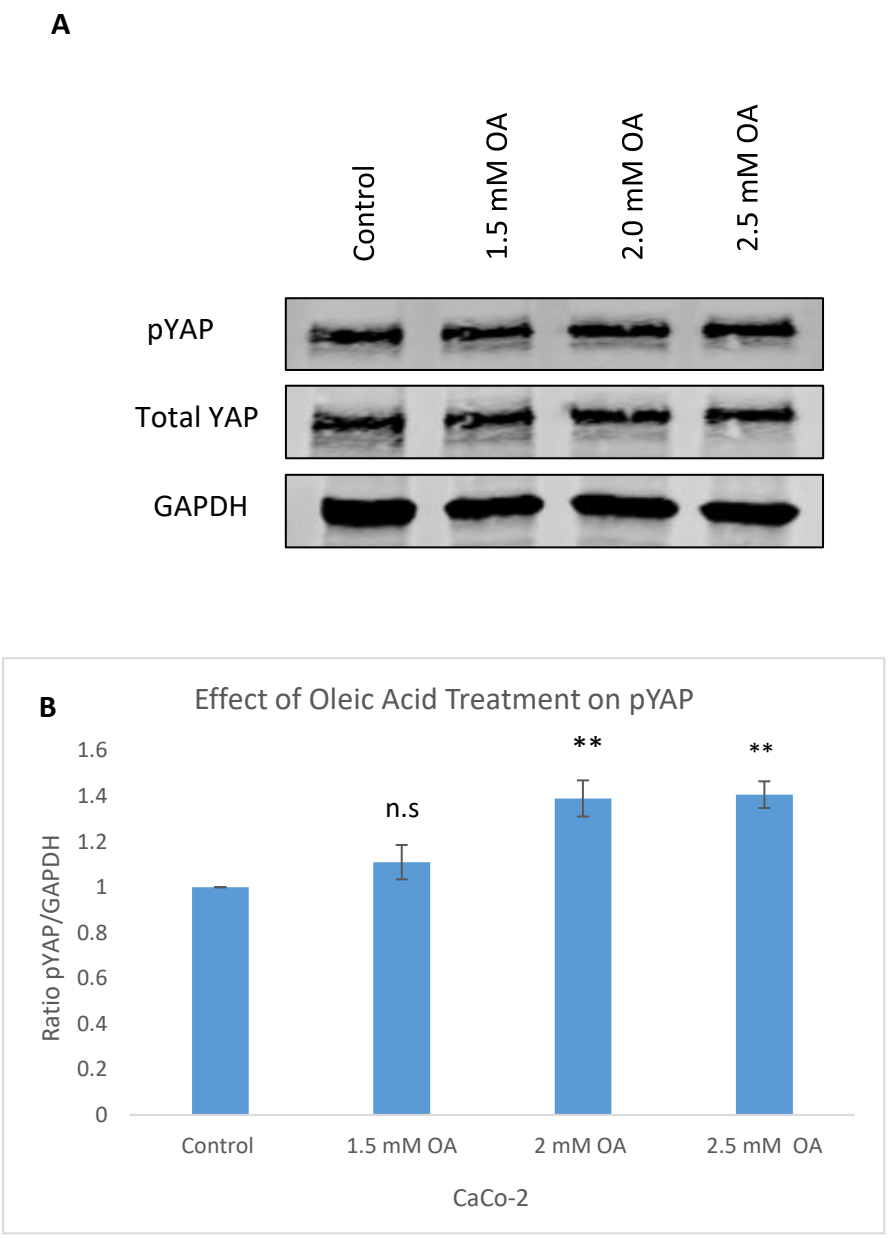

Figure 4.3 Effect of higher concentrations (1.5 mM, 2 mM, 2.5 mM) of oleic acid treatments on YAP (S127 site) phosphorylation in CaCo-2 cell line by western-blot analysis. (A) Western blot image of the effect of oleic acid treatments with 1.5 mM, 2 mM and 2.5 mM concentrations on phosphorylation levels of YAP in Caco-2 cells. (B) Quantification graph of phosphorylation levels of YAP versus GAPDH upon treatment of oleic acid with various concentrations compared to control cells. (C) Quantification graph of pYAP versus total YAP upon treatment of oleic acid with various concentrations compared to control cells. Graph was obtained represented as mean ± standard deviation (SD), N=1. Statistical importance of control versus different concentrations of oleic acid was determined by T-Test relating to YAP (S127) phosphorylation levels with p values above 0.05 which are statistically not-significant; $p>0.05$ and $**p\leq0.01$, statistically significant.

4.3 Effect of Lipid Treatments in CaCo-2 Cells on YAP Phosphorylation

CaCo-2 cells were treated with either 2 mM oleic acid, 0.5 mM palmitic acid or a combination of both to examine if differing lipids would have an effect of on the phosphorylation level of YAP. Each experiment was repeated 3 times, N=3. Observation of an effect with treatments with 2 mM oleic and 0.5 mM palmitic acid is not hugely obvious in the immunoblot image in Figure 4.4(A) when compared to control band but, the 2 mM oleic acid and 0.5 mM palmitic acid was quite clearly increased. This is also clearly reflected in Figure 4.4(B) that treatments of oleic and palmitic acid correlates with the deactivation of YAP by a significant increase in phosphorylation levels compared to control cells. CaCo-2 cells treated with oleic acid concentration of 2 mM were shown to increase phosphorylation level of YAP significantly, $p<0.05$. Treatment of CaCo-2 cells with palmitic acid resulted in higher YAP deactivation by increasing the phosphorylation level of YAP by 2.5 fold compared to oleic acid treatment. The remarkable increase in pYAP levels when treated with 0.5 mM palmitic acid is statistically significant with $p<0.05$. However, treatment of cells with a combination of oleic acid and palmitic acid did not result in higher phosphorylation of YAP and may have had an opposite effect in that both lipids may have affected one another, the increase in pYAP levels in combined treatments was thus statistically not significant when compared to control cells.

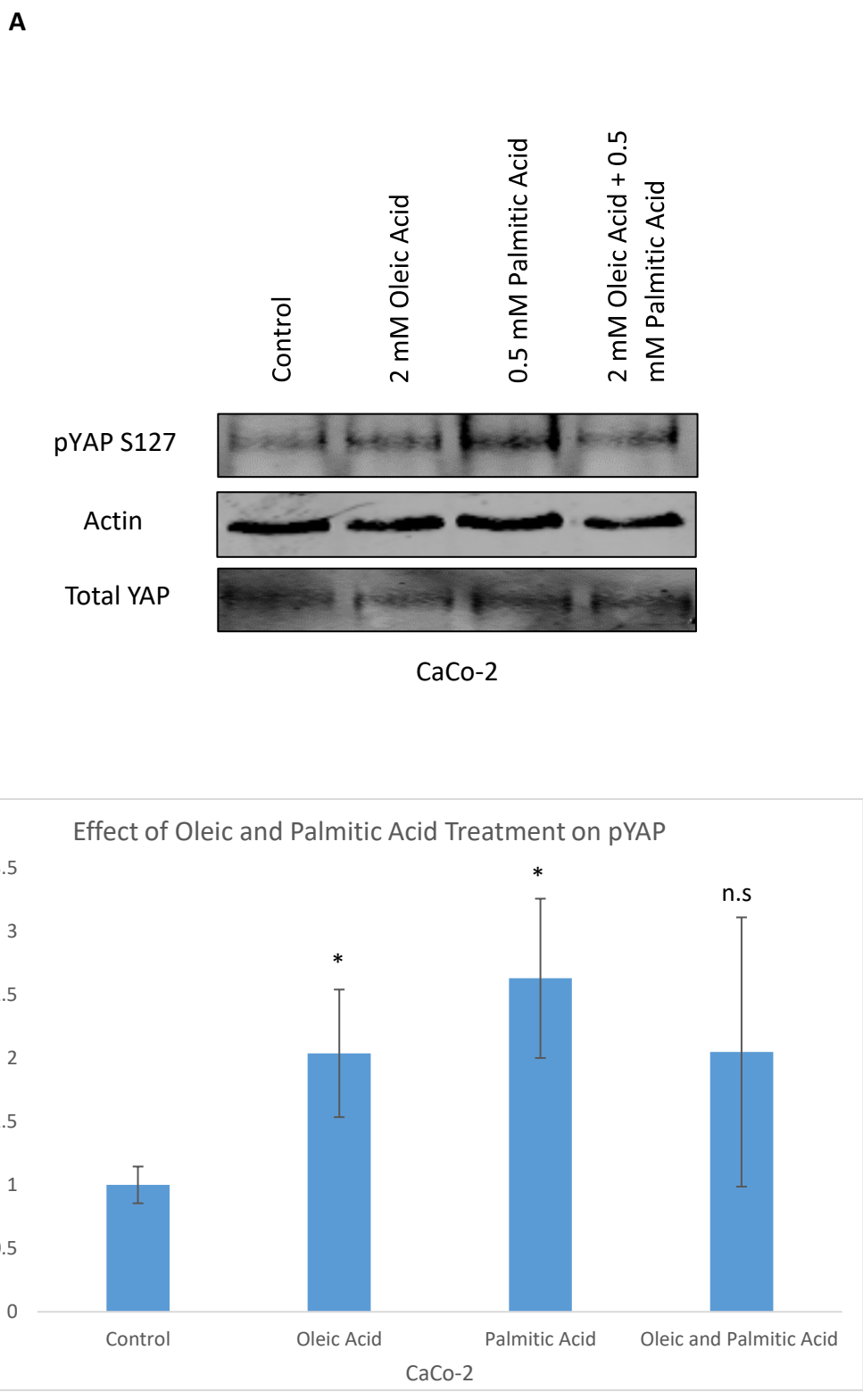

Figure 4.4 Effect of both oleic acid and palmitic acid treatments on YAP (S127 site) phosphorylation in Caco-2 cell line by western-blot analysis.(A) Western blot image of the effect of 2 mM oleic acid, 0.5 mM palmitic acid and combination of oleic and palmitic acid treatment on phosphorylation levels in Caco-2 cells. Representative blots from one experiment are displayed from three repeats (B) Quantification graph of phosphorylation levels of YAP upon treatments of oleic and palmitic acid compared to control cells. Graph was obtained from the pooled data of 3

independent experiments and represented as mean ± standard deviation (SD), N=3. Statistical importance of control versus 2 mM oleic acid and 0.5 mM palmitic acid was determined by T-Test , relating to YAP (S127) phosphorylation with a p value of 0.03 and 0.01 accordingly; $p<0.05$ which are statistically significant. T-Test was also done for control against combination of oleic and palmitic acid treatment and p value of 0.17 was obtained which is statistically not-significant; $p>0.05$.

It was quite evident that lipids had an effect on YAP activation in CaCo-2 cells, so the same was tested in Hep-G2 cells which have a central role in the regulation and metabolism of lipids (Paramitha *et al*., 2021).

4.4 Effect of different Palmitic Acid concentrations on YAP phosphorylation in Hep-G2 cells

Hep-G2 cells were used to determine the effect of lipid treatments on YAP activity. Primarily, palmitic acid at concentrations of 0.25 mM, 0.5 mM and 1 mM were used to treat Hep-G2 cells to observe the effect on YAP phosphorylation levels. Figure 4.5(A) displays western-blot images of palmitic acid treatments. An increase in pYAP levels when the cells were treated with palmitic acid was observable with an increased signal in comparison to control. Quantification graphs in Figure 4.5(B&C) shows the increase in pYAP levels as seen in the immunoblot. All palmitic acid concentrations resulted in deactivation of YAP by causing an increase in pYAP levels however, the 0.5 mM was shown to have the most significant increase in pYAP level amongst all concentrations which again, as with oleic acid maybe due to an optimal saturation of the system.

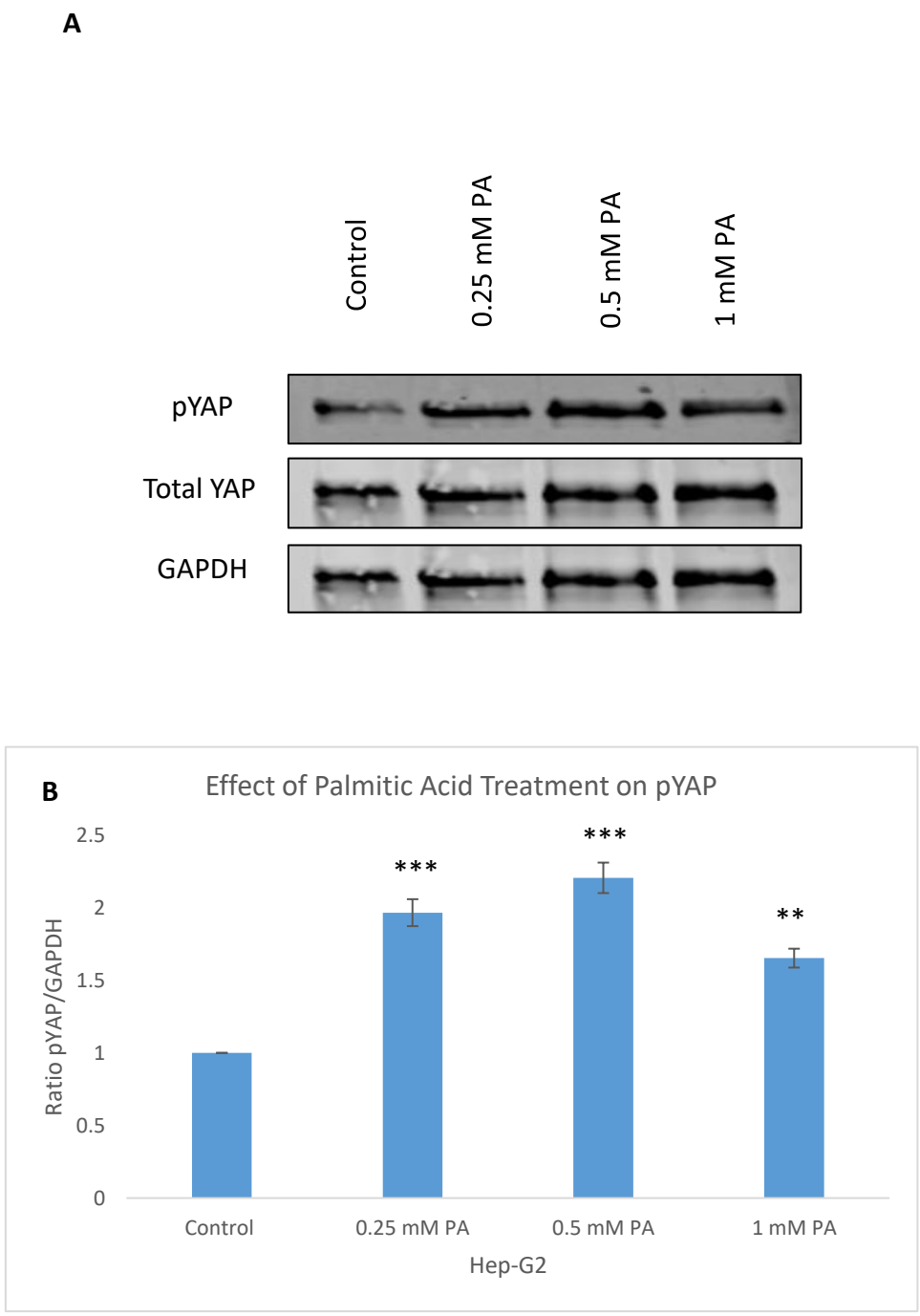

Figure 4.5 Effect of palmitic acid treatments in different concentrations (0.25 mM, 0.5 mM and 1 mM respectively) on YAP (S127 site) phosphorylation in Hep-G2 cell line by western-blot analysis. (A) Western blot image of the effect of palmitic acid treatments with different concentrations on phosphorylation levels of YAP in Hep-G2 cells. (B) Quantification graph of phosphorylation levels of YAP versus GAPDH upon treatment of palmitic acid with various concentrations. (C) Quantification graph of pYAP versus total YAP upon treatment of palmitic acid with various concentrations. Graph was represented as mean ± standard deviation (SD), N=1. Statistical importance of control versus different concentrations of palmitic acid was determined by T-Test relating to YAP (S127) phosphorylation levels with p values; **p≤0.01 and p≤0.001 which are statistically significant.

4.5 Effect of different Oleic Acid concentrations on YAP phosphorylation in Hep-G2 cells

Hep-G2 cells were next treated with both low and high oleic acid concentrations of 0.5 mM, 1 mM and 2 mM. Figure 4.6(A) displays the immunoblot for oleic acid treatments at varying concentrations. Each OA treatment was repeated 3 times, N=3. In contrast to the CaCo-2 result, both low and high concentration of oleic acid led to an increase in the YAP phosphorylation levels thus potential inactivation of the protein. A quantification graph in Figure 4.6(B) indicates a significant increase of pYAP in oleic acid treated cells at all concentrations.

A

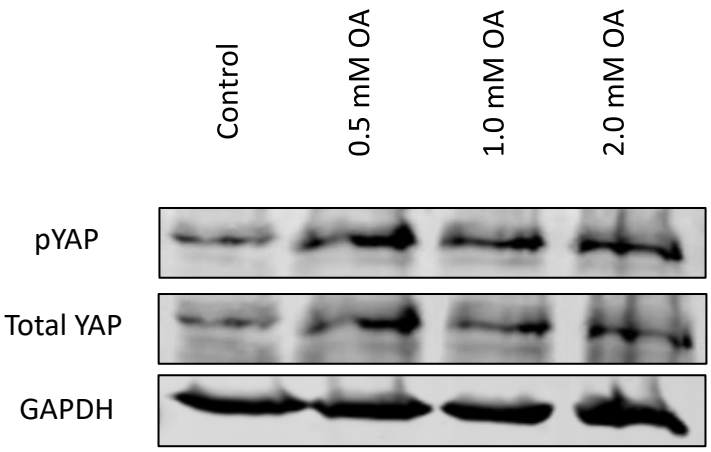

B

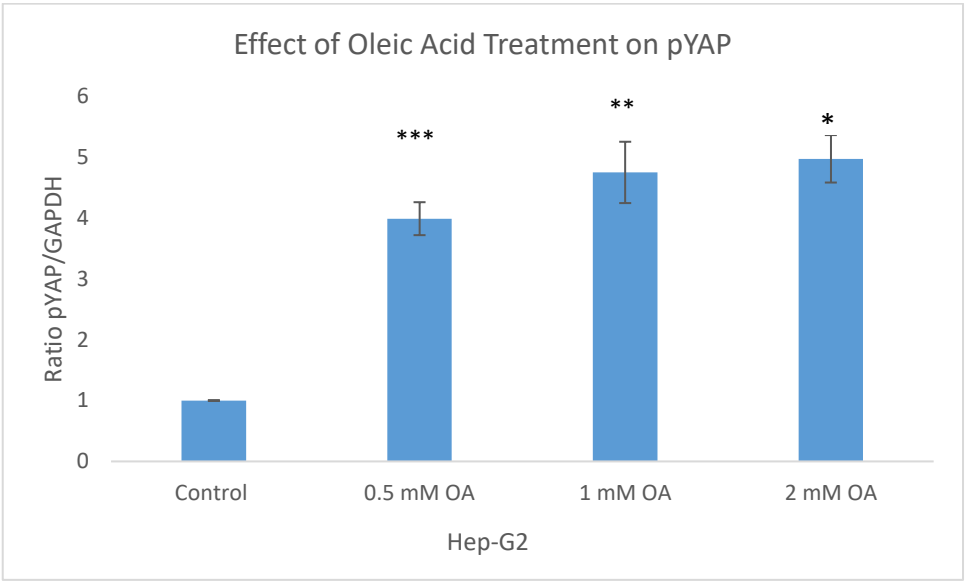

Figure 4.6 Effect of oleic acid treatments using different concentrations on YAP phosphorylation in Hep-G2 cellS line by immnoblot analysis. (A) Immunoblot of an effect of oleic acid treatments with different concentrations on phosphorylation levels of YAP in Hep-G2 cells. (B) A quantification graph of phosphorylation levels of YAP versus GAPDH upon treatment of oleic acid with various concentrations. (C) Quantification graph of pYAP versus total YAP upon treatment of oleic acid with various concentrations. Graph was obtained from the pooled data of 3 independent experiments and represented as mean ± standard deviation (SD), N=3. Statistical importance of control versus

different concentrations of oleic acid was determined by T-Test relating to YAP (S127) phosphorylation levels with p values; *p≤0.05, **p≤0.01 and ***p≤0.001, statistically significant.

4.6 Effect of lipids on protein-protein interactions by Co-immunoprecipitation

It has been shown that lipids have an effect on YAP phosphorylation and possibly activation. Therefore, assessment of oleic acid treatment and interactions between YAP and the novel proteins discovered previously was undertaken. CaCo-2 cells were thus treated with 2 mM oleic acid (the concentration that had an effect on YAP) and after 4 hours cells were lysed. The cells were incubated with antibodies against proteins of interest conjugated to beads. The inputs and Co-IP fractions were subjected to immunoprecipitation and interacting proteins were analysed by immunoblotting. The experiment was repeated 3 times, N=3. The interaction between the YAP and CD2AP validated in previous chapter at Figure 3.2 was a starting point. Cells treated with oleic acid disrupted the interaction between YAP and CD2AP. The decrease in the signal of YAP represented in the immunoblot in Figure 4.7 after oleic acid treatment shows distruption in interaction with CD2AP. Thus active YAP seems to be required for binding to CD2AP. This was also seen with a marked decrease with the interaction between talin and CD2AP.

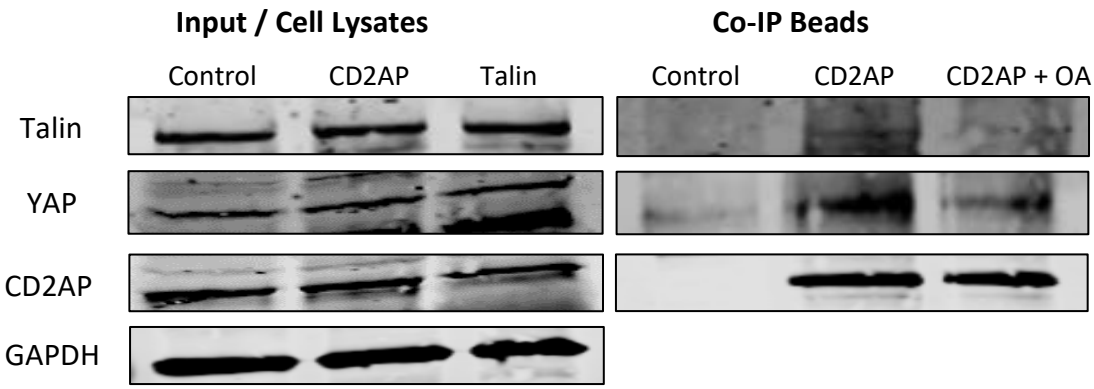

Figure 4.7 Co-Immunoprecipitation showing the interaction of YAP with CD2AP decreases with oleic acid treatment. CaCo-2 cells were treated with 2 mM oleic acid and after 4 hours cells were lysed. Cell lysates were incubated with antibodies against CD2AP conjugated to beads. Both inputs and Co-IP fractions were subjected to immunoprecipitation and proteins present were analysed by immunoblotting. Interaction of CD2AP immunoprecipitates with YAP and talin were found to decrease after the oleic acid treatment. Representative blots from one experiment are displayed amongst 3 independent repeats.

4.7 Evaluation of lipid droplets upon siRNA knockdown of specific proteins

As mentioned in chapter 3, a novel complex was characterised with specific ECM/Hippo proteins linked the Hippo signalling pathway and the ECM which potentially could be via lipid metabolism. The components of the complex were depleted by siRNA-mediated knockdown, individually to determine whether they also played a role in lipid droplet formation and thus provide a further link to lipid metabolism. The formation of lipid droplets was evaluated via immunofluorescence in Hep-G2 and CaCo-2 cells.

4.7.1 Hep-G2 Cells

Hep-G2 cells were cultured and transfected with siRNAs of control, YAP, CD2AP, Talin and Ezrin. After 72 hours of transfection, cells were incubated with 1mM oleic acid for 24 hours. Lipid droplets were stained using the LipidSpot^{TM} 488 Lipid Droplet Stain (green) and nucleus with DAPI (blue). Immunofluorescence images of lipid droplets with and without oleic acid treatment upon siRNA knockdowns in Figure 4.8 were obtained with Floid microscope at 20X magnification. The experiment was repeated 3 times, N=3. In control siRNA, addition of oleic acid increased the lipid droplets as expected. However, knockdown of specific proteins had a significant effect on lipid droplet formation in Hep-G2 cells. siRNA-mediated knockdown of YAP, CD2AP, Talin and Ezrin appeared to show a significant increase in lipid droplet formation upon addition of oleic acid compared to cells without oleic acid, suggesting that these members of the complex may in fact regulate lipid droplet formation in cells.

4.7.2 CaCo-2 Cells

The same procedure was repeated in CaCo-2 cells to assess the effect of knockdown of YAP, CD2AP, Talin and Ezrin on lipid droplet formation and shown in Figure 4.9. Depletion of proteins had a reverse effect on the formation of lipid droplets in CaCo-2 cells compared to Hep-G2 cells. A significant decrease was observed in lipid droplets after the siRNA-mediated knockdown of YAP, CD2AP, Talin and Ezrin which indicates that components of the complex have an important effect on lipid droplet formation in CaCo-2 cells however, in what role are they involved in is not known. The silencing of YAP, CD2AP, Talin and Ezrin had the opposite effects on the formation of lipid droplets in Hep-G2 and CaCo-2 cells. The

cell type can be the major determinant of this dissimilarity as Hep-G2 cells are liver cells and central for the regulation and metabolism of lipids (Paramitha *et al*., 2021).

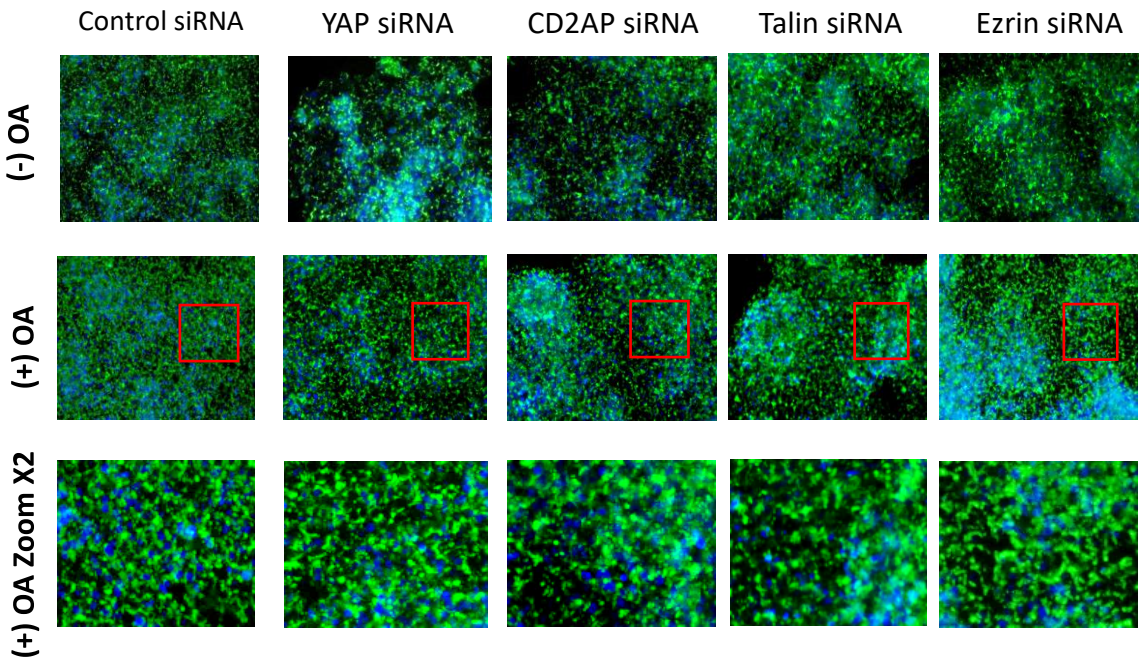

Figure 4.8 Immunofluorescence images of lipid droplets with and without oleic acid treatment upon siRNA knockdowns of YAP, CD2AP, Talin and Ezrin obtained with Floid microscope at 20X magnification in Hep-G2 cell line. Hep-G2 cells were cultured and transfected with siRNAs against control, YAP, CD2AP, Talin and Ezrin) and after 72h of transfection, incubated with 1 mM oleic acid for 24h. Lipid droplets were visualised using the LipidSpot™ 488 Lipid Droplet Stain (green) and nucleus with DAPI (blue). A 2X zoom is provided for clarity of image. Representative IF images from one experiment are displayed amongst 3 independent repeats.

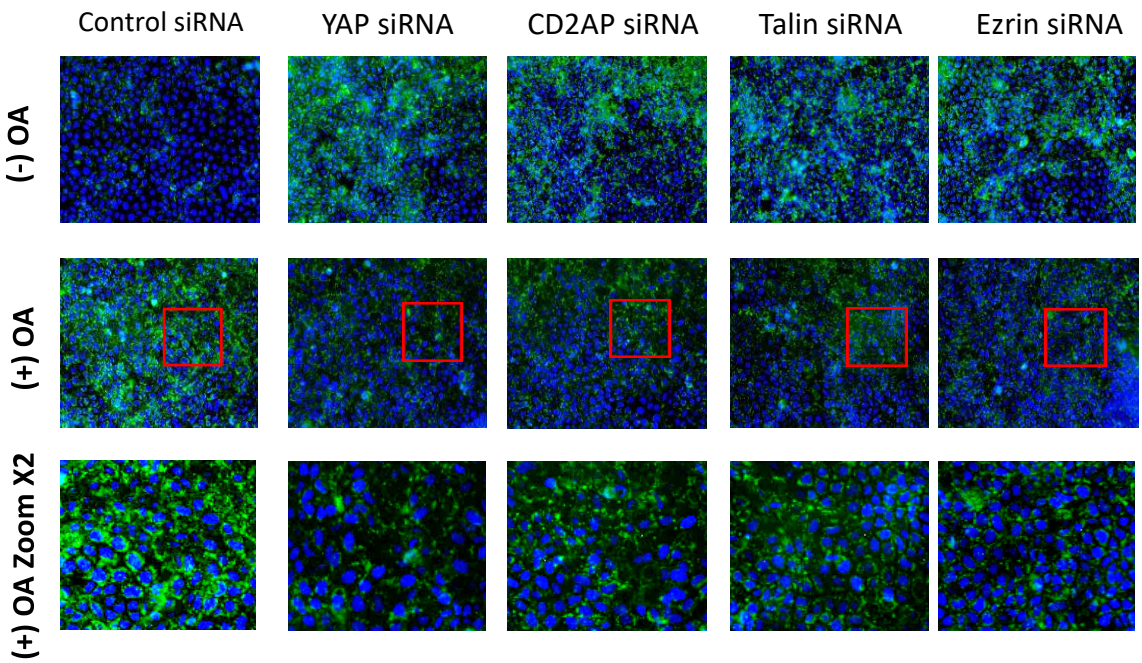

Figure 4.9 Immunofluorescence images of lipid droplets with and without oleic acid treatment upon siRNA knockdowns of YAP, CD2AP, Talin and Ezrin obtained with Floid microscope at 20X magnification in CaCo-2 cell line. CaCo-2 cells were cultured and transfected with siRNAs (Control, YAP, CD2AP, Talin and Ezrin) and after 72h of transfection, incubated with 1 mM oleic acid for 24h. Lipid droplets were visualised using the LipidSpot™ 488 Lipid Droplet Stain (green) and nucleus with DAPI (blue). A 2X zoom is provided for clarity of image. Representative IF images from one experiment are displayed amongst 3 independent repeats.

Based on the findings, it can be suggested that lipids have an effect on YAP phosphorylation and thus activation state. Lipids can disrupt the interaction between the ECM and YAP and finally that siRNA of the novel members of the complex can have differing effects on lipid droplet formation and metabolism dependant on the cell line, which also underlies the influence of the Hippo signalling pathway in lipid metabolism. Following this, observation of the translocation of YAP in a cell, following lipid manipulation was investigated.

4.8 Translocation of YAP upon lipid manipulation and the effect of lipid treatment on complex members

4.8.1 CaCo-2 Cells

As reported in Figures 4.2 and 4.3, 2 mM oleic acid treatment in CaCo-2 cells resulted in increased levels of YAP phosphorylation on its serine 127 site (Figure 4.2&4.3). If this affects activation, translocation of YAP from nucleus to cytoplasm would be expected upon its inactivation. In order to observe, the translocation of YAP upon oleic acid stimulation in CaCo-2 cells, cells were visualised by fluorescence staining using an immunofluorescence microscope. The effect of oleic acid treatment on the cellular location of YAP and on the other complex members was assessed in both confluent and sparse CaCo-2 cells. CaCo-2 cells were grown on coverslips, with cells treated with 2 mM oleic acid and then fixed with 4% PFA before co-stained with YAP, CD2AP, Talin, Ezrin antibodies (stained with CY3 in red) and Hoechst stain (DAPI in blue) for cell nuclei. Immunofluorescence images of cells were obtained with Evos fl fluorescence microscope at 20X magnification. Each experiment was repeated 4 times, N=4. Upon treatment of oleic acid, nuclear YAP was decreased compared to cells without oleic acid in confluent CaCo-2 cells. The YAP was clearly, strongly nuclear before addition of oleic acid and there was a strong decrease in nuclear YAP after addition of oleic acid with a translocation of the protein to a cytoplasmic pool as seen in Figure 4.10(A). This was consistent with the western-blot data (Figure 4.2&4.3). Interestingly, there was not much change in CD2AP after OA treatment (Figure 4.10(B)) however, oleic acid affected talin and ezrin localisation as both talin and ezrin staining were decreased in OA treated confluent CaCo-2 cells as shown in Figure 4.10C and D respectively. The pattern was same in oleic acid treated sparse CaCo-2 cells with YAP becoming more cytoplasmic

rather than nuclear, with no change in CD2AP and a decrease in talin and ezrin staining (Figure 4.11).

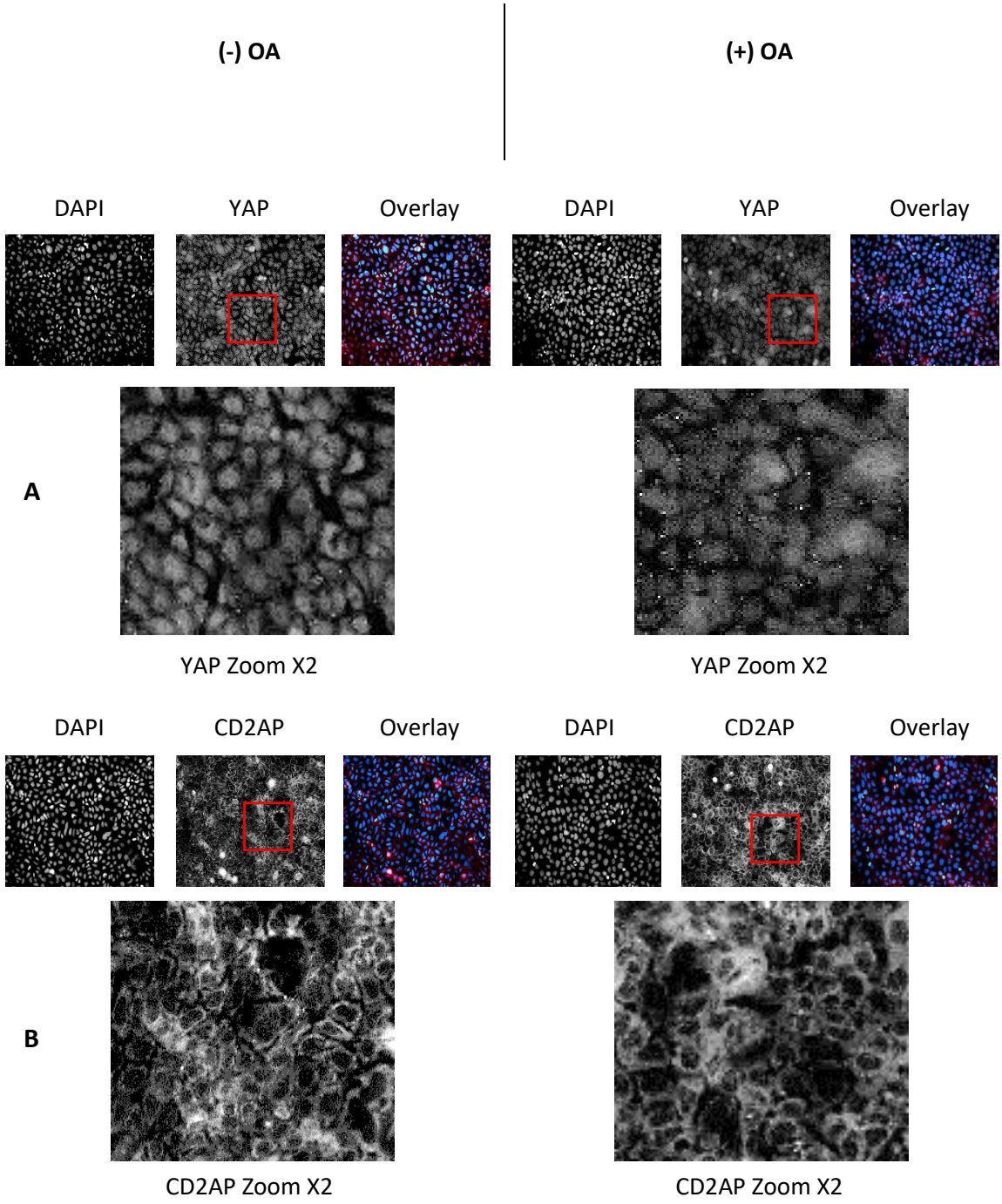

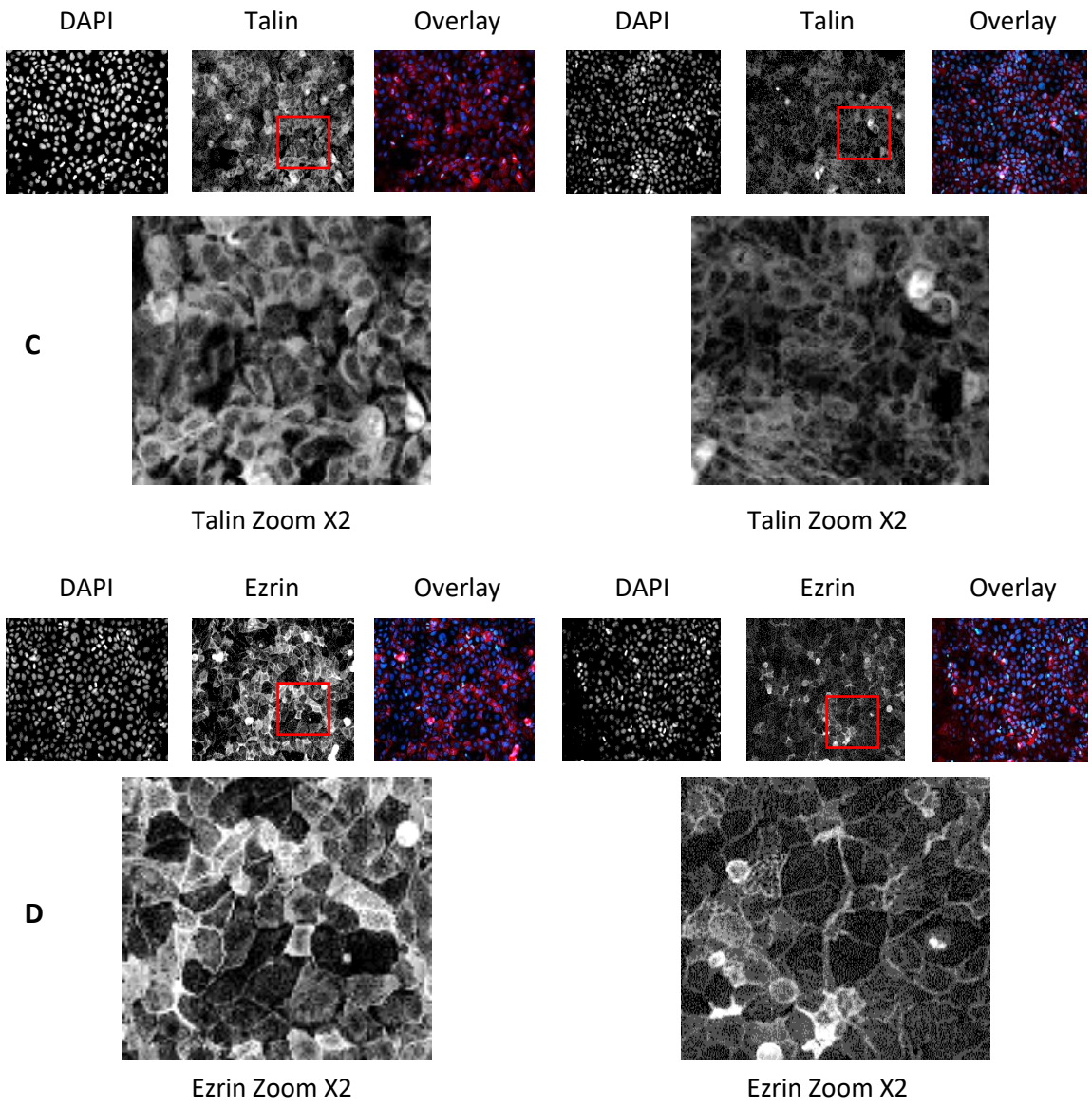

Figure 4.10 Cellular localization of YAP, CD2AP, Talin and Ezrin determined by immunofluorescence in confluent CaCo-2 cells with oleic acid treatment. Immunofluorescence images of cells obtained with Evos fl fluorescence microscope at 20X magnification. CaCo-2 cells were grown on coverslips, cells were treated with 2 mM oleic acid and then fixed with 4% PFA before co-stained with YAP, CD2AP, Talin, Ezrin antibodies and Hoechst stain (DAPI) for cell nuclei. YAP, CD2AP, Talin and Ezrin stained with CY3 and appear in red. Images were acquired separately. A 2X zoom is provided for clarity of image. (A) showing cellular localisation of YAP where (B), (C) and (D) showing cellular localisation of CD2AP, Talin and Ezrin respectively with OA treatment. Representative IF images from one experiment are displayed amongst 4 independent repeats.

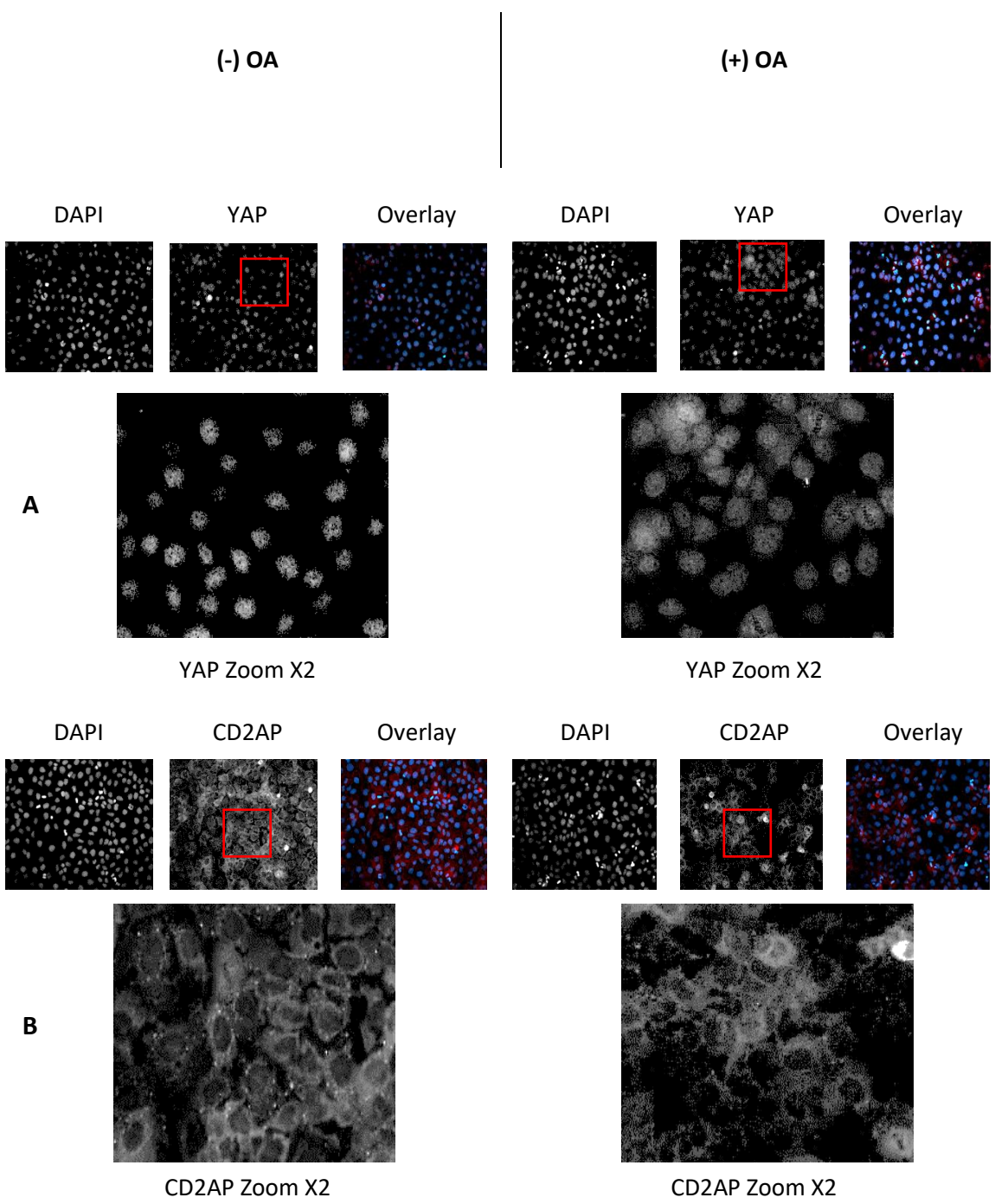
(-) OA
(+) OA
DAPI
YAP
Overlay
DAPI
YAP
Overlay
A
YAP Zoom X2
YAP Zoom X2
DAPI
CD2AP
Overlay
DAPI
CD2AP
Overlay
B
CD2AP Zoom X2
CD2AP Zoom X2

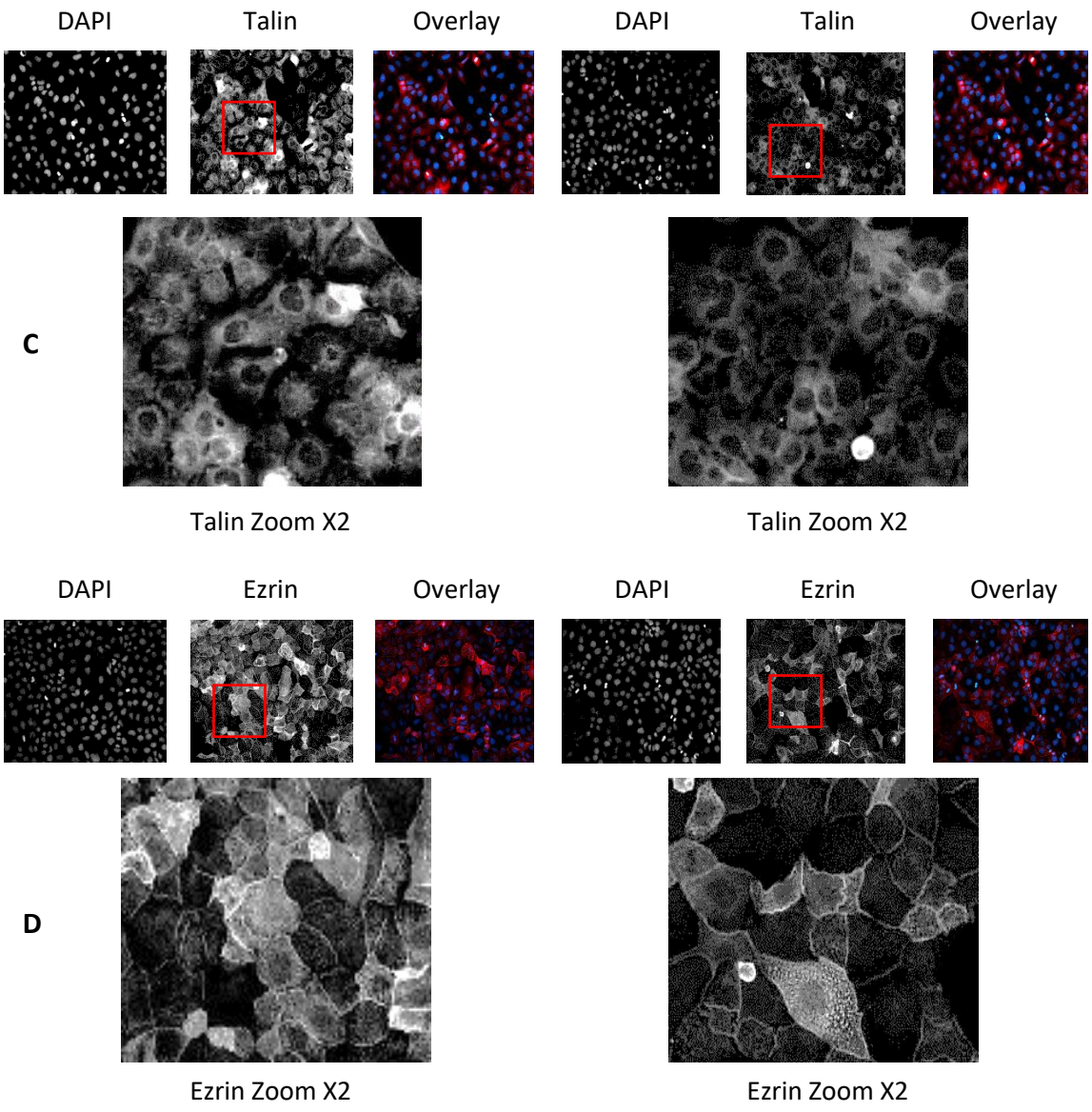

Figure 4.11 Cellular localization of YAP, CD2AP, Talin and Ezrin determined by immunofluorescence in sparse CaCo-2 cells with oleic acid treatment. Immunofluorescence images of cells obtained with Evos fl fluorescence microscope at 20X magnification. CaCo-2 cells were grown on coverslips, +OA cells were treated with 2 mM oleic acid and then fixed with 4% PFA before co-stained with YAP, CD2AP, Talin, Ezrin antibodies and Hoechst stain (DAPI) for cell nuclei. YAP, CD2AP, Talin and Ezrin stained with CY3 and appear in red. Images were acquired separately and overlay images were shown. A 2X zoom is provided for clarity of image. (A) showing cellular localisation of YAP where (B), (C) and (D) showing cellular localisation of CD2AP, Talin and Ezrin respectively with OA treatment. Representative IF images from one experiment are displayed amongst 4 independent repeats.

4.8.2 Hep-G2 Cells

The effect of oleic acid treatment on cellular location of YAP and complex members was assessed in Hep-G2 by immunofluorescence staining in confluent and sparse Hep-G2 cells. Hep-G2 cells were grown on coverslips, cells were treated with 2 mM oleic acid and then fixed with 4% PFA before co-stained with YAP, CD2AP, Talin antibodies (stained with CY3 in red) and Hoechst stain (DAPI in blue) for cell nuclei. Immunofluorescence images of cells were obtained with Evos fl fluorescence microscope at 20X magnification. Each experiment was repeated 4 times, N=4. Hep-G2 cells treated with oleic acid resulted previously in YAP inactivation in the immunoblot analysis via increase in pYAP level (Figure 4.6) which again was consistent with the immunofluorescence data we obtained, as nuclear YAP was strongly decreased and became more cytoplasmic upon oleic acid treatment when compared to untreated cells in both confluent and sparse Hep-G2 cells, thus establishing that YAP was inactivated. There was no change in CD2AP as seen in CaCo-2 cells, but there was also no effect on Talin levels after oleic acid treatment in both confluent and sparse Hep-G2 cells. The Hep-G2 cells grow in monolayers with a flat-morphology thus perceiving less signals from the ECM and this could be the reason for not observing any effect on the ECM proteins upon addition of OA (Figure 4.12 and 4.13). Ezrin did not give a clear stain for assessment.

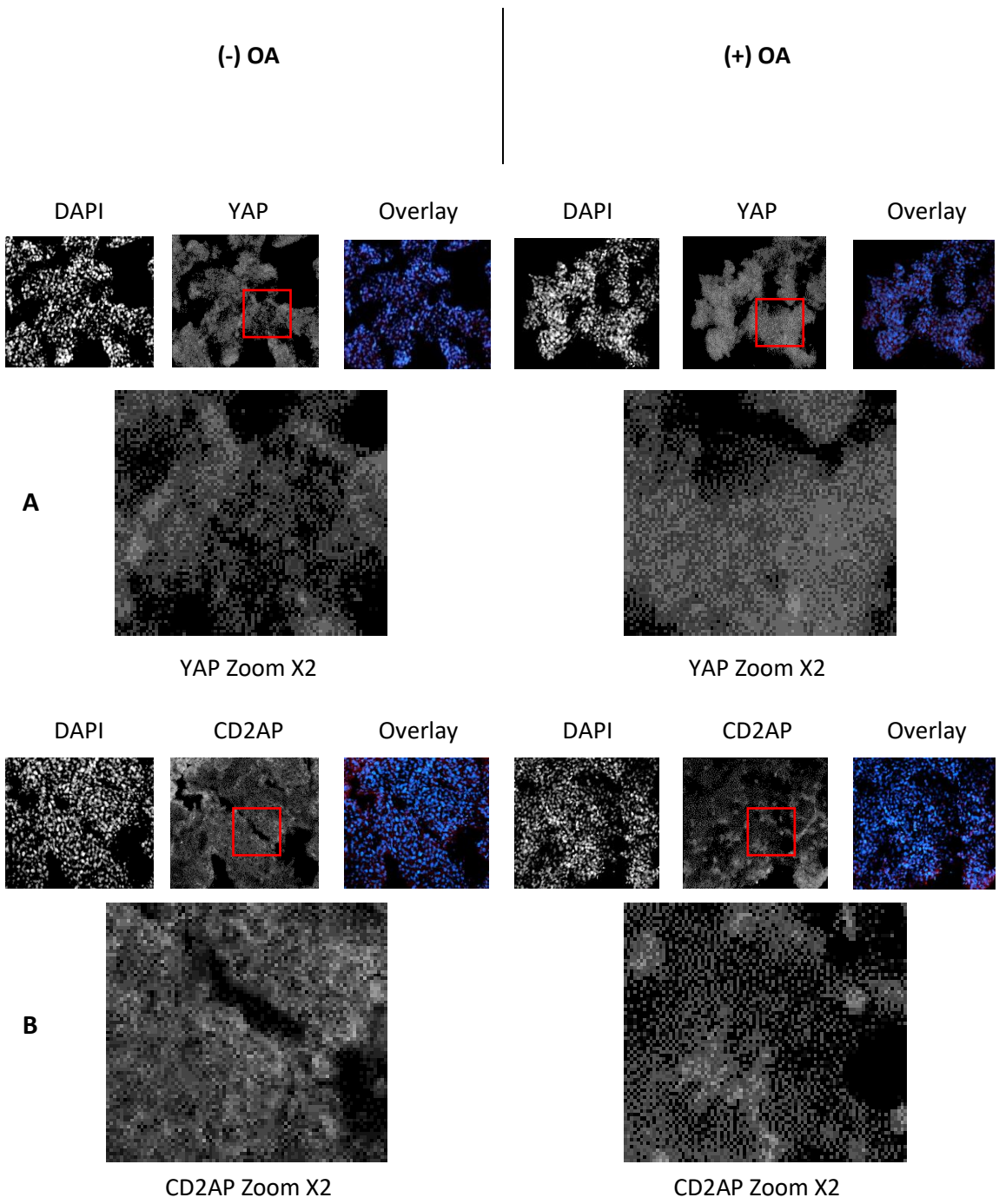
(-) OA
(+) OA
DAPI
YAP
Overlay
DAPI
YAP
Overlay
A
YAP Zoom X2
YAP Zoom X2
DAPI
CD2AP
Overlay
DAPI
CD2AP
Overlay
B
CD2AP Zoom X2
CD2AP Zoom X2

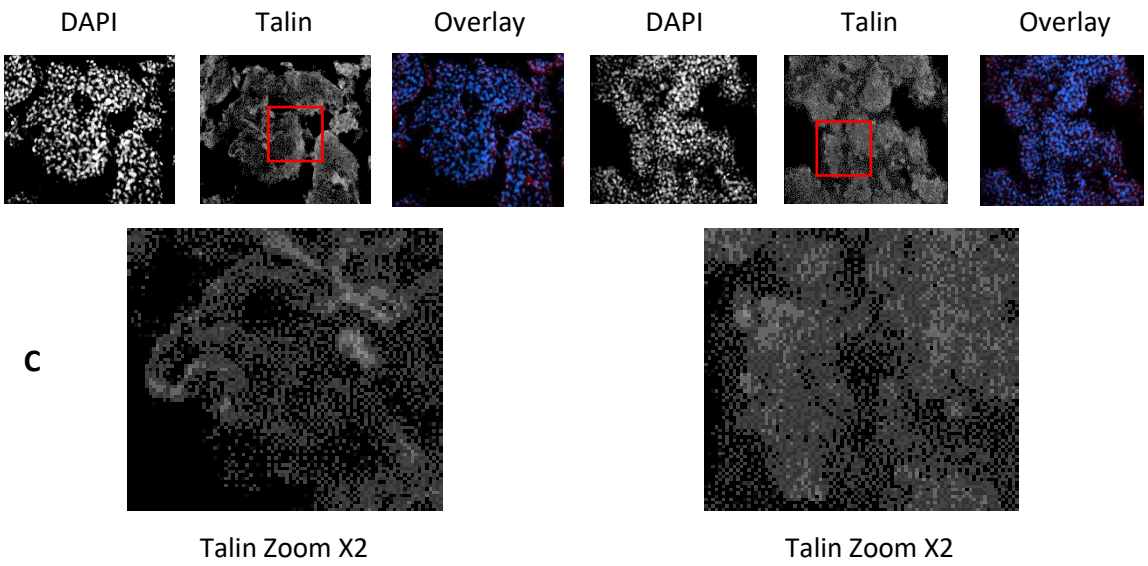

Figure 4.12 Cellular localization of YAP, CD2AP and Talin determined by immunofluorescence in confluent Hep-G2 cells with oleic acid treatment. Immunofluorescence images of cells obtained with Evos fl fluorescence microscope at 20X magnification. Hep-G2 cells were grown on coverslips, +OA cells were treated with 2 mM oleic acid and then fixed with 4% PFA before co-stained with YAP, CD2AP, Talin antibodies and Hoechst stain (DAPI) for cell nuclei. YAP, CD2AP and Talin stained with CY3 and appear in red. Images were acquired separately and overlay images were shown. A 2X zoom is provided for clarity of image. (A) showing cellular localisation of YAP where (B) and (C) showing cellular localisation of CD2AP and Talin respectively with OA treatment. Representative IF images from one experiment are displayed amongst 4 independent repeats.

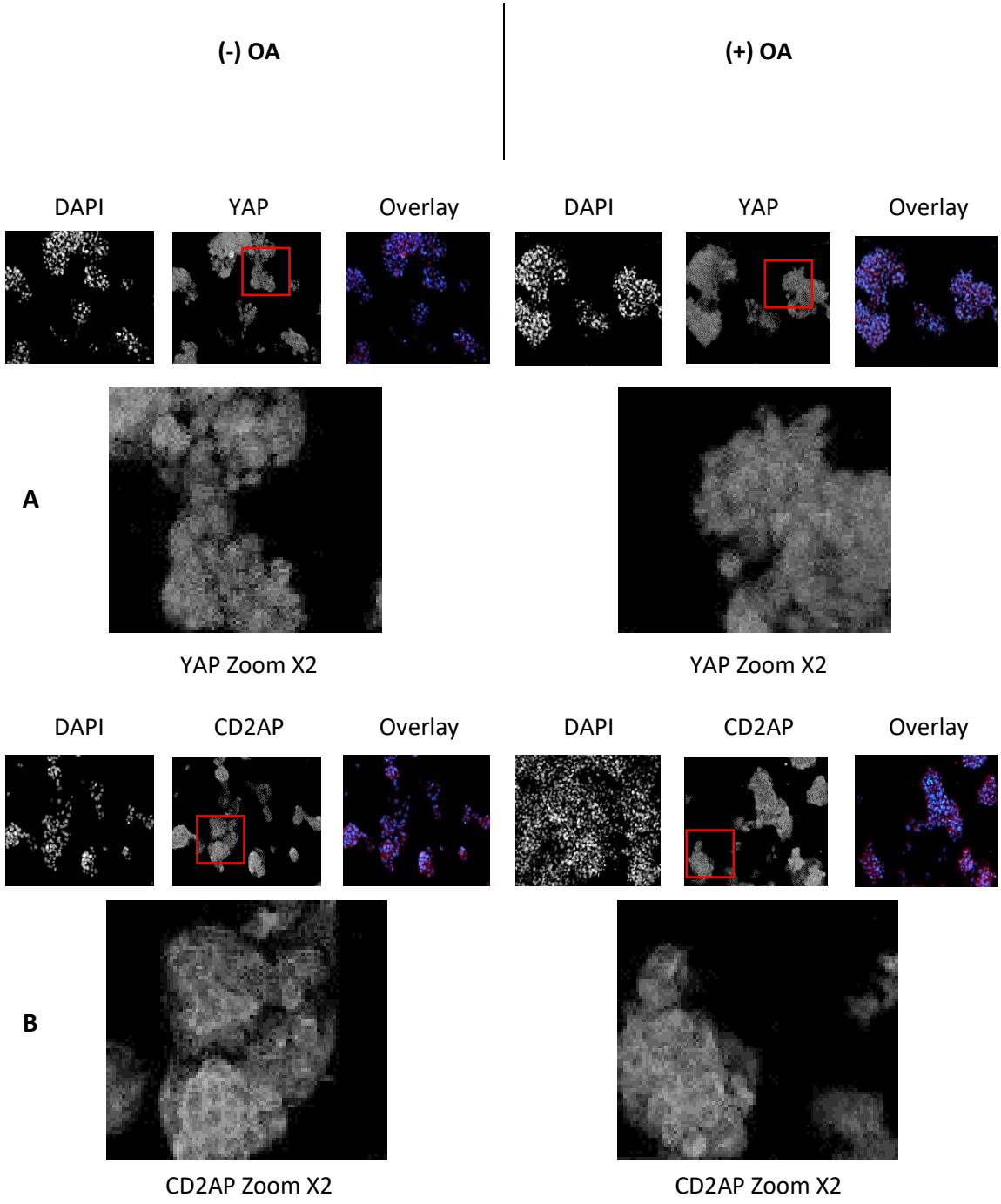
(-) OA
(+) OA
DAPI
YAP
Overlay
DAPI
YAP
Overlay
A
YAP Zoom X2
YAP Zoom X2
DAPI
CD2AP
Overlay
DAPI
CD2AP
Overlay
B
CD2AP Zoom X2
CD2AP Zoom X2

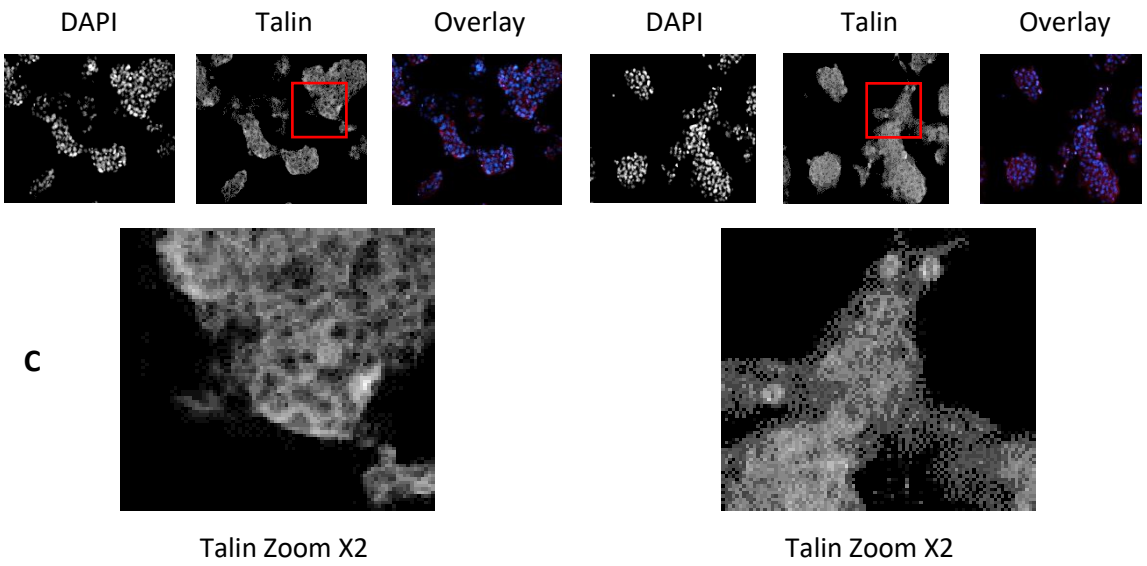

Figure 4.13 Cellular localization of YAP, CD2AP and Talin determined by immunofluorescence in sparse Hep-G2 cells with oleic acid treatment. Immunofluorescence images of cells obtained with Evos fl fluorescence microscope at 20X magnification. Hep-G2 cells were grown on coverslips, +OA cells were treated with 2 mM oleic acid and then fixed with 4% PFA before co-stained with YAP, CD2AP, Talin antibodies and Hoechst stain (DAPI) for cell nuclei. YAP, CD2AP and Talin stained with CY3 and appear in red. Images were acquired separately and overlay images were shown. A 2X zoom is provided for clarity of image. (A) showing cellular localisation of YAP where (B) and (C) showing cellular localisation of CD2AP and Talin respectively with OA treatment. Representative IF images from one experiment are displayed amongst 4 independent repeats.

CHAPTER 5. EFFECT OF LIPID METABOLISM ON THE HIPPO SIGNALLING PATHWAY *IN-VIVO* IN A PLANARIAN ANIMAL MODEL SYSTEM

CHAPTER 5. EFFECT OF LIPID METABOLISM ON THE HIPPO SIGNALLING PATHWAY *IN-VIVO* IN A PLANARIAN ANIMAL MODEL SYSTEM

This chapter focuses on the effect of the most abundant fatty acids; oleic and palmitic acid on the expression levels of *Hippo* and *Yorkie*; one of the most important genes of Hippo signalling pathway in Planarian. Two different species of Planarian; *Dugesia Lugubris* and *Schmidtea mediterranea* have been used as an *in-vivo* model organism to study the effect of lipid metabolism on the Hippo signalling pathway as their outstanding regenerative ability ease the study of complex physiological processes (Ge *et al*., 2022). Both species were microinjected with designated treatments (oleic acid or palmitic acid) as indicated in Materials and Methods section (2.1.13) and compared to control. RT-qPCR was performed to measure the relative fold gene expression of *Hippo* and *Yorkie* after injections at given time intervals. Beta actin (ACBT) was used as a housekeeping gene in the quantification of gene expression as it is the most stable reference gene expressed in the regeneration process of planarian (Yuwen *et al*., 2011). *Schmidtea* mediterranea planarian was used for determining the duration of wound closure upon oleic acid treatment.

5.1 Effect of Oleic Acid Microinjection on *Dugesia Lugubris* Regenerating Trunk Fragments

Dugesia Lugubris worms were cut into 3 fragments of head, trunk and tail. Trunks were microinjected with planarian water for control and with oleic acid for fatty acid treatment respectively as indicated. Whole planarian without any injection was used get a baseline for the experiment. The injected trunk fragments were examined at Day 5 and Day 7. The RNA was extracted and cDNA was synthesised for qPCR reaction to measure the relative fold gene expressions of *Hippo* and *Yorkie*. Figure 5.0 shows the data derived from the qPCR

reaction. No significant change was observed in the expression of *Hippo* gene with oleic acid treated trunks however, that was not the case for the expression of *Yorkie* gene in trunks treated with oleic acid. Expression of the *Yorkie* gene increased in Day 5 untreated trunk and when treated with an oleic acid significant decrease was observed in the expression of *Yorkie* on both Day 5 and Day 7 comparatively as seen in Figure 5.0. In the control, the *Yorkie* gene in day 5 trunk fragment left untreated increased prominently due to rapid regeneration of the *Dugesia Lugubris*. However, the regeneration process was inhibited upon oleic acid injection with a remarkable decrease in the expression of *Yorkie* gene. An analysis of variance (two-way ANOVA) showed that the overall interaction was significant DF (4), MS (1.705), F (4,50)=7.511 , ****p<0.0001. Post hoc analysis using the BONFERRONI's multiple comparisons test for significance indicated that expression of *Yorkie* for Day 5 untreated vs Day 5 Oleic Acid and Day 5 untreated vs Day 7 Oleic Acid were statistically significant with **p=0.001 and **p=0.0018 respectively. The expression of *Yorkie* for whole worm vs day 5 untreated is not statistically significant but has very close p value of 0.0528 (Figure 5.0).

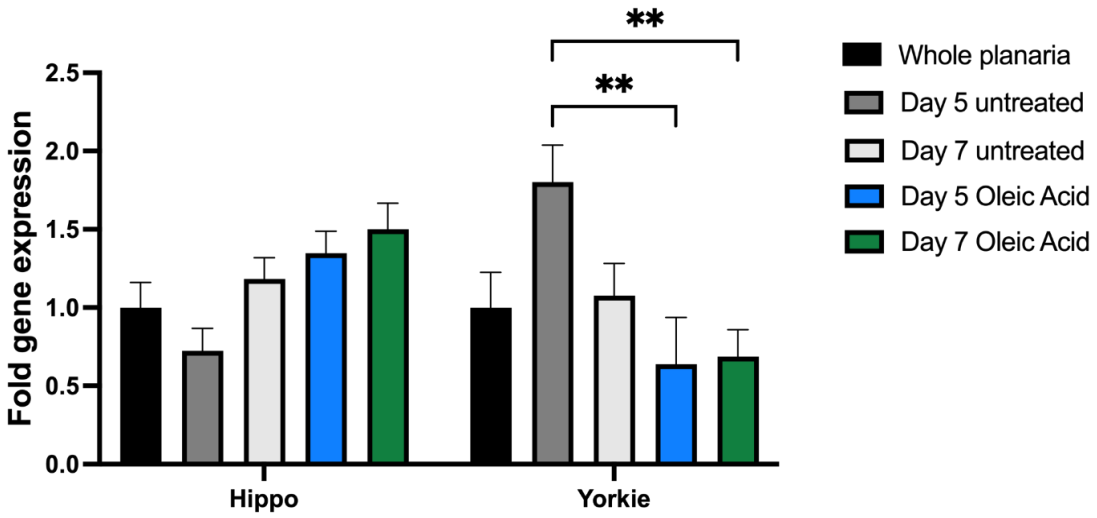

Figure 5.0. The change in fold expression of Hippo and Yorkie genes upon Oleic Acid treatment in Dugesia Lugubris trunks derived from qPCR data. Trunks of Dugesia Lugubris worms were injected with Oleic Acid. The expression of Hippo and Yorkie genes in oleic acid treated trunks at Day 5 and Day 7 were compared to Day 5 untreated trunk. RT-qPCR was performed to measure the relative fold gene expression of Hippo and Yorkie in Dugesia Lugubris trunks. ACBT was used as a housekeeping gene in the quantification of gene expression. Overall significant difference was obtained by two-way ANOVA with ****p<0.0001. Comparison between Day 5 untreated versus Day5 Oleic Acid and Day7 Oleic Acid were performed using Bonferroni's multiple comparisons test; **P<0.05. Error bars represent ± SEM, N=12.

5.2 Effect of Oleic Acid Microinjection on Wound Resolution in *Schmidtea mediterranea*

Schmidtea mediterranea worms were microinjected with oleic acid and days taken for site of injury to resolve were observed and compared to control worms which were injected with planarian water only over a period of time. Figure 5.1 represents the images of sham *Schmidtea mediterranea* worms injected with planarian water and treated *Schmidtea mediterranea* worms injected with oleic acid. The worms were examined for the wound resolution after injection at Day 2 and Day 7. The days taken for the wounds to resolve were evaluated after oleic acid injection. As seen in Figure 5.1 site of injury of the sham

worms injected with water only was resolved at Day 2 with no sign of wound present whilst oleic acid treated *Schmidtea mediterranea* worms got a site of injury even after 7 days of injection. Thus, oleic acid was shown to slow down the wound closure process. The arrows in Figure 5.1 indicate the site of injury for oleic acid treated *S.Med* at Day 2 and Day 7. The different timing of wound resolution as days in oleic acid treated *S.Med* versus control was shown as a scatter plot in Figure 5.2. Black dots indicate the *S.Med* worms without any site of injury thus fully resolved wound. Most of the sham worm wounds appeared to resolve before day 5, around day 2. Injection of oleic acid delayed the wound resolution like 5 days as wounds of oleic acid injected *S.Med* worms fully resolved after day 5 around day 7. Two of the oleic acid injected worms resolved at Day 19. Thus oleic acid did not stop but inhibited the wound resolution process. Statistically significant differences are indicated for wound resolution data when treated with oleic acid comparatively to sham. The p-value was calculated by two-tailed Mann-Whitney U test, significant at **P=0.007.

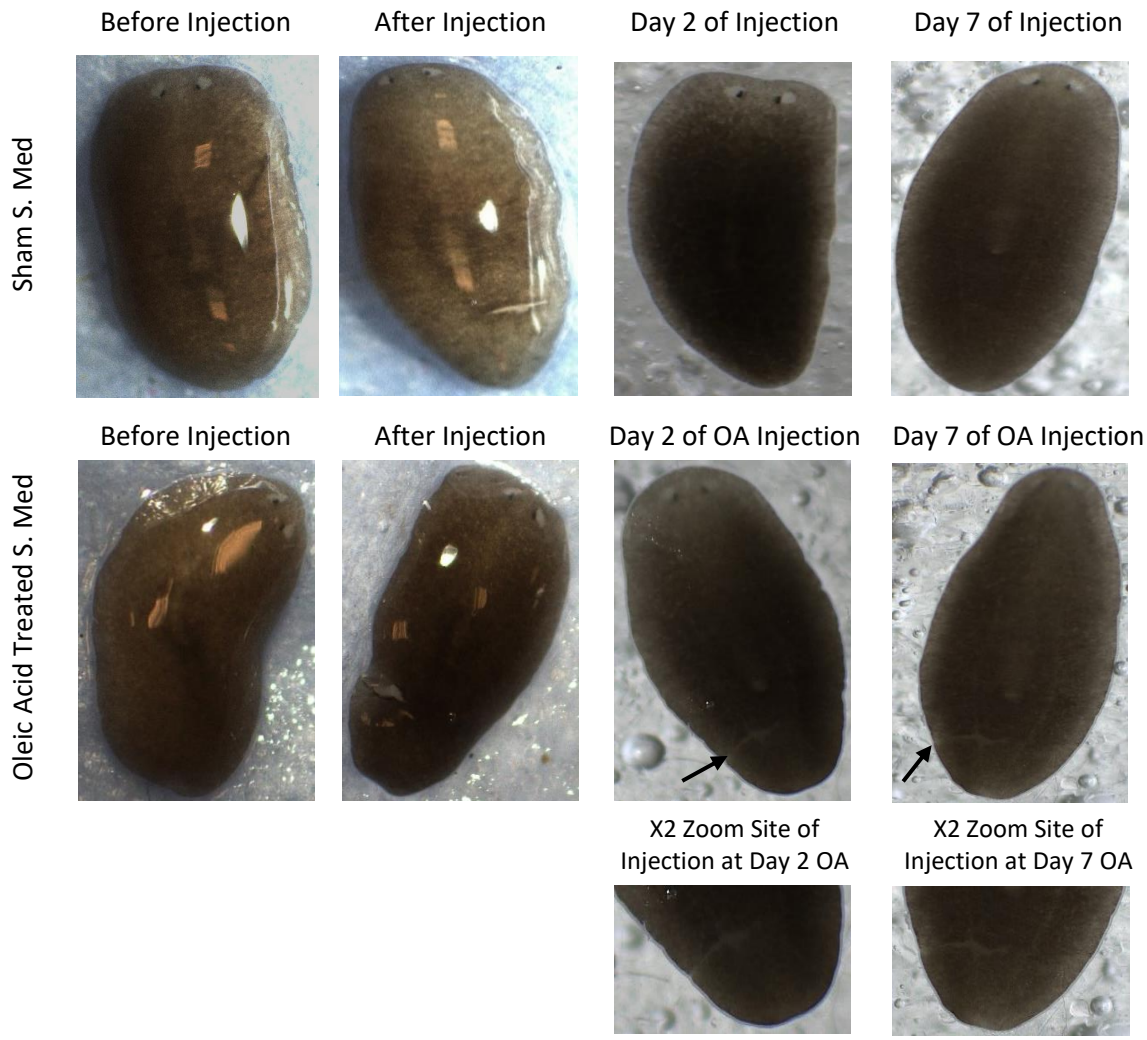

Figure 5.1. The images of S.Med worms showing the wound resolution for Control and Oleic Acid treated worms at indicated days. An image of worm represented before and after the microinjection. Control worm was injected with S.Med water and treated worm was injected with Oleic Acid. Resolution of wounds was presented at Day 2 and Day 7. An arrow indicates the site of injury for oleic acid treated S.Med at Day 2 and Day 7. An inset of focused image shows the site of injury for Day 2 and Day 7 oleic acid treated S.Med planaria.

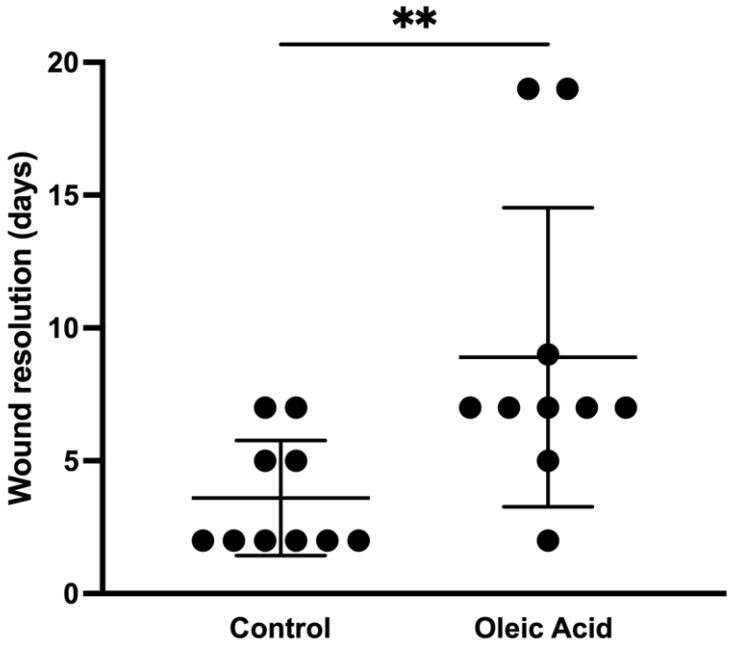

Figure 5.2. Evaluation of wound resolution in S.Med after oleic acid treatment compared to control. S.Med worms were microinjected with oleic acid and days taken for site of injury to resolve were observed and compared to control worms over time. The scatter plot shows the different timing of wound resolution as days in Oleic Acid treated S.Med versus control. Black dots represents the S.Med worms without wound. Statistically significant differences are indicated, N=10. The p-value was calculated by Mann-Whitney U test, significant at **P< 0.05.

5.3 Effect of Oleic Acid Microinjection on the Expression of *Hippo* and *Yorkie* Genes in *Schmidtea mediterranea*

Schmidtea mediterranea worms were injected with oleic acid as indicated and examined after 7 and 14 days of injection. Oleic acid injected *S.Med* worms at day 7 and day 14 were compared to controls at day 7 and day 14. RNA was extracted and cDNA was synthesised for qPCR reaction to measure the relative gene expression of *Hippo* and *Yorkie*. Figure 5.3 shows the data derived from qPCR reaction. Expression of the *Hippo* gene was elevated significantly after oleic acid injection compared to control on both Day 7 and Day 14 activating the Hippo signalling pathway which results in an inhibition of cell proliferation.

There is an observable decrease trend in expression of Yorkie after 14 days of oleic acid injection versus control thus change is statistically not significant. An analysis of variance (two-way ANOVA) showed that the overall interaction was significant DF (3), MS (0.3012), F (3,16)= 7.072 , **p=0.0031. Also gene expression and treatment-time were significant with values of DF(1), MS(0.8546), F(1,16)=20.07, ***p=0.0004 and DF(3), MS(0.2343), F(3,16)=5.501, **p=0.0086 respectively. Post hoc analysis using the BONFERRONI's multiple comparisons test for significance indicated that expression of *Hippo* for Control 7 Days versus Oleic Acid 7 Days; Control 14 Days versus Oleic Acid 7 Days and Oleic Acid 7 Days versus Oleic Acid 14 Days were statistically significant; **P=0.0014, **p=0.0014 and *p=0.0235 respectively.

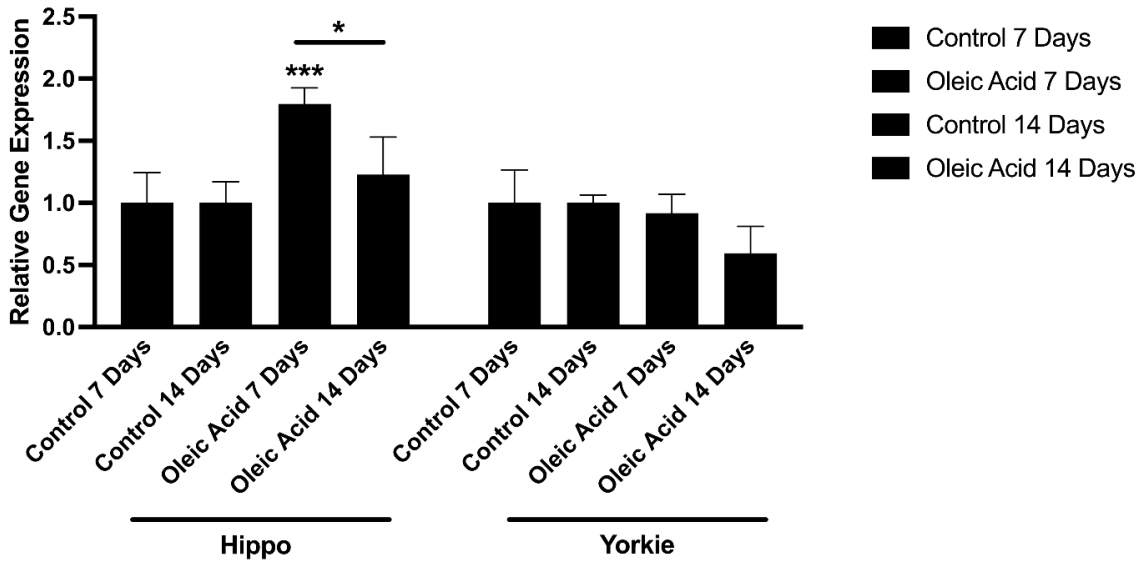

Figure 5.3. The change in relative expression of Hippo and Yorkie genes upon Oleic Acid treatment in *Schmidtea mediterranea* derived from qPCR data. *Schmidtea mediterranea* worms were injected with Oleic Acid. The expression of Hippo and Yorkie genes in oleic acid treated worms at Day 7 and Day 14 were compared to Control at Day 7 and Day 14. RT-qPCR was performed to measure the relative gene expression of Hippo and Yorkie in *Schmidtea mediterranea* worms. ACBT was used as a housekeeping gene in the quantification of gene expression. Overall significant interaction was obtained by two-way ANOVA with **p<0.05. Statistically significant increase was

obtained in expression of Hippo gene in oleic acid treated S.Med (***p<0.05). Comparison between Control 7 Days versus Oleic Acid 7 Days; Control 14 Days versus Oleic Acid 7 Days and Oleic Acid 7 Days versus Oleic Acid 14 Days performed using Bonferroni's multiple comparisons test found statistically significant; **P<0.05. Error bars represent ± SEM, N=6.

5.4 Effect of Palmitic Acid Microinjection on Expression of *Hippo* and *Yorkie* Genes in *Schmidtea mediterranea*

The *Schmidtea mediterranea* worms were microinjected with palmitic acid as indicated and examined after 7 and 14 days of injection. Palmitic acid injected *S.Med* worms at day 7 and day 14 were compared to controls at day 7 and day 14. The RNA was extracted and cDNA was synthesised for qPCR reaction to measure the relative gene expression of *Hippo* and *Yorkie.* Figure 5.4 shows the data derived from qPCR reaction. In the expression of *Hippo* gene no change was observed after palmitic acid injected on both Day 7 and Day 14. There is a traceable but non-significant decrease in expression of *Yorkie* after 14 days of palmitic acid injection versus control. An analysis of variance (two-way ANOVA) showed that there is no significance in overall interaction, p>0.05. Post hoc analysis using the BONFERRONI's multiple comparisons test for significance indicated that expression of *Hippo* and *Yorkie* upon palmitic acid injection were not statistically significant, p>0.05.

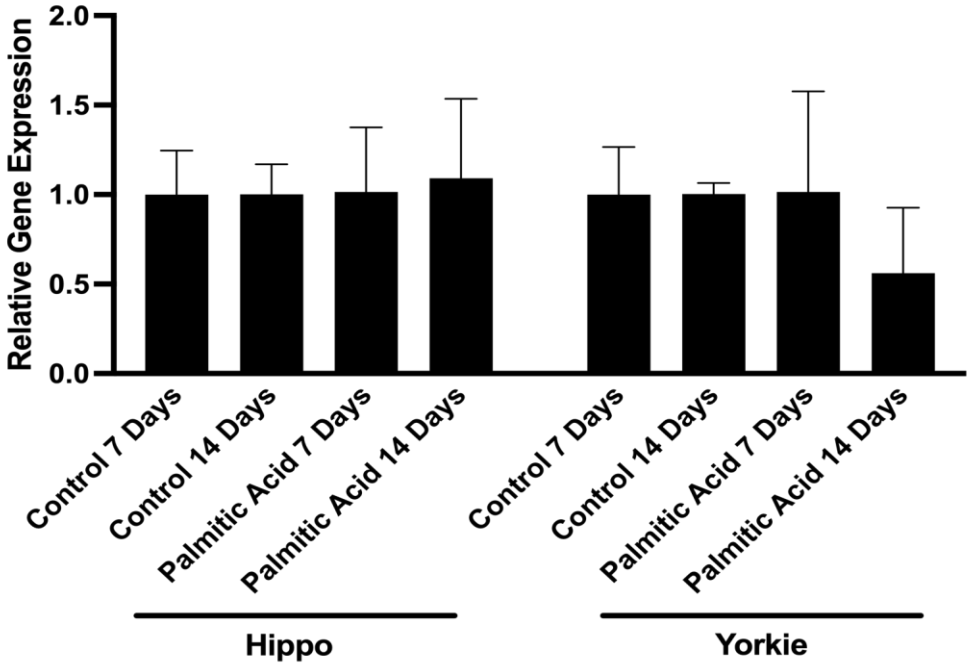

Figure 5.4. The change in relative expression of Hippo and Yorkie genes upon Palmitic Acid treatment in *Schmidtea mediterranea* derived from qPCR data. *Schmidtea mediterranea* worms were injected with Palmitic Acid. The expression of Hippo and Yorkie genes in palmitic acid treated worms at Day 7 and Day 14 were compared to Control at Day 7 and Day 14. RT-qPCR was performed to measure the relative gene expression of Hippo and Yorkie in *Schmidtea mediterranea* worms. ACBT was used as a housekeeping gene in the quantification of gene expression. No statistical significance was obtained by two-way ANOVA test in palmitic acid treated S. Med planaria. Error bars represent ± SEM, N=6.

CHAPTER 6. MASS SPECTROSCOPY AND RNA-SEQUENCING TO DETERMINE NOVEL PROTEIN INTERACTIONS AND EXPRESSION OF SPECIFIC GENES WITH THE HIPPO SIGNALLING PATHWAY DURING LIPID METABOLISM

CHAPTER 6. MASS SPECTROSCOPY AND RNA-SEQUENCING TO DETERMINE NOVEL PROTEIN INTERACTIONS AND EXPRESSION OF SPECIFIC GENES WITH THE HIPPO SIGNALLING PATHWAY DURING LIPID METABOLISM

This chapter focuses to determine the novel protein interactions and expression of specific genes with the Hippo signalling pathway during lipid metabolism via mass spectroscopy (MS) and RNA-Sequencing analysis respectively. Primarily, samples for MS analysis were prepared by Co-immunoprecipitation assay as stated in section 2.1.9 of Materials & Methods chapter. The samples were subjected to SDS-Page analysis and the protein of interests on the gel were sent off for MS analysis to assess the change in binding partners of YAP upon addition of oleic acid in CaCo-2 cells. Numerous YAP-interactors obtained in MS analysis are shown in Figure 6.0. Oleic acid was shown to abolish the interaction of several proteins with YAP. Among them, most importantly oleic acid disrupted the interaction of YAP with Ezrin and Radixin which are members of ERM-family proteins and are involved in the regulation of Hippo signalling pathway (Ponuwei, 2016). As described in the previous chapter, oleic acid in CaCo-2 cells resulted in decreased expression of ezrin thus, reduced Ezrin-YAP interaction observed in MS analysis was as anticipated, showing that OA somehow disrupts the interaction and affects the activity of YAP.

Moreover, OA did not disrupted the interaction of angiomotin family protein member; AMOLT2 with YAP as AMOLT2 has a tumour suppressor potential leading to inhibition of YAP like OA (Zhao *et al*., 2011).

Control	YAP IP	YAP IP + Oleic Acid	Uniprot Accession No	Protein name	Gene name
			P13647	Keratin, type II cytoskeletal 5	KRT5
			P46937	Transcriptional coactivator YAP1	YAP1
			P02533	Keratin, type I cytoskeletal 14	KRT14
			Q13123	Protein Red	IK
			P15311	Ezrin	EZR
			P14923	Junction plakoglobin	JUP
			P23588	Eukaryotic translation initiation factor 4B	EIF4B
			Q86YZ3	Hornerin	HRNR
			P35241	Radixin	RDX
			P33993	DNA replication licensing factor MCM7	MCM7
			P40227	T-complex protein 1 subunit zeta	CCT6A
			Q15061	WD repeat-containing protein 43	WDR43
			O95429	BAG family molecular chaperone regulator	BAG4
			P54886	Delta-1-pyrroline-5-carboxylate synthase	ALDH18A1
			Q9BZZ5	Apoptosis inhibitor 5	API5
			O95453	Poly(A)-specific ribonuclease PARN	PARN
			P43243	Matrin-3	MATR3
			P16401	Histone H1.5	H1-5
			P48444	Coatomer subunit delta	ARCN1
			Q9H8H0	Nucleolar protein 11	NOL11
			P16403	Histone H1.2	H1-2
			Q9Y3X0	Coiled-coil domain-containing protein 9	CCDC9
			Q9NYF8	Bcl-2-associated transcription factor 1	BCLAF1
			Q9Y5Q8	General transcription factor 3C polypeptide 5	GTF3C5
			Q8WVV9	Heterogeneous nuclear ribonucleoprotein L-like	HNRNPLL
			Q9UBD5	Origin recognition complex subunit 3	ORC3

			Q86XZ4	*Spermatogenesis-associated serine-rich protein 2*	*SPATS2*
			Q8WWY3	*U4/U6 small nuclear ribonucleoprotein Prp31*	*PRPF31*
			P07477	*Serine protease 1*	*PRSS1*
			P50990	*T-complex protein 1 subunit theta*	*CCT8*
			Q9NVP1	*ATP-dependent RNA helicase DDX18*	*DDX18*
			Q99829	*Copine-1*	*CPNE1*
			Q06330	*Recombining binding protein suppressor of hairless*	*RBPJ*
			P42166	*Lamina-associated polypeptide 2, isoform alpha*	*TMPO*
			Q9P2K5	*Myelin expression factor 2*	*MYEF2*
			Q9Y2J4	*Angiomotin-like protein 2*	*AMOTL2*
			P06748	*Nucleophosmin*	*NPM1*

	NEGATIVE
	POSITIVE

Figure 6.0 Mass-spectrometry analysis of change in binding partners of YAP upon addition of oleic acid. List of YAP-associated proteins identified in the mass-spectrometry analysis showing the change of YAP binding partners in response of oleic acid.

Thereafter, the expression of specific genes within the Hippo signalling pathway upon addition of oleic acid was analysed by RNA-Sequencing in CaCo-2 cells. The cell samples were prepared according to the protocol in Section 2.1.11 of Materials&Methods chapter and were sent to GENEWIZ for RNA-Sequencing analysis. Expression of target genes upon OA treatment were represented as heat map in Figure 6.1. The blue represents the expression of genes that were downregulated with OA whereas red represents the expression of genes that were upregulated with OA. Amongst several genes that are

downregulated with OA addition, MYC and ANKRD1 genes were identified as downstream target genes of YAP (Choi *et al*., 2018; Zheng *et al*., 2020). MYC, the oncogenic transcription factor is an evolutionary conserved target of the Hippo signalling pathway induced by YAP driving oncogenic activity (Zheng and Pan, 2019). The expression of *Myc* is highly elevated in most human cancers inducing proliferation and progression of tumours (Madden *et al*., 2021). ANKRD1 is also the well-known downstream transcription factor of YAP target genes (Zheng *et al*., 2020; Ou *et al*., 2021). Moreover, matrix metalloproteinase-1 (MMP1) expression was also downregulated with the addition of OA which has been shown to promote carcinogenesis and metastasis by degrading the extracellular matrix and encouring angiogenesis (Liu et al., 2012).

Oleic acid caused upregulation of many genes involved in Hippo signalling pathway shown in red. FRMD6 is one of the most important, as it has been established as a key upstream component of the Hippo signalling pathway resulting in inactivation of YAP (Kronenberg *et al*., 2020; Guan *et al*., 2019). Like FRMD6, TAOK1 is also a Hippo signalling pathway activator leading to inactivation of YAP (Meng, Moroishi and Guan, 2016). WWC2 is also an upstream regulator of Hippo signalling pathway and shown to suppress invasion and metastasis of hepatocellular carcinoma by preventing YAP transcriptional acivity (Zhang et al., 2017; Höffken et al., 2021). Moreover, PTPN14 is also an important upstream regulator of Hippo signalling pathway and with OA, its expression was also observed to be upregulated (Wilson *et al*., 2016). PTPN14 shown to have a potential tumor suppressor role in prostate cancer through modulation of LATS1/YAP signalling (Wang et al., 2020). Interestingly, the binding factor of YAP; TEAD1 in the Hippo signalling pathway was upregulated upon addition of OA. This was surprising as YAP was inactivated with OA.

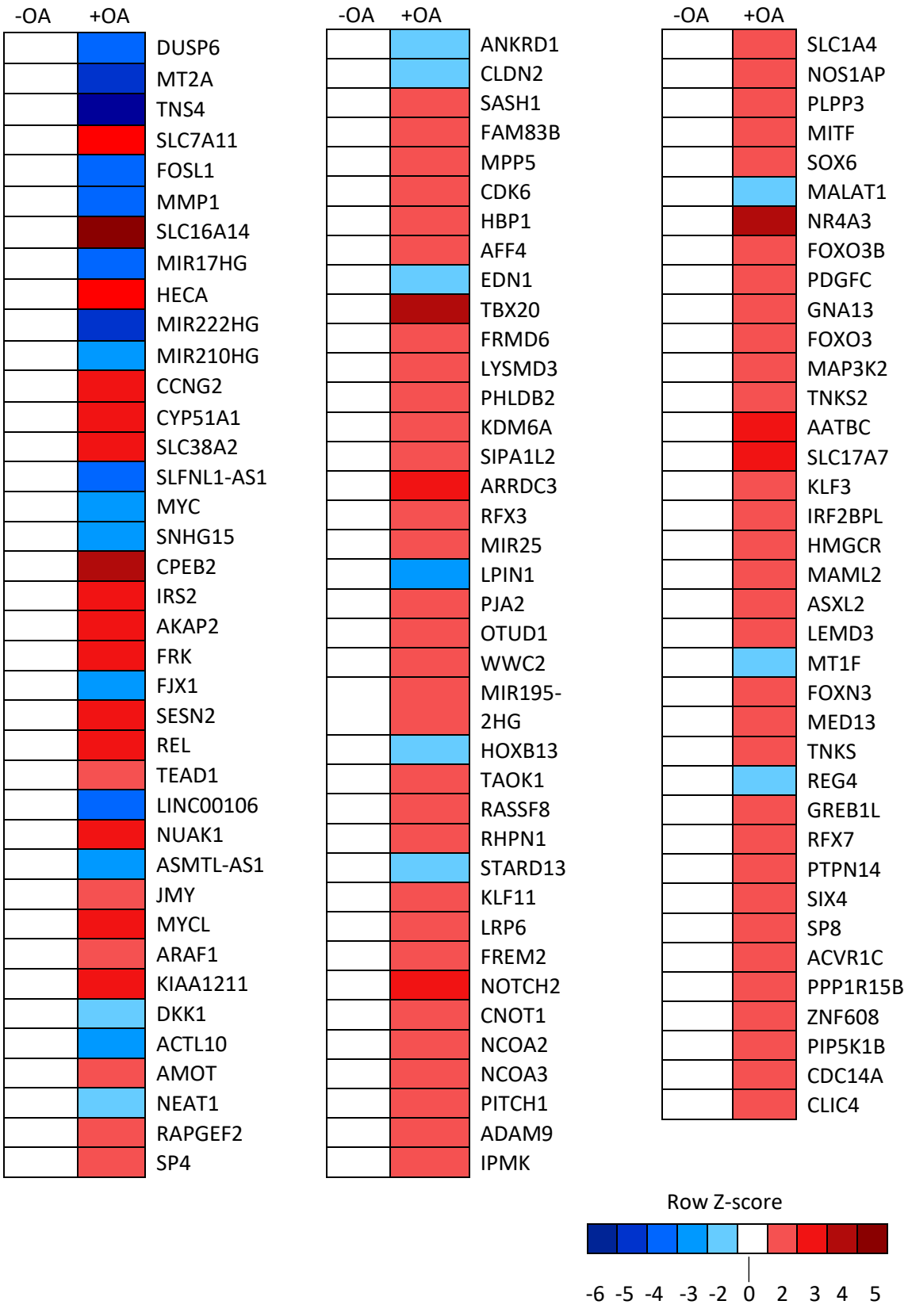

Figure 6.1 Expression of YAP target genes upon addition of oleic acid (OA) analysed by RNA-Sequencing. Heat map showing the YAP-target genes in control (- OA) and in OA-treated (+ OA) CaCo-2 cells. Blue represents down-regulation and red represents up-regulation of target gene expressions.

CHAPTER 7. DISCUSSION

CHAPTER 7. DISCUSSION

The Hippo signalling pathway is a critical biochemical signalling pathway in the context of tissue growth (Kwon, Kim and Jho, 2021; Zygulska, Krzemieniecki and Pierzchalski, 2017). One of the primary regulatory targets of Hippo signalling is the YAP transcriptional coactivator. YAP has been implicated as an oncogene in many published studies (Yimlamai, Fowl and Camargo, 2015; Zhao *et al*., 2007; Park and Guan, 2013). Activation of YAP via the canonical hippo signalling pathway depends on its phosphorylation status on five key HxRxxS consensus motifs, including S127. The LATS kinases phosphorylate YAP on these crucial sites to repress its oncogenic activity and inactivate the protein (Zhao *et al*., 2007; Park and Guan, 2013).

The extracellular matrix (ECM) is also known to play a crucial role in the regulation of Hippo signalling pathway (Moroishi, Hansen and Guan, 2015), however, the connection between the ECM, Hippo signalling pathway and lipid metabolism has not yet been fully established. What we know from previous research is that Src can activate YAP by direct phosphorylation at multiple tyrosine positions (Tyr-341, Tyr-357 and Tyr-394) to induce transcription of target genes (Cunnigham and Hansen, 2022; Dasgupta and McCollum, 2019).

7.1 Characterisation of a Novel Hippo/ECM Protein Complex

During the course of this project, an important and novel protein complex was characterised which for the first time couples the Hippo signalling pathway, the ECM and lipid metabolism. Hep-G2 and CaCo-2 cells were selected during the project as a preferred model systems due to their physiological suitability and susceptibility and link to the ECM.

Previous studies have validated that various ECM proteins including Enigma family proteins with PDZ and LIM domains were implicated in YAP regulation (Elbediwy *et al*., 2018). Talin2 was found in mass spectroscopy studies to interact directly with YAP (Elbediwy *et al*., 2018). This potential interaction between the Hippo signalling pathway effector YAP and the ECM protein Talin was validated using a Co-immunoprecipitation assay. Talin-family members could be a novel and important interactor of the Hippo signalling pathway by acting as a mechanosensors in the regulation of YAP through the ECM (Elbediwy *et al*., 2018; Cobbault *et al*., 2020).

Activity and stability of YAP through the ECM involves a range of proteins including talin, vinculin and PDLIM family proteins. External forces sensed by integrins are transmitted to talin family members allowing YAP and accessory proteins to act as a mechanosensors. Talin is relevant for intracellular mechanical connection as it's unfolding upon mechanical cues leads to focal adhesion formation thus integrin signalling; crucial in YAP regulation (Elosegui-Artola *et al*., 2017). A candidate approach was used to identify components which may bind to this YAP/Talin complex and 3 other components of the ECM were identified, which were CD2AP, PDLIM7 and Ezrin. YAP was found to directly interact with Ezrin while Talin acted as a linker to YAP and the other members of the complex by interacting with both ECM proteins; CD2AP and PDLIM7. YAP has been found previously to also directly link to PDLIM7 (Elbediwy *et al*., 2018). Further co-immunoprecipitation assays were implemented with CD2AP also shown to interact with PDLIM7 and YAP. The interaction of YAP/Talin complex with PDLIM7 was expected as a previous study confirmed that binding of Enigma proteins; PDLIM5 and PDLIM7 is required for the translocation of YAP to the nucleus, thence its activation (Elbediwy *et al*., 2018). Ezrin which was also confirmed to interact with the YAP/Talin complex, has an important role in the regulation of Hippo

signalling pathway as its phosphorylation has been previously shown to promote activation of YAP (Kawaguchi and Asano, 2022; Xue *et al*., 2020; Quan *et al*., 2018).

CD2-associated protein (CD2AP), actin-assembly regulator has been also found as a component of the complex by interacting with YAP (Schiffer *et al*., 2004; Lehtonen, Zhao and Lehtonen, 2002). CD2AP regulates actin dynamics by binding to F-actin capping protein, CapZ (Elbediwy *et al*., 2012). There is no evidence for direct interaction of CD2AP with YAP, however, CapZ was shown to restrict YAP/TAZ activity of cells experiencing low mechanical stress and interaction of CD2AP with CapZ is a requirement for junction formation and actin assembly (Aragona *et al*., 2013; Elbediwy *et al*., 2012). Thus, interaction of CD2AP and YAP directly although not been shown in this project is a distinct possibility under the correct conditions possibly when encountering mechanical stress; so CD2AP may be involved in the regulation of the Hippo signalling pathway via mechanotransduction. Thus, taken this all together, a significant and novel complex connecting the Hippo signalling pathway, the ECM and lipids can be described (Figure 7.0).

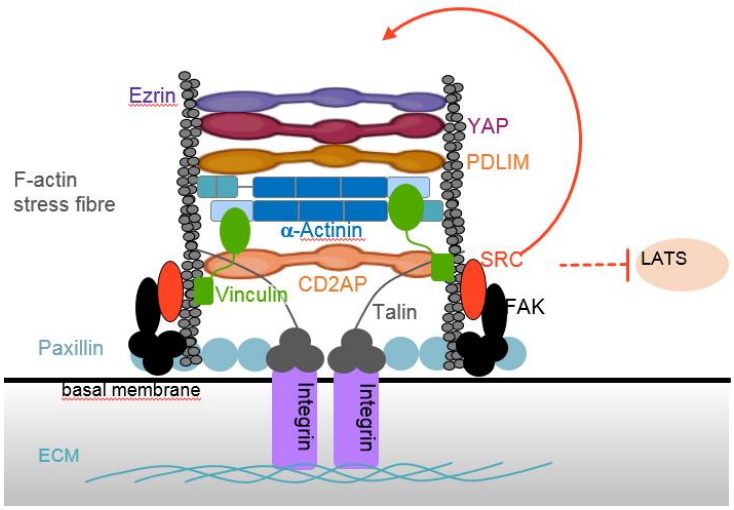

Figure 7.0 The Hippo/ECM protein complex. Schematic diagram of the protein complex consisting of YAP, Talin, PDLIM, CD2AP and Ezrin coupling the Hippo signalling pathway and the ECM (Adapted from; Elbediwy et al., 2018).

After the characterisation of the novel protein complex, determination of the effect of removal of one member of the complex on other key members of the complex using siRNA-mediated knockdowns was determined.

Depletion of YAP and Talin caused a significant deceleration in the migration of cells, whereas this was not observed upon CD2AP and Ezrin depletion. The results obtained upon depletion of YAP and Talin were expected. The transcriptional co-activator, YAP has a role in the expression of genes involved in cell proliferation, migration and anti-apoptosis (Jiang *et al*., 2021; Yu and Guan, 2013; Zeng and Dong; 2021). Transcription of genes is essential for persistent cellular migration and in the regulation of focal adhesion maturation as an inhibition of transcription results in migration arrest due to enhanced cytoskeletal tension, stress fiber formation and larger FAs. As previously reported, YAP/TAZ has a requirement for continuous cell migration and is involved in the control of cytoskeletal tension and FA maturation. In migrating cells, newly formed FAs provide attachment of the cell to the ECM and coupling of the actin cytoskeleton to FAs which allows force exertion thus leading to cellular migration. Published studies demonstrated that depletion of YAP/TAZ reduces directional movement of the cells and impairs continuous migration resulting in remarkably slowed migration (Nair and Wirtz, 2019; Mason *et al*., 2019). A study by Zhao *et al.* (2020) stated that depletion of YAP resulted in a significant decrease in cell motility and alterations in the arrangement of the actin cytoskeleton. Moreover, in colorectal cancer (CRC), YAP was shown to be overexpressed and promote cellular migration, EMT and thus invasion. Downregulation YAP expression in CRC resulted in inhibition of cell migration (Jiang *et al*., 2021; Cheng *et al*., 2020). Therefore, the decrease of cellular migration in CaCo-2 cells upon YAP knockdown is consistent with published studies.

Talin residing at focal adhesions is a requirement for sustained cell growth and traction force generation (Rahikainen *et al*., 2019). Several studies have described an influence of

talin1 and talin2 on cellular migration and invasion (Liang et al., 2018; Ji et al., 2021). Talin2 depletion in breast cancer cells and hepatocellular carcinoma cells was shown to inhibit the growth, invasion and migration of cells (Liang *et al*., 2018). Moreover, Talin-1 knockdown in colorectal cancer cells was shown to reduce rate of proliferation, migration and invasiveness of cells via regulation of the key epithelial-to-mesenchymal (EMT) pathway (Ji *et al*., 2021). A study by Zhang *et al.* (2008), validated that presence of talin is essential for continuous cell spreading as depletion of talin severely affected FA dependent pathways that are required for cell adhesion and migration. Therefore, the slowdown of cellular migration upon depletion of talin was expected.

As mentioned, the CD2AP-CapZ interaction is well established and and CapZ has been shown to restrict the activity of YAP/TAZ (Aragona *et al*., 2013; Elbediwy *et al*., 2012). In gastric cancer, expression of CD2AP was found to be downregulated, causing increased migration and invasion. Downregulation of CD2AP increased metastatic gastric cancer cells by interacting with CAPZA1 to encourage cell adhesion and cytoskeleton assembly whereas its upregulation resulted in considerable decrease of cell migration and invasion (Xie *et al*., 2020). CD2-associated protein recruits actin-capping protein to the cortactin (Src kinase substrate) at the leading edge of cell which is essential to define lamellipodium formation and necessary for cellular migration (Zhao *et al*., 2013). The effect of CD2AP on cell migration can be dependent on these accessory proteins and that might be the reason for not observing any clear effect in cellular migration of CaCo-2 cells upon its knockdown.

Moreover, depletion of ezrin in CaCo-2, a colorectal cancer cell line did not reduce the migration of cells. What was interesting was that a study in cervical cancer cell lines revealed that depletion of ezrin inhibited cellular migration (Xi and Tang, 2020). The same result was also obtained in hepatocellular carcinoma with decreased invasiveness of cells upon ezrin depletion (Xi and Tang, 2020). Also, migration ability of breast cancer cells was

inhibited by the silencing of ezrin. However, in human intrahepatic cholangiocarcinoma, downregulation of ezrin led to an increase in metastatic phenotype of the cells (Li *et al*., 2019). This inconsistency suggests that the effect of ezrin in various cancer cell line differs.

As talin depletion affected the cellular migration of CaCo-2 cells, talin isoforms (talin1 & talin2) were silenced individually to see if their depletion affected the phosphorylation of YAP at its most common canonical phosphorylation site (S127). (Cunningham and Hansen, 2022; Kwon, Kim and Jho, 2021; Han, 2019). Both Talin1 and Talin2 isoforms interact with YAP. Upon sensing mechanical stress, Talin1 unfolds and binds to vinculin resulting in nuclear translocation of YAP and adhesion growth whereas Talin2 interacts with F-actin polymers and an Integrin-FA cascade to promote the activation of YAP through Src kinases (Zhao, Lykov and Tzeng, 2022; Rausch and Hansen, 2020; Zhang *et al*., 2019). Integrin-Src signaling can affect YAP phosphorylation by LATS1/2 modulation or via Src activation of FAK. YAP can also be activated via direct tyrosine phosphorylation (Elbediwy *et al*., 2018). Association of YAP with a talin-integrin-actin complex allows Src to directly phosphorylate YAP at multiple positions to ensure activation independently of hippo signalling pathway regulation; these sites are all tyrosines and are as follows: Tyr-341, Tyr-357 and Tyr-394 and this promotes YAP nuclear translocation and transcriptional activity (Cunnigham and Hansen, 2022; Dasgupta and McCollum, 2019).

Depletion of Enigma proteins resulted in cytoplasmic sequestration of YAP and reduced Src-kinase dependent YAP phosphorylation (Elbediwy *et al*., 2018; Rausch and Hansen, 2020). A study by Elbediwy *et al*. (2016), showed that basal contact and consequently integrin-Src signalling is the main determinant of YAP/TAZ nuclear localization in basal layer cells and skin tumours. Upon loss of basal contact, YAP/TAZ was shown to be cytoplasmic. Integrin-Src signalling is crucial to assist stabilization and nuclear localization of YAP in the basal layer of cells. The study by Elbediwy *et al.* (2016), also confirmed antagonistic apical

and basal polarity signals in columnar epithelial cells (CaCo-2) act as key mechanical controllers in the determination of YAP cellular localization. Cells plated at low density with a flat morphology occupy an extensive basal surface area and thus invoke integrin-Src signalling. Activation of integrin-Src signalling via these basal signals result in inhibition of LATS kinases and promotes YAP nuclear localization by decreasing p-YAP levels in human CaCo-2 epithelial cells. In contrast, columnar epithelial cells are able to differentiate an apical domain and induce relocalization of YAP to the cytoplasm by increasing the p-YAP levels through the activation of LATS kinases and subsequently activation of the hippo signalling pathway. Thus, contact with the basement membrane localize YAP to drive various transcriptional activities via integrins (Elbediwy *et al*., 2016).

Based on the findings of similar studies, knockdown of both talin1 and talin2 was expected to inactivate and sequester YAP in the cytoplasm by increasing phosphorylation of the YAP S127 site as Talin is involved in nuclear translocation of YAP. Knockdown of talin2 increased pYAP levels and suppressed its activity in Hep-G2 cells (Figure 3.11) whereas it showed an opposite effect by decreasing pYAP levels in CaCo-2 cells (Figure 3.12). This contradictory set of results might be as a result of basal activation signals that are independent of LATS and the canonical pathway and thus serine YAP phosphorylation (Elbediwy *et al*., 2016).Talin2 depletion might inactivate YAP via decreased tyrosine phosphorylation by Src kinases rather than phosphorylation of S127 site by LATS family kinases. This could be the reason why no increase was observed in S127 YAP phosphorylation levels upon Talin2 knockdown in CaCo-2 cells.

The other potential issue is the level of Talin2 RNAi depletion, which may not be as efficient and thus may have not had much effect on the levels of pYAP. Assessing protein level of Talin2 is required, however because of low levels of talin2, depletion can be difficult to detect. Moreover, cell type could be an important determinant of Hippo signalling pathway

regulation for the dissimilarity, as YAP maybe regulated differently in CaCo-2 cells. CaCo-2s are columnar epithelial cells with very structural apical and basal column shape whereas Hep-G2 cells retain flat morphology and do not receive apical and basal signals as strongly as CaCo-2 cells so this indifference between apical and basal layers may also have a role in the regulation of the protein.

However, interestingly, the knockdown of Talin1 showed opposite effects to talin2 by decreasing pYAP S127 levels in both cell lines (Figure 3.10 & 3.12). Therefore, both talin1 and talin2 were depleted in CaCo-2 cells to observe if the result obtained upon knockdown of only one of the isoforms was due to redundancy of siRNA; however, the result obtained was the same with depletion of talin1 upon depletion of both talin isoforms.

Next, the effects of knockdown of individual components of the complex on the subcellular location of YAP in both confluent and sparse conditions in CaCo-2 and Hep-G2 cells was determined. Immunofluorescence staining of YAP was used to determine the effect of individual complex members on the translocation of YAP between the nucleus (active) and cytoplasm (inactive) in the context of CD2AP/Talin/Ezrin siRNA depletion.

YAP in the control state was observed to be cytoplasmic in highly dense cells and translocated into the nucleus when cells were at low density. Cell density and cell-to-cell contact are prominent regulators of YAP nuclear/cytoplasmic shuttling (Zhao *et al*., 2007; Cai, Wang and Meng, 2021). At high density, the physical connections between cells increases (adherent and tight junctions), leading to cytoplasmic retention of YAP through activation of LATS kinases in a Hippo signalling dependant process (Wang *et al*., 2021; Ko and Guan, 2018; Meng, Moroishi and Guan, 2016; Park and Guan, 2013). When the cells are in a confluent state, the Hippo signalling pathway becomes activated by perceiving a signal from the adherens junctions leading to phosphorylation of YAP by upstream LATS1/2

kinases resulting in translocation of YAP to the cytoplasm. This results in a loss of myosin-II contractile activity and actin-stress fibers formation and cytoplasmic retention of YAP (Pavel *et al*., 2018; Das *et al*., 2016). When cells are sparse, LATS1/2 kinases become inactivated and the level of YAP dependent hippo phosphorylation is low due to absence of adherens junctions which shuttles YAP into the nucleus (Zheng and Pan, 2019; Dobrokhotov *et al*., 2018). The cytoskeleton is perturbed with myosin-II contractile activity and actin stress fibers increased promoting activation of YAP by translocation into the nucleus (Pavel *et al*., 2018; Das *et al*., 2016).

Depletion of YAP led to an observation of less CD2AP, Talin and Ezrin only in confluent CaCo-2 conditions. This could be due to the morphological and functional characteristic of CaCo-2 cells as they express a polarized columnar epithelia when differentiated (Hiebl *et al*., 2020). Upon reaching confluency, tight junctions form between the adjacent cells and establish a barrier among the upper and lower parts of the cell resulting in apical-basal polarity (Lea, 2015). This polarity is maintained when the cell contacts with the ECM and receives various signals from polarity proteins, junctional cadherin and focal adhesions (Piroli, Blanchette and Jabberzadeh, 2019). The antagonistic apical and basal polarity signals in columnar epithelial cells (CaCo-2) act as key controllers for YAP cellular localization. Differentiation of CaCo-2 cells to form an apical domain at high density induce localization of YAP to the cytoplasm due to activation of the apical hippo signalling pathway, while cells at low density with an extensive basal surface area localize YAP to the nucleus via integrins (Elbediwy *et al*., 2016). Therefore, silencing expression of YAP is expected to lower the expression of ECM proteins at high density preventing their morphological actions. In Hep-G2 no effect was observed upon YAP depletion which might be due to the morphology of Hep-G2 cells as they do not express a columnar-epithelia like

CaCo-2 cells.

Depletion of CD2AP had no effect on the subcellular location or expression of YAP in both cell lines which shows that depletion of CD2AP is not efficient to shuttle YAP between the nucleus and cytoplasm. Previous studies elucidated the importance of F-actin capping proteins as negative regulators of YAP/TAZ in human mammary epithelial cells (Seo and Kim, 2018). At high density, cells encounter contact inhibition, YAP/TAZ is inactivated and rendered cytoplasmic by CapZ and its depletion results in activation and nuclear localization of YAP/TAZ (Aragona *et al*., 2013). Therefore, as was previously found, CD2AP interacted with CapZ (Elbediwy *et al*., 2012) and its knockdown was expected to affect the location of YAP but that was not the case. The direct interaction between CD2AP and YAP still needs to be unravelled to understand the relationship of CD2AP and how it can stabilize YAP in the cell lines tested.

The effect of Talin knockdown on YAP location was clear as depletion resulted in shuttling of YAP to the cytoplasm and assumed inactivation. Talin as a mechanosensor manages the transmission of tension between the actin cytoskeleton and the ECM with FAs and participates in integrin activation (Zhao, Lykov and Tzeng, 2022). Cells that are in high density sense the softness of cells around them whereas cells at low density only sense the substrate stiffness in which they are cultured in. This mechanosensing is crucial for the organization of cells, as mechanical forces sensed through the cytoskeletal tension upon different cell densities dictate the behaviour of cells (Wells, 2018).Based on mechanical tension, talin, triggers FAK and Src activation and results in increased cellular proliferation by promoting YAP nuclear localization and activation (Dasgupta and McCollum, 2019).

A study conducted by Nikolopoulou *et al.* (2022), elucidated the importance of talin in mechanosensing as talin depleted epithelial cells were unable to sense and translate

microenvironmental forces into cell responses by translocating YAP into nucleus. Talin deficient epithelial cells were unable to spread and YAP was mainly sequestered in the cytoplasm. Talin was also depleted in retinal blood vessels and resulted in a reduced localization of nuclear YAP (Nikolopoulou er al., 2022). Moreover, talin depleted cells were shown to inhibit formation of FAs and YAP nuclear localization (Virdi and Pethe, 2021). Research by Nikolopoulou *et al.* (2022) suggests that talin is essential for nuclear localization of YAP, and results matched this as depletion of talin translocated YAP into cytoplasm. YAP was nuclear in sparse cells and upon depletion of talin YAP translocated into cytoplasm whereas in confluent conditions, YAP was equally nuclear/cytoplasmic and became clearly cytoplasmic upon Talin knockdown in both cell lines.

In CaCo-2 cells, the knockdown of ezrin is shown to affect localisation of YAP, as ezrin depleted cells were shown to have higher levels of cytoplasmic YAP. In previous studies, Ezrin was found to induce nuclear translocation of YAP by phosphorylating the protein in pancreatic cancer cells through activation of the Akt/mTOR pathways and promote vascular endothelial cell migration by translocation of YAP to the nucleus (Quan *et al*., 2019; Chen *et al*., 2021). Moreover, skin fibroblast cell size was reduced by depletion of ezrin through impairment of YAP nuclear translocation which functionally indicated that ezrin depletion could inhibit YAP target genes and skin fibroblast proliferation by preventing its nuclear translocation and sequestering YAP in cytoplasm (Quan *et al*., 2018). Therefore, the results obtained upon depletion of ezrin in CaCo-2 cells are in agreement with the previous studies indicating that ezrin is important for YAP nuclear translocation. However, knockdown of ezrin had no effect on YAP in Hep-G2 cells which are hepatocellular carcinoma cells. A study conducted by Xue *et al*. (2020), reported that in hepatocellular carcinomas, phosphorylated-ezrin (at Thr567) activate YAP by increasing its expression. Phosphorylation of ezrin results in a conformational change of ezrin from a folded state

into unfolded state leading to its association with the plasma membrane to regulate YAP and growth of hepatocellular carcinoma cells (Xue *et al*., 2020). That might be the reason for lack of effect on YAP with depletion of wild-type ezrin in hepatocytes as maybe only the p-ezrin affects the activity of YAP (Xue *et al*., 2020).

7.2 The Regulation of the Novel Protein Complex by Lipid Metabolism

The next aspect was to determine the effect of lipid metabolism on the Hippo signalling effector YAP and the novel components of the Hippo/ECM complex and assess whether the complex characterised in this research regulates or is regulated by lipid manipulation. In this study, the most abundant free fatty acids, oleic and palmitic acid were used and their effect on the Hippo signalling pathway tested using CaCo-2 and Hep-G2 cells. The effect of lipid manipulation on cellular migration was assessed by scratch assays using CaCo-2 cells. The effect of addition of lipids on YAP and its activity was assessed by analysing the phosphorylation state of YAP, using key LATS dependant phosphorylation site serine 127. pYAP levels were drastically modified with a statistically significant increase in phosphorylation of YAP at S127 site. To justify the observed pYAP levels upon lipids addition, immunofluorescence was used to validate whether addition of lipids interfered with the localization of proteins of the identified complex. Finally, the levels of lipid droplet formation by addition of oleic acid in conjunction with depletion of proteins within the complex was evaluated using again immunofluorescence microscopy. The experiments provide a new insight into the relationship of lipid metabolism with the ECM and Hippo signalling pathway.

Previously published studies have elucidated the effects of oleic acid and palmitic acid on various cell types involving different signalling and metabolic pathways. The effect of oleic

acid which is an n-9 monounsaturated fatty acid (Liu *et al*., 2013) has been examined in many different cancerous cell lines. Oleic acid has been shown to have various effects on cancer cell proliferation, migration and invasion. For example, proliferation and migration was induced in MCF-7 and MDA-MB-231 breast cancer cell lines through the activity of FFAR1/4, EGFR, AKT and PI3K whilst invasion was mediated through a PI3K/Akt dependent pathway (Soto-Guzman *et al*., 2008 and Marcial-Medina *et al*., 2019). Oleic acid was also found to promote proliferation and migration of highly metastatic cancer cells via enhanced β-oxidation, mediated by activation of AMPK, whereas in low metastatic cancer cells it was found to have an inhibitory effect and inhibit growth and survival of cancerous cells (Li *et al*., 2014). On the contrary, OA was shown to have an ability to inhibit proliferation and have anticancer effects in many cancer cell lines such as prostate, breast and colorectal cancer (Jiang *et al*., 2017; Farag and Z. Gad, 2022). Oleic acid was also found to have anti-proliferative effects in breast cancer by suppressing HER2 gene expression and on hepatocellular carcinoma by reducing autophagy (Menendez *et al*., 2005; Guilitti *et al*., 2021) and a strong anti-proliferative effect on Tongue Squamous cell carcinomas (TSCC) by inducing cell cycle arrest in the G0/G1 phase of mitosis and cell death via autophagy and apoptosis through the Akt/mTOR pathway (Jiang *et al*., 2017). However, there are no studies on the effects of oleic acid on the activity of YAP and its mechanism of action in the Hippo signalling pathway.

Palmitic acid on the other hand was shown to reduce the ability of prostate cancer cells to invade across ECM barriers by suppressing the secretion of exosomes and exosome-associated molecules (Maly and Hofmann, 2020). A study published by Yuan *et al*. (2017) showed that palmitic acid dysregulates the Hippo-YAP pathway through inducing mitochondrial damage. Upon damage, cytosolic DNA sensor cGAS and STING is activated resulting in IRF3 activation which in turn induces the expression of the Hippo signalling

pathway kinase MST1 and phosphorylation of YAP. Therefore; nuclear YAP and its function is prevented resulting in inhibition of endothelial cell proliferation, migration and tube formation. Functionally, overexpression of YAP or MST1 knockdown obstruct the inhibitory effect of PA on endothelial cell proliferation (Yuan *et al*., 2017; Koo and Guan, 2018). These observations suggest that palmitic acid leads to an increase of Hippo signalling pathway dependant YAP phosphorylation levels thus inactivation.

Observations from previously published studies in other cell lines (Menendez *et al*., 2005; Guilitti *et al*., 2021; Yuan *et al.,* 2017; Jiang *et al.,* 2017) show similar results for cellular migration upon administration of 2 mM oleic and 0.5 mM palmitic acid as migration of CaCo-2 cells was also significantly reduced upon wounding. The decrease in cellular migration could be due to the lipids causing inactivation of YAP. To test this hypothesis, activity of YAP was assessed by quantifying its S127 phosphorylation levels after addition of lipids. Treatment of CaCo-2 and Hep-G2 cells with 2mM oleic acid significantly increased the level of YAP phosphorylation thus subsequent inactivation of the transcriptional co-activator of Hippo signalling pathway and its retention in the cytoplasm, inhibiting cellular proliferation. An increase in phosphorylation of YAP was also observed when cells were treated with 0.5 mM palmitic acid. Thus, both lipids; oleic and palmitic acid inhibited YAP by increasing its hippo dependant phosphorylation on the S127 site resulting in cytoplasmic retention of YAP and thus decreased cell proliferation. A lower OA concentration also resulted in an increase of pYAP levels in Hep-G2 cells, however, almost no significant effect was observed in CaCo-2 cells with low concentrations of OA and controls with no added OA. Morphology of CaCo-2 cells can be the reason for not observing any effect with low OA concentrations as they are columnar epithelial cells with antagonistic apical and basal signals. Moreover, this could be due to experimental variation including variation due to

sample preparation, measurement, technical replication of experimental protocols and experimental factors.

Cells were also treated with a combination of oleic and palmitic acid with the assumption that combination treatment may result in a higher level of YAP phosphorylation, but that was not the case as pYAP levels, although increased in comparison to control, decreased when combined compared to treatment alone and no significant effect was therefore observed. This may be due to the attenuation of the palmitic acid effect by oleic acid when combined.

Ricchi *et al.* (2008), studied insulin signalling impairment, by administration of both oleic acid and palmitic acid. The study found that combination of the two fatty acids lowered insulin signalling impairment compared to palmitic acid alone suggesting a protective effect of oleic acid. The protective feature of oleic acid might be the reason for the increase of pYAP levels when combined with palmitic acid.

After confirming the effect of lipids on YAP phosphorylation and activity, OA was again used to test if the interaction between YAP and the members of the complex was affected. Oleic acid was shown to disrupt the interaction of YAP with CD2AP and the interaction of Talin with CD2AP. As seen previously, oleic acid resulted in inactivation of YAP by hippo signalling dependant phosphorylation and inactivation of YAP by OA prevents the protein binding to CD2AP thus it appears that active YAP is required for binding to CD2AP. As previously shown, talin acted as a linker to YAP and the other complex members by interacting with ECM proteins, inactivation of YAP and talin with OA could prevent talin acting as a linker to bind to CD2AP and therefore decrease the interaction between YAP and CD2AP. However, why this is the case remains unclear and would warrant further study.

To get a further understanding of the effect of lipid manipulation on the ECM/Hippo complex, the cellular location of YAP and the components of the complex were visualized by fluorescence staining. YAP was expected to translocate from the nucleus to cytoplasm as it was shown to be inactivated with an increased phosphorylation level upon OA treatment. This was achieved in both CaCo-2 and Hep-G2 cells as nuclear YAP was decreased, and the cytoplasmic pool of the protein was increased after oleic acid treatment. CD2-associated protein (CD2AP) was not affected by treatment with OA, but OA was shown to decrease the levels of talin and ezrin in CaCo-2 cells. CaCo-2 cells have a strong ECM as previously mentioned, so signals coming from the base activating the integrin-src signalling pathway through talin would encourage nuclear YAP localization. Addition of lipids might interfere with this process affecting talin and decreasing its expression at protein level, thus making it unable to interact with integrins and Src to activate YAP leading its retention in cytoplasm (Elbediwy *et al*., 2016). However, OA only affected the localisation of YAP with no clear effect on the components of the complex in Hep-G2 cells. The morphology of the Hep-G2 cells can be the reason as Hep-G2 cells grow as mono-layers, retain a flat morphology (Bokhari *et al*., 2007), with less extracellular matrix based signalling and thus perturbed integrin/Src signal does not occur hence why oleic acid did not have any effect on the ECM proteins in Hep-G2 cells.

Cellular lipid metabolism was further evaluated through the effects of components of the complex on lipid droplet formation. The regulation of changes in lipid droplet size and number is not fully understood. Previous studies indicate that lipid droplet formation stimulated by oleic acid supplementation is regulated through the activation of the FFAR4 fatty acid receptor through the involvement of PI3K, AKT and phospholipase D activity in hepatoma cell line, Huh-7 cells (Rohwedder *et al*., 2014). Therefore, establishing if the Hippo signalling pathway component, YAP and its complex members were involved directly

in lipid droplet formation in CaCo-2 and Hep-G2 cells would be novel. Depletion of YAP, CD2AP, Talin and Ezrin appeared to have an increase in lipid droplet formation in Hep-G2 cells treated with oleic acid, whereas a significant decrease in lipid droplet formation was observed upon knockdown of the proteins in treated CaCo-2 cells. The presence of the components of the complex was shown to be essential in lipid droplet formation in CaCo-2 cells but how these proteins contribute to this is not known and needs further research. The cell type can be the major determinant of this dissimilarity, as Hep-G2s (hepatocellular carcinoma cells) are liver cells and may store and or metabolise lipids differently to CaCo-2 cells (Paramitha *et al*., 2021). Research by Li *et al.* (2021), measured the effect of oleic acid lipid deposition on actin cytoskeleton arrangements in Hep-G2 cells. Upon oleic acid treatment, Hep-G2 cells showed an obvious lipid deposition with increased density and the size of lipid droplets. This had no direct effect on actin cytoskeleton rearrangements, as actin filaments remained intact confirming that the observed increase was dependent on intracellular lipid deposition not on the remodelling of the actin cytoskeleton (Li *et al*., 2021). As observed in this research, depletion of components of the complex did not result in a decrease in lipid droplet formation, instead more lipid droplets were observed in Hep-G2 cells therefore ECM proteins that can interact or link to the actin cytoskeleton are not directly involved in lipid droplet formation in Hep-G2 cells, as no significant change was observed in actin cytoskeleton remodelling, as shown in the previously published study. However, this was not the case in CaCo-2 cells as presence of actin-related ECM proteins and YAP were shown to have an essential role in lipid droplet formation. The clearly defined apical-basal polarity which differentiates in CaCo-2 cells is suggestive of a lot of remodelling of the actin cytoskeleton through ECM cross-linkage. This may interfere with lipid droplet formation which might explain the significant reduction in LD formation upon complex protein depletion. Several proteomics studies have revealed that lipids droplets are

embedded with various proteins and presence of specific proteins on the LD surface facilitate their movement along the cytoskeleton to allow their interaction with signalling molecules resulting in diverse functionality such as membrane trafficking and intracellular signalling (Demignot, Beilstein and Morel, 2014; Ding *et al*., 2012). Proteins involved in lipid droplets can vary among different cell types and also within a single cell due to various lipid droplet populations and can be dependent on cell physiopathology (Demignot, Beilstein and Morel, 2014). A proteomics study by Ding *et al*. (2012), identified that both Talin1 and Talin2 were associated with lipid droplets isolated from mouse white adipocytes. Thus, CaCo-2 cells may result in actin cytoskeleton remodelling upon oleic acid treatment and involve talin and other components of the complex and subsequent activation of YAP and thus result in lipid droplet formation, however there is no clear evidence about which proteins and signalling pathways are involved in lipid droplet formation in CaCo-2 cells. Further studies on how the complex may regulate lipid droplet formation would be required, including assessing if complex members bind to lipid droplets and or the actin cytoskeleton. It would be interesting to analyse lipid metabolism in the context of an *in vivo* model.

7.3 Assessing the Link between YAP and Lipid Metabolism *in vivo*

In order to assess the effect of lipid metabolism in a physiologically relevant system, it was decided to use planarian flatworms. Planarian flatworms have been used as a model organism to great effect in research as the presence of pluripotent stem cells throughout their body facilitate the examination of complex physiological processes (Ge *et al*., 2022) . In this project oleic and palmitic acid were used to examine effects on the expression levels of *Hippo* (ortholog of Mats) and the Planarian ortholog of YAP, known as *Yorkie* in two

different planarian species: *Dugesia Lugubris* and *Schmidtea Mediterranea*. The precise measurement of *Hippo* and *Yorkie* gene expression levels after fatty acid microinjection was measured by using real-time quantitative reverse transcription PCR (RT-qPCR). Beta actin (ACBT) was used as a reference (housekeeping/loading control) gene in the quantification of gene expression in this part of the project as it is the most stable reference gene expressed in the regeneration process of planarian (Yuwen *et al*., 2011).

The Hippo signalling pathway has been previously implicated in the regeneration process of Planarian flatworms (Hayashi, Yokoyama and Tamura, 2015). Planarians are considered an excellent in vivo model organism to study regeneration processes owing to a large pluripotent stem cell population throughout their body (Cote, Simental and Reddien, 2019; Ge *et al*., 2022). Two highly flexible systems are required for the process of planarian regeneration. Pluripotent neoblasts lead to production of any kind of new cells whereas muscle cells give instructions for regeneration of planarian (Karami *et al*., 2015). Planarians, when cut into pieces can regenerate their body parts and maintain themselves; heads, tails, sides and became a complete worm within days (Reddien, 2018; Angerer *et al*., 2019).

To study the expression of *Hippo* and *Yorkie* genes during regeneration and following oleic acid microinjection, *Dugesia Lugubris* worms were cut into three pieces and the trunk part of the worm's body was used. Whole planarian worms were used as a baseline in the experiment without any microinjections. The trunk fragments were microinjected with water and oleic acid, before being examined at Day 5 and Day 7 post treatment. There was no significant change in the expression of the *Hippo* gene when *Dugesia Lugubris* trunks were treated with oleic acid. However, significant changes were observed in *Yorkie* gene expression upon oleic acid treatment of *Dugesia Lugubris* trunks. *Yorkie* gene expression was increased significantly at Day 5 untreated trunk when compared to the whole planarian. The reason for a prominent increase in *Yorkie* gene expression maybe due to the

rapid regeneration of the *Dugesia Lugubris* trunk fragment. Recently published studies revealed the function of the yap/yorkie gene in regeneration using various flatworm species (Hayashi, Yokoyama and Tamura, 2015; Hwang *et al*., 2015). Primarily, in the basal flatworm *Mac-rostomum lignano*, expression of YAP is shown to be upregulated in regenerating stem cells (neoblasts) to promote proliferation, as conversely, the knockdown of the Mac-Yap gene by RNAi in *M.lignano* basal flatworm caused a reduction in proliferation during homeostasis (Hayashi, Yokoyama and Tamura, 2015; Hwang *et al*., 2015). Another species of freshwater planarian, *Dugesia japonica* was also used to assess the role of the *Yorkie* gene. The knockdown of *yki* gene in *Dugesia japonica* also resulted in a decrease in stem cell proliferation during homeostasis again showing that expression of yap/yki gene is essential for stem cell proliferation during regeneration and homeostasis *in vivo* (Hwang *et al*., 2015). Therefore, an increase in *Yorkie* gene expression of *Dugesia Lugubris* trunks is a necessity during the regeneration process in this species showing the same phenotypic pattern with the *M. lignano* and *Dugesia japonica* species (Hayashi, Yokoyama and Tamura, 2015; Hwang *et al*., 2015).

A decrease in *Yorkie* gene expression of *Dugesia Lugubris* trunks resulted in an inhibition of regeneration upon oleic acid microinjection. The decrease in *Yorkie* expression is observable after oleic acid injection on both Day 5 and Day 7 when compared with untreated Day 5 control. The lipid profile of planarian; Dugesia anceps was observed in a previously published study (Angerer *et al*., 2019) and the regenerating planarian shown to contain less unsaturated fatty acids (Angerer *et al*., 2019). Oleic acid is a mono-unsaturated fatty acid so addition of oleic acid may interfere with the regeneration process of *Dugesia Lugubris* somehow and that can be the reason of reduced *Yorkie* gene expression (Giulitti *et al*., 2021).

The next part of the project was to investigate *Schmidtea mediterranea (S.med) planaria,* in order to determine the duration of wound closure upon oleic acid treatment. *S.med* worms were microinjected with oleic acid and worms were examined for wound resolution after 2 and 7 days respectively. The results obtained clearly indicated that oleic acid injection slowed down the wound healing process, as most of the control worms fully closed around day 2 whereas OA injected worms mostly closed around day 7. Thus, it can be concluded that OA significantly inhibited the wound healing process of *S.med.* The effect of OA wound closure could be due to the effect of the lipid on the regulation of *Hippo (hpo)* and *Yorkie (Yki)* genes. Oleic acid injection in *S.med* may have resulted in slowdown of wound resolution processes by decreasing the expression of *Yorkie* gene and increasing the expression of *Hippo* gene. Therefore, it was expected to observe changes in the expression of *Yorkie* gene upon OA injection but no effect was observed in its expression. This effect could be a Hippo signalling pathway independent of *Yorkie.* A previous study found that the conserved consensus Warts/Lats phosphorylation motif in flies and vertebrates was mutated in *Smed-Yorkie* with a lysine instead of arginine becoming refractory to phosphorylation (Lin and Pearson, 2014). This might be the potential reason for Hippo signalling independent regulation of *S.Med Yorkie*.

Several studies elucidated the importance of the Hippo signalling cascade effector; *Yki* in multiple aspects of pleiotropic processes (Lin and Pearson, 2017; Lin and Pearson, 2014). *S.med* planarian has been shown to possess a single ortholog of *Yorkie* exhibiting pleiotropic functions (Lin and Pearson, 2014). The *Smed/yorkie* was shown to be essential for the restriction of stem cell proliferation and maintenance of excretory system homeostasis of planarian (Lin and Pearson, 2014). It is also known that, a proper axial patterning requires *Yorkie (yki).* Thus, *yki* act as a key gene for the integration of cell regulation and spatial tissue patterning (Lin and Pearson, 2014). A recent study has shown

that *Smed-yki* is essential to regulate a normal wound response and proper size upon injury as *yki* gene deficient *S.med* worms were unable to express injury-induced genes and preserve correct scaling in response to injury (Fu, Plouffe and Guan, 2017).

In *S.Med* planarian, a significant elevation of *Hippo* gene expression was observed upon OA injection in comparison to control at Day 7 and 14 resulting in activation of Hippo signalling pathway thus decrease of cell proliferation (Figure 5.3). In planarians, Hippo signalling is shown to be essential to maintain a stable differentiated state of the cell population, to regulate cell cycle progression and also to provide balance among apoptotic and mitotic cells (de Sousa *et al*., 2018). Downregulation of the Hippo signalling pathway in planarian resulted in overgrowths and undifferentiated tissue regions without affecting the body size and number of cells. This was due to a cell cycle arrest, inhibition of apoptosis and increase in cellular dedifferentiation of post-mitotic cells (Ge at al., 2022; Pasual-Carreras *et al*., 2020; de Sousa *et al*., 2019). Inhibition of Hippo in *S.med* planarian led to an overgrown phenotype with a reduction in apoptosis and increase in mitosis without changing the cell number and body size (not inferring with cell proliferation) confirming that inhibition of hippo signalling pathway does not increase cell cycle activity, instead arresting cells at M phase thus rendering cells unable to reach and sustain their proper fate by preventing stable differentiation (de Sousa *et al*., 2018; de Sousa *et al*., 2019). Therefore, an increase in *Hippo* gene expression after oleic acid injection was expected as OA was shown to inhibit wound healing process thus preventing cells to differentiate and regenerate properly.

Palmitic acid was also tested in *S.med* worms to assess whether the lipid is having an effect on the expression of *Hippo* and *Yorkie* genes. After completing the experiments, surprisingly no significant effect was observed with both genes. Previous studies have shown that palmitic acid rescued regeneration defects in starved planarians (Gutierrez-Gutierrez *et al*., 2021). Palmitic acid supplementation elevated the survival of starved

planarian by preventing regeneration failure and implicated that lipid metabolism is an essential requirement for regeneration under starvation (Gutierrez-Gutierrez *et al*., 2021). However, what effect it has on *S.med* worms under normal conditions and on Hippo signalling pathway is not known as the expression of *Hippo* and *Yorkie* genes were not affected upon its administration. The different effects of oleic and palmitic acid on *S.med* worms does need further investigation as different results were obtained upon their administration. However, the results gathered with oleic acid *in-vivo* are consistent with the results obtained in mammalian cells of CaCo-2 and Hep-G2 as all results obtained in this project indicate that lipids in part interact/manipulate the Hippo signalling pathway to regulation its activation state.

7.4 Identifying Key Protein and Gene Transcriptional Targets of YAP using Lipid Metabolism

The last aspect of this project was to assess both protein interactions and gene changes upon lipid treatments and if the hippo signalling pathway is affected by this. Assessment to determine if the binding partners of YAP changed upon addition of lipids was carried out in order to try to understand the mechanism of action of YAP, the ECM and lipid metabolism. In order to analyse this, mass spectroscopy analysis in CaCo-2 cells with samples of YAP with and without oleic acid treatment was undertaken. Numerous well-known interactors of YAP were verified, which provide reassurance that a successful mass spectroscopy analysis was performed. Among the various YAP interactors, most importantly, interaction of Ezrin and Radixin with YAP, found in untreated samples, was abolished upon addition of oleic acid, suggesting that oleic acid disrupted the interaction of YAP with Ezrin and Radixin. Following on from the previous data observed with ezrin, the decrease of the YAP-Ezrin

interaction upon OA treatment was to be expected from MS analysis. The decrease in the expression of ezrin upon addition of OA in CaCo-2 cells can also be clearly seen in immunofluorescence images (Figures 4.9 & 4.10). Ezrin depletion was shown to result in reduced skin fibroblast cell size by sequestering YAP in cytoplasm in previously published studies (Quan *et al*., 2018). Phosphorylated ezrin in hepatocellular carcinomas was shown to directly regulate Hippo signalling pathway leading to YAP activation (Xue *et al*., 2020). Moreover, phosphorylation of ezrin at T567 was also shown to possess a fundamental role in cellular migration by modulating the mechanical features and cytoskeletal organization of the cells (Zhang *et al*., 2020).

Radixin as with ezrin, is a member of ERM-family protein linking actin filaments to the plasma membrane and plays a crucial role in signal transduction. Depletion of radixin is shown to reduce migration and invasion of gastric cancer cells by regulating adhesion proteins (Zhu *et al*., 2016). The role of Radixin by itself in the Hippo signalling pathway is not known as there are no published studies. However, the MS analysis revealed that it interacts with the Hippo signalling pathway effector YAP and its interaction was abolished upon addition of oleic acid which suggests that it has an essential role in the regulation of Hippo signalling pathway. Thus, both Ezrin and Radixin, are involved in the regulation of Hippo signalling pathway and this regulation may be via mechanotransduction.

Angiomotin (AMOT) family proteins were previously specified as a negative regulator of YAP, resulting in inhibition of its activity (Kim *et al*., 2016; Moleirinho *et al*., 2017). Angiomotin can directly bind and sequester YAP in the cytoplasm independently of phosphorylation (Yang and Wang, 2017; Moleirinho *et al*., 2017; Seo and Kim, 2017). Angiomotin can also suppress the activity of YAP by promoting its phosphorylation via LATS kinases (Seo and Kim, 2017; Moleirinho *et al*., 2017). At high density cell culture, AMOTs positioned at tight junctions are necessary to sustain cytoplasmic localisation of YAP

(Karaman and Halder, 2018). The angiomotin family protein member; AMOTL2 was shown to a be potent YAP inhibitor as its depletion promoted EMT and elevated proliferation of MCF10A cells via activation of YAP (Wang *et al*., 2012; Han, Yang and Wang, 2017). A previous study in polarized kidney cells found that depletion of AMOTL2 resulted in activation of YAP by increasing its nuclear localisation thus decreasing its tight-junction localization which in turn promoted targeted YAP-induced gene expression. Thus, AMOT family proteins exhibit tumour suppressor potential via inhibition of YAP (Zhao *et al*., 2011). Therefore, OA addition did not lead to reduced AMOT-YAP interaction in Mass Spectroscopy analysis as AMOT was also involved in inhibition of YAP activity in a similar way to OA.

An RNA-Sequencing (RNA-Seq) approach was used to analyse the expression of specific genes within the Hippo signalling pathway in CaCo-2 cells upon addition of lipids. YAP-regulated genes were expected to be downregulated upon addition of OA as previously shown OA resulted in inactivation of YAP. Genes that are downregulated upon addition of OA were represented in shades of blue (Figure 6.1). Amongst several genes that are downregulated with OA addition, *MYC* and *ANKRD1* genes were identified as downstream target genes of YAP (Choi *et al*., 2018; Zheng *et al*., 2020). The oncogenic transcription factor, *Myc* is evolutionary conserved target of the Hippo signalling pathway induced by YAP for increased oncogenic activity (Zheng and Pan, 2019). The expression of *Myc* is highly elevated in most human cancers inducing proliferation and encourages tumour progression (Madden *et al*., 2021). Active YAP interacts with TEAD family members in the nucleus resulting in YAP-TEAD complex formation, which in turn activate the transcription of *c-Myc* gene to promote cell proliferation (Han. 2019; Croci *et al*., 2017). Interaction of YAP with *c-Myc* is shown to be critical in hepatocarcinogenesis (Xiao *et al*., 2013). A significant

correlation was found in the expressions of YAP and MYC in human gastric cancers (Choi *et al*., 2018).

ANKRD1 (Ankyrin repeat domain containing protein 1), is also a well-known downstream transcription factor of YAP target genes as knockdown of YAP significantly downregulated the expression of *ANKRD1* gene in intestinal fibroblasts (Zheng *et al*., 2020; Ou *et al*., 2021).

In addition, Malat1 has been shown to increase cell proliferation and migration through its upregulated expression via YAP in several cancers (Zygulska, Krzemieniecki and Pierzchalski, 2017). Direct binding of MALAT1 with YAP promotes stabilisation of YAP in the nucleus and induces transcriptional activity which in turn positively regulates the stemness of esophageal and ovarian cancer cells (Syllaios *et al*., 2021; Wu *et al*., 2020). Moreover, YAP-induced MALAT1 encourages epithelial to mesenchymal transition (EMT) of colorectal cancer cells (Sun *et al*., 2019).

As mentioned, MYC, ANKRD1 and MALAT1 interact with active YAP to execute their roles. Therefore, their downregulation with OA was expected as inactivated YAP is unable to interact with them to drive the expression of genes involved in cell proliferation.

Oleic acid caused upregulation of many genes involved in Hippo signalling pathway which were represented in shades of red in (Figure 6.1). FRMD6 is one of the most important genes that has been upregulated upon addition of oleic acid. FRMD6 has been established as a key upstream component of the Hippo signalling pathway activating the core Hippo kinases and resulting in inactivation of the transcriptional co-activator YAP (Kronenberg *et al*., 2020; Guan *et al*., 2019). Thus, FRMD6 is an upstream Hippo signalling pathway activator and has also been identified as a tumour suppressor as its expression is highly suppressed in various human cancers (Haldrup *et al*., 2021; Coffey, 2021). Downregulation of FRMD6 promotes proliferation and migration resulting in tumorigenesis which mimics

the YAP overexpression phenotype (Kronenberg *et al*., 2020; Guan *et al*., 2019). In prostate cancer, knockdown of FRMD6 caused increased Hippo/YAP and c-MYC signalling thus elevating the oncogenic transformation promoting viability and proliferation of prostate cancer cells (Haldrup *et al*., 2021). Like FRMD6, TAOK-1 has also been found to modulate and activate the Hippo signalling cascade by direct phosphorylation of MST1/2 kinases leading to inactivation of YAP (Meng, Moroishi and Guan, 2016). A previous study also showed that TAOK1 can also activate LATS1/2 directly. Thus, activation of Hippo signalling pathway by TAOK1 could suppress activity of YAP (Fang *et al*., 2020). Therefore, their upregulation upon lipid treatment was not surprising as OA also prevented activation of YAP.

Moreover, PTPN14 is also an important upstream regulator of the Hippo signalling pathway and with administration of OA, expression of PTPN14 gene was also observed to be upregulated (Wilson *et al*., 2016). PTPN14 was described as a possible tumour suppressor by negatively regulating YAP's oncogenic actions (Wilson *et al*., 2016). PTPN14 directly interacts with YAP, leading to cytoplasmic sequestration, thus its inactivation to supress cell proliferation is dependent on cell density (Wang *et al*., 2012). PTPN14 also interacts with LATS1 kinase of the Hippo signalling pathway to increase the phosphorylated state of YAP (p-S127) resulting in inhibition of YAP activity (Wilson *et al*., 2014). It has been shown that downregulation of PTPN14 stimulates oncogenic transformation of cells in a similar way to YAP overexpression (Wilson *et al*., 2016).

The expression of AMOT was also upregulated as a result of OA administration. AMOT suppresses activation of YAP leading to its cytoplasmic sequestration. Moreover, a study conducted by Yamaguchi and Taouk (2020), stated that interaction of both AMOT and PTPN14 with YAP inhibits its activity by localising YAP upon the plasma membrane. Thus,

upregulation of both PTPN14 and AMOT with oleic acid was clearly observed in this research.

Interestingly, the expression of TEAD1 which is the binding factor of YAP in the Hippo signalling pathway was upregulated upon addition of OA which was surprising. The downregulation of TEAD1 was expected because YAP was inactivated with OA. TEAD family transcription factors exist as 4 homologous members; TEAD1, TEAD2, TEAD3 and TEAD4 and play a key role in Hippo signalling pathway. They interact with YAP/TAZ in the nucleus to drive expression of target genes induced by YAP. Interaction of YAP with TEADs is a requisite for effective transcriptional activity (Fan *et al*., 2022; Li *et al*., 2010). Therefore, with OA, we were expecting to observe downregulated TEAD1 expression as YAP would be inactivated however that was not the case. The reason for this observation might be due to the redundancy with other TEAD homologs which do not appear in the RNA-Seq data.

In conclusion, interaction of YAP with the ECM proteins; Talin, CD2AP, PDLIM7 and Ezrin revealed a novel protein complex linking the Hippo signalling pathway, the ECM and lipid metabolism. The activity of YAP was shown to be regulated by the ECM as the translocation of YAP between the nucleus and cytoplasm was affected upon siRNA-mediated depletion of complex members. Lipids were shown to inhibit the activation of YAP by increasing its phosphorylation level. Oleic acid was also shown to disrupt the interaction between the members of the complex and resulted in cytoplasmic sequestration of YAP. The study on lipid droplet formation with OA addition in the context of siRNA-mediated knockdowns of the complex members in CaCo-2 and Hep-G2 cells also provided a new insight into the link between lipid metabolism, ECM and Hippo signalling pathway. Moreover, the effect of lipids was tested *in vivo* using Planarian to assess physiological relevance of this and results obtained with oleic acid were consistent with the results obtained in mammalian CaCo-2 and Hep-G2 cells in this research. Finally, change of YAP-binding partners and expression

of target genes were analysed following addition of exogenous lipids by mass spectroscopy and RNA-sequencing. Oleic acid was found to abolish the interaction of Ezrin and Radixin with YAP. The expression of downstream YAP targets were found to be downregulated whereas key upstream target genes of YAP were upregulated upon addition of OA.

As results indicate, lipid metabolism plays an important role in the functionality of Hippo pathway through a novel ECM complex as an increase of lipid content in the cell weakens the interaction among the ECM proteins and YAP to manipulate the signalling of the Hippo pathway. The positive correlation between the Hippo signalling pathway, ECM and lipid metabolism can potentially be utilised to develop targets for the production of beneficial therapeutic agents in the treatment of diseases such as cancer, diabetes and obesity which involve dysregulation of Hippo signalling pathway. Dasatinib and Verteporfin are promising antitumor drugs clinically used for chemotherapeutics and chemosensitizers. Both drugs inhibit YAP oncogene resulting in inhibition of transcriptional activity of downstream targets of YAP. Dasatinib prevents nuclear YAP localisation by acting as a Src inhibitor whereas Verteporfin prevents the interaction of YAP with TEAD blocking the oncogenic activity of YAP (Oku et al., 2015; Feng et al., 2016; Wang et al., 2016). A lipid-based drug can be developed and introduced into cancer treatment in combination with chemotheraphy to disturb the interaction of ECM proteins (CD2AP, Talin, Ezrin and PDLIM7) and prevent the activation of YAP oncogene by sequestering YAP in cytoplasm to inhibit proliferation, migration and invasion of tumors. After that, phase-I clinical trial can be carried out to ascertain the safety and efficiency of the newly developed lipid based drug on early stage of cancer. And if the treatment became successful in preventing the activation of YAP oncogene thus cancer progression; it can also be tested on different types of cancers such as colon, stomach, breast, and ovarian. In addition, targeting genes whose expression is altered by lipids and are critical for cancer progression may provide an

important avenue for cancer therapy. Moreover, in previously published study the transcriptional co-activators YAP/TAZ and their target genes were found to become activated during obesity in human and mouse adipocytes (Wang et al., 2020) thus inhibition of YAP with the addition of lipids may help to prevent the formation of obesity. Oleic acid (OA) is a commonly occurring, monounsaturated fatty acid found in olive oil (Sales-Campos *et al*., 2013; Giulitti *et al*., 2021) and as the treatment of cells with oleic acid inhibited the YAP activation it can be integrated more in people's diet to prevent the formation of obesity.

7.5 Future Work

Mass spectroscopy analysis can also be used to detect the protein phosphorylation and activation state of YAP interacting proteins upon addition of lipids after the determination of protein-protein interactions. In addition, RNA-sequencing can be used to determine the effect of different lipids (like palmitic acid, linoleic acid and linolenic acid) on the expression of specific genes with the Hippo signalling during lipid metabolism. Moreover, a proteomics study can be performed to identify if the protein members of the novel complex is associated with lipid droplets isolated from colorectal adenocarcinoma and hepatocellular carcinoma cells (CaCo-2 and Hep-G2 cells). PIP5K1C has been shown previously to bind directly to Talin2 so it would be interesting to assess the link of PIP5K1C to the novel complex characterised in this research and also to observe if binding of PIP5K1C affects the activation of YAP by immunoblot of pYAP as well as localization to the nucleus in immunofluorescence stains. Talin2 has three specific domains, an N terminal head (FERM) domain, a linker domain and a C-terminal tail domain. The other key experiment is generate

truncated plasmids using a pCMV-flag plasmid as a host and performing PCRs of the Talin2 domains and then to perform overexpression of the plasmids using Lipofectamine 3000 in cell culture before analyzing by Immunoblot, immunofluorescence and Co-immunoprecipitations of all three domains to assess which domains of the protein bind to YAP as well as PIP5K1C. The novel complex characterised can be investigated in a metabolic specific cell line; in adipocytes. Adipocytes can expand when subjected to increased fats without multiplying; induction of hypertrophy without hyperplasia. The novel YAP complex characterised in this research can be used to investigate the role of adipocyte hypertrophy and hyperplasia and to assess what role does YAP (a potent hyperplasia trigger) plays in this and whether manipulation of lipids and ECM proteins could prevent the formation of obesity. The adipocytes can be plated on differing stiffness's of matrix using collagen/fibronectin and by changing the lipid content of the cell simultaneously to analyse the expression levels of YAP/Talin/CD2AP/Ezrin/PDLIM7 and their associated target gene by qPCR. By affecting the levels of lipids, we can also assess if YAP can be prevented from being inactivated and using a constitutively active version of YAP known as YAP 5SA mutated in the five serine residues which are targeted by LATS kinases, we can observe the effects on cellular morphology and associated Hippo pathway proteins. Therefore, it will be interesting to see if we can manipulate YAP to rescue hypertrophy and whether extracellular matrix proteins play a role in this to ultimately find a therapy for obesity and build-up of lipids intracellularly.

8.0 – REFERENCES

REFERENCES

Abrass, C. K. (2004). Cellular lipid metabolism and the role of lipids in progressive renal disease. *American Journal of Nephrology*, *24*(1), 46–53.

Accioly, M. T. *et al.* (2008) "Lipid bodies are reservoirs of cyclooxygenase-2 and sites of prostaglandin-E2 synthesis in colon cancer cells," *Cancer research*, 68(6), pp. 1732–1740.

Adair, B. D. *et al.* (2014) "Structure of the kidney slit diaphragm adapter protein CD2-associated protein as determined with electron microscopy," *Journal of the American Society of Nephrology: JASN*, 25(7), pp. 1465–1473.

Angerer, T. B. *et al.* (2019) "Insights into the histology of planarian flatworm Phagocata gracilis based on location specific, intact lipid information provided by GCIB-ToF-SIMS imaging," *Biochimica et biophysica acta. Molecular and cell biology of lipids*, 1864(5), pp. 733–743.

Antelmi, E. *et al.* (2013) "ß1 integrin binding phosphorylates ezrin at T567 to activate a lipid raft signalsome driving invadopodia activity and invasion," *PloS one*, 8(9), p. e75113.

Aragona, M. *et al.* (2013) "A mechanical checkpoint controls multicellular growth through YAP/TAZ regulation by actin-processing factors," *Cell*, 154(5), pp. 1047–1059.

Ardestani, A., Lupse, B., & Maedler, K. (2018). Hippo signaling: Key emerging pathway in cellular and whole-body metabolism. *Trends in Endocrinology and Metabolism: TEM*, *29*(7), 492–509.

Arpin, M. *et al.* (2011) "Emerging role for ERM proteins in cell adhesion and migration," *Cell adhesion & migration*, 5(2), pp. 199–206.

Aw Yong, K. M., Sun, Y., Merajver, S. D., & Fu, J. (2017). Mechanotransduction-induced reversible phenotypic switching in prostate cancer cells. *Biophysical Journal*, *112*(6), 1236–1245.

Aylon, Y. *et al.* (2016) "The LATS2 tumor suppressor inhibits SREBP and suppresses hepatic cholesterol accumulation," *European journal of cancer (Oxford, England: 1990)*, 61, p. S164.

Bae, S. J. and Luo, X. (2018) "Activation mechanisms of the Hippo kinase signaling cascade," *Bioscience reports*, 38(4), p. BSR20171469.

Bian, X. *et al.* (2021) "Lipid metabolism and cancer," *The journal of experimental medicine*, 218(1). doi: 10.1084/jem.20201606.

Bokhari, M., Carnachan, R. J., Cameron, N. R., & Przyborski, S. A. (2007). Culture of HepG2 liver cells on three dimensional polystyrene scaffolds enhances cell structure and function during toxicological challenge. *Journal of Anatomy*, *211*(4), 567–576.

Bouchard, A. *et al.* (2020) "Hippo signal transduction mechanisms in T cell immunity," *Immune network*, 20(5), p. e36.

Broders-Bondon, F., Nguyen Ho-Bouldoires, T. H., Fernandez-Sanchez, M.-E., & Farge, E. (2018). Mechanotransduction in tumor progression: The dark side of the force. *The Journal of Cell Biology*, *217*(5), 1571–1587.

Cai, X., Wang, K.-C. and Meng, Z. (2021) "Mechanoregulation of YAP and TAZ in cellular homeostasis and disease progression," *Frontiers in cell and developmental biology*, 9, p. 673599.

Calderwood, D. A. (2004). Talin controls integrin activation. *Biochemical Society Transactions*, *32*(Pt3), 434–437.

Calses, P. C. *et al.* (2019) “Hippo pathway in cancer: Aberrant regulation and therapeutic opportunities,” *Trends in cancer*, 5(5), pp. 297–307.

Chakraborty, S. and Hong, W. (2018) “Linking extracellular matrix agrin to the Hippo pathway in liver cancer and beyond,” *Cancers*, 10(2).

Chakraborty, S. *et al.* (2017). Agrin as a mechanotransduction signal regulating YAP through the hippo pathway. *Cell Reports*, *18*(10), 2464–2479.

Chen, Q. *et al.* (2021). Ezrin regulates synovial angiogenesis in rheumatoid arthritis through YAP and Akt signalling. *Journal of Cellular and Molecular Medicine*, *25*(19), 9378–9389.

Cheng, D., Jin, L., Chen, Y., Xi, X., & Guo, Y. (2020). YAP promotes epithelial mesenchymal transition by upregulating Slug expression in human colorectal cancer cells. *International Journal of Clinical and Experimental Pathology*, *13*(4), 701–710.

Cheng, J. *et al.* (2020) “The role and regulatory mechanism of Hippo signaling components in the neuronal system,” *Frontiers in immunology*, 11, p. 281.

Chinthalapudi, K., Rangarajan, E. S. and Izard, T. (2018) “The interaction of talin with the cell membrane is essential for integrin activation and focal adhesion formation,” *Proceedings of the National Academy of Sciences of the United States of America*, 115(41), pp. 10339–10344.

Chinthalapudi, K., Rangarajan, E. S., & Izard, T. (2018). The interaction of talin with the cell membrane is essential for integrin activation and focal adhesion formation. *Proceedings of the National Academy of Sciences of the United States of America*, *115*(41), 10339–10344.

Choi, W. *et al.* (2018). YAP/TAZ initiates gastric tumorigenesis via upregulation of MYC. *Cancer Research*, *78*(12), 3306–3320.

Cobbaut, M. *et al.* (2020). Dysfunctional mechanotransduction through the YAP/TAZ/Hippo pathway as a feature of chronic disease. *Cells (Basel, Switzerland)*, *9*(1), 151.

Coffey, K. (2021). Targeting the Hippo pathway in prostate cancer: What's new? *Cancers*, *13*(4), 611.

Cote, L. E., Simental, E. and Reddien, P. W. (2019) "Muscle functions as a connective tissue and source of extracellular matrix in planarians," *Nature communications*, 10(1), p. 1592.

Critchley, D. R., & Gingras, A. R. (2008). Talin at a glance. *Journal of Cell Science*, *121*(Pt 9), 1345–1347.

Croci, O. *et al.* (2017). Transcriptional integration of mitogenic and mechanical signals by Myc and YAP. *Genes & Development*, *31*(20), 2017–2022.

Cummins, T. D. *et al.* (2018) "PAWS1 controls cytoskeletal dynamics and cell migration through association with the SH3 adaptor CD2AP," *Journal of cell science*, 131(1).

Cunningham, R. and Hansen, C. G. (2022) "The Hippo pathway in cancer: YAP/TAZ and TEAD as therapeutic targets in cancer," *Clinical science (London, England: 1979)*, 136(3), pp. 197–222.

Das, A., Fischer, R. S., Pan, D., & Waterman, C. M. (2016). YAP nuclear localization in the absence of cell-cell contact is mediated by a filamentous actin-dependent, myosin II- and phospho-YAP-independent pathway during extracellular matrix mechanosensing. *The Journal of Biological Chemistry*, *291*(12), 6096–6110.

Dasgupta, I. and McCollum, D. (2019) "Control of cellular responses to mechanical cues through YAP/TAZ regulation," *The journal of biological chemistry*, 294(46), pp. 17693–17706.

Davis, J. R. and Tapon, N. (2019) "Hippo signalling during development," *Development (Cambridge, England)*, 146(18), p. dev167106.

de Sousa, N. *et al.* (2018) "Hippo signaling controls cell cycle and restricts cell plasticity in planarians," *PLoS biology*, 16(1), p. e2002399.

de Sousa, N. *et al.* (2019) "Functional characterization of salvador and warts in planarians," *Matters*.

Demignot, S., Beilstein, F., & Morel, E. (2014). Triglyceride-rich lipoproteins and cytosolic lipid droplets in enterocytes: key players in intestinal physiology and metabolic disorders. *Biochimie*, *96*, 48–55.

DeRan, M. *et al.* (2014). Energy stress regulates hippo-YAP signaling involving AMPK-mediated regulation of angiomotin-like 1 protein. *Cell Reports*, *9*(2), 495–503.

Di Benedetto, G. *et al.* (2021) "YAP and TAZ mediators at the crossroad between metabolic and cellular reprogramming," *Metabolites*, 11(3), p. 154.

Ding, Y. *et al.* (2012) “Proteomic profiling of lipid droplet-associated proteins in primary adipocytes of normal and obese mouse,” *Acta biochimica et biophysica Sinica*, 44(5), pp. 394–406.

Dobrokhotov, O., Samsonov, M., Sokabe, M., & Hirata, H. (2018). Mechanoregulation and pathology of YAP/TAZ via Hippo and non-Hippo mechanisms. *Clinical and Translational Medicine*, *7*(1), 23.

Dupont, S. (2016). Role of YAP/TAZ in cell-matrix adhesion-mediated signalling and mechanotransduction. *Experimental Cell Research*, *343*(1), 42–53.

Elbediwy, A. *et al.* (2012) “Epithelial junction formation requires confinement of Cdc42 activity by a novel SH3BP1 complex,” *The journal of cell biology*, 198(4), pp. 677–693.

Elbediwy, A. *et al.* (2018). Enigma proteins regulate YAP mechanotransduction. *Journal of Cell Science*, *131*(22), jcs221788.

Elbediwy, A. *et al.* (2016). Integrin signalling regulates YAP and TAZ to control skin homeostasis. *Journal of Cell Science*, *129*(11), e1.1-e1.1.

Elosegui-Artola, A. *et al.* (2017) “Force triggers YAP nuclear entry by regulating transport across nuclear pores,” *Cell*, 171(6), pp. 1397-1410.e14.

Eynaudi, A. *et al.* (2021) “Differential effects of oleic and palmitic acids on lipid droplet-mitochondria interaction in the hepatic cell line HepG2,” *Frontiers in nutrition*, 8, p. 775382.

Fan, M. *et al.* (2022). Covalent disruptor of YAP-TEAD association suppresses defective Hippo signaling. *ELife*, *11*.

Fang, C.-Y., Lai, T.-C., Hsiao, M., & Chang, Y.-C. (2020). The diverse roles of TAO kinases in health and diseases. *International Journal of Molecular Sciences*, *21*(20), 7463.

Farag, M. A., & Gad, M. Z. (2022). Omega-9 fatty acids: potential roles in inflammation and cancer management. *Journal, Genetic Engineering & Biotechnology*, *20*(1), 48.

Feng, J. *et al.* (2016) "Verteporfin, a suppressor of YAP-TEAD complex, presents promising antitumor properties on ovarian cancer," *OncoTargets and therapy*, 9, pp. 5371–5381. doi: 10.2147/OTT.S109979.

Fu, Y. *et al.* (2021) "Lipid metabolism in cancer progression and therapeutic strategies," *MedComm*, 2(1), pp. 27–59. doi: 10.1002/mco2.27.

Fu, V., Plouffe, S. W. and Guan, K.-L. (2017) "The Hippo pathway in organ development, homeostasis, and regeneration," *Current opinion in cell biology*, 49, pp. 99–107.

Ge, X.-Y. *et al.* (2022) "An insight into planarian regeneration," *Cell proliferation*, 55(9), p. e13276.

Giulitti, F. *et al.* (2021) "Anti-tumor effect of oleic acid in hepatocellular carcinoma cell lines via autophagy reduction," *Frontiers in cell and developmental biology*, 9, p. 629182.

Gough, R. E., & Goult, B. T. (2018). The tale of two talins - two isoforms to fine-tune integrin signalling. *FEBS Letters*, *592*(12), 2108–2125.

Goult, B. T., Yan, J., & Schwartz, M. A. (2018). Talin as a mechanosensitive signaling hub. *The Journal of Cell Biology*, *217*(11), 3776–3784.

Guan, C., Chang, Z., Gu, X., & Liu, R. (2019). MTA2 promotes HCC progression through repressing FRMD6, a key upstream component of hippo signaling pathway. *Biochemical and Biophysical Research Communications*, *515*(1), 112–118.

Gumbiner, B. M., & Kim, N.-G. (2014). The Hippo-YAP signaling pathway and contact inhibition of growth. *Development (Cambridge, England)*, *141*(6), e607–e607.

Gutiérrez-Gutiérrez, Ó. *et al.* (2021). Regeneration in starved planarians depends on TRiC/CCT subunits modulating the unfolded protein response. *EMBO Reports*, *22*(8), e52905.

Haining, A. W. M., Lieberthal, T. J., & Del Río Hernández, A. (2016). Talin: a mechanosensitive molecule in health and disease. *FASEB Journal: Official Publication of the Federation of American Societies for Experimental Biology*, *30*(6), 2073–2085.

Haldrup, J. *et al.* (2021). FRMD6 has tumor suppressor functions in prostate cancer. *Oncogene*, *40*(4), 763–776.

Han, H., Yang, B. and Wang, W. (2017) “Angiomotin-like 2 interacts with and negatively regulates AKT,” *Oncogene*, 36(32), pp. 4662–4669.

Han, Y. (2019) “Analysis of the role of the Hippo pathway in cancer,” *Journal of translational medicine*, 17(1), p. 116.

Harvey, K. F., Zhang, X. and Thomas, D. M. (2013) “The Hippo pathway and human cancer,” *Nature reviews. Cancer*, 13(4), pp. 246–257.

Hayashi, S., Yokoyama, H. and Tamura, K. (2015) “Roles of Hippo signaling pathway in size control of organ regeneration,” *Development, growth & differentiation*, 57(4), pp. 341–351.

Hiebl, V. *et al.* (2020). Caco-2 cells for measuring intestinal cholesterol transport - possibilities and limitations. *Biological Procedures Online*, *22*(1), 7.

Hoskin, V. *et al.* (2015) “Ezrin regulates focal adhesion and invadopodia dynamics by altering calpain activity to promote breast cancer cell invasion,” *Molecular biology of the cell*, 26(19), pp. 3464–3479.

Höffken, V. *et al.* (2021) “WWC proteins: Important regulators of Hippo signaling in cancer,” *Cancers*, 13(2), p. 306. doi: 10.3390/cancers13020306.

Hsu, P.-C. *et al.* (2020) “The crosstalk between Src and Hippo/YAP signaling pathways in non-small cell lung cancer (NSCLC),” *Cancers*, 12(6), p. 1361.

Hugo, C. *et al.* (1998) “The plasma membrane-actin linking protein, ezrin, is a glomerular epithelial cell marker in glomerulogenesis, in the adult kidney and in glomerular injury,” *Kidney international*, 54(6), pp. 1934–1944.

Hwang, B. *et al.* (2015) “Two distinct roles of the yorkie/yap gene during homeostasis in the planarian Dugesia japonica,” *Development, growth & differentiation*, 57(3), pp. 209–217.

Ibar, C. and Irvine, K. D. (2020) “Integration of Hippo-YAP signaling with metabolism,” *Developmental cell*, 54(2), pp. 256–267.

Islam, M. S. *et al.* (2021) “Extracellular matrix and Hippo signaling as therapeutic targets of antifibrotic compounds for uterine fibroids,” *Clinical and translational medicine*, 11(7), p. e475.

Ji, L., Jiang, F., Cui, X., & Qin, C. (2021). Talin1 knockdown prohibits the proliferation and migration of colorectal cancer cells via the EMT signaling pathway. *Oncology Letters*, *22*(3), 682.

Jiang, L., Wang, W., He, Q., Wu, Y., Lu, Z., Sun, J., Liu, Z., Shao, Y., & Wang, A. (2017). Oleic acid induces apoptosis and autophagy in the treatment of Tongue Squamous cell carcinomas. *Scientific Reports*, *7*(1), 11277.

Jiang, L. *et al.* (2021). YAP promotes the proliferation and migration of colorectal cancer cells through the Glut3/AMPK signaling pathway. *Oncology Letters*, *21*(4), 312.

Johnson, R. and Halder, G. (2014) “The two faces of Hippo: targeting the Hippo pathway for regenerative medicine and cancer treatment,” *Nature reviews. Drug discovery*, 13(1), pp. 63–79.

Karaman, R., & Halder, G. (2018). Cell junctions in hippo signaling. *Cold Spring Harbor Perspectives in Biology*, *10*(5), a028753.

Karami, A., Tebyanian, H., Goodarzi, V., & Shiri, S. (2015). Planarians: An in vivo model for regenerative medicine. *International Journal of Stem Cells*, *8*(2), 128–133.

Kawaguchi, K. and Asano, S. (2022) “Pathophysiological roles of actin-binding scaffold protein, ezrin,” *International journal of molecular sciences*, 23(6), p. 3246.

Kelley, C. F. *et al.* (2020) “Phosphoinositides regulate force-independent interactions between talin, vinculin, and actin,” *eLife*, 9.

Khaldoun, S. A. *et al.* (2014) “Autophagosomes contribute to intracellular lipid distribution in enterocytes,” *Molecular biology of the cell*, 25(1), pp. 118–132.

Kim, Miju *et al.* (2016) “Role of Angiomotin-like 2 mono-ubiquitination on YAP inhibition,” *EMBO reports*, 17(1), pp. 64–78.

Kim, N.-G. and Gumbiner, B. M. (2015) “Adhesion to fibronectin regulates Hippo signaling via the FAK-Src-PI3K pathway,” *The journal of cell biology*, 210(3), pp. 503–515.

Klapholz, B., & Brown, N. H. (2017). Talin – the master of integrin adhesions. *Journal of Cell Science*, *130*(15), 2435–2446.

Koo, J. H., & Guan, K.-L. (2018). Interplay between YAP/TAZ and metabolism. *Cell Metabolism*, *28*(2), 196–206.

Kronenberg, N. M. *et al.* (2020). Willin/FRMD6 influences mechanical phenotype and neuronal differentiation in mammalian cells by regulating ERK1/2 activity. *Frontiers in Cellular Neuroscience*, *14*, 552213.

Kwon, H., Kim, J. and Jho, E.-H. (2021) “Role of the Hippo pathway and mechanisms for controlling cellular localization of YAP/TAZ,” *The FEBS journal*, 289(19), pp. 5798–5818.

Lamar, J. M. *et al.* (2012) “The Hippo pathway target, YAP, promotes metastasis through its TEAD-interaction domain,” *Proceedings of the National Academy of Sciences of the United States of America*, 109(37), pp. E2441-50.

Lamar, J. M. *et al.* (2019) “SRC tyrosine kinase activates the YAP/TAZ axis and thereby drives tumor growth and metastasis,” *The journal of biological chemistry*, 294(7), pp. 2302–2317.

Lea, T. (2015). Caco-2 Cell Line. In *The Impact of Food Bioactives on Health* (pp. 103–111). Springer International Publishing.

Lee, J. and Ridgway, N. D. (2018) “Phosphatidylcholine synthesis regulates triglyceride storage and chylomicron secretion by Caco2 cells,” *The Journal of Lipid Research*, 59(10), pp. 1940–1950.

Lee, U., Cho, E.-Y. and Jho, E.-H. (2022) “Regulation of Hippo signaling by metabolic pathways in cancer,” *Biochimica et biophysica acta. Molecular cell research*, 1869(4), p. 119201.

Lehtonen, S., Zhao, F. and Lehtonen, E. (2002) “CD2-associated protein directly interacts with the actin cytoskeleton,” *American journal of physiology. Renal physiology*, 283(4), pp. F734-43.

Li, L. *et al.* (2017). The role of talin2 in breast cancer tumorigenesis and metastasis. *Oncotarget*, *8*(63), 106876–106887.

Li, N. *et al.* (2019). Ezrin promotes breast cancer progression by modulating AKT signals. *British Journal of Cancer*, *120*(7), 703–713.

Li, R., Bu, Y., Yang, C., & Wang, J. (2021). Effects of lipid deposition on viscoelastic response in human hepatic cell line HepG2. *Frontiers in Physiology*, *12*, 684121.

Li, S. *et al.* (2014). High metastaticgastric and breast cancer cells consume oleic acid in an AMPK dependent manner. *PloS One*, *9*(5), e97330.

Li, Z. *et al.* (2010). Structural insights into the YAP and TEAD complex. *Genes & Development*, *24*(3), 235–240.

Liang, Y. *et al.* (2018). Talin2 regulates breast cancer cell migration and invasion by apoptosis. *Oncology Letters*.

Lin, A. Y. T. and Pearson, B. J. (2017) "Yorkie is required to restrict the injury responses in planarians," *PLoS genetics*, 13(7), p. e1006874.

Lin, A. Y. T., & Pearson, B. J. (2014). Planarian yorkie/YAP functions to integrate adult stem cell proliferation, organ homeostasis and maintenance of axial patterning. *Development (Cambridge, England)*, *141*(6), 1197–1208.

Lin, D., Chun, T.-H. and Kang, L. (2016) "Adipose extracellular matrix remodelling in obesity and insulin resistance," *Biochemical pharmacology*, 119, pp. 8–16.

Liu, H. *et al.* (2012) "The role of MMP-1 in breast cancer growth and metastasis to the brain in a xenograft model," *BMC cancer*, 12, p. 583. doi: 10.1186/1471-2407-12-583.

Liu, Q., Liu, X. and Song, G. (2021) "The Hippo pathway: A master regulatory network important in cancer," *Cells (Basel, Switzerland)*, 10(6), p. 1416.

Liu, Z. *et al.* (2013). Effects of oleic acid on cell proliferation through an integrin-linked kinase signaling pathway in 786-O renal cell carcinoma cells. *Oncology Letters*, *5*(4), 1395–1399.

Lomakin, A., Nader, G. and Piel, M. (2017) "Forcing entry into the nucleus," *Developmental cell*, 43(5), pp. 547–548.

Madden, S. K. *et al.* (2021). Taking the Myc out of cancer: toward therapeutic strategies to directly inhibit c-Myc. *Molecular Cancer*, *20*(1), 3.

Makhutova, O. N. *et al.* (2009) "Fatty acid content and composition of freshwater Planaria dendrocoelopsis sp. (planariidae, Turbellaria, Platyhelminthes) from the Yenisei river," *Journal of Siberian Federal University Biology*, 2(2), pp. 135–144.

Maly, I. V., & Hofmann, W. A. (2020). Effect of palmitic acid on exosome-mediated secretion and invasive motility in prostate cancer cells. *Molecules (Basel, Switzerland)*, *25*(12), 2722.

Marsick, B. M., San Miguel-Ruiz, J. E. and Letourneau, P. C. (2012) "Activation of ezrin/radixin/moesin mediates attractive growth cone guidance through regulation of growth cone actin and adhesion receptors," *The Journal of neuroscience: the official journal of the Society for Neuroscience*, 32(1), pp. 282–296.

Mason, D. E. *et al.* (2019). YAP and TAZ limit cytoskeletal and focal adhesion maturation to enable persistent cell motility. *The Journal of Cell Biology*, *218*(4), 1369–1389.

Maugeri-Saccà, M., & De Maria, R. (2018). The Hippo pathway in normal development and cancer. *Pharmacology & Therapeutics*, *186*, 60–72.

Menendez, J. A., Vellon, L., Colomer, R., & Lupu, R. (2005). Oleic acid, the main monounsaturated fatty acid of olive oil, suppresses Her-2/neu (erbB-2) expression and synergistically enhances the growth inhibitory effects of trastuzumab (Herceptin) in breast cancer cells with Her-2/neu oncogene amplification. *Annals of Oncology*, *16*(3), 359–371.

Meng, Z., Moroishi, T., & Guan, K.-L. (2016). Mechanisms of Hippo pathway regulation. *Genes & Development*, *30*(1), 1–17.

Misra, J. R., & Irvine, K. D. (2018). The Hippo signaling network and its biological functions. *Annual Review of Genetics*, *52*(1), 65–87.

Mohri, Z., Del Rio Hernandez, A., & Krams, R. (2017). The emerging role of YAP/TAZ in mechanotransduction. *Journal of Thoracic Disease*, *9*(5), E507–E509.

Moleirinho, S. *et al.* (2017) "Regulation of localization and function of the transcriptional co-activator YAP by angiomotin," *eLife*, 6.

Moroishi, T., Hansen, C. G., & Guan, K.-L. (2015). The emerging roles of YAP and TAZ in cancer. *Nature Reviews. Cancer*, *15*(2), 73–79.

Moya, I. M., & Halder, G. (2016). The Hippo pathway in cellular reprogramming and regeneration of different organs. *Current Opinion in Cell Biology*, *43*, 62–68.

Nair, P. R., & Wirtz, D. (2019). Enabling migration by moderation: YAP/TAZ are essential for persistent migration. *The Journal of Cell Biology*, *218*(4), 1092–1093.

Nguyen-Lefebvre, A. T. *et al.* (2021) "The hippo pathway: A master regulator of liver metabolism, regeneration, and disease," *FASEB journal: official publication of the Federation of American Societies for Experimental Biology*, 35(5), p. e21570.

Nikolopoulou, P. *et al.* (2022). Talin regulates steady-state tensional homeostasis to drive vascular morphodynamics and cancer. In *bioRxiv*.

Ou, W. *et al.* (2021). Increased expression of yes-associated protein/YAP and transcriptional coactivator with PDZ-binding motif/TAZ activates intestinal fibroblasts to promote intestinal obstruction in Crohn's disease. *EBioMedicine*, *69*(103452), 103452.

Paramitha, P. N. *et al.* (2021). Raman study on lipid droplets in hepatic cells co-cultured with fatty acids. *International Journal of Molecular Sciences*, *22*(14), 7378.

Park, H. W., & Guan, K.-L. (2013). Regulation of the Hippo pathway and implications for anticancer drug development. *Trends in Pharmacological Sciences*, *34*(10), 581–589.

Pascual-Carreras, E. *et al.* (2020) "Planarian cell number depends on blitzschnell, a novel gene family that balances cell proliferation and cell death," *Development (Cambridge, England)*, 147(7), p. dev184044.

Pavel, M. *et al.* (2018). Contact inhibition controls cell survival and proliferation via YAP/TAZ-autophagy axis. *Nature Communications*, *9*(1), 2961.

Piroli, M. E., Blanchette, J. O., & Jabbarzadeh, E. (2019). Polarity as a physiological modulator of cell function. *Frontiers in Bioscience (Landmark Edition)*, *24*(3), 451–462.

Ponuwei, G. A. (2016) "A glimpse of the ERM proteins," *Journal of biomedical science*, 23(1), p. 35.

Qi, L. *et al.* (2016). Talin2-mediated traction force drives matrix degradation and cell invasion. *Journal of Cell Science*, *129*(19), 3661–3674.

Oku, Y. *et al.* (2015) "Small molecules inhibiting the nuclear localization of YAP/TAZ for chemotherapeutics and chemosensitizers against breast cancers," *FEBS open bio*, 5(1), pp. 542–549. doi: 10.1016/j.fob.2015.06.007.

Quan, C. *et al.* (2018) "Ezrin regulates skin fibroblast size/mechanical properties and YAP-dependent proliferation," *Journal of cell communication and signaling*, 12(3), pp. 549–560.

Quan, C. *et al.* (2019) “Ezrin promotes pancreatic cancer cell proliferation and invasion through activating the Akt/mTOR pathway and inducing YAP translocation,” *Cancer management and research*, 11, pp. 6553–6566.

Rahikainen, R. *et al.* (2017) “Mechanical stability of talin rod controls cell migration and substrate sensing,” *Scientific reports*, 7(1), p. 3571.

Rahikainen, R. *et al.* (2019) “Talin-mediated force transmission and talin rod domain unfolding independently regulate adhesion signaling,” *Journal of cell science*, 132(7), p. jcs226514.

Rausch, V., & Hansen, C. G. (2020). The Hippo pathway, YAP/TAZ, and the plasma membrane. *Trends in Cell Biology*, *30*(1), 32–48.

Reddien, P. W. (2018) “The cellular and molecular basis for planarian regeneration,” *Cell*, 175(2), pp. 327–345.

Ricchi, M. *et al.* (2009). Differential effect of oleic and palmitic acid on lipid accumulation and apoptosis in cultured hepatocytes. *Journal of Gastroenterology and Hepatology*, *24*(5), 830–840.

Rohwedder, A., Zhang, Q., Rudge, S. A., & Wakelam, M. J. O. (2014). Lipid droplet formation in response to oleic acid in Huh-7 cells is mediated by the fatty acid receptor FFAR4. *Journal of Cell Science*, *127*(Pt 14), 3104–3115.

Sales-Campos, H. *et al.* (2013). An overview of the modulatory effects of oleic acid in health and disease. *Mini Reviews in Medicinal Chemistry*, *13*(2), 201–210.

Santos, C. P., & Schulze, A. (2012). Lipid metabolism in cancer. *FEBS Journal*, *279*(15), 2610–2623.

Schiffer, M. *et al.* (2004) “A novel role for the adaptor molecule CD2-associated protein in transforming growth factor-beta-induced apoptosis,” *The journal of biological chemistry*, 279(35), pp. 37004–37012.

Seo, J. and Kim, J. (2018) “Regulation of Hippo signaling by actin remodeling,” *BMB reports*, 51(3), pp. 151–156.

Seong, J., Wang, N. and Wang, Y. (2013) “Mechanotransduction at focal adhesions: from physiology to cancer development,” *Journal of cellular and molecular medicine*, 17(5), pp. 597-604.

Shamsan, G. A., & Odde, D. J. (2019). Emerging technologies in mechanotransduction research. *Current Opinion in Chemical Biology*, *53*, 125–130.

Shen, J. *et al.* (2018) “Hippo component YAP promotes focal adhesion and tumour aggressiveness via transcriptionally activating THBS1/FAK signalling in breast cancer,” *Journal of experimental & clinical cancer research: CR*, 37(1).

Shu, Z. *et al.* (2019). A functional interaction between Hippo-YAP signalling and SREBPs mediates hepatic steatosis in diabetic mice. *Journal of Cellular and Molecular Medicine*, *23*(5), 3616–3628.

Si, Y. *et al.* (2017) “Src inhibits the Hippo tumor suppressor pathway through tyrosine phosphorylation of Lats1,” *Cancer research*, 77(18), pp. 4868–4880.

Song, X. *et al.* (2020) “Acetylation of ezrin regulates membrane-cytoskeleton interaction underlying CCL18-elicited cell migration,” *Journal of molecular cell biology*, 12(6), pp. 424–437.

Staley, B. K. and Irvine, K. D. (2012) “Hippo signaling in Drosophila: recent advances and insights” *Developmental dynamics: an official publication of the American Association of Anatomists*, 241(1), pp. 3–15.

Sun, Z., Guo, S. S., & Fässler, R. (2016). Integrin-mediated mechanotransduction. *The Journal of Cell Biology*, *215*(4), 445–456.

Sun, Z. *et al.* (2019). YAP1-induced MALAT1 promotes epithelial-mesenchymal transition and angiogenesis by sponging miR-126-5p in colorectal cancer. *Oncogene*, *38*(14), 2627–2644.

Syllaios, A. *et al.* (2021). Pathways and role of MALAT1 in esophageal and gastric cancer. *Oncology Letters*, *21*(5), 343.

Tadokoro, S. *et al.* (2003). Talin binding to integrin ß tails: A final common step in integrin activation. *Science (New York, N.Y.)*, *302*(5642), 103–106.

Virdi, J. K. and Pethe, P. (2021) “Biomaterials regulate mechanosensors YAP/TAZ in stem cell growth and differentiation,” *Tissue engineering and regenerative medicine*, 18(2), pp. 199–215.

Wang, C. *et al.* (2016) “Verteporfin inhibits YAP function through up-regulating 14-3-3σ sequestering YAP in the cytoplasm,” *American journal of cancer research*, 6(1), pp. 27–37.

Wang, L. *et al.* (2020) “YAP and TAZ protect against white adipocyte cell death during obesity,” *Nature communications*, 11(1), p. 5455. doi: 10.1038/s41467-020-19229-3.

Wang, M. *et al.* (2021) “The regulatory networks of the Hippo signaling pathway in cancer development,” *Journal of cancer*, 12(20), pp. 6216–6230.

Wang, R. *et al.* (2020) “PTPN14 acts as a candidate tumor suppressor in prostate cancer and inhibits cell proliferation and invasion through modulating LATS1/YAP signaling,” *Molecular and cellular probes*, 53(101642), p. 101642. doi: 10.1016/j.mcp.2020.101642.

Wang, W. *et al.* (2012). PTPN14 is required for the density-dependent control of YAP1. *Genes & Development*, *26*(17), 1959–1971.

Wang, Y. and Brieher, W. M. (2019) “CD2AP links actin to PI3 kinase activity to extend epithelial cell height and constrain cell area,” *The journal of cell biology*, 219(1), p. jcb.201812087.

Wells, R. G. (2008). The role of matrix stiffness in regulating cell behavior. *Hepatology (Baltimore, Md.)*, *47*(4), 1394–1400.

Werneburg, N., Gores, G. J. and Smoot, R. L. (2020) “The Hippo pathway and YAP signaling: Emerging concepts in regulation, signaling, and experimental targeting strategies with implications for hepatobiliary malignancies,” *Gene expression*, 20(1), pp. 67–74.

Wilson, K. E. *et al.* (2014). PTPN14 forms a complex with Kibra and LATS1 proteins and negatively regulates the YAP oncogenic function. *The Journal of Biological Chemistry*, *289*(34), 23693–23700.

Wilson, K. E., Yang, N., Mussell, A. L., & Zhang, J. (2016). The regulatory role of KIBRA and PTPN14 in Hippo signaling and beyond. *Genes*, *7*(6), 23.

Wu, X. *et al.* (2020). The long non-coding RNA MALAT1 enhances ovarian cancer cell stemness by inhibiting YAP translocation from nucleus to cytoplasm. *Medical Science Monitor: International Medical Journal of Experimental and Clinical Research*, *26*, e922012.

Xi, M., & Tang, W. (2020). Knockdown of Ezrin inhibited migration and invasion of cervical cancer cells in vitro. *International Journal of Immunopathology and Pharmacology*, *34*, 2058738420930899.

Xiao, W. *et al.* (2013). Mutual interaction between YAP and c-Myc is critical for carcinogenesis in liver cancer. *Biochemical and Biophysical Research Communications*, *439*(2), 167–172.

Xiao, Y. and Dong, J. (2021) "The Hippo signaling pathway in cancer: A cell cycle perspective," *Cancers*, 13(24), p. 6214.

Xie, W. *et al.* (2020). CD2AP inhibits metastasis in gastric cancer by promoting cellular adhesion and cytoskeleton assembly. *Molecular Carcinogenesis*, *59*(4), 339–352.

Xue, Y. *et al.* (2020) "Phosphorylated Ezrin (Thr567) regulates Hippo pathway and yes-associated protein (Yap) in liver," *The American journal of pathology*, 190(7), pp. 1427–1437.

Yamaguchi, H. and Taouk, G. M. (2020) "A potential role of YAP/TAZ in the interplay between metastasis and metabolic alterations," *Frontiers in oncology*, 10, p. 928.

Yang, D. *et al.* (2021) “The Hippo signaling pathway: The trader of tumor microenvironment,” *Frontiers in oncology*, 11, p. 772134.

Yimlamai, D., Fowl, B. H., & Camargo, F. D. (2015). Emerging evidence on the role of the Hippo/YAP pathway in liver physiology and cancer. *Journal of Hepatology*, *63*(6), 1491–1501.

Yu, F.-X., & Guan, K.-L. (2013). The Hippo pathway: regulators and regulations. *Genes & Development*, *27*(4), 355–371.

Yuan, L. *et al.* (2017). Palmitic acid dysregulates the Hippo–YAP pathway and inhibits angiogenesis by inducing mitochondrial damage and activating the cytosolic DNA sensor cGAS–STING–IRF3 signaling mechanism. *The Journal of Biological Chemistry*, *292*(36), 15002–15015.

Yuwen, Y.-Q. *et al.* (2011) “Evaluation of endogenous reference genes for analysis of gene expression with real-time RT-PCR during planarian regeneration,” *Molecular biology reports*, 38(7), pp. 4423–4428.

Zanconato, F., Battilana, G., Cordenonsi, M., & Piccolo, S. (2016). YAP/TAZ as therapeutic targets in cancer. *Current Opinion in Pharmacology*, *29*, 26–33.

Zanconato, F., Cordenonsi, M., & Piccolo, S. (2016). YAP/TAZ at the roots of cancer. *Cancer Cell*, *29*(6), 783–803.

Zeng, R. and Dong, J. (2021) “The Hippo signaling pathway in drug resistance in cancer,” *Cancers*, 13(2), p. 318.

Zeng, R., & Dong, J. (2021). The Hippo signaling pathway in drug resistance in cancer. *Cancers*, *13*(2), 318.

Zhang, J. *et al.* (2019). Mechanotransduction and cytoskeleton remodeling shaping YAP1 in gastric tumorigenesis. *International Journal of Molecular Sciences*, *20*(7), 1576.

Zhang, X. *et al.* (2008) "Talin depletion reveals independence of initial cell spreading from integrin activation and traction," *Nature cell biology*, 10(9), pp. 1062–1068.

Zhang, X. *et al.* (2020). Ezrin phosphorylation at T567 modulates cell migration, mechanical properties, and cytoskeletal organization. *International Journal of Molecular Sciences*, *21*(2), 435.

Zhang, X. *et al.* (2018). The role of YAP/TAZ activity in cancer metabolic reprogramming. *Molecular Cancer*, *17*(1), 134.

Zhang, Y. *et al.* (2017) "WWC2 is an independent prognostic factor and prevents invasion via Hippo signalling in hepatocellular carcinoma," *Journal of cellular and molecular medicine*, 21(12), pp. 3718–3729. doi: 10.1111/jcmm.13281.

Zhao, B. *et al.* (2011) "Angiomotin is a novel Hippo pathway component that inhibits YAP oncoprotein," *Genes & development*, 25(1), pp. 51–63.

Zhao, B. *et al.* (2012) "Cell detachment activates the Hippo pathway via cytoskeleton reorganization to induce anoikis," *Genes & development*, 26(1), pp. 54–68.

Zhao, B., Li, L., Lei, Q., & Guan, K.-L. (2010). The Hippo-YAP pathway in organ size control and tumorigenesis: an updated version. *Genes & Development*, *24*(9), 862–874.

Zhao, B. *et al.* (2007). Inactivation of YAP oncoprotein by the Hippo pathway is involved in cell contact inhibition and tissue growth control. *Genes & Development*, *21*(21), 2747–2761.

Zhao, J. *et al.* (2013). CD2AP links cortactin and capping protein at the cell periphery to facilitate formation of lamellipodia. *Molecular and Cellular Biology*, *33*(1), 38–47.

Zhao, Y., Lykov, N. and Tzeng, C. (2022) “Talin‑1 interaction network in cellular mechanotransduction (Review),” *International journal of molecular medicine*, 49(5).

Zheng, C. *et al.* (2020). YAP activation and implications in patients and a mouse model of biliary atresia. *Frontiers in Pediatrics*, *8*, 618226.

Zheng, Y. and Pan, D. (2019) “The Hippo signaling pathway in development and disease,” *Developmental cell*, 50(3), pp. 264–282.

Zhu, Y.-W. *et al.* (2016). Knockdown of radixin suppresses gastric cancer metastasis in vitro by up-regulation of E-cadherin via NF-κB/snail pathway. *Cellular Physiology and Biochemistry: International Journal of Experimental Cellular Physiology, Biochemistry, and Pharmacology*, *39*(6), 2509–2521.

Zygulska, A. L., Krzemieniecki, K. and Pierzchalski, P. (2017) “Hippo pathway - brief overview of its relevance in cancer,” *Journal of physiology and pharmacology: an official journal of the Polish Physiological Society*, 68(3), pp. 311–335.

APPENDIX

MATERIALS

Cell Culture Maintenance and Supplements

Manufacturer	Material
Gibco®	DMEM(1X) Dulbecco's Modified Eagle Medium [+] 4.5g/L D-Glucose, L-Glutamine [+] Pyruvate REF 41966-029 LOT 2436354
Gibco®	Penicillin-Streptomycin REF 15140-122 LOT 2145456
Gibco®	0.5% Trypsin-EDTA (10X) REF 15400-054
Sigma-Aldrich	D8537-500ML Dulbecco's Phosphate Buffered Saline Modified, without calcium chloride and magnesium chloride LOT RNBK7105
Sigma-Aldrich	Foetal Bovine Serum (FBS)

SiRNA Transfection

Manufacturer	Material
Gibco®	Opti-MEM® I (1X) Reduced-Serum Medium REF: 31985-062
Invitrogen	Lipofectamine® RNAiMAX Transfection Reagent REF 13778-075 LOT 2158124
Dharmacon™	5X siRNA Buffer 0.2 um Sterile Filtered
Dharmacon™	siGENOME™ Control Pool Non-Targeting #1, 20 nmol Catalog: D001206-13-20 LOT 2673245
Dharmacon™	siGENOME SMARTpool Human YAP1, 20nmol Cat # M-012200-00 Lot#: 170616
Dharmacon™	siGENOME SMARTpool Human TLN1, 5nmol Cat # M-012949-00-0005 Lot#: 191114
Dharmacon™	siGENOME SMARTpool Human TLN2, 5nmol

	Cat # M-012909-01-0005 Lot#: 191114
Dharmacon™	siGENOME SMARTpool Human CD2AP, 5nmol Cat # M-012799-02-0005 Lot#:220302
Dharmacon™	siGENOME SMARTpool Human EZR, 5nmol Cat # M-017370-02-0005 Lot#:220302

Antibodies

Manufacturer	**Antibody**	**Host**	**Immuno-blotting Dilution**	**Immuno-fluorescence Dilution**	**Immuno-precipitation Dilution (ug)**
CST (Cell Signalling Technology)	Phospho-YAP (Ser127) rabbit antibody 100 ul Catalog no. #4911 LOT 5	Rabbit	1:500	-	-
Santa Cruz Biotechnology	YAP (63.7), mouse monoclonal IgG_{28} 100ug/ml Catalog no. sc-101199	Mouse Monoclonal	1:500	1:200	5
Santa Cruz Biotechnology	CD2AP (B-4), mouse monoclonal IgG_1 200ug/ml Catalog no. sc-25272	Mouse Monoclonal	1:500	1:200	5
Santa Cruz Biotechnology	GAPDH (6C5), mouse monoclonal IgG_1 100ug/ml Catalog no. sc-32233	Mouse Monoclonal	1:1000	-	-
Santa Cruz Biotechnology	YAP (H-125), rabbit polyclonal IgG 200 ug/ml Catalog no. sc-15407	Rabbit Polyclonal	-	1:200	-

Sigma-Aldrich	T3287-2ML Monoclonal Anti-Talin antibody produced in mouse Lot # 049M4782V	Mouse	1:500	1:200	2
Sigma-Aldrich	Anti-Actin, N-terminal antibody-Catalog no. A2103	Rabbit	1:1000	-	-
Novus Biologicals	pAb anti-PDLIM7 Lot A105841 0.1 ml Immunogen affinity purified Rabbit Sera 0.1 mg/ml Catalog no. NBP1-84841	Rabbit Polyclonal	1:500	-	5
LI-COR	IRDye 800 CW Donkey anti-Mouse-Catalog no. 926-32212	Donkey	1:2500	-	-
LI-COR	IRDye 680 RD Donkey anti-Rabbit-Catalog no. 926-68073	Donkey	1:2500	-	-
Jackson Immunoresearch	CY3 (Donkey)	Mouse	-	1:300	-
Jackson Immunoresearch	CY3 (Goat)	Rabbit	-	1:300	-
Jackson Immunoresearch	FITC (Donkey)	Mouse	-	1:300	-
Jackson Immunoresearch	FITC (Donkey)	Rabbit	-	1:300	-

Fatty Acid Treatments

Manufacturer	Fatty Acid
Sigma-Aldrich	Oleic Acid-Albumin from Bovine Serum, O3008 - 5 mL (Oleic Acid-BSA Complex)
	Albumin, Bovine-Palmitic Acid, A7922

Cell Lysis (Sample) Buffer

Manufacturer	Material
ThermoFisher	3.6 ml of Tris-Glycine SDS 2X Buffer
	400 of NuPage LDS Sample Reducing Agent (10X)

SDS-Page Gels (10%) & Buffers

Separating Gel	Stacking Gel
10 mL of 30% (w/v) Acrylamide: 0.8 % (w/v) Bis-Acryl-amide Stock Solution (37.5:1) (National Diagnostics)	3 mL of 30% (w/v) Acrylamide: 0.8 % (w/v) Bis-Acryl-amide Stock Solution (37.5:1) (National Diagnostics)
7.8 mL of 4X ProtoGel Resolving Buffer (1.5 M Tris-HCl, 0,4% SDS, pH 8.8) (National Diagnostics)	4 mL of ProtoGel Stacking Buffer (0.5 M Tris HCl 0.4% SDS, pH 6.8) (National Diagnostics)
9.15 mL of H_2O	8.5 mL of H_2O
3 mL of 1% Ammonium Persulfate (APS) (Sigma Aldrich)	1.6 mL of 1% Ammonium Persulfate (APS) (Sigma Aldrich)
50 µL of Tetramethyl-ethylene Diamine (TEMED) (Sigma Aldrich)	50 µL of Tetramethyl-ethylene Diamine (TEMED) (Sigma Aldrich)

10X Stock Running Buffer	**1L Transfer Buffer**
0.25M TRIS	100 mL of TRIS/Glycine/SDS 10X Solution (Fisher BioReagents)
1.92M Glycine	200 mL of Methanol
1% SDS	700 ml of H_2O

Western Blotting

Destain Solution	**20% Tween**	**PBS**	**PBS-Tween**
7.5 % acetic acid (FisherScientific)	10 ml Tween (Sigma Aldrich)	10 Phosphate-buffered saline tablets (OXOID)	5 ml of 20% Tween
20% methanol (VWR Chemicals)	H_2O up to 50 ml	H_2O up to 1L	PBS up to 1L
H_2O up to 1L			

Co-Immunoprecipitation (Co-IP)

Magnetic Beads	MCE® MedChemExpress Protein A/G Magnetic Beads 1mL Cat.#HY-K0202 Lot# 114185
Inhibitors	Sigma Aldrich P0044-1 ML Phosphatase Inhibitor Cocktail 3 Batch # 0000080384
	Sigma Aldrich P2714-1BTL Protease Inhibitor Cocktail Powder LOT # 068M4099V
Wash Buffer	Phosphate Buffered Saline (PBS) (Sigma Aldrich)
Lysis Buffer	50 l of Triton X-100 (Sigma Aldrich) in 10 ml PBS

Immunofluorescence

Blocking Buffer	Ab Dilution/Permabilization Buffer	4% PFA
1.0 g of 1% BSA powder (Sigma Aldrich)	40 ml of blocking buffer	1 ampul of PFA (ThermoScientific)
0.07 g of 20 mM Glycine (Fisher Bioreagents)	200 ul of 20% Triton	300 ml of PBS
100 ml of 1X PBS		

Planaria

Manufacturer	Material
Sigma Aldrich	S4438-100RXN SYBR® Green Jumpstart™ Taq ReadyMix™ PCode 1003364281
BIO-RAD	iScript cDNA Synthesis Kit Cat# 1708890 Batch 64408847